

**Prediction of Particulate Fouling in Reverse Osmosis Systems
MFI-UF Method Development and Application**

Abunada, M.B.M.

DOI

[10.4233/uuid:58a8de05-9b30-4009-93bb-1b671eed3bee](https://doi.org/10.4233/uuid:58a8de05-9b30-4009-93bb-1b671eed3bee)

Publication date

2023

Document Version

Final published version

Citation (APA)

Abunada, M. B. M. (2023). *Prediction of Particulate Fouling in Reverse Osmosis Systems: MFI-UF Method Development and Application*. [Dissertation (TU Delft), Delft University of Technology, IHE Delft Institute for Water Education]. <https://doi.org/10.4233/uuid:58a8de05-9b30-4009-93bb-1b671eed3bee>

Important note

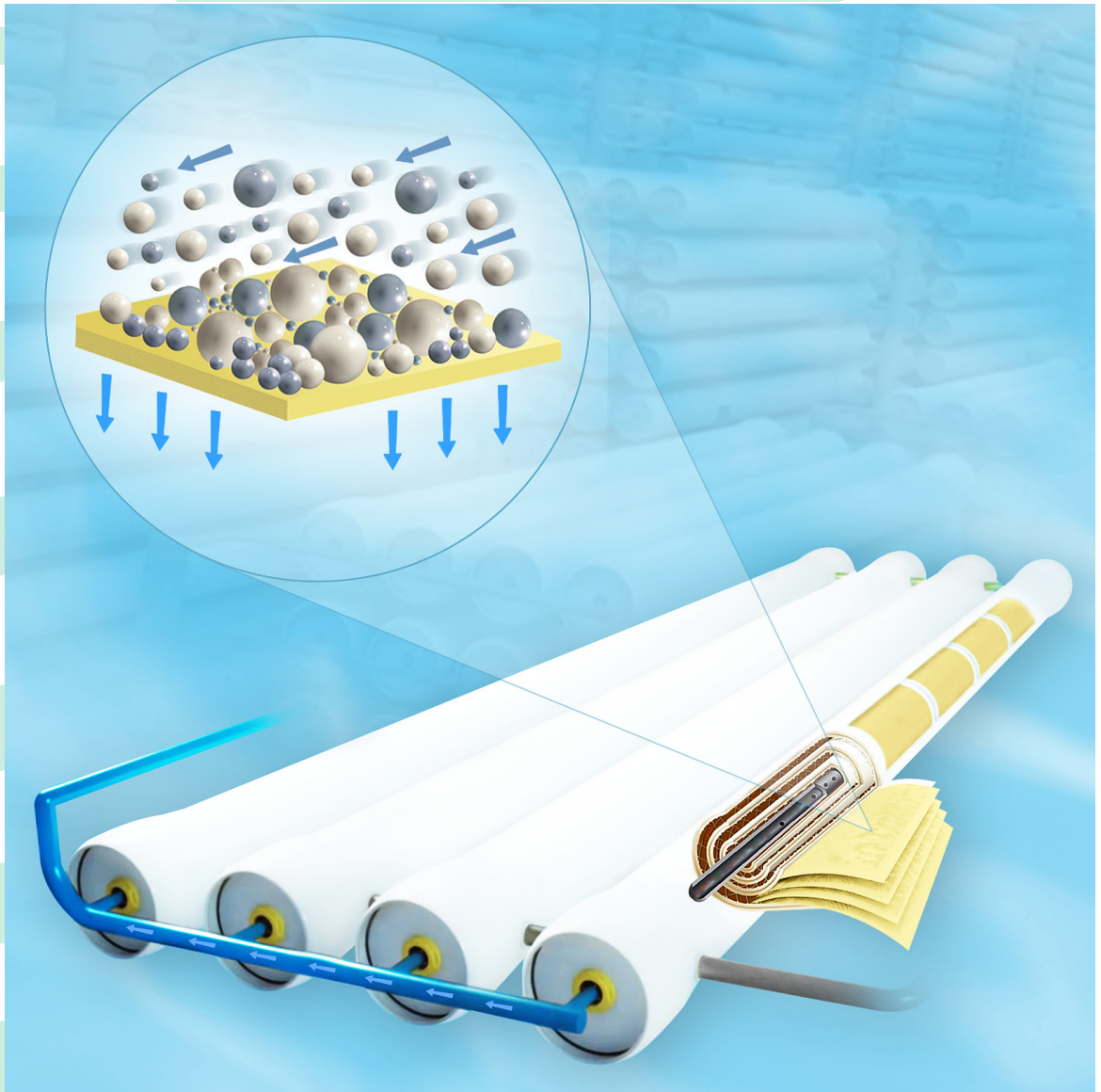
To cite this publication, please use the final published version (if applicable).
Please check the document version above.

Copyright

Other than for strictly personal use, it is not permitted to download, forward or distribute the text or part of it, without the consent of the author(s) and/or copyright holder(s), unless the work is under an open content license such as Creative Commons.

Takedown policy

Please contact us and provide details if you believe this document breaches copyrights.
We will remove access to the work immediately and investigate your claim.



Prediction of Particulate Fouling in Reverse Osmosis Systems

MFI-UF Method Development and Application

Mohanad Abunada

Prediction of Particulate Fouling in Reverse Osmosis Systems:
MFI-UF Method Development and Application

Mohanad Abunada

Prediction of Particulate Fouling in Reverse Osmosis Systems:
MFI-UF Method Development and Application

DISSERTATION

for the purpose of obtaining the degree of doctor
at Delft University of Technology
by the authority of the Rector Magnificus prof.dr.ir. T.H.J.J. van der Hagen,
chair of the Board for Doctorates
and
in fulfilment of the requirement of the Rector of IHE Delft
Institute for Water Education, Prof.dr. E.J. Moors,
to be defended in public on
Wednesday, 18 October 2023 at 12:30 hours

by

Mohanad ABUNADA
Master of Science in Urban Water Engineering and Management,
IHE Delft Institute for Water Education
born in Benghazi, Libya

This dissertation has been approved by the (co)promotors.

Composition of the doctoral committee:

Rector Magnificus TU Delft	chairperson
Rector IHE Delft	vice-chairperson
Prof.dr. M. D. Kennedy	IHE Delft / TU Delft, promotor
Dr. N. Dhakal	IHE Delft, copromotor

Independent members:

Dr. A.M.M. Al-hadidi	FUJIFILM Europe B.V.
Prof.dr.ir. J.A.M.H. Hofman	University of Bath, UK
Prof.dr.ir. L.C. Rietveld	TU Delft
Prof.dr.ir. W.G.J. van der Meer	University of Twente
Prof.dr. M.E. McClain	IHE Delft / TU Delft, reserve member

This research was conducted under the auspices of the Graduate School for Socio-Economic and Natural Sciences of the Environment (SENSE)

© 2023, Mohanad Abunada

Although all care is taken to ensure integrity and the quality of this publication and the information herein, no responsibility is assumed by the publishers, the author nor IHE Delft for any damage to the property or persons as a result of operation or use of this publication and/or the information contained herein.

A pdf version of this work will be made available as Open Access via <https://ihedelftrepository.contentdm.oclc.org/> This version is licensed under the Creative Commons Attribution-Non Commercial 4.0 International License, <http://creativecommons.org/licenses/by-nc/4.0/>

Published by IHE Delft Institute for Water Education

www.un-ihe.org

ISBN 978-90-73445-55-0

To my late parents...

ACKNOWLEDGEMENTS

I would like to express my thanks and appreciation to all persons who guided and supported me during my PhD journey.

First of all, I would like to express my sincere gratitude to my promotor Prof. Maria D. Kennedy for her supervision, guidance and assistance during my PhD study as well as for her kind support on the personal level. My thanks to my supervisors Prof. Noreddine Ghaffour and Dr. Nirajan Dhakal for their support and valuable inputs during my research. Thanks also to Dr. Sergio Salinas for his supervision and support in the first year of my PhD. I would like also to thank Prof. Jan C. Schippers for his voluntary support and for his valuable advices and critical discussions during my PhD progress which strongly helped me to identify the research problems and solutions in a deeper way as well as through a broad picture.

I would like to thank ‘Netherlands Fellowship Programme’ (currently ‘Orange Knowledge Programme’) – Nuffic for funding my PhD at IHE-Delft. Thanks to European Union’s Horizon 2020 Research and Innovation Programme and the Department of Biotechnology - Government of India for co-funding part of my PhD research. Thanks also to Lamminga Foundation - TU Delft for covering the costs of presenting my PhD research in international conferences. Thanks to Jolanda Boots from IHE-Delft who facilitated the reception of these funds.

Thanks to PWN and Evides water treatment companies in the Netherlands for their cooperation and facilitation of my field work by giving access to collect samples and operation data from their RO plants. Thanks to Herman Smit and Emmanuelle from PWN, and David Moed and Vincent Toussaint from Evides, for providing all kind support during the field work.

Thanks to the Rectorate and Graduate school at IHE-Delft for following up my PhD progress and facilitating my PhD graduation. Thanks to the Rector Prof. Eddy Moors, Prof. Michael McClain, Dr. Schalk Jan van Anandel, Anique Karsten and Floor Felix. Thanks also for the Management Officers of our department; Bianca Wassenaar and Selvi Pransiska for facilitating the progress meetings and the other agenda.

Thanks to the IHE-Delft laboratory staff for the support during my laboratory work as well as for the discussion on research related topics. Thanks to Fred Kruis, Ferdi Battes, Berend Lolkema, Peter Heerings, Frank Wiegman, Lyzette Robbemont and Zina Al Saffar.

Many thanks to the MSc students with whom I worked during my PhD research, namely Yuke Li, Pamela Ajok, Raffay Gulrez and William Z. Andyar. I wish you all success in your career and further education.

My thanks to all my friends and colleagues at IHE-Delft for the support and unforgettable moments. Special thanks go to my friends: Ahmad Mahmoud, Nasir Mangal, Mohaned Sousi and Motasem Abushaban for their endless and valuable support and nice memories during my PhD research especially in the beginning of the laboratory work. Many thanks also to my other friends who joined me in the PhD journey: Ahmad Ghandour, Omar Abdeldayem, Nazanin Moradi, Yuli Ekowati, Hesham Elmilady, Taha Al Washali, Musaed Aklan, Mary Barrios Hernandez, Shahnoor Hasan and Fiona Zakaria (R.I.P). Thanks to the MSA family at IHE-Delft for the nice gatherings and celebrations. Thanks as well for my other Palestinian friends and their families for the nice gatherings. Thanks to Mohammad Aljerjawi, Alaaeddin Swidan, Alaa Ouda, Almohanad Abusultan, Mamoun Althuluth, Karam Abu Shammala, Yousef Albuhaishi and Abdulqader Mahmoud.

Many thanks to my colleagues at Invest International for all supporting and motivating words.

Finally and most importantly, I would like to express my thanks and appreciation to my own family. I am infinitely grateful to my late parents for all endless support, love and care and for everything they did for me. All words are not enough to express my thanks to them. Many thanks to my brothers Loai, Ahmad and Mohammad for all support, prayers and wishes. Thanks also to all my family relatives who have been always sharing their greetings and wishes. Finally, my big thanks to the fruit of my life, to my sweetheart lovely daughter Wajd for her love and patience and for making my life more colourful and worth living.

SUMMARY

The application of reverse osmosis (RO) membranes in water treatment has rapidly grown over the last few decades thanks to the continuous advancements in both design and operation. However, RO membrane fouling still remains a key challenge. Fouling can cause a decline in membrane permeability, which requires higher operational energy and more frequent membrane cleaning/replacement to maintain stable water production, which eventually results in increased O&M costs. Particulate fouling, due to the deposition of particles and colloids onto RO membranes, is one of the types of fouling persistently experienced in RO systems. Therefore, there is a real need for a reliable method to predict particulate fouling in order to effectively monitor and control the performance of RO systems.

The ASTM methods, i.e. Silt Density Index (SDI) and Modified Fouling Index (MFI), are commonly used to assess the particulate fouling. However, many research articles have demonstrated the limitations of these methods. One of the main drawbacks is that both SDI and MFI simulate particulate fouling of RO using a 0.45 μm membrane, and thus neither method assesses the effect of small colloids ($< 0.45 \mu\text{m}$) which are more likely to be responsible for RO membrane fouling. Consequently, a more promising method; the Modified Fouling Index – Ultrafiltration (MFI-UF) was developed, whereby a UF membrane is used in order to capture and assess smaller colloids. Moreover, the MFI-UF method was developed further to operate at constant flux filtration to closely simulate RO systems which mostly operate at constant flux as well.

The main objective of this PhD research was to further develop and apply the MFI-UF method (constant flux) to verify its accuracy, reproducibility and applicability to predict particulate fouling in RO systems. Subsequently, a complete protocol for the MFI-UF method was proposed. The PhD thesis is structured in six chapters, with Chapter 1 providing a general introduction and Chapter 6 summarizing the main conclusions and future perspectives of this research.

Chapter 2 investigates the calibration and validation of the MFI-UF method to measure particulate fouling in RO. Firstly, MFI-UF calibration was examined using solutions of standard particles of dextran (150 kDa) and polystyrene (25 nm). Two main criteria were investigated: (i) the linearity of the MFI-UF with particle concentration at both the low and high range of fouling potential and (ii) the reproducibility of the MFI-UF linearity. Dextran solutions showed good linearity over the entire range of measured MFI-UF. However, linearity was not reproducible, and variable results were produced with different batches of dextran prepared under the same conditions. This was attributed to the structure of the dextran polymers which could be sensitive to slight variations in the chemical and/or physical conditions during the preparation of dextran solutions, resulting in different sizes of dextran particles and consequently different MFI-UF values. For

polystyrene solutions, the MFI-UF was linear over particle concentration. However, MFI-UF values in the lower range (i.e. $\text{MFI-UF} < 5,000 \text{ s/L}^2$) appeared slightly underestimated. In addition, the slopes of the calibration lines obtained for polystyrene solutions were similar for a wide range of flux rates ($50\text{-}200 \text{ L/m}^2\cdot\text{h}$). This was attributed to the fact that polystyrene particles in a filter cake may be difficult to rearrange or compress even when the flux increases since they are monodisperse and rigid in nature. As a result, the porosities of filter cakes formed from polystyrene particles (and thus the measured MFI-UF values) were similar at different flux rates. This result suggests that a monodisperse polystyrene particle solution may not be suitable for MFI-UF calibration since it cannot detect the effect of pump errors (if any) on the flux rate. Therefore, the study recommended to select and test a heterogeneous mixture of polystyrene particles (with different particle sizes and shapes) to overcome the limitations of monodisperse polystyrene particles. Secondly, the MFI-UF was validated using natural (surface) water under a wide range of testing conditions (at a flux of 20, 100 and $200 \text{ L/m}^2\cdot\text{h}$ using 5, 10 and 100 kDa membranes). Strong MFI-UF linearity was obtained over the entire range of measured MFI-UF. Thus, the MFI-UF method was validated to measure different levels of particulate fouling in RO. In addition, this result confirmed the robustness of the MFI-UF method to detect variations in particulate fouling potential due to a change in the quality of RO feed water.

Chapter 3 investigates the effect of surface porosity of UF membranes used to measure MFI-UF. For this purpose, a new approach was developed to quantify the effect of surface porosity of 5, 10, 50 and 100 kDa membranes using suspensions of pre-washed polystyrene particles (75 nm). Polystyrene particles were washed by stirred filtration (using an Amicon cell), to remove any surfactant material and particle fractions smaller than the pores of 5-100 kDa UF membranes. This was a prerequisite to ensure that the polystyrene particles retaining on 5-100 kDa membranes during the MFI-UF tests are equivalent in load and properties (i.e. same cake properties and thus same specific cake resistance on all membranes). Consequently, any difference in the measured MFI-UF can be attributed to the surface porosity of the membrane independently of the membrane pore size. MFI-UF measurements were combined with high-resolution SEM analysis to characterize the surface porosity of the 5-100 kDa membranes. The results showed that the lower the membrane MWCO, the lower the membrane surface porosity, and the more non-uniformly the pores are distributed over the membrane surface. This could result in cake formation being limited to the porous regions of the membrane surface, and consequently lead to smaller effective membrane filtration area, and thus higher local fluxes. Eventually, an overestimated MFI-UF (and overestimated particulate fouling prediction) would be obtained. Accordingly, correction factors of 0.4-1.0 were proposed for the MFI-UF measured with UF membranes in the range of 5-100 kDa, respectively.

Chapter 4 deals with the application of the MFI-UF method to predict particulate fouling rates in two full-scale RO plants. The MFI-UF was measured using 5, 10 and 100 kDa membranes at same flux applied in the RO plants ($20\text{-}26 \text{ L/m}^2\cdot\text{h}$). The particle disposition

factor (Ω) was calculated to simulate particle deposition in RO cross-flow filtration, and subsequently the particulate fouling rates in RO plants were predicted using the MFI-UF fouling prediction model. Other types of fouling (i.e. scaling, organic and biological fouling) were also evaluated based on threshold reference values. However, in all cases it was concluded that particulate fouling was likely to be the most dominant fouling in the two RO plants studied. For the first RO plant, the results showed that the fouling rates predicted based on the MFI-UF measured with the 100 kDa membrane had the best agreement with the actual fouling observed in the RO plant (with 3-11% deviation). For the second RO plant, the particulate fouling rate predicted based on the 10 kDa membrane agreed the best with the fouling observed in the plant (with only 2% deviation). Nevertheless, the fouling rate predicted based on the 100 kDa membrane showed also a good agreement with the observed fouling rate (with 15% deviation). However, the fouling rates predicted based on the MFI-UF measured with the 5 kDa membrane were apparently overestimated for both RO plants. The reason was attributed to the correction factor used to correct the effect of surface porosity of MF-UF membranes, which was still overestimated in the case of 5 kDa membrane. Accordingly, the results could indicate that 10-100 kDa is mostly the suitable range of MWCO of MFI-UF membranes for predicting particulate fouling in RO plants.

Chapter 5 introduces a complete testing protocol for the MFI-UF method, based on the result of the MFI-UF development and application investigated in the previous chapters of this study (Chapter 2-4). The protocol describes the MFI-UF testing procedures required to ensure the accuracy and reproducibility of MFI-UF measurements. It addresses all details related to the MFI-UF set-up, membranes, operating conditions and calculation. For MFI-UF calculation, a new numerical algorithm was successfully developed based on regression modelling which calculates the MFI-UF value automatically upon the completion of the MFI-UF test. The introduced protocol focuses on MFI-UF measurement at constant flux in the range of 20-200 L/m².h using flat-sheet polyethersulfone (PES) UF membranes with MWCO of 5-100 kDa.

Overall, the development and application of the MFI-UF method including the testing protocol addressed in this study provide a reliable tool to accurately measure particulate fouling and predict its rate in RO systems, which can support engineers, operators and researchers to design, operate and monitor RO systems more effectively. Additional research is recommended to select and test heterogenous standard particles for MFI-UF calibration to overcome the aforesaid limitations obtained with the dextran and monodisperse polystyrene particles. Moreover, further research is required to quantify the effect of surface porosity of MFI-UF membrane using different types of particles which exhibit similar properties to particles that exist in real water. Future research should also focus on applying the MFI-UF method to predict particulate fouling rates in more RO plants treating different types of water and operating under different conditions. In addition, further work is needed to develop an automated MFI-UF system which can be connected online in RO plants to predict and report particulate fouling rate in real time.

SAMENVATTING

Het toepassen van omgekeerde osmose (reverse osmosis (RO)) membranen in de behandeling van water is de afgelopen decennia snel gegroeid dankzij voortdurende vorderingen in zowel ontwerp als uitvoering. Desondanks presenteert vervuiling van RO-membranen nog steeds een belangrijke uitdaging. Vervuiling kan een afname van de membraanpermeabiliteit veroorzaken, wat een hogere operationele energie vereist en meer frequente schoonmaak/vervanging van membranen om een stabiele waterproductie te waarborgen, wat uiteindelijk resulteert in verhoogde kosten. Vervuiling door de afzetting van deeltjes en colloïden op de RO-membranen is één van de soorten vervuiling die aanhoudend ervaren worden in RO-systemen. Daarom is er sprake van een serieuze behoefte aan een betrouwbare methode om de vervuiling van deeltjes te voorspellen ten behoeve van het effectief monitoren en controleren van de prestatie van RO-systemen.

De ASTM-methoden, d.w.z. Silt Density Index (SDI) en Modified Fouling Index (MFI), worden vaak gebruikt voor het beoordelen van vervuiling door deeltjes. Veel onderzoeksartikelen hebben echter de beperkingen van deze methoden aangetoond. Eén van de belangrijkste nadelen is dat zowel SDI als MFI de vervuiling van RO simuleren met behulp van een 0.45 µm membraan, waardoor geen van de methoden de invloed van kleine colloïden (< 0.45 µm) beoordeelt, welke een grotere kans hebben om verantwoordelijk te zijn voor RO-membraanvervuiling. Als gevolg daarvan werd er een veelbelovender methode ontwikkeld; de Modified Fouling Index – Ultrafiltration (MFI-UF), waarbij een UF-membraan gebruikt wordt voor het vangen en beoordelen van kleinere colloïden. Bovendien is de MFI-UF methode verder ontwikkeld om te opereren bij constante fluxfiltratie om ook RO-systemen die voornamelijk bij constante flux opereren nauwkeurig te simuleren.

Het belangrijkste doel van dit onderzoek was om de MFI-UF methode (constante flux) verder te ontwikkelen en toe te passen om de nauwkeurigheid, reproduceerbaarheid, en toepasbaarheid om vervuiling door deeltjes in RO-systemen te voorspellen ervan te verifiëren. Nadien was een compleet protocol voor de MFI-UF methode voorgesteld. Het proefschrift is opgebouwd uit zes hoofdstukken, waarvan Hoofdstuk 1 een algemene introductie geeft en Hoofdstuk 6 de belangrijkste conclusies en toekomstperspectieven van dit onderzoek samenvat.

Hoofdstuk 2 onderzoekt de kalibratie en validatie van de MFI-UF methode om vervuiling door deeltjes in RO te meten. Allereerst werd de kalibratie van de MFI-UF methode getoetst met behulp van oplossingen van standaard deeltjes dextraan (150 kDa) en polystyreen (25 nm). Twee hoofdcriteria werden onderzocht: (i) de lineariteit van de MFI-UF methode met deeltjesconcentratie bij zowel laag als hoog bereik van

vervuilingspotentieel en (ii) de reproduceerbaarheid van de lineariteit van de MFI-UF methode. Dextraanoplossingen lieten een goede lineariteit zien over het volledige bereik van gemeten MFI-UF. Dit was echter niet reproduceerbaar en variabele resultaten werden verkregen voor verschillende partijen dextraan, bereid onder gelijke omstandigheden. Dit werd toegewezen aan de structuur van de dextraanpolymeren die gevoelig kan zijn voor lichte variaties in de chemische en/of fysieke omstandigheden tijdens de bereiding van dextraanoplossingen wat resulteert in verschillende grootten van dextraandeeltjes en, als gevolg daarvan, verschillende MFI-UF waarden. Voor polystyreen oplossingen was de MFI-UF lineair over de deeltjesconcentratie. De MFI-UF waarden in het lagere bereik (d.w.z. $MFI-UF < 5,000 \text{ s/L}^2$) leken echter enigszins onderschat. Daarnaast waren de hellingen van de voor polystyreen oplossingen verkregen kalibratielijnen vergelijkbaar voor een groot bereik van fluxsnelheid (50-200 L/m².h). Dit werd toegewezen aan het feit dat, zelfs als de flux toeneemt, het lastig kan zijn om polystyreendeeltjes in een filterkoek te herschikken of samen te drukken, aangezien deze van nature monodispers en rigide zijn. Als gevolg hiervan was de porositeit van filterkoeken gevormd uit polystyreendeeltjes (en dus de gemeten MFI-UF-waarden) vergelijkbaar bij verschillende fluxsnelheden. Dit resultaat suggereert dat het kan zijn dat een oplossing van monodisperse polystyreendeeltjes niet geschikt is voor MFI-UF kalibratie, aangezien het niet de effecten van pompfouten op de fluxsnelheid (als deze voorkomen) kan detecteren. Daarom adviseerde de studie om een heterogene mix van polystyreendeeltjes (met verschillende deeltjesgrootten en vormen) te selecteren en testen om de beperkingen van monodisperse polystyreendeeltjes te overwinnen. Ten tweede was de MFI-UF methode gevalideerd door middel van het gebruik van natuurlijk (oppervlakte)water onder een groot bereik van testomstandigheden (bij een flux van 20, 100 en 200 L/m².h. gebruikmakende van 5, 10 en 100 kDa membranen). Sterke MFI-UF lineariteit was verkregen over het volledige bereik van gemeten MFI-UF. De MFI-UF methode was dus gevalideerd om verschillende niveaus van vervuiling door deeltjes in RO te meten. Bovendien bevestigde dit resultaat de robuustheid van de MFI-UF methode om variaties in vervuiling door deeltjes veroorzaakt door veranderingen in de kwaliteit van RO-voedingswater te detecteren.

Hoofdstuk 3 onderzoekt het effect van de porositeit van het oppervlak van UF-membranen die gebruikt worden om MFI-UF te meten. Voor dit doeleinde werd een nieuwe aanpak ontwikkeld om het effect van de porositeit van het oppervlak van 5, 10, 50 en 100 kDa membranen te kwantificeren met behulp van suspensies van voorgewassen polystyreendeeltjes (75 nm). Polystyreendeeltjes werden gewassen door geroerde filtratie (met behulp van een Amicon-cel) om al het oppervlakte-actieve materiaal en deeltjesfracties kleiner dan de poriën van 5-100 kDa UF-membranen te verwijderen. Dit was een voorwaarde ervoor te zorgen dat de polystyreendeeltjes die tijdens de MFI-UF-tests op membranen van 5-100 kDa worden vastgehouden, gelijkwaardig zijn wat betreft belasting en eigenschappen (d.w.z. dezelfde koekeigenschappen en dus dezelfde specifieke koekweerstand op alle membranen). Vervolgens kan elk verschil in de gemeten

MFI-UF worden toegeschreven aan de oppervlakteporositeit van het membraan, onafhankelijk van de poriëgrootte van het membraan. MFI-UF metingen werden gecombineerd met hoge resolutie SEM analyse om de porositeit van het oppervlak van de 5-100 kDa membranen te karakteriseren. De resultaten lieten zien dat hoe lager de membraan MWCO was, des te lager de porositeit het membraanoppervlak was en des te ongelijkmatiger de poriën verdeeld waren over het membraanoppervlak. Dit zou kunnen resulteren in koekformatie die beperkt blijft tot de poreuze gebieden van het membraanoppervlak, en vervolgens leidt tot een kleiner effectief membraanfiltratieoppervlak en, dus hogere fluxen. Uiteindelijk zou een overschatte MFI-UF (en een overschatte voorspelling van vervuiling door deeltjes) worden verkregen. Overeenkomstig werden correctiefactoren van 0.4-1.0 voorgesteld voor de gemeten MFI-UF met UF-membranen in het bereik van respectievelijk 5-100 kDa.

Hoofdstuk 4 behandelt de toepassing van de MFI-UF methode om de vervuilingssnelheid door deeltjes in twee grootschalige RO-installaties te voorspellen. De MFI-UF werd gemeten met behulp van 5, 10 en 100 kDa membranen bij dezelfde flux die werd toegepast in de RO-installaties (20-26 L/m².h). De deeltjesdispositiefactor (Ω) werd berekend om de deeltjesafzetting bij RO-dwarsstroomfiltratie te simuleren, en vervolgens werd de vervuiling door deeltjes in RO-installaties voorspeld met behulp van het MFI-UF-vervuilingsvoorspellingsmodel. Andere soorten vervuiling (d.w.z. scaling, organische en biologische vervuiling) werden ook geëvalueerd op basis van drempelreferentiewaarden. Desalniettemin, werd in alle gevallen geconcludeerd dat vervuiling door deeltjes waarschijnlijk de meest dominante vervuiling was in de bestudeerde RO-installaties. Voor de eerste RO-installatie, toonden de resultaten aan dat de voorspelde vervuilingswaarden op basis van de MFI-UF, gemeten met het 100 kDa-membraan, de beste overeenkomst hadden met de werkelijke vervuiling waargenomen in de RO-installatie (met een afwijking van 3-11%). Voor de tweede RO-installatie kwam de voorspelde vervuiling door deeltjes op basis van het 10 kDa-membraan het meest overeen met de vervuiling die in de installatie werd waargenomen (met een afwijking van slechts 2%). Toch liet de vervuilingssnelheid op basis van het 100 kDa membraan ook een goede overeenkomst zien met de vervuilingssnelheid die werd waargenomen (met een afwijking van 15%). De voorspelde vervuilingssnelheden op basis van de MFI-UF gemeten met het 5 kDa-membraan bleken echter overschat voor beide RO-installaties. De oorzaak hiervan werd toegeschreven aan de correctiefactor die werd gebruikt om de effecten op oppervlakteporositeit van de MF-UF membranen te corrigeren, welke still overschat werd in het geval van het 5 kDa membraan. Overeenkomstig zouden de resultaten erop kunnen wijzen dat het bereik van 10-100 kDa het meest passend is voor MWCO van MFI-UF membranen voor het voorspellen van vervuiling door deeltjes in RO-installaties.

Hoofdstuk 5 introduceert een volledig testprotocol voor de MFI-UF methode op basis van het resultaat van de MFI-UF ontwikkeling en toepassing die is onderzocht in de voorgaande hoofdstukken van dit onderzoek (Hoofdstuk 2-4). Het protocol beschrijft de

MFI-UF testprocedures die vereist zijn om de nauwkeurigheid en reproduceerbaarheid van de MFI-UF metingen te waarborgen. Het behandelt alle details met betrekking tot de MFI-UF-opstelling, membranen, bedrijfsomstandigheden en berekening. Voor de MFI-UF berekening werd met succes een nieuw numeriek algoritme ontwikkeld op basis van regressiemodellering welke de MFI-UF waarde automatisch berekend na voltooiing van de MFI-UF test. Het geïntroduceerde protocol richt zich op MFI-UF-metingen bij constante flux in het bereik van 20-200 L/m².h met behulp van vlakke polyethersulfon (PES) UF-membranen met een MWCO van 5-100 kDa.

Over het geheel genomen bieden de ontwikkeling en toepassing van de MFI-UF-methode, inclusief het testprotocol dat in deze studie wordt behandeld, een betrouwbaar hulpmiddel om vervuiling door deeltjes nauwkeurig te meten en de snelheid ervan in RO-systemen te voorspellen. Dit kan ingenieurs, operators en onderzoekers ondersteunen bij het ontwerpen, bedienen en het effectiever monitoren van RO-systemen. Aanvullend onderzoek wordt aanbevolen om heterogene standaarddeeltjes te selecteren en te testen voor MFI-UF-kalibratie om de bovengenoemde beperkingen die zijn verkregen met de dextraan- en monodisperse polystyreendeeltjes te overwinnen. Bovendien is verder onderzoek nodig om het effect van de oppervlakteporositeit van het MFI-UF-membraan te kwantificeren met behulp van verschillende soorten deeltjes die vergelijkbare eigenschappen vertonen als deeltjes die in echt water voorkomen. Toekomstig onderzoek zou zich ook moeten richten op de toepassing van de MFI-UF-methode om de mate van vervuiling door deeltjes te voorspellen in meer RO-installaties die verschillende soorten water behandelen en onder verschillende omstandigheden werken. Daarnaast is er verder werk nodig om een geautomatiseerd MFI-UF-systeem te ontwikkelen dat online kan worden aangesloten in RO-installaties om de mate van vervuiling door deeltjes direct te voorspellen en te rapporteren.

CONTENTS

Acknowledgements	vii
Summary	ix
Samenvatting.....	xiii
Contents.....	xvii
1 Introduction.....	1
1.1 Background	2
1.2 Particulate fouling	5
1.2.1 Particles	5
1.2.2 Fouling mechanisms	6
1.3 Particulate fouling prediction methods –brief review.....	6
1.3.1 Silt density index	7
1.3.2 Modified fouling index	10
1.3.3 Modified fouling index – ultrafiltration.....	11
1.3.4 Cross-flow sampler modified fouling index	13
1.3.5 Modified fouling index – nanofiltration	15
1.3.6 Combined/multiple modified fouling indices.....	15
1.3.7 Feed fouling monitor	15
1.3.8 Flow field-flow fractionation	16
1.3.9 Differential mobility analyser.....	16
1.3.10 Artificial intelligence	17
1.4 Problem statement.....	18
1.5 Research objectives.....	19
1.6 Thesis outline	20
1.7 Annexes	21
Annex 1.7.1: Summary of particulate fouling assessment methods	21
2 Calibrating and validating the MFI-UF method to measure particulate fouling in Reverse Osmosis	25
2.1 Introduction.....	26
2.2 Theoretical background	27
2.3 Materials and methods	29
2.3.1 MFI-UF set-up.....	29
2.3.2 MFI-UF membranes	30
2.3.3 MFI-UF calibration using standard particle solutions.....	30

2.3.4	MFI-UF validation using natural water	31
2.4	Results and discussion	32
2.4.1	MFI-UF calibration using standard solutions	32
2.4.2	MFI-UF validation using natural water (canal water)	36
2.5	Conclusions.....	38
3	Quantifying the effect of the surface porosity of MFI-UF membrane.....	41
3.1	Introduction.....	42
3.2	Theoretical background	45
3.3	Materials and Methods.....	47
3.3.1	MFI-UF measurement	47
3.3.2	MFI-UF membranes	47
3.3.3	Characterization of MFI-UF membrane surface	48
3.3.4	Theoretical demonstration of membrane surface porosity effect during the MFI-UF testing	48
3.3.5	Approach to quantify the effect of membrane surface porosity on the measured MFI-UF.....	49
3.3.6	Identification of membrane holder support effect on the membrane surface porosity	55
3.3.7	Applying the MFI-UF to predict particulate fouling in a full-scale RO plant – with and without a correction for the surface porosity of the MFI-UF membrane	56
3.4	Results and discussion	56
3.4.1	Membrane surface characterization – SEM analysis.....	56
3.4.2	Theoretical effect of membrane surface porosity during the MFI-UF testing	59
3.4.3	Quantifying the effect of membrane surface porosity on the measured MFI-UF	60
3.4.4	Correcting the effect of membrane surface porosity on the measured MFI-UF	62
3.4.5	Effect of membrane holder support on membrane surface porosity	63
3.4.6	Effect of membrane surface porosity on the prediction of particulate fouling in a full-scale RO plant	64
3.5	Conclusions.....	66
3.6	Annexes	68
Annex 3.6.1:	Particle technical sheet.....	68
Annex 3.6.2:	Preliminary investigations of polystyrene particle washing	74
4	Prediction of Particulate Fouling in Full-Scale Reverse Osmosis Plants Using the MFI-UF Method	79
4.1	Introduction.....	80

4.2	Theoretical background	82
4.2.1	MFI-UF fouling prediction model.....	84
4.3	Materials and methods	84
4.3.1	Full-scale RO plants and sample collection	85
4.3.2	MFI-UF measurement	88
4.3.3	Prediction of particulate fouling rates in RO plants	89
4.3.4	Identification of actual fouling observed in RO plants.....	89
4.3.5	Comparison between predicted and observed fouling rates in RO plants	91
4.4	Results and discussion	91
4.4.1	MFI-UF of RO feed and RO concentrate	91
4.4.2	Actual fouling observed in the RO plants	94
4.4.3	Comparison between predicted and observed fouling rates in RO plants	96
4.5	Conclusions.....	99
4.6	Annexes	102
	Annex 4.6.1: Supplementary data.....	102
5	Protocol for the MFI-UF at Constant Flux to Measure Particulate Fouling in Reverse Osmosis	105
5.1	Introduction.....	106
5.1.1	MFI-UF theoretical background.....	107
5.2	MFI-UF set-up	109
5.2.1	Set-up assembly	109
5.2.2	Set-up quality control	111
5.3	Membrane	114
5.3.1	Membrane selection.....	114
5.3.2	Membrane cleaning	115
5.3.3	Membrane resistance	117
5.3.4	Effect of membrane surface porosity.....	119
5.3.5	Membrane plane direction	119
5.4	MFI-UF testing conditions.....	120
5.4.1	Feed water temperature	120
5.4.2	Flux rate.....	121
5.4.3	Test duration	122
5.5	MFI-UF calculation	125
5.6	Step-by-step MFI-UF testing procedure	127
5.7	Conclusions.....	133
5.8	Annexes	135
	Annex 5.8.1: Cake creep during the filtration of feed water consisting of inert particles.....	135

Annex 5.8.2: Correction of water temperature variation during MFI-UF test	138
Annex 5.8.3: Example of manual MFI-UF calculation	140
Annex 5.8.4: MFI-UF calculation algorithm	142
6 Conclusions and future perspectives	163
6.1. Conclusions.....	164
6.1.1 Calibration and validation of the MFI-UF method.....	164
6.1.2 Effect of surface porosity of the MFI-UF membrane.....	165
6.1.3 Application of the MFI-UF method to predict particulate fouling in RO systems	165
6.1.4 MFI-UF testing protocol.....	166
6.2 Future perspectives	168
References.....	171
List of acronyms	181
List of Tables.....	183
List of Figures	184
About the author.....	187

1

INTRODUCTION

1.1 BACKGROUND

Freshwater represents one of the most essential elements for human life. Despite that water covers about 71% of the Earth's surface, less than 1% of the available water is accessible freshwater. The use of freshwater has been increasing worldwide over the past decades due to the continuous population growth, socio-economic development and consumption patterns change. According to the report of UNESCO (2020), global water use is expected to continue in growth by about 1% per year until 2050, which accounts for around 30% increase above current water consumption levels. The increase in water use, combined with the impact of climate change, has led to the deterioration of available sources of freshwater and converted many parts over the world into water-scarce regions. Currently, more than 50% of world's population experiences severe water scarcity for at least one month per year, while this percentage is predicted to rise in the coming years (UNESCO, 2020).

Among the different options to mitigate water scarcity (such as water conservation, water reuse, rainwater harvesting and others), water desalination has been considered as a promised alternative (March, 2015). This is basically because around 40% of world population are living in coastal areas (United Nations, 2017). Since the beginning of the 21st century, the growth of water desalination has rapidly increased (Figure 1.1) as a result of the technological improvements and the subsequent significant cost reduction. By 2020, water desalination capacity comprised about 110 million m³/day of the global water supplies (DesalData, 2020). It even now represents the major national share of water supply in many countries, such as the Arabian Gulf countries which have very limited freshwater resources. Kuwait, for instance, relies 100% on water desalination to supply freshwater for domestic and industrial use (Sawe, 2017).

There are several techniques to desalinate water, and they can be classified mainly into; (i) membrane-based desalination processes such as reverse osmosis (RO), nanofiltration (NF) and electrodialysis (ED), and (ii) thermal desalination (or distillation) such as multi-stage flash (MSF), multi-effect distillation (MED) and vapour compression (VC). At present, RO desalination is the dominant technique with around 70% of the total current global desalination capacity, as shown in Figure 1.2 (DesalData, 2020). This is basically attributed to the RO technology advances entailing the simplicity of design and operation, reduction in energy consumption and compactness of the plant footprint, which all made water production cost lower in comparison with other desalination techniques (Ahmed et al., 2020). Currently, the unit cost of water produced by new RO desalination plants could fall down to around 0.5 US\$/m³ and it is estimated to reach 0.3 US\$/m³ within 20 years (World Bank, 2019).

The use of RO technology has not been limited only to seawater and brackish water desalination, but it has also been extended to surface water (such as rivers and lakes) and

wastewater treatment, due to the high effectiveness of RO membranes to remove a wide variety of impurities (Figure 1.3).

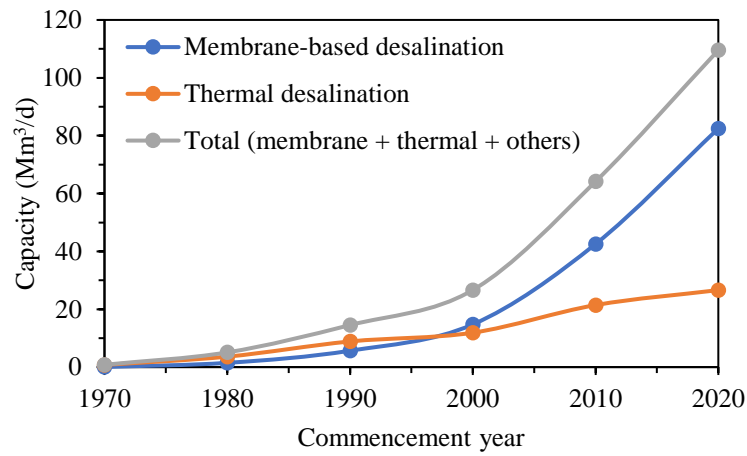


Figure 1.1: Global desalination capacity increase between 1970 and 2020 (DesalData, 2020)

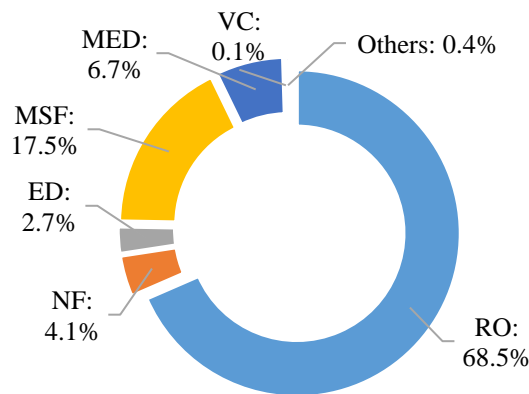


Figure 1.2: Global market share of the different desalination technologies (DesalData, 2020)

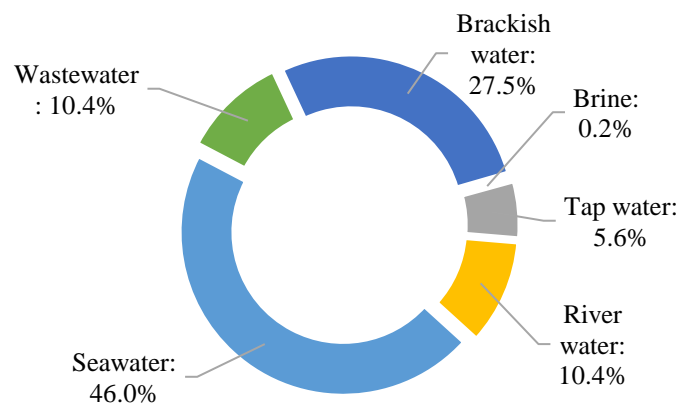


Figure 1.3: Global RO capacity with regards to the water source (DesalData, 2020)

However, membrane fouling is still a major issue affecting the efficiency and sustainability of RO applications. Membrane fouling can cause a decline in membrane permeability which results in increased energy and chemical consumption and frequent membrane cleaning/replacement, which leads eventually to an increase in the total production cost. In addition, the greenhouse gas emissions from the increased energy consumption as well as the disposal of chemical residuals and replaced RO modules can still have negative impacts on the environment (Khoo et al., 2021).

Membrane fouling occurs due to the accumulation of constituents (foulants) in the feed water on the membrane, which consequently hinders water transport through the membrane and reduces its permeability. It is dominated by a combination of various physicochemical factors, including: (i) foulant characteristics (composition, size, charge and concentration), (ii) feed water chemistry (pH and ionic strength), (iii) membrane properties (surface roughness, charge and hydrophobicity), and (iv) operation conditions (flux rate, cross-flow velocity and water temperature) (Li and Elimelech, 2004; Tang et al., 2011). The foulants accumulated on the membrane can be reversible in which case they can be physically removed by flushing the membrane surface, or irreversible and thus require (extensive) chemical cleaning for their removal (Guo et al., 2012).

Membrane fouling can be classified into four main forms, depending on the type of the foulants and the mechanism of interaction with the membrane (Salinas-Rodríguez et al., 2021):

1. Particulate/colloidal fouling: particles deposit onto membrane and accumulate on its surface in cake/gel layer,
2. Organic fouling: organic compounds attach to the membrane by adsorption,
3. Biofouling: microorganisms adhere and grow on the membrane and form biofilms, and
4. Scaling: inorganic dissolved compounds precipitate on the membrane surface as a result of exceeding their solubility.

Another phenomenon is the concentration polarization (CP) which occurs when the salts rejected by the RO membrane accumulate gradually near its surface, whereby the salt concentration exceeds the concentration in the bulk solution. CP does not only restrict the permeation flow (due to the elevated osmotic pressure), but also leads to increased salt passage through the membrane (Barger and Carnahan, 1991). The influence of CP can be even more severe in the presence of a cake layer on membrane surface. In this case, the cake can hinder the back diffusion of rejected salts and significantly enhance the CP, resulting in so-called 'cake enhanced concentration polarization' (Hoek and Elimelech, 2003).

Assessment of fouling potential is very important in order to determine the approach to be applied to control it and prevent/mitigate its effect, such as: identifying the cleaning

frequency of RO membranes, optimizing the operation conditions of the RO system, improving/upgrading the pre-treatment of RO feed (Goh et al., 2018).

This research focuses on particulate/colloidal fouling as a one of the most persistent problems experienced in RO systems. Particularly, the research aims at developing an assessment method that can accurately predict the particulate fouling in RO systems. Accordingly, the following sections focus further on particulate fouling.

1.2 PARTICULATE FOULING

Particulate fouling is mainly caused by the particles which are not removed by the pre-treatment processes and eventually retain and accumulate on the membrane surface. The type and nature of the particles and the mechanisms how they foul the membrane are addressed in section 1.2.1 and 1.2.2.

1.2.1 Particles

Particles causing membrane fouling are generally referred to the suspended solids (>1000 nm) and colloids (1-1000 nm). Particles can be classified based on their composition into three main types: (i) inorganic particles such as clays, silts, and oxides/hydroxides of silica, iron, aluminium and manganese, (ii) organic particles of high molecular weight such as polysaccharides, proteins, extracellular polymer substances (EPS) and transparent exopolymer particles (TEP), and (iii) biological particles which comprise microorganisms such as algae and bacteria (as long as not growing in biofilms) (Gregory, 2006; Au et al., 2011; Salinas-Rodriguez, 2011).

Another common particle classification includes two distinct groups; hydrophilic and hydrophobic. Hydrophilic particles are basically water-soluble macromolecules, such as much of natural organic matter (NOM). On the other hand, hydrophobic particles are insoluble and dispersed in water, like inorganic materials such as clay and oxides. The most important difference between the two groups is that the hydrophilic particles are thermodynamically stable and can remain indefinitely in solution (if no chemical or biological change occurs). Conversely, the hydrophobic particles may irreversibly aggregate with time. However, the distinction between the hydrophilic and hydrophobic particles is often fuzzy because, for instance, organic matter may adsorb on inorganic particles, and therefore the latter may acquire in this case some hydrophilic characteristics (Gregory, 2005).

In terms of the electrical charge, particles have mostly a negative charge. This knowledge led the membrane manufacturers to produce membranes with negative charge to repel the particles in the feed water passing the membrane and reduce their fouling potential.

Nevertheless, this electrostatic repulsion can be influenced by the pH and ionic strength of feed water (Belfort et al., 1994).

1.2.2 Fouling mechanisms

Particulate fouling can generally occur in four main mechanisms, as shown in Figure 1.4; (i) complete blocking (Figure 1.4 (a)): each depositing particle block a pore completely without overlaying other particles, (ii) standard blocking (Figure 1.4 (b)): pores are constricted by the attachment of deposited particles into pore walls, (iii) intermediate blocking (Figure 1.4 (c)): particles may block pores and start to overlay with other particles on membrane surface, and (iv) cake/gel formation (Figure 1.4 (d)): particles deposit and accumulate over each other forming such a cake/gel layer on membrane surface taking over the role of water transport through the membrane (Yang et al., 2022). Cake/gel may be further clogged and compressed due to the additional load of depositing particles, where compressed cake/gel filtration becomes the dominant fouling mechanism (Boerlage et al., 2003b). For microfiltration (MF) membranes, particulate fouling can be described typically by pore blocking mechanism. Whereas, for RO, NF and tight ultrafiltration (UF) membranes, cake/gel filtration is considered the dominant particulate fouling mechanism (Zhu and Elimelech, 1997).

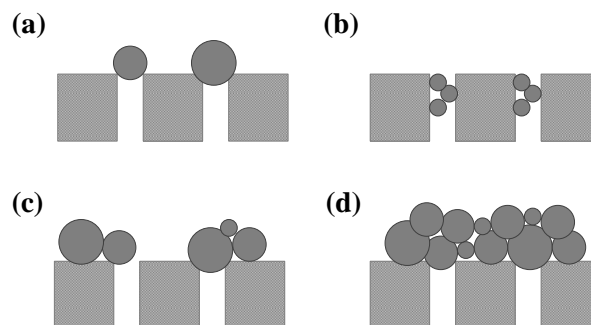


Figure 1.4: Mechanisms of particulate fouling: (a) complete blocking, (b) standard blocking, (c) intermediate blocking, and (d) cake/gel formation (Yang et al., 2022)

1.3 PARTICULATE FOULING PREDICTION METHODS –BRIEF REVIEW

Prediction of particulate fouling potential is very important to optimize the performance of RO systems at both the design stage as well as during operation. Traditional water quality monitoring measures, such as turbidity, particle counts and suspended solids are commonly used to indicate the particle concentration in feed water. However, these measures cannot indicate the resistance resulting from the deposition of particles on RO membrane, and thus they are unsuitable to predict particulate fouling. For this reason, several alternative methods have been developed and introduced in the scientific literature.

Currently, the ASTM standard indices; the silt density index (SDI) and modified fouling index (MFI-0.45) are the most common methods applied to measure the particulate fouling potential of RO feed water (ASTM, 2014; ASTM, 2015). However, both indices have deficiencies limiting their reliability (illustrated in section 1.3.1 and 1.3.2). Consequently, a lot of researches have been carried out to further develop the SDI and MFI-0.45 methods in order to predict the particulate fouling potential more accurately. In addition, other researches have also focused on developing new methods independently of the SDI and MFI-0.45. The following sections (1.3.1-1.3.10) review the state of the art of the particulate fouling assessment methods, including their theoretical principle and the key pros and cons (summarized in Annex 1.7.1).

1.3.1 Silt density index

The silt density index (SDI) is the most widely applied method worldwide to measure the particulate fouling potential of RO feed water (Alhadidi et al., 2012). It is an empirical test developed initially by DuPont Co., and then has been introduced as a standard method in the ASTM (code: D4189) (ASTM, 2014). The test basically measures the rate at which a MF membrane is fouled. This is done by filtering the feed water through a 0.45 µm membrane in dead-end mode at a constant pressure of 207 kPa, using the set-up schemed in Figure 1.5 (ASTM, 2014).

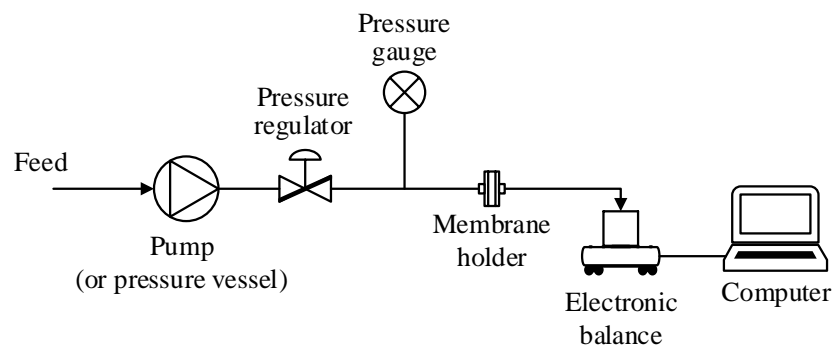


Figure 1.5: Scheme of SDI set-up (adapted from ASTM (2014))

During the test, the filtered volume is recorded over time, and then the SDI value can be calculated by Equation (1.1) (ASTM, 2014).

$$SDI_T = \frac{\%P}{T} = \frac{\left(1 - \frac{t_i}{t_f}\right) \times 100}{T} \quad (1.1)$$

Where t_i is the time required to collect the initial filtered water volume, and t_f is the time required to collect the same water volume after time $T = 15$ min from the start of the test. The volume collected during both times is 500 mL, which is based on a 47 mm diameter

membrane. If the membrane diameter is different, then the filtered volume can be adjusted proportionally to the membrane surface area. $\%P$ is the membrane plugging ratio, and it should not exceed 75%. If P is $> 75\%$, then t_f should be re-measured based on a shorter T of 10 or 5 min. Accordingly, based on Equation (1.1), the range of SDI values is listed in Table 1.1. The guideline of most of the RO membrane manufacturers is to maintain SDI_{15min} at ≤ 5 for the RO feed, while an SDI_{15min} value of < 3 is recommended to minimize the particulate fouling potential (DOW, 2011; Hydranautics, 2016).

Table 1.1: Range of SDI values

Total elapsed time (T)	SDI (%/min)	
	Full range	At $\%P = 75\%$ (maximum accepted value)
5 min	0 – 20	15
10 min	0 – 10	7.5
15 min	0 – 6.7	5

Despite that the SDI method is a standard method and has been applied for many years, however, it has several deficiencies which limit its reliability. The key deficiency is that it is not based on any fouling mechanism, and hence it cannot be used to simulate and predict the development of particulate fouling in RO (Schippers and Verdouw, 1980). Therefore, the SDI value cannot reflect the degree of membrane fouling, whereby serious fouling may possibly occur even when the SDI value is low (Yiantsios et al., 2005). Moreover, the SDI has no linear correlation with the concentration of particles in the feed water, and it is mathematically limited to a maximum value (Table 1.1). This means that a maximum SDI value can always be obtained once the particles in the feed water exceed a certain concentration. In addition, the method does not simulate the real operation in RO since it is performed at constant pressure in dead-end mode, while RO systems operate in practice at constant flux at cross-flow filtration. Besides, it does not evaluate the effect of particles/colloids smaller than 0.45 μm , which are most likely responsible for the fouling of RO membranes (Schippers et al., 1985). Another major deficiency is the lack of standardization of the testing conditions, namely; water temperature, transmembrane pressure and membrane resistance. It is known that in case of any variation in these parameters, then the feed flow and thus the load of particles brought to the SDI membrane during the test will vary as well. As a result, different plugging rates and thus different SDI values can be obtained for same feed water (Alhadidi et al., 2011c). Consequently, to overcome the aforementioned deficiencies, new SDI-based methods were developed as alternatives, such as the normalized SDI and volume-based SDI (addressed below in section 1.3.1.1 and 1.3.1.2).

1.3.1.1 Normalized SDI

Alhadidi et al. (2011b) proposed to normalize the SDI to the testing conditions, namely; water temperature (20 °C), transmembrane pressure (207 kPa) and membrane resistance ($1.29 \times 10^{10} \text{ m}^{-1}$), to improve the accuracy of the SDI. The normalized SDI (referred to as SDI⁺) was derived based on the mathematical relationship between the SDI and the modified fouling index (section 1.3.2), assuming that (i) the cake/gel filtration mechanism is the only fouling mechanism that occurs during the SDI test, and (ii) the variation in particle retention during the test is negligible. However, the SDI is based on a mixture of both pore blocking and cake/gel filtration, such that pore blocking is the dominant mechanism in the beginning of the test. Furthermore, the particles smaller than 0.45 µm can pass initially through the SDI membrane but may be later retained onto it due to pore plugging/narrowing, and hence particle retention can vary during the test. This means that the assumptions applied to develop the SDI⁺ are not fully covering the reality, despite the fact that it could improve the accuracy of SDI (Alhadidi et al., 2011b). In addition, the SDI⁺ could not overcome the other deficiencies of the standard SDI; i.e. it is based on no fouling mechanism, it has no correlation with particle concentration, it is operated at constant pressure at dead-end filtration unlike the RO operation in practice, it doesn't consider the effect of small colloids (< 0.45 µm), and it cannot be used to predict the rate of particulate fouling in RO.

1.3.1.2 Volume-based SDI

Volume-based SDI (SDI_v) was developed by Alhadidi et al. (2011c) as an alternative to the standard SDI to eliminate the effect of testing conditions (i.e. water temperature, transmembrane pressure and membrane resistance). The new test is performed by following the same procedure of the standard SDI, but the second water volume is collected after a fixed filtered volume (V) instead of a fixed filtration time (T). Hence, in this case, the fouling load during the test (i.e. the amount of particles depositing on the SDI membrane) will be the same at any testing condition because the filtered volume is fixed, unlike the case in the standard SDI where the fouling load can be different during the test as the filtered volume may change due to the testing conditions variation (as illustrated in section 1.3.1). The experimental and mathematical outputs confirmed that the SDI_v is independent of the testing conditions. In addition, the SDI_v showed a better linear correlation with particles concentration compared with the standard SDI, particularly when complete blocking is the dominant fouling mechanism during the test. However, as the standard SDI, the SDI_v is performed at constant pressure at dead-end filtration unlike the operation of RO systems in practice, it doesn't evaluate the effect of small colloids (< 0.45 µm), and it cannot be used to predict the rate of particulate fouling in RO.

1.3.2 Modified fouling index

The modified fouling index (MFI or MFI-0.45) was developed by Schippers and Verdouw (1980). In 2015, ASTM adopted the MFI-0.45 (code: D8002) as an alternative method to the SDI to measure the particulate fouling potential of RO feed water (ASTM, 2015). In contrast with the SDI, the MFI-0.45 is based on cake/gel filtration which is the dominant particulate fouling mechanism in RO membranes (Zhu and Elimelech, 1997). In addition, the MFI-0.45 is corrected to reference testing conditions (i.e. water temperature and transmembrane pressure), and a linear correlation exists between the MFI value and the particle concentration (Schippers and Verdouw, 1980).

The MFI-0.45 test can be performed using the same set-up as the SDI test (Figure 1.5), where the feed water is filtered through a 0.45 μm membrane in dead-end mode at a constant pressure of 2 bar. Subsequently, the relationship between the reciprocal flow and filtered volume is plotted. The output plot (Figure 1.6) represents basically the fouling rate of MFI-0.45 membrane which typically takes place in three subsequent phases (i) pore blocking, (ii) cake/gel formation, and (iii) cake/gel compression and/or cake/gel pores narrowing. The MFI is then determined based on the cake/gel filtration phase.

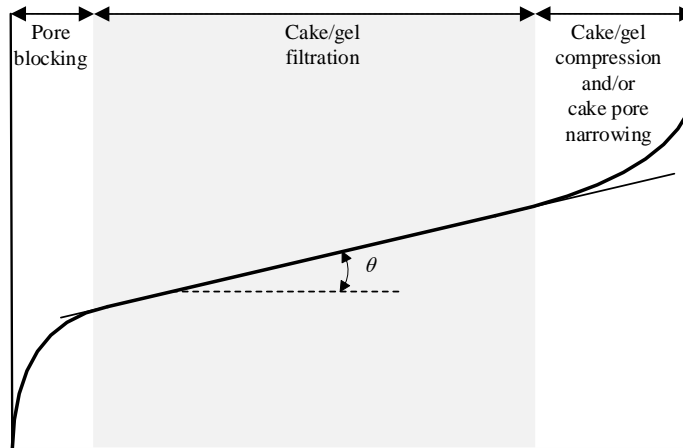


Figure 1.6: Typical filtration curve at constant pressure (t/V vs V) and at constant flux (ΔP vs t) (Boerlage et al., 1998; Boerlage et al., 2004)

At constant pressure, the cake/gel filtration can be described by the linear formula shown in Equation (1.2) (Schippers and Verdouw, 1980).

$$\frac{t}{V} = \frac{\eta \cdot R_m}{\Delta P \cdot A} + \frac{\eta \cdot I}{2\Delta P \cdot A^2} \cdot V \quad (1.2)$$

Where t is the filtration time, V is the filtered volume, R_m is the clean membrane resistance, A is the membrane surface area, ΔP is the transmembrane pressure, and η is the feed water viscosity. The parameter I is the fouling index which describes the fouling

potential of feed water. It is the product of the specific cake resistance (α) and particles concentration in feed water (C) as shown in Equation (1.3) (Boerlage et al., 1998).

$$I = \alpha \cdot C \quad (1.3)$$

The value of I can be calculated based on the slope of cake/gel filtration phase demonstrated during the MFI-0.45 test, as shown in Equation (1.4).

$$I = \frac{2\Delta P \cdot A^2}{\eta} \cdot \tan \theta \quad (1.4)$$

By definition, the MFI is the fouling index (I) corrected to the reference testing conditions, namely; (i) membrane surface area ($A_o = 13.8 \times 10^{-4} \text{ m}^2$), (ii) transmembrane pressure ($\Delta P_o = 2 \text{ bar}$) and (iii) water viscosity ($\eta_{20^\circ\text{C}} = 1 \times 10^{-6} \text{ kPa}\cdot\text{s}$), as shown in Equation (1.5) (Schippers and Verdouw, 1980). The values of these reference conditions were basically defined so that the reporting of MFI value becomes convenient and corresponds to the SDI value. For instance, the MFI of 1 s/L^2 is equivalent more or less to an SDI value of 1 (Salinas-Rodriguez, 2011).

$$MFI = \frac{\eta_{20^\circ\text{C}} \cdot I}{2\Delta P_o \cdot A_o^2} \quad (1.5)$$

The measured MFI value could be used as an input in a mathematical model to predict the rate of the flux decline in RO due to the particulate fouling (Schippers et al., 1981). However, it was found that the predicted rate is too far low to explain the actual fouling of RO membranes observed in reality. The reason was attributed to the pore size of the MFI-0.45 membrane which cannot retain smaller particles ($< 0.45 \text{ um}$) present in RO feed water. Accordingly, to improve the accuracy of fouling prediction, Schippers et al. (1985) suggested to perform the MFI test with a tighter membrane with a pore size of 0.05 um (referred to as MFI-0.05). Nevertheless, it was found that the particles smaller than 0.05 um , which are not retained by the membrane, are most likely responsible for the fouling of RO membranes (Schippers et al., 1985).

1.3.3 Modified fouling index – ultrafiltration

The modified fouling index – ultrafiltration (MFI-UF) method was developed by Boerlage et al. (1997), where a UF membrane is used in the place of a 0.45 um MFI membrane in order to capture the small particles and measure their effect on the RO membrane fouling. The characterisation, verification and application of the MFI-UF were then further investigated in subsequent studies (Boerlage et al., 1998; Boerlage et al., 2000; Boerlage et al., 2002b; Boerlage et al., 2003a; Boerlage et al., 2003b). Initially, the

test was performed at constant pressure using the same set-up and procedure as the MFI-0.45 test. Different hollow fibre UF membranes with various molecular weight cut-off (MWCO) and materials were examined. Eventually, polyacrylonitrile (PAN) membrane with MWCO of 13 kDa was recommended as a reference. The outputs of MFI-UF and MFI-0.45 were compared using different types of feed water (Boerlage et al., 2000; Boerlage et al., 2003a). It was found that the MFI-UF is 400-1900 higher than the MFI-0.45 value, which confirmed the advantage of MFI-UF to incorporate the effect of the small colloids which are not retained during the MFI-0.45 test.

As mentioned above, the MFI-UF test was performed initially at constant pressure, which is unlike RO membrane systems which are usually operated in constant flux mode. It was found that the flux rate observed during the MFI-UF test is (initially) around 10-1000 times higher than that applied in the RO (Boerlage et al., 2004). As a result, the cake formed on the MFI-UF membrane could be highly compressed in comparison to that formed on RO membranes. Accordingly, to simulate more closely the particulate fouling behaviour in RO membranes, the MFI-UF was developed further by Boerlage et al. (2004) to operate at constant flux filtration. One more advantage is the test duration which was found markedly shorter at constant flux compared with the case at constant pressure. Later, Salinas-Rodríguez et al. (2015) investigated and developed the MFI-UF at constant flux using flat sheet membranes with MWCO of 10-100 kDa.

The MFI-UF test at constant flux can be performed using the set-up shown in the scheme in Figure 1.7. The feed water is filtered at constant flux (J) through a UF membrane placed in a dead-end filter holder, and simultaneously the pressure increases due to the membrane fouling and is recorded and plotted over time. The shape of the resulting plot is typically similar to that demonstrated during the MFI-0.45 test (Figure 1.6).

At constant flux filtration, cake/gel filtration phase is described as shown in Equation (1.6) (Boerlage et al., 2004).

$$\Delta P = J \cdot \eta \cdot R_m + J^2 \cdot \eta \cdot I \cdot t \quad (1.6)$$

Accordingly, the fouling index (I) is calculated from the slope of cake/gel filtration phase as shown in Equation (1.7), and then the MFI-UF value is obtained based on I and the reference testing conditions using the same MFI-0.4 equation (Equation (1.5)). Hence, the MFI-UF measured at constant flux can be compared with the MFI-0.45, as both indices would have same measuring unit (s/L^2).

$$I = \frac{1}{J^2 \cdot \eta} \cdot \tan \theta \quad (1.7)$$

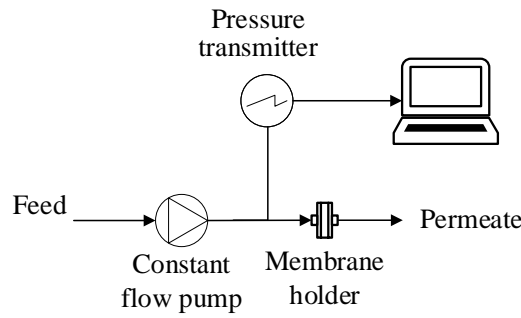


Figure 1.7: Scheme of MFI-UF set-up at constant flux filtration

1.3.3.1. MFI-UF (constant flux) fouling prediction model

The MFI-UF value measured at constant flux can be incorporated in the model shown in Equation (1.8) to predict the particulate fouling rate of RO membranes, which is described by the increase in net driving pressure (ΔNDP) over time (Schippers et al., 1981). The model was derived based on the assumption that the NDP increase is attributed only to the cake/gel formation on RO membranes excluding the effect of scaling and biofouling.

$$\frac{\Delta NDP}{t} = \frac{2\Delta P_o \cdot A_o^2 \cdot \eta \cdot J^2 \cdot \Omega \cdot MFI-UF}{\eta_{20^\circ C}} \quad (1.8)$$

The particle deposition factor (Ω) in the model is a correction factor to simulate particle deposition in RO filtration. This is because RO systems operate at cross-flow filtration and not in dead-end mode as the case in the MFI-UF test. As a result, not all the particles in the feed water that is filtered through RO membranes actually deposit on the membrane surface, where some fraction of the particles is back-transported to the concentrate due to tangential flow. Therefore, the particle deposition factor represents that portion of particles in the feed water which are filtered through the RO membrane, and actually deposit and remain on the membrane surface. The factor can be determined, using Equation (1.9), based on the MFI-UF of RO feed, MFI-UF of RO concentrate and the RO recovery rate (R). Ideally, the Ω value may vary between 0 and 1; where $\Omega = 0$ indicates no particle deposition, and $\Omega = 1$ indicates that all particles in the feed water portion passing the RO membrane deposited onto the membrane (Salinas-Rodríguez et al., 2015).

$$\Omega = \frac{1}{R} + \frac{MFI-UF_{concentrate}}{MFI-UF_{feed}} \cdot \left(1 - \frac{1}{R}\right) \quad (1.9)$$

1.3.4 Cross-flow sampler modified fouling index

Sim et al. (2010) developed the cross-flow sampler modified fouling index (CFS-MFI-UF) as an extension of the MFI-UF to account for the RO cross-flow hydrodynamic

conditions; where a cross-flow sampler (CFS) is connected prior to the MFI-UF set-up at constant flux mode. The CFS includes a cross-flow cell fractionating the particles in the feed water under the same hydrodynamic conditions applied in the actual RO filtration. For this purpose, a non-retentive membrane with relatively large straight-through pores was used ($\geq 5 \mu\text{m}$), so that all particles moving near the membrane surface are captured and permeate through. Hence, the permeate collected from the CFS thereby could contain all the potential particles which would likely deposit on the RO membrane. Subsequently, the particulate fouling potential of the collected CFS permeate is measured by the MFI-UF.

Several experiments were conducted to compare the outputs of the CFS-MFI-UF with the MFI-UF, using different types of feed water (Sim et al., 2010). In all results, the MFI-UF was higher than the CFS-MFI-UF value, with a difference of 10-40%. This was basically because during the MFI-UF test, all the particles in feed water transfer toward the MFI-UF membrane. On the other hand, in the case of CFS-MFI-UF, only the particles which permeated through the CFS transfer to the MFI-UF membrane. However, the influence of CFS was found minor (i.e. negligible particles fractionation) when the feed water contained narrow particle size, where almost no difference was found between the outputs of both methods. Moreover, the CFS-MFI-UF method was found more sensitive than the MFI-UF in detecting changes in fouling potential due to the variation of feed water quality.

Fouling rate predicted by CFS-MFI-UF was also validated with actual RO fouling profile, where only about 11% deviation was found. However, the predicted fouling rate was underestimated when the salt concentration in feed water increased. This was attributed to the contribution of cake-enhanced osmotic pressure (CEOP), which was not considered in the CFS-MFI-UF measurement. Accordingly, Sim et al. (2011b) improved the prediction of the CFS-MFI-UF by incorporating the effect of CEOP. The preliminary results showed that the fouling prediction incorporating the effect of CEOP matches well with the actual RO fouling. Nevertheless, the prediction was only validated with synthetic water (silica suspension). This means that the particle characteristics required to estimate the CEOP (e.g. particle size, density and concentration) were known, unlike the case of RO feed water in practice where particle characteristics vary a lot and are difficult to quantify.

Despite the innovation of the CFS-MFI-UF method in simulating real RO operation conditions, it has a major drawback. The method doesn't consider the possible detachment of particles deposited on the RO membrane. This is because all the particles transferred to the CFS membrane can pass through. However, in RO cross-flow filtration, particle deposition is not static as deposited particles can be re-suspended and move away as a result of hydrodynamic shear forces and the impaction of other flowing particles (Henry et al., 2012). Therefore, the concept of the particle deposition factor incorporated in the MFI-UF method may have an advantage over the CFS approach, as it reflects not

only the deposition but also the detachment of particles from RO membranes by taking into account the relation between particle concentration in the RO feed and concentrate (Equation (1.9)). Another deficiency in the CFS-MFI-UF method is the relative complexity of the test set-up and procedure, which may also lead to increased probability of measurement errors and thus affect the accuracy of CFS-MFI-UF outputs.

1.3.5 Modified fouling index – nanofiltration

Khirani et al. (2006) proposed the modified fouling index – nanofiltration (MFI-NF) method, by replacing the 0.45 μm membrane used in the MFI-0.45 test with a NF membrane to capture very small colloids. Later, Ju and Hong (2014) developed the MFI-NF further by applying the method at the same pressure as is applied in RO systems in order to simulate the characteristics of cakes formed on RO membrane. The new method is referred to as the cake resistance simulator – modified fouling index nanofiltration (MFI-NF-CRS). However, the MFI-NF methods are problematic from the theoretical point of view. This is because the NF membrane can reject ions (Schäfer et al., 1998), and thus the measured MFI can be highly affected by the build-up of osmotic pressure (and concentration polarization) during the test. On the other hand, the MFI concept is based on cake/gel filtration only and doesn't account for the additional resistance caused by the osmotic pressure (Schippers and Verdouw, 1980). In addition, the proposed MFI-NF methods were performed at constant pressure, in contrary to the RO systems which mostly operate at constant flux filtration.

1.3.6 Combined/multiple modified fouling indices

Choi et al. (2009) developed the combined fouling index (CFI) which incorporates several MFI measurements. In this method, three MFI tests are performed in parallel; using hydrophilic MF, hydrophobic MF and hydrophilic UF membranes to distinct the fouling potential due to particles, hydrophobic organics and colloids, respectively. The resulted MFI values are then combined together in one value (CFI) using a developed mathematical model. Yu et al. (2010) and Ju et al. (2015) employed another multiple MFI system. They used MF, UF and NF (or tight UF) membranes in series to separate the particles, colloids and organics, respectively, where the MFI was measured during each separation. However, the resulting MFI values were presented schematically, and not quantified in one value as the case of CFI. Although the new combined/multiple MFI methods were claimed as more informative in explaining the fouling potential, they are considered complicated and time consuming, and hence difficult to apply in the practice.

1.3.7 Feed fouling monitor

Taheri et al. (2013) predicted particulate fouling in RO by incorporating the effect of CEOP. For this purpose, a feed fouling monitor (FFM) was used in combination with an

ultrasonic time domain reflectometry (UTDR). The FFM includes a cross-flow cell operating at the same hydrodynamic conditions as the RO. The cell includes a UF membrane to measure the fouling potential due to the particulate matter existed in the feed. The UTDR function is to measure the thickness of the cake developed on the RO membrane, which is required to estimate the CEOP. The information obtained by both monitors (i.e. FFM and UTDR) are then combined in a developed mathematical model to predict the rate fouling due to both the cake and CEOP.

Several experiments were carried out, where the fouling rates predicted based on FFM and UTDR showed a good match with the actual fouling observed in RO. However, the feed samples used in these experiments included synthetic water (suspensions of silica colloids mixed with NaCl). Therefore, the information of particle characteristics (e.g. particle size, density, and concentration) required to estimate the CEOP were known. However, this information is difficult to measure for real RO feed water in practice. Besides, the set-up and testing procedures are considered complicated and relatively time consuming, which can limit the application of the method in the practice.

1.3.8 Flow field-flow fractionation

Several studies focused on estimating particulate fouling by using the flow field-flow fractionation (FI-FFF) analysis (Wright et al., 2001; Hartmann and Williams, 2002; Moon and Cho, 2005; Pellegrino et al., 2005; Hong et al., 2009; Kim et al., 2009). FI-FFF is an analytical technique developed by Giddings et al. (1976) to separate and characterize particles in feed water based on their size. In this technique, a feed water sample flows along a channel containing a membrane sheet, while a cross-flow stream is induced at right angles to the feed flow. Consequently, particles retained by the membrane are fractionated and positioned as a result of the balance between the applied cross-flow field and back diffusion of particles. Particles are then transported to the outlet of the flow channel and detected with a UV detector. Finally, the particle retention time distribution can be described by a fractogram, which can be employed to assess (qualitatively and quantitatively) the fouling potential of feed water. The main advantage of FI-FFF technique is the simulation of hydrodynamic conditions in RO cross-flow filtration (i.e. permeation flux and cross-flow velocity). However, the FI-FFF is not based on any fouling mechanism, and therefore, it cannot be used to predict the rate of fouling.

1.3.9 Differential mobility analyser

Park et al. (2013) determined the particulate fouling potential by measuring the concentration of particles using a differential mobility analyser (DMA), which was developed in previous works (Park et al., 2009a; Park et al., 2009b). In this technique, feed water is aerosolized by an atomizer into liquid droplets. The droplets are dried through diffusion driers, and thus the particles exited in the droplets become suspended

in the air. The particles are then introduced into the DMA, which separates the particles in terms of size based on their electrical mobility. Subsequently, the number of particles in each size range are counted by a condensation particle counter located downstream of the DMA. Finally, the fouling potential of feed water can be measured by integrating the particle size distribution (referred to as ‘number concentration’ of particles). However, in addition to its complexity, this technique cannot simulate membrane fouling in RO as it doesn’t involve any membrane fouling mechanism.

1.3.10 Artificial intelligence

Artificial intelligence (AI) has been used by several researchers to predict membrane fouling. Various AI techniques have been successfully employed, such as artificial neural networks, fuzzy logic and genetic algorithm. The artificial neural networks (ANN) is the most widely used technique due its principle flexibility, simplicity and accuracy (Niu et al., 2022).

Several RO performance parameters were used as outputs in the ANN modelling to indicate and predict the fouling of RO membranes (in real-time). In most of ANN models, permeate flux/flow and slat passage were used as target outputs, while other parameters such as feed flow rate, pressure, temperature and conductivity were used as inputs to feed the model (Niemi et al., 1995; Al-Shayji and Liu, 2002; Jafar and Zilouchian, 2002; Abbas and Al-Bastaki, 2005; Lee et al., 2009; Libotean et al., 2009; Khayet et al., 2011; Moradi et al., 2013; Barello et al., 2014; Aish et al., 2015; Salgado-Reyna et al., 2015).

Despite the significant advances and accurate results achieved in the prediction of RO membrane fouling using ANN technique, there are still several issues. ANN models may have poor reproducibility due to the random weight and bias factors used in the ANN model (weight and bias are important parameters used in machine learning models such as ANN). Besides, the accuracy of ANN models depends highly on the availability of a large set of data for model training and validation. However, this data may not be large enough for some (new) RO systems and thus the model may fail to predict the membrane fouling accurately (Niu et al., 2022). Moreover, most of the ANN models used RO operational parameters such as feed flow rate, pressure and temperature as inputs to the model to predict membrane fouling. However, membrane fouling depends strongly on foulant characteristics (i.e. type, size, charge and concertation), which may even vary over time (Tang et al., 2011). Nevertheless, these factors were not considered in the ANN models reviewed above. Finally, prediction of membrane fouling using ANN technique (and other AI modes) cannot provide deep insight into the type (i.e. reason) of fouling, which makes it difficult to determine the actions to be taken to prevent/mitigate the fouling impact.

1.4 PROBLEM STATEMENT

Particulate fouling is one of the problems experienced in RO plants. The availability of a reliable method to accurately assess and monitor the particulate fouling potential and predict its development rate is very important in order to effectively control the RO system. The MFI-UF method operating at constant flux and incorporating the concept of a particle deposition factor is considered a promising method that can closely simulate particulate fouling in RO plants (as addressed in section 1.3 and summarized in Annex 1.7.1). Nevertheless, further research is required to verify the accuracy, reproducibility and applicability of the MFI-UF method, as addressed in the following points.

1. MFI-UF calibration and validation

Measured MFI-UF values are highly dependent on the accuracy and reproducibility of the measurement set-up. However, the instruments that make up the MFI-UF measurement set-up, specifically the pump and pressure transmitter, may drift over time due to malfunction, over-loading and environmental conditions, which may eventually result in errors in the outputs of these instruments. The instrument errors may even be exacerbated by other factors such as (invisible) water leakage from the set-up and existence of air bubbles (Salinas-Rodríguez et al., 2015). Consequently, these errors may lead to an inaccurate MFI-UF value, and subsequently result in an inaccurate particulate fouling prediction.

To ensure the accuracy and consistency of MFI-UF measurements, the MF-UF method should be calibrated. MFI-UF calibration can be demonstrated by verifying a reproducible linear relationship between the MFI-UF value and particle concentration of a standard (reference) solution under certain testing conditions. This was verified for the MFI-0.45 method using a standard solution of Formazine particles (Schippers and Verdouw, 1980; ASTM, 2015). However, until now, no standard solution has been proposed and tested for the calibration of the MFI-UF method.

Moreover, in practice, the MFI-UF is measured for natural water (e.g. RO feed water) which usually includes a wide range of particles with different properties than those of particles existing in standard solutions. Therefore, the linear relationship between the MFI-UF and particle concentration should not be only verified with standard solutions but also with natural water, to simulate more closely the case in real RO systems.

2. MFI-UF membrane surface porosity

In addition to the MFI-UF set-up, MFI-UF also depends strongly on the MWCO of the MFI-UF membrane used in the test. The lower the membrane MWCO, the smaller the membrane pore size, and thus the more the particles which can be captured by the MFI-UF membrane, which eventually results in a higher measured MFI-UF value (Salinas-Rodríguez et al., 2015). Furthermore, Boerlage et al. (2002b) indicated that the lower the

membrane MWCO, the lower the surface porosity and the more non-uniformly the pores are distributed over membrane surface. This could result in smaller effective membrane filtration area, and subsequently higher local flux which might lead to an overestimated MFI-UF value. The effect of membrane surface porosity on measured particulate fouling was also suggested in other several studies (Ethier and Kamm, 1989; Fane et al., 1991; Güell and Davis, 1996; Chandler and Zydney, 2006). However, no method was proposed to quantify the effect of membrane surface porosity, which still needs to be investigated.

3. MFI-UF application in full-scale RO plants

The application of the MFI-UF to predict the particulate fouling in full-scale RO plants is still very limited. In addition, the particulate fouling rates predicted based on MFI-UF have been never compared with the actual fouling observed in reality, and hence, the accuracy of fouling prediction has remained questionable. Therefore, it is important to apply the MFI-UF to predict the particulate fouling in full-scale RO plants and compare the predicted fouling with the actual fouling rates observed in the plants.

4. MFI-UF test protocol

Finally, unlike the ASTM MFI-0.45, there is no a (standard) protocol which can be followed to perform the MFI-UF test at constant flux, which may affect the accuracy and reproducibility of MFI-UF measurement. Therefore, it is important to introduce a complete testing protocol including the description of MFI-UF set-up, membranes, testing conditions, calculations, and quality control procedures.

1.5 RESEARCH OBJECTIVES

The overall goal of this research is to provide a reliable method which can accurately assess particulate fouling and predict its development rate in RO plants. For this purpose, the research aims to further develop and apply the MFI-UF method at constant flux to verify and improve its accuracy, reproducibility and applicability. Accordingly, the following are the main research objectives.

- (1) To calibrate and validate the MFI-UF method using solutions of standard particles and natural water.
- (2) To Investigate and quantify the effect of surface porosity of the MFI-UF membrane on the measured MFI-UF value.
- (3) To apply the MFI-UF to predict the rate of particulate fouling in full-scale RO plants, and compare the predicted rates with the actual fouling observed in the plants.
- (4) To describe a complete protocol to perform the MFI-UF test at constant flux, describing the MFI-UF set-up, membranes, testing conditions, calculations and quality control procedures.

1.6 THESIS OUTLINE

This thesis is made-up of six chapters, described as follows.

- Chapter 1: Presents the introduction of this research, including general background on desalination, RO technology and membrane fouling. The chapter focuses specifically on the measurement and prediction of particulate fouling, which is the scope of this research. Finally, the chapter addresses the research justifications and objectives.
- Chapter 2: Describes the MFI-UF calibration and validation approach.
- Chapter 3: Investigates the effect of surface porosity of MFI-UF membranes on the measured MFI-UF values.
- Chapter 4: Addresses the application and verification of MFI-UF method to predict particulate fouling rates in full-scale RO plants.
- Chapter 5: Introduces a new protocol to perform the MFI-UF test accurately.
- Chapter 6: Provides a summary of the main conclusions and future perspectives.

1.7 ANNEXES

Annex 1.7.1: Summary of particulate fouling assessment methods

Table A1.1: Key advantages and disadvantages of particulate fouling assessment methods

Method	Main advantages	Main disadvantages	Reference
Silt density index (SDI)	<ul style="list-style-type: none">- Simple (can be used even by non-professionals).	<ul style="list-style-type: none">- Based on no fouling mechanism.- No linear correlation with particle concentration.- No correction for testing conditions.- Colloids smaller than 0.45 μm are not evaluated.- Performed at constant pressure.- Performed at dead-end filtration.- Cannot be used to predict the fouling rate in RO.	ASTM (2014)
Normalized SDI (SDI ⁺)	<ul style="list-style-type: none">- Simple- Corrected for reference testing conditions.	<ul style="list-style-type: none">- Based on no fouling mechanism.- No linear correlation with particles concentration.- Colloids smaller than 0.45 μm are not evaluated.- Performed at constant pressure.- Performed at dead-end filtration.- Cannot be used to predict the fouling rate in RO.	Alhadidi et al. (2011b); Alhadidi et al. (2011c); Alhadidi et al. (2012)

Volume-based SDI (SDI _v)	<ul style="list-style-type: none"> - Simple. - Independent on testing conditions. - Has better linear correlation with particles concentration compared with the standard SDI, particularly when the complete blocking is the dominant fouling mechanism. 	<ul style="list-style-type: none"> - Colloids smaller than 0.45 µm are not evaluated. - Performed at constant pressure. - Performed at dead-end filtration. - Cannot be used to predict the fouling rate in RO. 	Alhadidi et al. (2011c)
Modified fouling index (MFI-0.45)	<ul style="list-style-type: none"> - Based on cake/gel filtration mechanism. - Linearly correlated to particles concentration. - Corrected for reference testing conditions. - Can be used to predict the fouling rate in RO (i.e. flux decline rate). - Cross-flow hydrodynamic conditions can be simulated by particle deposition factor. 	<ul style="list-style-type: none"> - Colloids smaller than 0.45 µm are not evaluated. - Performed at constant pressure. 	Schippers and Verdouw (1980); ASTM (2015)
Modified fouling index - ultrafiltration (MFI-UF) at constant pressure	<ul style="list-style-type: none"> - Based on MFI concept (see MFI-0.45). - Can be used to predict the fouling rate in RO (i.e. flux decline rate). - Small colloids can be evaluated. - Cross-flow hydrodynamic conditions can be simulated by particle deposition factor. 	<ul style="list-style-type: none"> - Performed at constant pressure. 	Boerlage et al. (1997); Boerlage et al. (1998); Boerlage et al. (2000); Boerlage et al. (2002b); Boerlage et al. (2003a); Boerlage et al. (2003b)
Modified fouling index - ultrafiltration (MFI-UF) at constant flux	<ul style="list-style-type: none"> - Based on MFI concept (see MFI-0.45). - Small colloids can be evaluated. - Performed at constant flux. - Can be used to predict fouling rate in RO. - Cross-flow conditions can be simulated by particle deposition factor. 	<p>Has specific limitations which can affect its accuracy, addressed in details in the research justifications in section 1.3.10 (however, these limitations also exist in the other fouling prediction methods which are based on the MFI concept).</p>	Boerlage et al. (2004); Salinas-Rodríguez et al. (2015)

Cross-flow sampler modified fouling index ultrafiltration (CFS-MFI-UF)	<ul style="list-style-type: none"> - Based on MFI concept (see MFI-0.45). - Small colloids can be evaluated. - Performed at constant flux. - Can be used to predict fouling rate in RO. - Cross-flow conditions can be simulated by cross-flow sampler. - CEOP effect was incorporated (but only validated with synthetic water). 	<ul style="list-style-type: none"> - Cross-flow sampler does not consider particle detachment during RO cross-flow filtration, and thus the fouling prediction may be overestimated. - Relatively complicated. 	Sim et al. (2010); Sim et al. (2011a); Sim et al. (2011b)
Modified fouling index - nanofiltration (MFI-NF)	<ul style="list-style-type: none"> - Based on MFI concept (see MFI-0.45). - Very small (nano)colloids can be evaluated. - Can be used to predict the fouling rate in RO (i.e. flux decline rate). 	<ul style="list-style-type: none"> - Theoretically it might not valid as NF membranes can reject salts, while the effect of osmotic resulted by the rejected salts accumulation is not incorporated in the MFI concept. - Performed at constant pressure. 	Khirani et al. (2006); Ju and Hong (2014)
Combined/multiple modified fouling index	<ul style="list-style-type: none"> - Based on MFI concept (see MFI-0.45). - Predicts fouling potential due to different types of particles. 	<ul style="list-style-type: none"> - Complicated and time consuming. 	Choi et al. (2009); Yu et al. (2010); Ju et al. (2015)
Feed fouling monitor (FFM)	<ul style="list-style-type: none"> - Based on cake/gel filtration and CEOP (but only validated with synthetic water). - Small colloids can be evaluated. - Performed at cross-flow conditions. - Can be used to predict fouling rate in RO. 	<ul style="list-style-type: none"> - Complicated. 	Taheri et al. (2013)
Flow field-flow fractionation (FI-FFF)	<ul style="list-style-type: none"> - Performed at cross-flow conditions. - Characterizing the particles based on their size. 	<ul style="list-style-type: none"> - Based on no fouling mechanism. - Cannot be used to predict the fouling rate in RO. 	Wright et al. (2001); Hartmann and Williams (2002); Moon and Cho (2005); Pellegrino et al. (2005);

			Hong et al. (2009); Kim et al. (2009)
Differential mobility analyser (DMA)	<ul style="list-style-type: none"> - Characterizing the particles based on their size. 	<ul style="list-style-type: none"> - Very complicated. - Based on no fouling mechanism. - Cannot be used to predict the fouling rate in RO. 	Park et al. (2013)
Artificial intelligence (AI) – artificial neural networks (ANN)	<ul style="list-style-type: none"> - Intelligent method (i.e. self-learning capabilities) - Does not need experimental work. - Real-time fouling prediction. 	<ul style="list-style-type: none"> - May have poor reproducibility due to the random weight and bias factors used in the model. - Model accuracy depends highly on large set of data which may not be available for some (new) RO systems. - Foulant characteristics (i.e. type, size, charge and concertation) were not considered in the reviewed models. - May not distinguish between the types of fouling. 	Niemi et al. (1995); Al-Shayji and Liu (2002); Jafar and Zilouchian (2002); Abbas and Al-Bastaki (2005); Lee et al. (2009); Libotean et al. (2009); Khayet et al. (2011); Moradi et al. (2013); Barello et al. (2014); Aish et al. (2015); Salgado-Reyna et al. (2015)

2

CALIBRATING AND VALIDATING THE MFI-UF METHOD TO MEASURE PARTICULATE FOULING IN REVERSE OSMOSIS

This study aimed to calibrate and validate the MFI-UF method in order to ensure the accuracy of particulate fouling measurements in RO. Firstly, MFI-UF calibration was examined using two solutions of standard particles (dextran and polystyrene). Two main criteria were investigated; (i) MFI-UF linearity with particle concentration at both low and high range of fouling potential, and (ii) reproducibility of MFI-UF linearity. Dextran solutions showed a strong MFI-UF linearity over the entire range of measured MFI-UF. However, the linearity was not reproducible, and different batches of dextran prepared under the same conditions produced very variable results. For polystyrene solutions, the MFI-UF linearity was verified at the higher range of MFI-UF ($> 10,000 \text{ s/L}^2$), while the MFI-UF at the lower range ($< 5,000 \text{ s/L}^2$) appeared to be underestimated. Secondly, MFI-UF validation was investigated using natural (surface) water under a wide range of testing conditions (at 20, 50 and 200 $\text{L/m}^2\cdot\text{h}$ using 5, 10 and 100 kDa membranes). Strong MFI-UF linearity was obtained over the entire range of measured MFI-UF (up to $70,000 \text{ s/L}^2$). Thus, the MFI-UF method was validated to measure different levels of particulate fouling in RO. Future research focussing on MFI-UF calibration is still required by selecting, preparing and testing heterogenous mixtures of standard particles.

2.1 INTRODUCTION

The application of reverse osmosis (RO) membranes in water treatment has rapidly grown over the last few decades. Despite the continuous advances, membrane fouling is still a major problem challenging the performance of this technology. Particulate fouling due to deposition of particles and colloids onto the membrane is one of the fouling types experienced in RO systems. Membrane fouling can cause a decline in the membrane permeability, which requires higher operational pressure and more frequent membrane cleaning/replacement to maintain stable water production. Therefore, there is a real need for a reliable method to assess the particulate fouling potential of RO feed in order to effectively control the operation of the RO systems.

The ASTM standard methods, i.e. Silt Density Index (SDI) and Modified Fouling Index (MFI-0.45), are commonly used to assess the particulate fouling potential of RO feed (ASTM, 2014; ASTM, 2015). The MFI-0.45 has advantages over the SDI as (i) it is based on cake/gel filtration which is assumed to be the dominant fouling mechanism in RO, (ii) it is proportional to the particle concentration in feed water, and (iii) it can be corrected to reference testing conditions (Schippers and Verdouw, 1980). Nevertheless, the main drawback of the MFI-0.45 is the use of a membrane with a pore size of 0.45 μm to simulate fouling of RO membrane. Hence, the measured MFI is too low to explain the fouling rates in RO, since the small colloids ($< 0.45 \mu\text{m}$), which are likely the responsible for RO membrane fouling, are not considered (Schippers et al., 1985). For this reason, the MFI-UF method was developed, where the 0.45 μm membrane was replaced by an ultrafiltration (UF) membrane to capture and assess smaller colloids (Boerlage et al., 1997; Boerlage et al., 1998; Boerlage et al., 2002b; Boerlage et al., 2003b).

The MFI-UF test was initially performed at constant pressure. However, in practice most RO systems operate at a constant flux which is around 10-1000 times lower than the (initial) flux observed during an MFI-UF test performed at constant pressure. As a result, since high filtration fluxes can result in cake compression, it was observed that the cake formed on MFI-UF membranes under constant pressure filtration may be more compressed than the cake formed on RO membranes, and thus predicted particulate fouling may be overestimated (Boerlage et al., 2004). Consequently, to more accurately assess particulate fouling in RO, the MFI-UF was developed to operate at constant flux (Boerlage et al., 2004; Salinas-Rodríguez et al., 2015).

The measured MFI-UF depends on the properties of the UF membrane used in test, particularly the molecular weight cut-off (MWCO). The lower the MWCO of the MFI-UF membrane, the smaller the membrane pore size and the more the particles that can be retained by the membrane, which eventually results in a higher MFI-UF value (Salinas-Rodríguez et al., 2015).

In addition, the measured MFI-UF is highly dependent on the accuracy and reproducibility of the measurement set-up. The instrumentations that make up the MFI-UF set-up, particularly the (infusion) pump and pressure transmitter (explained in detail in section 2.3.1), may drift with time due to malfunction, over-loading/extensive using and environment conditions, which may eventually result in errors in the outputs of these instruments. Moreover, the instrument errors may even be exacerbated by improper test performance, due to (invisible) water leakage from the set-up and existence of air bubbles (Salinas-Rodríguez et al., 2015), or because of any user-made error. Consequently, these errors may lead to an inaccurate MFI-UF value, and eventually result in inaccurate particulate fouling prediction.

Therefore, to ensure accurate and consistent MFI-UF measurement, MF-UF set-up should be calibrated using a standard (reference) calibration solution. For the MFI-0.45 method, the calibration could be done using a standard solution of Formazine particles (ASTM, 2015). However, until now, no standard solution has been proposed or tested for the calibration of the MFI-UF method.

Moreover, in practice, the MFI-UF is measured for natural water (e.g. RO feed water) which usually includes a wide range of particles with different properties than those of standard calibration solutions. Therefore, in addition to the calibration of MFI-UF using a standard solution, the MFI-UF should be also validated using natural water. In both processes (i.e. calibration and validation), a linear correlation should be demonstrated between the MFI-UF value and particle concentration (as illustrated in section 2.2).

Accordingly, the aim of this study was to calibrate and validate the MFI-UF for accurate measurement of particulate fouling in RO. For this purpose, the research objectives were:

- (1) Examining the MFI-UF calibration using different calibration solutions of standard particles (dextran and polystyrene).
- (2) Validating the MFI-UF method using natural (surface) water as a representative of real water in RO systems.

2.2 THEORETICAL BACKGROUND

The MFI-UF is based on cake/gel filtration mechanism. At constant flux, cake/gel filtration can be defined by the linear correlation of the transmembrane pressure (ΔP) and the filtration time (t), as shown in Equation (2.1) (Boerlage et al., 2004).

$$\Delta P = J \cdot \eta \cdot R_m + J^2 \cdot \eta \cdot I \cdot t \quad (2.1)$$

Where J is the flux rate, η is the feed water viscosity, R_m is the clean membrane resistance, and I is the fouling index which describes the fouling potential of feed water. I is proportional to the product of the specific cake resistance (α) and particle concentration in the feed water (C), as shown in Equation (2.2) (Boerlage et al., 1998).

$$I = \alpha \cdot C \quad (2.2)$$

Specific cake resistance (α) can be defined based on Carman-Kozeny formula (Carman, 1938), as shown in Equation (2.3) (Boerlage et al., 1998), as a function of the cake porosity (ε), particle diameter (d) and particle density (ρ).

$$\alpha = \frac{180 \cdot (1 - \varepsilon)}{\rho \cdot d^2 \cdot \varepsilon^3} \quad (2.3)$$

The two parameters α and C are very difficult to measure accurately, especially for natural water. Therefore, the fouling index (I) can be determined experimentally through the MFI-UF test. During the MFI-UF test, transmembrane pressure increases over time in three sequential phases, as shown in Figure 2.1; (i) pore blocking (plus system start-up), (ii) cake/gel filtration and (iii) cake/gel compression and cake pores narrowing. The value of I can be determined from the slope of the linear phase of cake/gel filtration, using Equation (2.4).

$$I = \frac{1}{J^2 \cdot \eta} \cdot \text{slope} \quad (2.4)$$

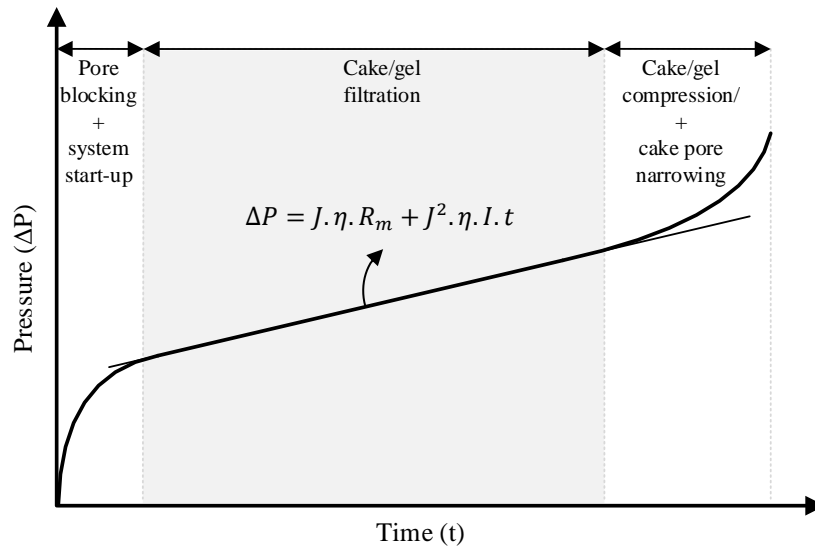


Figure 2.1: Typical filtration phases during the MFI-UF test performed at constant flux

The MFI-UF, by definition, is the value of I corrected to reference testing conditions, as shown Equation (2.5) (Schippers and Verdouw, 1980).

$$MFI-UF = \frac{\eta_{20^{\circ}\text{C}} \cdot I}{2 \cdot \Delta P_o \cdot A_o^2} \quad (2.5)$$

Where ΔP_o , $\eta_{20^{\circ}\text{C}}$ and A_o are the reference pressure, water viscosity and surface membrane area, respectively (Schippers and Verdouw, 1980).

By combining Equation (2.2), (2.3) and (2.5), the MFI-UF can be then defined by Equation (2.6), which demonstrates (theoretically) a linear correlation between the MFI-UF and particle concentration.

$$MFI-UF = \frac{90 \cdot \eta_{20^{\circ}\text{C}} \cdot (1 - \varepsilon) \cdot C}{\Delta P_o \cdot A_o^2 \cdot \rho \cdot d^2 \cdot \varepsilon^3} \quad (2.6)$$

2.3 MATERIALS AND METHODS

2.3.1 MFI-UF set-up

MFI-UF measurements were performed using the set-up schemed in Figure 2.2. The set-up simply consisted of three main items; infusion syringe pump (PHD ULTRA, Harvard Apparatus), pressure transmitter (PXM409, Omega and PMC51, Endress+Hauser) and membrane holder (Whatman) including the UF membrane. During the test, the water sample was delivered at a constant flow rate to the UF membrane. Simultaneously, the pressure transmitter recorded the transmembrane pressure (ΔP) over time (t) and transferred the data to a connected computer. Finally, the relationship between ΔP and t was plotted (as shown in Figure 2.1), and then the MFI-UF value was calculated based on Equation (2.4) and (2.5).

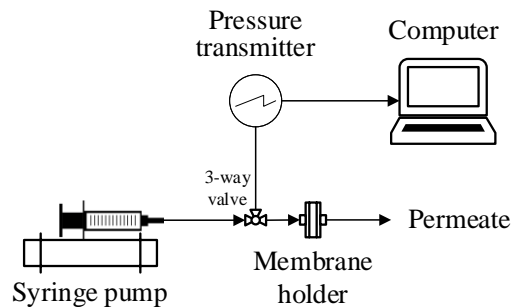


Figure 2.2: Scheme of MFI-UF set-up at constant flux filtration

2.3.2 MFI-UF membranes

Flat-sheet polyethersulfone (PES) UF membranes with molecular weight cut-off (MWCO) of 5, 10, and 100 kDa and surface diameter of 25 mm were used (Biomax, Millipore). All membranes were cleaned before use by filtering at least 100 mL of ultra-pure water (Milli-Q, Millipore) to remove any preservation materials used during membrane production. Clean membrane resistance (R_m) was measured prior to each MFI-UF measurement, based on Equation (2.7), to ensure that membranes were manufactured consistently and not damaged.

$$R_m = \frac{\Delta P}{J \cdot \eta} \quad (2.7)$$

2.3.3 MFI-UF calibration using standard particle solutions

MFI-UF calibration was examined using two solutions of different types of standard particles; dextran and polystyrene, as a representative of polymeric and well-defined particles, respectively. The applied testing conditions are detailed below and summarized in Table 2.1.

Dextran with a molecular weight of 150 kDa was used (Sigma-Aldrich). Dextran was supplied in a powder form. Dextran solutions with serial concentrations (Table 2.1) were prepared by dissolving the dextran in a 0.05 mol/L of potassium phosphate buffer solution of pH 7. The buffer solution was prepared by dissolving 3.15 g of KH_2PO_4 and 4.67 g of K_2HPO_4 in 1 L of ultra-pure water (Milli-Q, Millipore).

Polystyrene particles had a nominal size of 25 nm (Bangs Laboratories). The supplied polystyrene was suspended in a deionized water with a concentration of 10%. The suspension also included 0.5% sodium dodecyl sulphate (to stabilize the particles) and 0.1% sodium azide (to inhibit bacterial growth). Polystyrene solutions of different concentrations (Table 2.1) were prepared by adding ultra-pure water (Milli-Q, Millipore) to the supplied stock suspension.

Table 2.1: Testing conditions applied to examine the MFI-UF calibration using dextran and polystyrene solutions

Standard particles used in feed solution	Concentration	Flux	MFI-UF membrane
Dextran (150 kDa)	Lower range: 20-100 mg/L Higher range: 200-1000 mg/L	100 L/m ² .h	100 kDa
Polystyrene (25 nm)	Lower range: 1-25 mg/L Higher range: 50-150 mg/L	50, 100 and 200 L/m ² .h	100 kDa

The suitability of dextran and polystyrene solutions for MFI-UF calibration was examined based on 2 main criteria:

1. Verification of MFI-UF linearity at both the lower and higher range of particle concentration. For RO applications, it is important that the calibration/linearity range covers the MFI-UF of RO feed water. Based on the results addressed later in Chapter 4 (Abunada et al., 2023b), the MFI-UF values of different RO feed waters measured at the same testing conditions in Table 2.1 (i.e. at 100 L/m².h using 100 kDa membrane) were in the range of 550-1150 s/L², however, this range may be different for other types of RO feed.
2. Reproducibility of MFI-UF linearity under the same testing conditions (i.e. at same flux and same MFI-UF membrane MWCO).

2.3.4 MFI-UF validation using natural water

MFI-UF validation was investigated by verifying the linearity of the MFI-UF as a function of the particle concentration using natural surface water to simulate real water treated in RO systems in practice. For this purpose, several batches of canal water (CW) were collected (from Delft, Netherlands). The quality of CW varied based on the time of collection (season, month and even the time of day), where the turbidity ranged from 1.5 to 3.0 NTU, TOC from 11 to 18 mg/L, and EC from 600 to 800 uS/cm. Tap water was used to make dilutions of the CW to eliminate any effect of pH variation, as both CW and tap water had more or less same pH. Accordingly, all prepared CW dilutions had similar pH (7.9-8.1). Since tap water is not a particle-free solution (i.e. it also contains particles), it was filtered through a 10 kDa membrane before being used to dilute the CW, in order to avoid introducing additional particles into the diluted CW samples. Diluted CW samples were prepared in two ranges of concentrations; low and high (as shown in Table 2.2) to simulate the water with both low and high particle concentration such as RO feed and raw water, respectively.

Table 2.2: Testing conditions applied to assess the MFI-UF linearity using CW

Feed solution	Concentration *	Flux	MFI-UF membrane
Canal water (CW)	Lower range: 0-10% Higher range: 20-100%	20, 100 and 200 L/m ² .h	5, 10 and 100 kDa

* For example, 10% sample refers to a mixture of 10% of CW and 90% of diluting solution (prefiltered tap water). 0% sample refers to 0% of CW; i.e. only the diluting solution (prefiltered tap water).

In principle, MFI-UF linearity should be verified at the flux which is typically applied in RO systems, i.e. in the range of 10-35 L/m².h (DOW, 2011). However, at such a low flux range, the MFI-UF test may be very lengthy. Hence, MFI-UF can be measured at higher flux rates and then extrapolated linearly to the actual RO flux (Salinas-Rodríguez et al., 2012). Therefore, the MFI-UF linearity was investigated at a low flux of 20 L/m².h (similar to RO flux) as well as at higher flux rates of 100 and 200 L/m².h.

In addition, since the size of particles depositing onto RO membranes is unknown, the MFI-UF can be typically measured using UF membranes with a range of MWCO (Salinas-Rodríguez et al., 2015). Hence, the MFI-UF linearity was investigated using different UF membranes with MWCO of 5, 10 and 100 kDa.

2.4 RESULTS AND DISCUSSION

2.4.1 MFI-UF calibration using standard solutions

2.4.1.1 Dextran particle solution

2.4.1.1.1 Linearity verification

Figure 2.3 shows the relationship between the MFI-UF and dextran concentration at 100 L/m².h using a 100 kDa membrane. As can be observed, the calibration curve was linear over the entire range of dextran concentrations, with $R^2 > 0.99$.

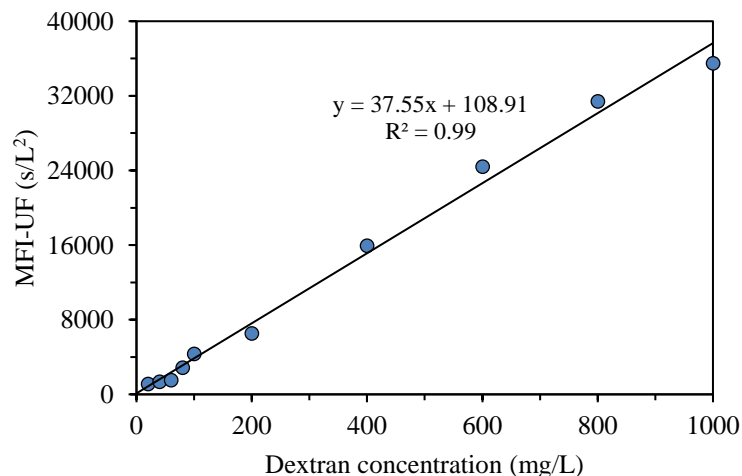


Figure 2.3: Relationship between MFI-UF and dextran concentration

2.4.1.1.2 Reproducibility

To verify the reproducibility of the MFI-UF calibration line demonstrated in Figure 2.3, the MFI-UF measurements were repeated at the same conditions (at 100 L/m².h using 100

kDa membrane) using a newly prepared dextran samples (prepared by the same stock dextran). The relationship between the MFI-UF and the dextran concentration of the new samples was also linear ($R^2 = 0.93$). However, the slope of the calibration line obtained with the different batches of dextran samples varied by around 70%, which indicated that the calibration line obtained with dextran solutions was not reproducible.

The reason that the MFI-UF calibration line was not reproducible with dextran solutions was assumed to be attributed to the diluting buffer solution used to prepare the dextran samples (potassium phosphate buffer solution). To confirm this further, the MFI-UF was measured using samples of dextran (50 mg/L) prepared with two diluting buffer solutions, where the diluting solutions were prepared based on the same procedure explained in section 2.3.3. As shown in Figure 2.4, the variation in the MFI-UF of dextran samples prepared with the same diluting solution was 12-15% (where MFI-UF measurements were performed in triplicate with each diluting solution). However, the variation in the average MFI-UF of dextran samples prepared with different diluting solution was $> 100\%$.

This result could be attributed to the structure of the dextran polymer chains (i.e. type, degree and length of branching) which could be sensitive to any slight variation in the chemical stability of the prepared diluting buffer solution. Another reason could be due to the sensitivity of dextran polymers to the stirring conditions (i.e. shear forces) during dissolving the dextran in the buffer solutions. Consequently, the size range of dextran particles might have been different for each of the prepared dextran samples shown in Figure 2.4. Hence, since the MFI-UF is highly dependent on particle size (Equation (2.6)), different range of MFI-UF values (and thus different calibration line) could be obtained when very small changes in the diluting buffer solution exist.

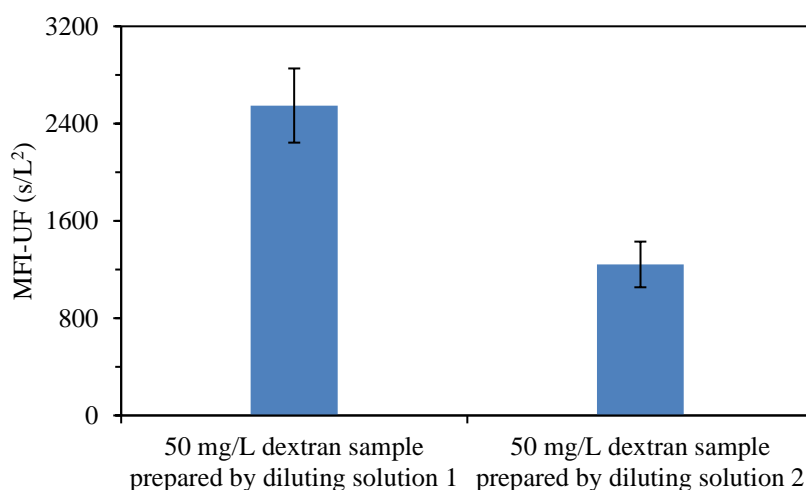


Figure 2.4: MFI-UF of dextran samples (50 mg/L) prepared with two diluting buffer solutions (where MFI-UF was measured in triplicate)

2.4.1.2 Polystyrene particle solution

2.4.1.2.1 Linearity verification

Figure 2.5 shows the relationship between MFI-UF and the concentration of polystyrene particles at 50, 100 and 200 L/m².h using 100 kDa membrane. The intercepts of the calibration lines were set to 40 s/L² which is the average MFI-UF value of the diluting blank solution (ultra-pure water) at these testing conditions. As observed, the fit of the calibration line to the measured MFI-UF values was similar in all cases; the higher MFI-UF values ($> \sim 10,000$ s/L²) of higher polystyrene concentration samples (50-150 mg/L) showed a good fit with the regression line, while the MFI-UF values obtained at lower particle concentration range (1-25 mg/L) showed a poor fit and appeared to be underestimated. The observation of this trend can be due to two reasons, as explained below.

One possible reason for this trend (shown in Figure 2.5) may be attributed to the surfactant portion in the prepared polystyrene samples (sodium dodecyl sulphate was present in the supplied polystyrene suspension as a surfactant to stabilize the particles). The surfactant concentration in the lower polystyrene concentration samples might have been too low to stabilize the particles. As a result, the polystyrene particles in the lower concentration samples could aggregate into larger particles, and hence lower (underestimated) MFI-UF was obtained (based on Equation (2.6)). To verify this hypothesis, the zeta potential (ZP) of polystyrene samples was measured using a zetasizer (Malvern, Nano-ZS). For all polystyrene samples (both of lower and higher polystyrene concentration), the ZP was similar with a value of $-61(\pm 1)$ mV (except for the polystyrene sample of 1 mg/L where the ZP was -50 mV). This indicated that the required surfactant portion was based on particle-surfactant ratio (i.e. the lower the particle concentration, the lower surfactant concentration is required to keep the particles stabilized), and thus the surfactant portion was sufficient even in the samples with lower polystyrene concentration. Therefore, the aggregation of polystyrene particles might not be the reason for the underestimated MFI-UF values observed at lower particle concentrations shown in Figure 2.5.

Another reason can be attributed to the inert nature of polystyrene particles resulting in the restriction of their attachment to the MFI-UF membrane surface as well as to each other during MFI-UF testing. This effect of the inert nature of polystyrene could be even further enhanced by several factors; (i) the presence of surfactant which could keep the polystyrene particles stabilized and unattached, (ii) the lateral water flow streams inside the MFI-UF membrane holder which could sweep the particles from the membrane surface, and (iii) the low density of polystyrene particles. Due to these factors, at lower polystyrene concentrations, a porous cake might have been formed above the MFI-UF membrane surface as shown in Figure 2.6 (a). Consequently, the MFI-UF values at lower particle concentrations were underestimated (below the calibration line). On the other

hand, at higher polystyrene concentrations, the load of particles was higher, which could subsequently overcome the aforementioned factors by pushing and holding the particles on the membrane surface, forming a more compacted cake as shown in Figure 2.6 (b). Therefore, the MFI-UF values at the higher range were fitted well by the calibration line (i.e. not underestimated as the case at the lower range).

The above explanation also clarifies the improvement of the fit of the calibration line at the lower range when the flux was higher (i.e. the MFI-UF values at the lower range were less underestimated when the flux was higher). This is because the higher the flux, the higher the permeation force acting on particles toward the membrane surface, which subsequently reduced the effect of the factors mentioned in above explanation.

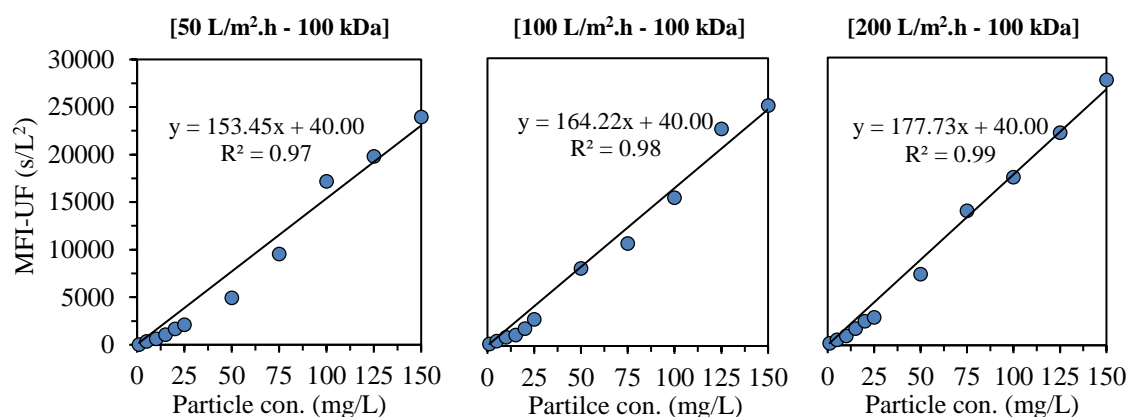


Figure 2.5: Relationship between MFI-UF and polystyrene concentration

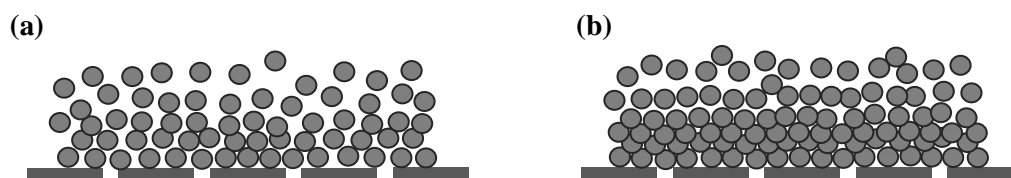


Figure 2.6: Hypothesized illustration of the cake formed by polystyrene particles in case of (a) lower particle concentration (b) higher particle concentration

2.4.1.2.2 Reproducibility

The reproducibility of the MFI-UF calibration line obtained with polystyrene solutions was examined at a flux of 100 L/m².h using a 100 kDa membrane, with newly prepared batches of polystyrene particle samples. The relationship between the MFI-UF and the concentration of the new polystyrene particles was similar to that demonstrated in Figure 2.5, where the slopes of the calibration lines obtained by the different batches of polystyrene samples were similar, with only 7% deviation.

However, the reproducibility of the calibration line obtained by polystyrene particle solutions appears to be similar regardless of the applied flux rate. Based on the results shown in Figure 2.5, the slopes of calibration lines were similar (with only 7% variation) although they were obtained at different flux rates (50, 100 and 200 L/m².h). In principle, increasing the flux directly impacts the re-arrangement of particles in the cake and simultaneously causes cake compression, which eventually results in a less-porous cake and thus higher MFI-UF value (Salinas-Rodriguez, 2011). However, the effect of the flux might be minor in the case of the tested polystyrene solutions. This is because the used polystyrene particles are monodisperse spheres, and hence particle re-arrangement in the cake is limited even when the flux increased from 50 to 200 L/m².h. In addition, since polystyrene particles are rigid (Kutscher et al., 2010), they are not expected to be strongly compressed as the flux is increased. Consequently, cake porosity and thus the measured MFI-UF values were similar at different flux rates, which resulted in similar calibration lines. This result suggests that MFI-UF calibration with polystyrene solution may not be able to detect errors in pump flow (if any), as the MFI-UF of a polystyrene sample would be similar even if the flux was different due to a pump error. However, using a heterogenous mixture of polystyrene particles (with different particle sizes and shapes) may improve the degree of the re-arrangement and compressibility of polystyrene particles in the cake and thus overcome the limitation of calibration mentioned above. Nevertheless, this needs further investigations.

2.4.2 MFI-UF validation using natural water (canal water)

Figure 2.7 shows the relationship between the MFI-UF and the particle concentration in canal water (CW) under different testing conditions (at flux rates of 20, 100 and 200 L/m².h using 5, 10 and 100 kDa membranes). As explained in section 2.3.4, the raw CW used to prepare the CW dilutions was different for each testing condition, since the raw CW was collected at different times of the year. This means that the water quality for each testing condition is different (turbidity = 1.5-3.0 NTU, TOC = 11-18 mg/L and EC = 600-800 uS/cm). Therefore, the effect of the flux and membrane MWCO on MFI-UF values (and thus on the slopes of linear relationships) in Figure 2.7 cannot be compared. For instance for the 10 kDa membrane, the MFI-UF values measured at 20 L/m².h were (accidentally) close to the corresponding MFI-UF values measured at a higher flux of 100 L/m².h. This is because the quality of raw CW used at 20 L/m².h was lower than that at 100 L/m².h (e.g. TOC was 16 and 11.2 mg/L for the raw CW used at 20 and 100 L/m².h, respectively).

As observed at all testing conditions, the relationship between the MFI-UF and the particle concentration was linear with $R^2 > 0.97$, regardless of the flux, membrane MWCO and water quality tested. This result verified that the MFI-UF method is valid (according to Equation (2.6)) and can be used to measure different levels of particulate

fouling potential at a wide range of testing conditions (at fluxes of 20-200 L/m².h using 5, 10 and 100 kDa membranes). In addition, the strong correlation between the MFI-UF and particle concentration also confirmed the robustness of the MFI-UF method to detect the variation in particulate fouling potential due to any changes in the water quality of RO feed water.

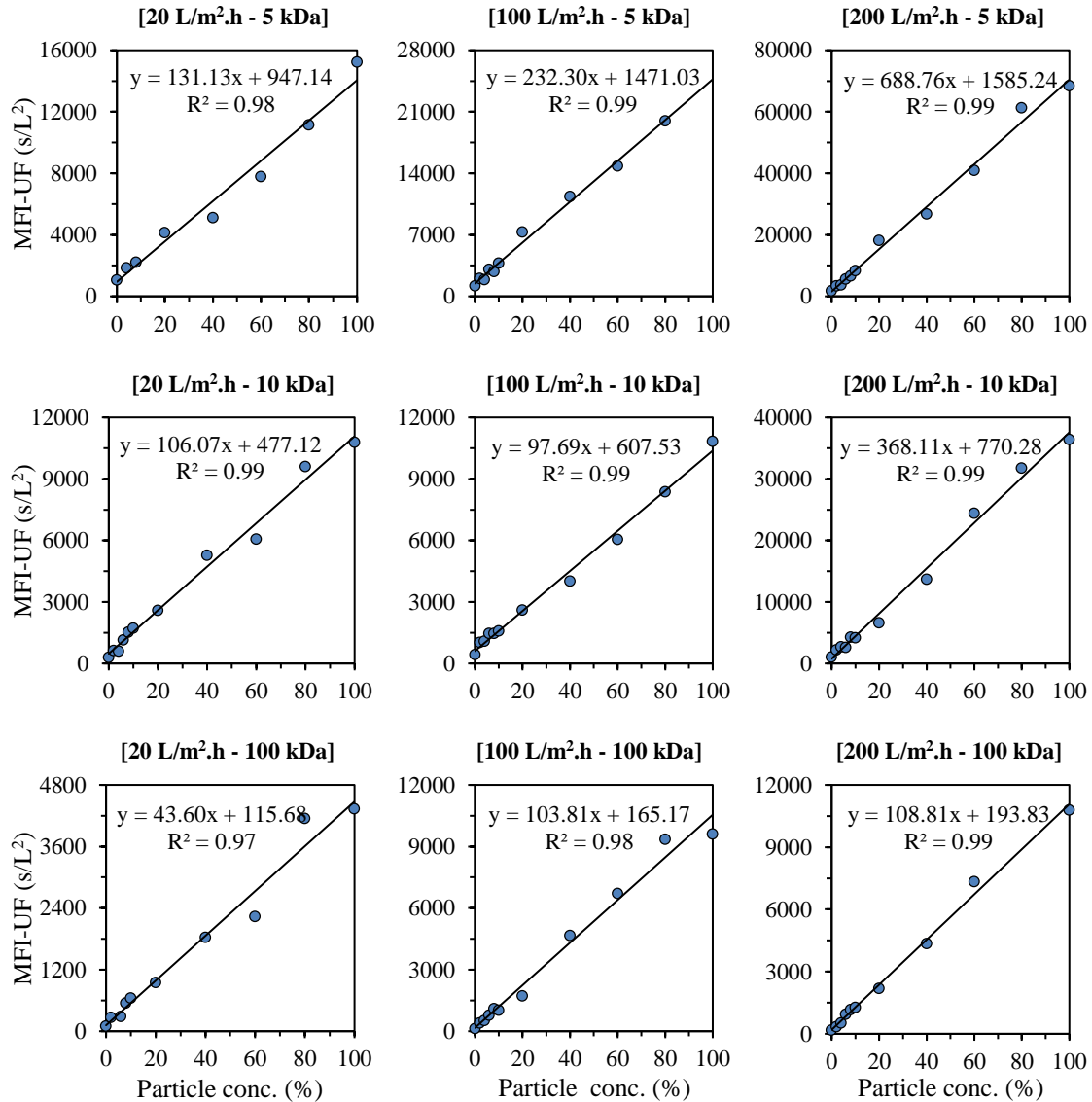


Figure 2.7: Relationship between MFI-UF and particle concentration in surface canal water at various testing conditions; at 20, 100 and 200 L/m².h using 5, 10 and 100 kDa membranes (the raw canal water used to prepare the dilutions was different at each testing condition; turbidity = 1.5-3.0 NTU, TOC = 11-18 mg/L and EC = 600-800 μ S/cm)

Based on Figure 2.7, the MFI-UF linearity range was verified up to around 70,000 s/L² (at 200 L/m².h using 5 kDa membrane). However, it is expected that the MFI-UF linearity could be extended to higher levels of MFI-UF in case of other types of water (with higher particle concentration) are used. Nevertheless, the observed linearity ranges (Figure 2.7) were confirmed to cover the MFI-UF levels along different RO plants measured in other works by Salinas-Rodríguez et al. (2012) and Abunada et al. (2023b) (see Chapter 4).

Nevertheless, the MFI-UF was validated using fresh water (canal water), while RO systems in practice may also be used to treat saline water; i.e. brackish groundwater and seawater. Regarding the application of the MFI-UF for saline water, Boerlage et al. (2003a) found that an increase in the salinity of a feed water (such as the case in seawater) can affect the cake resistance and thus the MFI-UF. The increase in salinity can initially compress the double layer around the particles which results in an increase in the cake resistance and thus a higher MFI-UF value. Once the increase in salinity becomes above the critical concentration of coagulation, particles start to aggregate into larger sizes leading to less cake resistance and thus lower MFI-UF value. Hence, in case seawater is used to validate the MFI-UF (i.e. instead of fresh surface water), the diluted seawater samples will have different salinity, which will affect the particle/cake properties as mentioned above. However, based on the MFI-UF principle (Equation (2.6)), the MFI-UF method can be validated if a linear relationship exists between the MFI-UF and particle concentration, assuming no change in particle/cake properties (i.e. particle size and density and cake porosity). Therefore, the MFI-UF of diluted seawater samples should be corrected to eliminate the effect of salinity (Boerlage et al., 2003a). Consequently, the corrected MFI-UF will only be a function of particle concentration, as the case in surface canal water used in this study.

2.5 CONCLUSIONS

This study aimed to calibrate and validate the MFI-UF for accurate measurement of particulate fouling in RO.

The MFI-UF calibration was examined using 2 solutions of standard particles (150 kDa dextran and 25 nm polystyrene particles). The calibration was examined based on: (i) verification of MFI-UF linearity at both the lower and higher range of MFI-UF, and (ii) reproducibility of MFI-UF linearity under the same testing conditions.

For dextran solutions, the relationship between the MFI-UF and particle concentration was strongly linear ($R^2 \approx 1$) over the entire range of MFI-UF. However, the calibration line was not reproducible with different batches of dextran solution prepared under the same conditions. The reason could be attributed to the dextran polymers which might be sensitive to very slight variation during dextran solution preparation (i.e. slight variation

in stirring conditions and/or chemical stability), which could consequently result in different particle sizes and thus different MFI-UF values when dextran samples (of same concentration) were prepared with different diluting solutions. Therefore, dextran solution was not deemed suitable for MFI-UF calibration.

For polystyrene solutions, a linear relationship between the MFI-UF and particle concentration was verified at the higher range of MFI-UF (i.e. $\text{MFI-UF} > 10,000 \text{ s/L}^2$), while the MFI-UF values at the lower range appeared to be underestimated. The explanation of this trend could be attributed to the inert nature of polystyrene particles which could restrict their attachment to the MFI-UF membrane surface as well as to each other during the MFI-UF test. Consequently, at lower concentration (i.e. load) of polystyrene particles, a more porous cake may have formed on the MFI-UF membranes and thus lower (i.e. underestimated) MFI-UF values were obtained. In addition, the calibration lines obtained for polystyrene solutions were similar over a wide range of flux rates (50-200 $\text{L/m}^2\cdot\text{h}$). This was attributed to the fact that the tested polystyrene particles were hardly re-arranged or compressed even when the flux was increased. Therefore, the cake porosity and thus the measured MFI-UF values were similar at different flux rates. These results indicated that the polystyrene particle solutions may not be able to detect errors in the pump (i.e. the MFI-UF of a polystyrene sample would be similar even if the flux changed due to any error in the pump).

The MFI-UF validation was investigated by verifying the linearity of MFI-UF using natural water (canal water), under a wide range of testing conditions (i.e. at flux of 20, 100 and 200 $\text{L/m}^2\cdot\text{h}$ using 5, 10 and 100 kDa membranes). At all testing conditions, the relationship between the MFI-UF and the particle concentration was strongly linear at both the lower and higher range of MFI-UF ($R^2 > 0.97$). The verified linearity ranges covered MFI-UF levels along different RO plants (measured in previous works).

In conclusion, the MFI-UF method was validated for measuring particulate fouling under a wide range of testing conditions. On the other hand, further research is still required to examine the MFI-UF calibration using more suitable solutions of standard particles. Based on the results of this study, the solution of polystyrene standard particles is considered promising as it is stable and reproducible (compared to dextran solution). However, further investigation is needed to select, prepare and test a suitable heterogenous mixture of polystyrene particles (with different particle sizes and shapes) to overcome the limitations of calibration mentioned above.

3

QUANTIFYING THE EFFECT OF THE SURFACE POROSITY OF MFI-UF MEMBRANE

This study aimed to quantify the effect of membrane surface porosity on particulate fouling predicted by the MFI-UF method at constant flux. Firstly, the surface porosity of polyethersulfone UF membranes (5-100 kDa) was determined using ultra-high resolution SEM. Thereafter, the MFI-UF was measured using suspensions of polystyrene particles (75 nm), which were pre-washed to remove surfactant and particle fractions smaller than the pores of MFI-UF membranes, thus ensuring complete retention of particles during MFI-UF measurements. Consequently, the MFI-UF values of washed polystyrene particle suspensions were independent of the pore size and depended only on the surface porosity of MFI-UF membrane. The results showed that the membrane surface porosity decreased with MWCO from 10.5% (100 kDa) to 0.6% (5 kDa), and consequently the MFI-UF increased from 3700 to 8700 s/L^2 , respectively. This increase in MFI-UF was attributed to the non-uniform distribution of membrane pores, which is exacerbated as surface porosity decreases. Consequently, preliminary correction factors of 0.4-1.0 were proposed for MFI-UF measured with UF membranes in the range 5-100 kDa. Nevertheless, additional research is required to establish correction factors for different types of feed water.

3.1 INTRODUCTION

Particulate fouling due to the deposition of particles/colloids on membrane surfaces is one of the problems experienced in many reverse osmosis (RO) membrane systems. Membrane fouling has several consequences, including: higher energy requirement and frequent membrane cleaning associated with increased use of chemicals and shorter membrane life (Alpatova et al., 2020). Therefore, a method to assess, monitor and predict particulate fouling potential is really essential to optimize the performance of RO systems.

Currently, the most common methods used to assess particulate fouling potential are the Silt Density Index (SDI) and the Modified Fouling Index (MFI or MFI-0.45), which are standard methods in ASTM (under designation code: D4189 and D8002, respectively) (ASTM, 2014; ASTM, 2015). The main advantage of the SDI is that it is simple to measure, even by non-professionals (Alhadidi et al., 2011a; Rachman et al., 2013). However, there have been growing doubts about its accuracy and reproducibility, attributed to the lack of correction factors for temperature, pressure and membrane resistance. Consequently, the SDI⁺ was developed where the SDI value is corrected for the aforementioned parameters (Alhadidi et al., 2011b; Alhadidi et al., 2011c). On the other hand, the MFI-0.45 has more advantages over the SDI as it is (i) derived based on cake/gel filtration, which is assumed to be the dominant particulate fouling mechanism in RO membranes, (ii) proportional to the particle concentration in feed water, and (iii) corrected for temperature and pressure (Schippers and Verdouw, 1980). The main drawback of the MFI-0.45 method is the use of a 0.45 μm membrane as a reference membrane to simulate the RO membrane. Hence, the particles/colloids smaller than 0.45 μm , which likely play a significant role in RO membrane fouling, are not considered in the method (Schippers et al., 1985). Consequently, the MFI-UF method was developed where an ultrafiltration (UF) membrane is used in order to capture smaller particles/colloids (Boerlage et al., 1997; Boerlage et al., 1998; Boerlage et al., 2000; Boerlage et al., 2003a; Boerlage et al., 2003b). The MFI-UF method was initially performed at constant pressure (as the MFI-0.45). However, most of RO systems in practice operate at constant flux which is around 10-1000 lower than the (initial) flux observed during the MFI-UF test at constant pressure. Therefore, the MFI-UF method was further developed to operate at constant flux filtration to more accurately simulate the operation of RO systems (Boerlage et al., 2004). The MFI-UF at constant flux was primarily measured using hollow fibre UF membranes (Boerlage et al., 2004), while afterwards, it was further developed using flat-sheet membranes (Salinas-Rodríguez et al., 2015).

MFI-UF depends strongly on the molecular weight cut-off (MWCO) of the UF membrane used in the measurement. The lower the membrane MWCO, the smaller the membrane pore size, which allows the retention of smaller particles by the MFI-UF membrane and eventually results in a higher measured MFI-UF value (Salinas-Rodríguez et al., 2015).

Accordingly, assuming the particles retained on different MWCO membranes are equivalent in load and properties (i.e. same cake properties and thus same specific cake resistance on all membranes), then the measured MFI-UF value is assumed to be independent of the membrane MWCO. However, this might not be the case, as the measured MFI-UF value may also be affected by the membrane surface porosity. Membranes with low surface porosity and a non-uniform distribution of pores will have a smaller effective filtration area compared with their geometric filtration area. Hence, the local permeation flux through the cake formed on the surface of a membrane with a non-uniform porosity is expected to be higher (Fane et al., 1991; Boerlage et al., 2002b). Subsequently, this may cause the particles in the cake to be re-arranged, and simultaneously the cake can be compressed (Salinas-Rodriguez, 2011). As a result, the cake resistance may increase, leading to a higher MFI-UF value for membranes with non-uniformly distributed pores.

Boerlage et al. (2002b) studied the effect of the surface porosity of hollow fibre polysulphone UF membranes on the MFI-UF measured at constant pressure filtration. The (field emission) scanning electron microscope (SEM) analyses showed that the membranes with MWCO from 1 to 100 kDa (same manufacturer) had a similar range of surface porosities (2-6%), but the distribution of pores over the membrane surface appeared in different patterns. For the membranes ranging in MWCO from 10 to 100 kDa, the pores were distributed uniformly over the entire membrane surface. On the other hand, in the case of the membranes with MWCO from 1 to 5 kDa, the pores were only present on striations running lengthwise across the membrane surface. As a result, the MFI-UF measured using 1-5 kDa membranes was substantially higher than that obtained for the same feed water based on 10-100 kDa membranes. It was hypothesized that in the case of 1-5 kDa membranes, the cake formation might be limited to the porous striations only, while the remaining non-porous part of membrane surface was not involved in filtration and therefore it was ineffective. Consequently, this could result in a denser cake with higher resistance, which could eventually lead to (artificially) overestimated MFI-UF values. However, it was suggested that the effect of membrane surface porosity would be diminished if the MFI-UF test continued for longer duration, as the cake may eventually cover the entire membrane surface. Nevertheless, this was not verified in that study.

The effect of membrane surface porosity was also observed with microfiltration (MF) membranes in several studies (Ethier and Kamm, 1989; Fane et al., 1991; Güell and Davis, 1996; Chandler and Zydny, 2006); where it was found that the rate of flux decline caused by cake/gel formation was faster when the membrane surface porosity was lower and non-uniformly distributed.

In addition, membrane surface porosity might also further decrease as a result of the influence of the membrane holder (housing) support which is placed underneath the membrane. This was reported by Nahrstedt and Camargo-Schmale (2008) and Salinas

Rodriguez et al. (2019) during the measurement of MFI-0.45 using several holder supports with different permeable surface areas. It was found that the non-permeable part of the holder support could block membrane pores which were directly in contact with the support. Consequently, it was found that the smaller the permeable surface area of the holder support, the lower the membrane surface porosity, the smaller the effective filtration area, and eventually the higher the measured MFI-0.45 value.

Although the studies reviewed above suggested/hypothesized the effect of membrane surface porosity on measured particulate fouling, the effect was not proven experimentally. In addition, the studies did not propose nor describe a method to quantify the effect of membrane surface porosity. Moreover, the aforementioned studies focused on constant pressure filtration using mostly MF membranes, while the latest development of the MFI-UF method utilizes UF membranes operating at a constant flux.

Therefore, the aim of this study was to verify and quantify the effect of membrane surface porosity on the MFI-UF measured at constant flux to improve particulate fouling prediction in RO systems. Flat-sheet polyethersulfone (PES) UF membranes with MWCO of 5, 10, 50 and 100 kDa were examined. The following research objectives were investigated:

- (1) To characterize the UF membranes used to measure the MFI-UF (5-100 kDa) in terms of their surface porosity and the distribution of pores across the surface using ultra-high resolution SEM.
- (2) To demonstrate (theoretically) the effect of membrane surface porosity on the effective filtration area during the MFI-UF test.
- (3) To develop an approach to quantify the effect of surface porosity on the MFI-UF measured with 5-100 kDa membranes. To achieve this, it was essential to ensure complete retention of particles on the 5-100 kDa membranes during the MFI-UF measurements in order to eliminate the effect of membrane pore size on the measured MFI-UF (i.e. to quantify the membrane surface porosity effect, the measured MFI-UF should be independent of the pore size and should depend only on the surface porosity of the membranes).
- (4) To identify whether the membrane holder support used in MFI-UF test affects the membrane surface porosity and thus the measured MFI-UF.
- (5) To illustrate the effect of surface porosity of MFI-UF membrane on particulate fouling prediction in a full-scale RO plant.

3.2 THEORETICAL BACKGROUND

MFI-UF was derived based on cake/gel filtration (Boerlage et al., 2004). At constant flux, cake/gel filtration can be defined by the linear relationship between the transmembrane pressure (ΔP) and filtration time (t), as described by Equation (3.1) (Boerlage et al., 2004).

$$\Delta P = J \cdot \eta \cdot R_m + J^2 \cdot \eta \cdot I \cdot t \quad (3.1)$$

Where J is the flux rate, η is the feed water viscosity, R_m is the clean membrane resistance, and I is the fouling index which describes the fouling potential of feed water.

The fouling index (I) is defined by the product of the specific cake resistance (α) and particle concentration in feed water (C), as shown in Equation (3.2) (Boerlage et al., 1998).

$$I = \alpha \cdot C \quad (3.2)$$

Specific cake resistance (α) can be defined according to the Carman-Kozeny equation (Carman, 1938) as a function of the porosity of the cake formed on the membrane surface (ε), particle diameter (d) and particle density (ρ), as shown in Equation (3.3) (Boerlage et al., 1998).

$$\alpha = \frac{180 \cdot (1 - \varepsilon)}{\rho \cdot d^2 \cdot \varepsilon^3} \quad (3.3)$$

The value of I can be determined through MFI-UF test. During the test, transmembrane pressure increases over time, typically, in three subsequent mechanisms, as shown in Figure 3.1; (i) pore blocking (plus system start-up), (ii) cake/gel filtration, and (iii) cake/gel compression and cake/gel pore narrowing. Subsequently, I value is determined from the slope of the linear phase of cake/gel filtration, as shown by Equation (3.4).

$$I = \frac{1}{J^2 \cdot \eta} \cdot slope \quad (3.4)$$

Then the MFI-UF, by definition, is determined based on I value and corrected to the reference testing conditions proposed by Schippers and Verdouw (1980), as shown in Equation (3.5), where ΔP_o , $\eta_{20^\circ\text{C}}$ and A_o are the reference pressure, water viscosity and membrane surface area, respectively.

$$MFI-UF = \frac{\eta_{20^\circ\text{C}} \cdot I}{2 \cdot \Delta P_o \cdot A_o^2} \quad (3.5)$$

MFI-UF can be also described by combining Equation (3.2), (3.3) and (3.5), as shown in Equation (3.6).

$$MFI-UF = \frac{90 \cdot \eta_{20^\circ C} \cdot (1 - \varepsilon) \cdot C}{\Delta P_o \cdot A_o^2 \cdot \rho \cdot d^2 \cdot \varepsilon^3} \quad (3.6)$$

The MFI-UF value can be used as an input in the model shown by Equation (3.7) to predict the particulate fouling rate in RO plants. The fouling rate is described by the increase in the net driving pressure (ΔNDP) due to the cake/gel formation on RO membrane, assuming no contribution by concentration polarization, scaling and biofouling (Schippers et al., 1981).

$$\frac{\Delta NDP}{t} = \frac{2 \cdot \Delta P_o \cdot A_o^2 \cdot J^2 \cdot \eta \cdot \Omega \cdot MFI-UF}{\eta_{20^\circ C}} \quad (3.7)$$

Since the MFI-UF is performed at dead-end filtration, the particles deposition factor (Ω) is incorporated in the prediction model to simulate the portion of particles depositing on RO membrane under cross-flow filtration. The deposition factor can be measured using Equation (3.8), based on the MFI-UF of RO feed, MFI-UF of RO concentrate and RO recovery rate (R). Ideally, the Ω value may vary between 0 and 1; where $\Omega = 0$ indicates no particle deposition, and $\Omega = 1$ indicates that all particles existed in the water passing the RO membrane deposited and remained on its surface (Salinas-Rodríguez et al., 2015).

$$\Omega = \frac{1}{R} + \frac{MFI-UF_{concentrate}}{MFI-UF_{feed}} \cdot \left(1 - \frac{1}{R}\right) \quad (3.8)$$

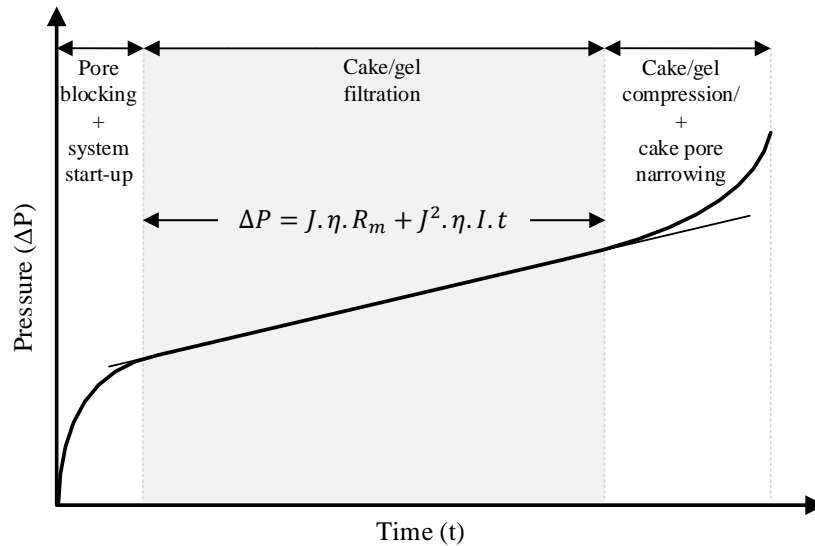


Figure 3.1: Typical filtration curve during an MFI-UF test at constant flux

3.3 MATERIALS AND METHODS

3.3.1 MFI-UF measurement

MFI-UF measurements were performed using the set-up presented in Figure 3.2. The set-up consisted of three main components: (i) infusion syringe pump (PHD ULTRA, Harvard Apparatus), (ii) pressure transmitter (PXM409, Omega), and (iii) membrane holder (Whatman) where the UF membrane was placed. Feed water was infused by the pump and filtered through the membrane at constant flow. Pump flow (Q) was set based on the membrane surface area (A) and the required flux rate (J), where $Q = J \cdot A$. The data of ΔP vs t was recorded by the pressure transmitter and transferred to a connected computer. Finally, the MFI-UF value was calculated based on Equation (3.4) and (3.5).

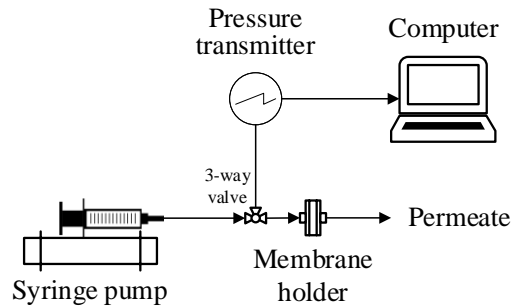


Figure 3.2: Scheme of MFI-UF set-up at constant flux filtration

3.3.2 MFI-UF membranes

The pore size of the MFI-UF membrane should be smaller than the particles in the feed water to be assessed. In RO filtration, the size range of particles that deposit on the RO membrane is not known. Therefore, in this study, a wide range of MWCOs was investigated for MFI-UF; 5, 10, 50, and 100 kDa. The selected UF membranes were made of polyethersulfone (PES), and had flat-sheet configuration with a surface diameter of 25 mm (Biomax, Millipore). All membranes were pre-cleaned by filtering at least 100 mL of ultra-pure water (Milli-Q, Millipore) at a constant flux of 200-300 L/m².h to remove preservation chemicals.

The clean membrane resistance (R_m) was measured prior to the MFI-UF measurement, to verify that the membranes are manufactured consistently and not damaged. R_m can be described by the Hagen-Poiseuille equation (Equation (3.9)) as a function of membrane thickness (Δx), tortuosity (τ), surface porosity (ϵ_m) and pore radius (r_p) (Salinas-Rodríguez et al., 2015).

$$R_m = \frac{8 \cdot \Delta x \cdot \tau}{\varepsilon_m \cdot r_p^2} \quad (3.9)$$

However, since the parameters above are not provided by the manufacturer, R_m was measured experimentally by filtering ultra-pure water (Milli-Q, Millipore) at constant flux, and then, R_m value was calculated using Equation (3.10).

$$R_m = \frac{\Delta P}{J \cdot \eta} \quad (3.10)$$

3.3.3 Characterization of MFI-UF membrane surface

The surface of MFI-UF membranes was characterized using ultra-high resolution SEM (FEI Magellan 400) at magnification of 500,000x and accelerated voltage of 3 kV. The images generated by the SEM were further processed using ImageJ software to identify the surface porosity and the distribution of pores over the membrane surface.

3.3.4 Theoretical demonstration of membrane surface porosity effect during the MFI-UF testing

According to Boerlage et al. (2002b), the effect of membrane surface porosity on the effective filtration area and thus on the measured MFI-UF may be expected to diminish if the duration of the MFI-UF test is very long. To demonstrate this, it was first important to understand how the cake develops on the membrane surface in relation to the uniformity of the membrane surface porosity.

It was hypothesized that the cake development on the membrane surface during the MFI-UF test progresses as shown in Figure 3.3. Just after pore blocking, the particles start to accumulate over and around the pores forming separated mounds of particles on the membrane surface (Figure 3.3 (a)). These mounds continue growing in a form of cake hemispheres which will expand on the membrane surface until they overlap (Figure 3.3 (b)). Consequently, continuous and even cake layers will eventually start to build up over the entire membrane surface (Figure 3.3 (c)).

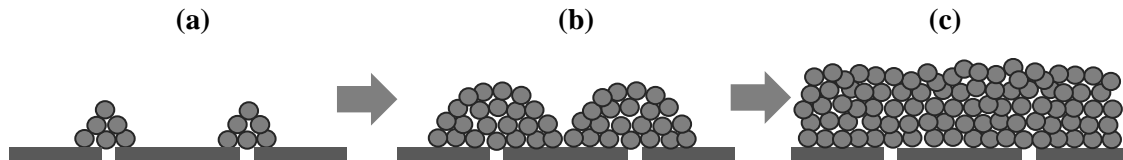


Figure 3.3: Schematic diagram illustrating the hypothesized cake development on the membrane surface during MFI-UF test; (a) separated mounds, (b) overlapping hemispheres, and (c) continuous/even layers

Based on the hypothesis above, the extent of the effect of membrane surface porosity was theoretically (i.e. non-experimentally) determined by calculating the approximate time required until the stage where the membrane surface area is completely covered by cake is reached, and thus the total area becomes effective in filtration (i.e. once the cake hemispheres overlap). Membrane pores were assumed to be uniformly distributed over the membrane surface (i.e. the distance between all membrane pores is identical).

Firstly, it was assumed that all membrane pores have the same size. Accordingly, the number of pores (N_p) was calculated by dividing the porous area by the average cross-sectional area of 1 membrane pore (A_p), where the porous area is the product of the membrane surface porosity (ε_m) and total membrane surface area (A), as shown in Equation (3.11).

$$N_p = \frac{\varepsilon_m \cdot A}{A_p} \quad (3.11)$$

Secondly, it was assumed that one cake hemisphere develops over each membrane pore. In addition, the developed hemispherical cake was assumed to be non-porous and incompressible. Hemisphere volume (V_{hc}) development was calculated by dividing the total cake volume over time by the number of pores (N_p). Where the total cake volume over time was calculated by the product of the feed flow (Q) and particles concentration in the feed (C) divided by particles density (ρ), as shown in Equation (3.12). Particles were assumed to be equivalent in density to the polystyrene particles ($\rho = 1.05 \text{ g/cm}^3$).

$$V_{hc} = \frac{Q \cdot C}{\rho} \cdot \frac{1}{N_p} \cdot t \quad (3.12)$$

Thirdly, based on the hemisphere volume, the hemisphere base area could be calculated over time. Accordingly, the hemispheres will cover the entire membranes surface once the summation of hemisphere base areas is equal to the total membrane surface area. At this stage, it is considered (theoretically) that the filtration area becomes stable over time and no longer impacted by the surface porosity of the membrane.

3.3.5 Approach to quantify the effect of membrane surface porosity on the measured MFI-UF

The theoretical demonstration of the effect of membrane surface porosity addressed in the previous section (3.3.4) was assessed experimentally by measuring the MFI-UF using different UF membranes (5, 10, 50 and 100 kDa).

A new approach was proposed to ensure complete retention of particles by the 5-100 kDa membranes during the MFI-UF test. Complete particle retention is a prerequisite in order

to ensure that the load of particles (and properties of cake) retained on all membranes are identical. Consequently, any difference in the measured MFI-UF can be attributed to the variation in surface porosity of the examined membranes. In case complete retention of particles is not achieved, then the observed differences in the measured MFI-UF can also be as a result of the variation in particle retention due to the different pore sizes of the UF membranes

Figure 3.4 shows the approach followed to ensure complete particle retention. The MFI-UF was measured for a feed suspension of particles in ultra-pure water (Milli-Q, Millipore) using 5-100 kDa membranes. Assuming that all particles are retained on the 5-100 kDa membranes (stage 1), then the measured MFI-UF of the permeates (stage 2) should be similar to the MFI-UF of ultra-pure water which is below the limit of detection (LOD) value; $\approx 200 \text{ s/L}^2$ (see section 3.3.5.1). All MFI-UF measurements were performed at a constant flux of $100 \text{ L/m}^2\cdot\text{h}$.

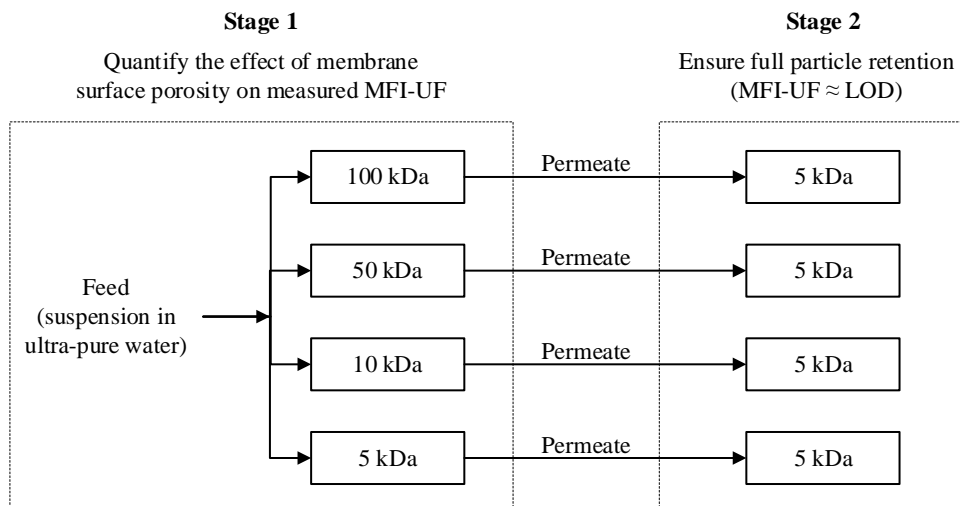


Figure 3.4: The newly developed approach to verify the effect of membrane surface porosity on the MFI-UF measured at constant flux

3.3.5.1 Limit of detection (LOD) measurement

LOD of the MFI-UF method was determined by measuring the MFI-UF of a blank solution of ultra-pure water at least 10 times. The LOD was measured at $100 \text{ L/m}^2\text{h}$ (which is the flux rate used to quantify the effect of surface porosity in this study). The value of LOD was calculated based on Equation (3.13) (Long and Winefordner, 1983). As observed from Table 3.1, higher LOD was found when the membrane MWCO was lower. This is because the lower the membrane MWCO, the higher the associated transmembrane pressure, and thus the higher the error of the pressure transmitter.

$$LOD = Avg + 3 \times StdDev \tag{3.13}$$

Table 3.1: LOD of MFI-UF at 100 L/m².h

Membrane MWCO	Avg (s/L ²)	StdDev (s/L ²)	LOD (s/L ²)
100 kDa	40	15	85
10 kDa	60	20	120
5 kDa	70	40	190

3.3.5.2 Preparation of feed samples used to quantify the effect of membrane surface porosity

The feed sample was initially prepared using monodisperse polystyrene particles (Bangs Laboratories). Polystyrene particles were the preferred choice to verify membrane surface porosity effect based on several criteria, including; (i) polystyrene particles are inert and are chemically very stable (Li et al., 2010), (ii) feed suspensions are easy to prepare (just by diluting the manufactured polystyrene suspension with ultra-pure water), (iii) polystyrene particles are commercially available and relatively inexpensive (price in 2020 was 200 Euro per 1.5 g of 10% concentration), and (iv) polystyrene particles have been used in particulate fouling tests by several researchers (Yiantsios and Karabelas, 1998; Brant and Childress, 2002; Spettmann et al., 2007; Lipp et al., 2009; Park et al., 2009b; Lohaus et al., 2018; Trinh et al., 2020). The selected polystyrene particles had a nominal size of 75 nm. Based on the technical manufacturing data sheet (shown in Annex 3.6.1), the particle size range (65-85 nm) was larger than the pore size range of the 5-100 kDa membranes (which were characterized by ultra-high resolution SEM in advance). Particles with a size significantly larger than the MWCO of the selected membranes were considered unsuitable as large particles are not expected to affect the MFI-UF considerably (since the MFI-UF is inversely proportional to the square of particle size, as shown in Equation (3.6)), and thus the effect of membrane surface porosity variation on the measured MFI-UF would not be noticeable in this case.

Preliminary investigations showed that feed suspension prepared with polystyrene particles could not ensure the criterion of complete particle retention, as the MFI-UF values of the collected permeates were considerably higher than the MFI-UF of ultra-pure (i.e. \gg LOD), as shown in Figure 3.5 (a). This means that the particle load on the 5-100 kDa membranes (stage 1) was different and thus the difference in the measured MFI-UF could not be attributed to the effect of membrane surface porosity only but also to the different retention of polystyrene particles achieved with each membrane. Based on the manufacturer's information, the high MFI-UF values measured for the UF permeates were mainly attributed to the existence of some small particle fractions and/or surfactant residual in the prepared suspensions, such that these small components could (partially) pass through the 5-100 kDa membranes (in stage 1) but probably were retained on the subsequent 5 kDa membranes (in stage 2) due to particle bridging (Hund et al., 2017).

3. Quantifying the effect of the surface porosity of MFI-UF membrane

In further trials, silver particles of 80 nm (Sigma-Aldrich) and pullulan particles of 800 kDa (Sigma-Aldrich) were also tested, both of which were larger than the pore size range of the 5-100 kDa membranes examined in this study (technical data sheets of both silver and pullulan particles are in Annex 3.6.1). Silver particles were selected as they are assumed to be more rigid and have less affinity to be fractured in comparison with polystyrene particles. Whereas, the pullulan particles are used as they are a standard reference material (for calibration in chromatography) and have a well-defined structure (Singh et al., 2008). Thus, for both particle types, negligible small particle fractions were expected in the prepared feed samples. Nevertheless, preliminary investigations showed that the feed samples prepared by both types of particles could not achieve the requirement of full particle retention, as shown in Figure 3.5 (b) and (c). The reason was also mainly attributed to the presence of small particle fractions which might have already existed in the supplied particles and/or were created during sample preparation (e.g. due to shear forces resulted by stirring).

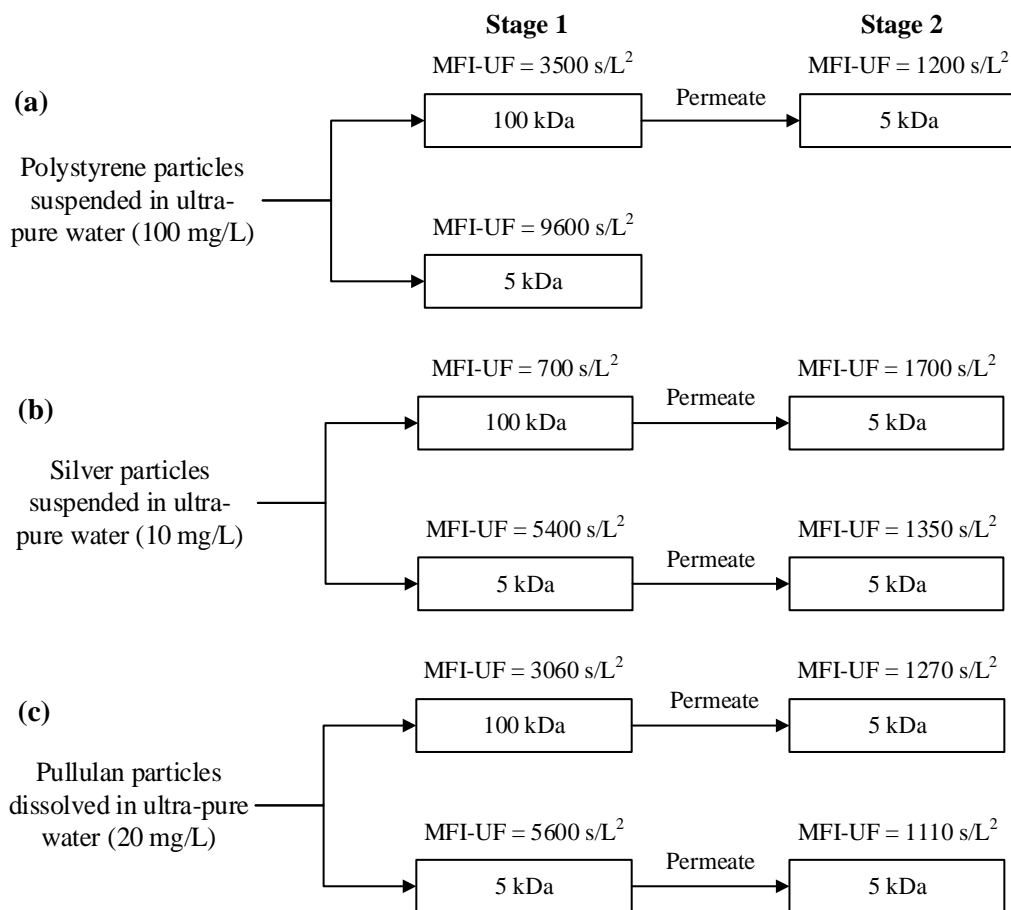


Figure 3.5: Preliminary investigation to verify the effect of membrane surface porosity on measured MFI-UF using feed suspensions/solutions of (a) unwashed polystyrene particles (75 nm), (b) silver particles (80 nm), and (c) pullulan particles (800 kDa)

Based on the above preliminary investigation, it was concluded that none of the commercially available particles tested in this study were suitable to be used as supplied, and an approach was developed to pre-wash the particles to remove the surfactant and the associated particle fractions that were smaller than the pore size of the 5-100 kDa membranes. In this study, particle washing was only investigated for the polystyrene particles, as they were considerably less expensive than the other particles (pullulan and silver).

3.3.5.3 Washing of polystyrene particles to remove surfactant and small particle fractions

The objective of polystyrene particle washing was to remove the small particle fractions and residual surfactant (sodium dodecyl sulphate) created or added during the manufacturing process. For this purpose, several particle washing techniques were investigated; centrifugation, dialysis, unstirred dead-end filtration and stirred dead-end filtration, where the efficiency of each technique was evaluated based on the approach described in Figure 3.4. Eventually, the stirred dead-end filtration, which was the most promising washing technique, yielded complete retention of the polystyrene particles (the results of all washing experiments are addressed in detail in Annex 3.6.2).

Polystyrene particles were washed by stirred filtration, as shown in Figure 3.6; using a 200 mL dead-end stirred cell (Amicon, Millipore) equipped with a 500 kDa PES membrane (Biomax, Millipore). The MWCO of the cell membrane (500 kDa) was selected so that small particle fractions and surfactant in the polystyrene particle suspension could pass through while retaining only the larger particles (> 500 kDa). Thus, this ensures that the washed particles (i.e. retained on the 500 kDa membrane) should be completely retained on the 5-100 kDa membranes. The washing procedure was as follows.

1. A prepared suspension of polystyrene particles (200 mg/L) was placed in the Amicon cell.
2. The connected pressure vessel was filled with ultra-pure water (Milli-Q, Millipore).
3. The stirred filtration of the polystyrene suspension was started simultaneously while filling the cell with ultra-pure water from the pressure vessel (i.e. the inflow of ultra-pure water in the cell = the outflow of filtrate from the cell). Hence, during filtration, the polystyrene particles were washed (by the ultra-pure water) while small fractions of particles as well as surfactant were filtered through the 500 kDa membrane.
4. The total organic carbon (TOC) of the filtrate was measured during filtration (every 30 min).
5. The filtration was stopped once the TOC of the filtrate equalled that of the ultra-pure water (TOC < 0.2 mg/L), which confirmed that most small fractions and surfactant

3. Quantifying the effect of the surface porosity of MFI-UF membrane

were filtered through the 500 kDa membrane. Thereby, the suspension remaining in the cell after filtration comprised washed polystyrene particles (larger than 500 kDa).

6. The washed particle suspension which remained in the cell was then used to quantify the effect of membrane surface porosity (Figure 3.4) on the MFI-UF. The concentration of washed polystyrene particles was estimated by measuring the TOC of the suspension, where the percentage of carbon in polystyrene (C_8H_8)_n is 92%. Accordingly, the washed polystyrene concentration equalled $TOC/0.92$.

Particle washing by stirred filtration was initially investigated at a constant pressure of 250 mbar. In this scenario, the washing process lasted for around 6 hours, and at that point the TOC of the filtrate was < 0.2 mg/L, which was the criterion indicating that washing was complete. However, in many cases, washing was insufficient since the feed suspension of washed polystyrene particles did not satisfy the criterion of complete particle retention described in Figure 3.4 (stage 2), whereby the MFI-UF of the permeate was considerably higher than the target value (results are presented in Annex 3.6.2). The reason was attributed to pore blocking of the Amicon cell membrane (500 kDa) which could restrict part of the small particle fractions and surfactant from passing through the 500 kDa membrane.

Consequently, washing was enhanced by performing the stirred filtration at a lower pressure of 100 mbar to reduce the flux rate and thus minimize membrane pore blocking. In addition, the 500 kDa membrane in the Amicon cell was replaced twice during the washing process (i.e. 3 membranes were used in total), where steps 1-5 mentioned above were repeated after each membrane replacement. The overall washing process required around 8 hours. Particle washing conducted under these conditions (i.e. at 100 mbar using 3 different 500 kDa membranes in the Amicon cell for a period of 8 hours) was successful and satisfied the criterion of complete particle retention (Figure 3.4 (stage 2)), and the MFI-UF values of all UF permeates were less than the LOD (< 200 s/L²) as shown in Figure 3.7.

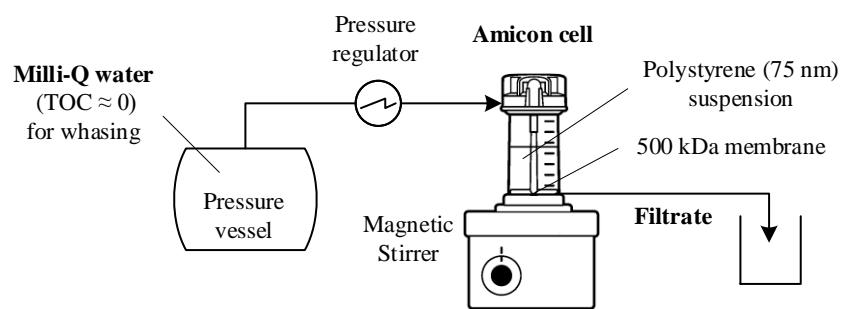


Figure 3.6: Polystyrene particle washing approach using stirred UF filtration at constant pressure

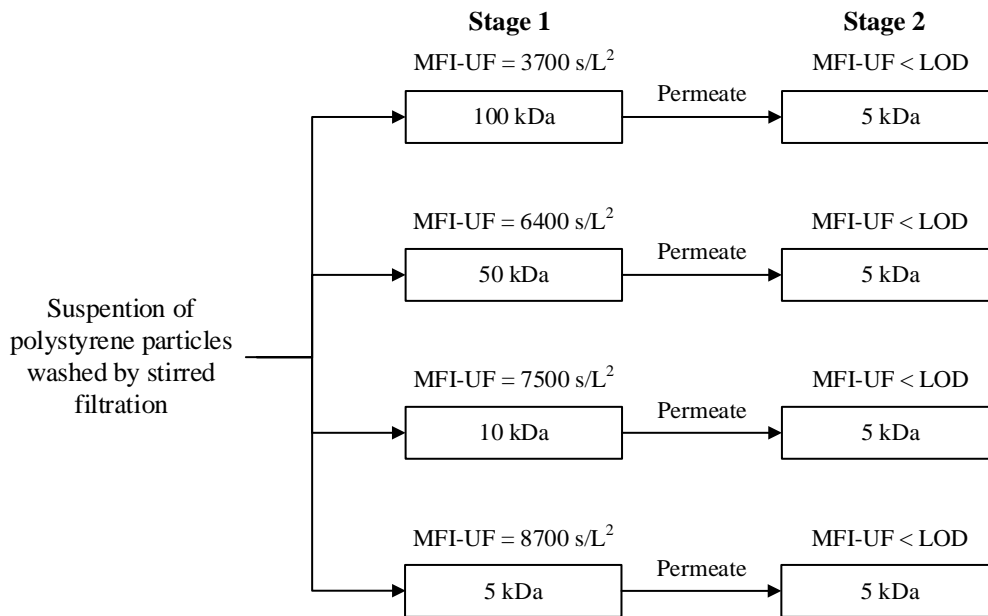


Figure 3.7: Verified the effect of membrane surface porosity on the MFI-UF using a suspension of polystyrene particles washed by stirred dead-end filtration (Amicon cell)

3.3.6 Identification of membrane holder support effect on the membrane surface porosity

The effect of the membrane holder support pad on membrane surface porosity and thus on the measured MFI-UF was investigated using the membrane holder support shown in Figure 3.8 (Whatman). The support pad had two sides with different surface engravings; channels (Figure 3.8 (a)) and perforations (Figure 3.8 (b)). The ratio of the permeable area to the total surface area of the pad was around 50% and 25% for the channelled and perforated sides, respectively.

The effect of the support pad on the membrane surface porosity was investigated by measuring and comparing the clean resistance (R_m) measured with each side of the pad. This was done for the 10 kDa membrane (low MWCO) and 100 kDa membrane (high MWCO), at a constant flux of 200 L/m².h (using Equation (3.10)). Four replicated measurements were carried out with each pad side.

Based on Equation (3.9), R_m is inversely proportional to the membrane surface porosity. Therefore, in case the contact between the support pad and the membrane blocks some membrane pores and thus reduces the surface porosity, then it is expected that the R_m measured based on the perforated side should be higher than that of the channelled side (since the non-permeable part of the perforated side is higher, and thus the possible reduction in membrane surface porosity due to pore blocking is expected to be higher).

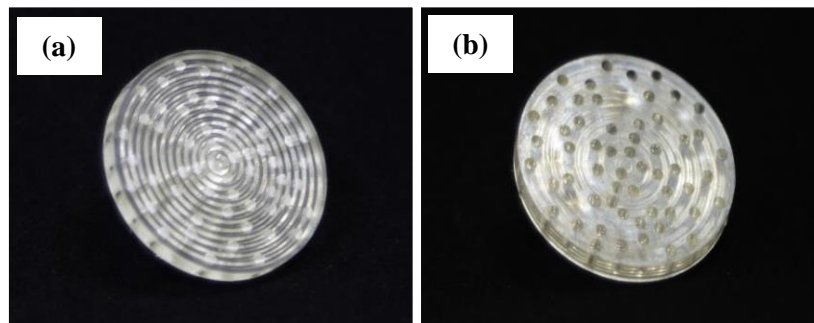


Figure 3.8: Membrane holder support pad; (a) channelled side, and (b) perforated side

3.3.7 Applying the MFI-UF to predict particulate fouling in a full-scale RO plant – with and without a correction for the surface porosity of the MFI-UF membrane

To illustrate the effect of surface porosity of the MFI-UF membrane, the MFI-UF was applied to predict the particulate fouling rate in a full-scale RO drinking water treatment plant. The RO plant produces drinking water from surface water with conventional pre-treatment processes, comprising micro strainers, coagulation, sedimentation, rapid sand filtration and granular activated carbon filtration, followed by 150 kDa UF membranes, and then 2-stage RO membranes. Water samples were collected from the RO feed and RO concentrate of the first stage ($J = 26 \text{ L/m}^2\cdot\text{h}$, $R = 57\%$). The MFI-UF of the collected RO feed and concentrate samples was measured using 5-10 kDa membranes at the same flux rate applied in the RO plant ($26 \text{ L/m}^2\cdot\text{h}$). Subsequently, the deposition factor (Ω) was determined (Equation (3.8)), and the NDP increase rate was predicted (Equation (3.7)) for each MFI-UF membrane. Finally, the agreement between the NDP increase rate observed in the plant and the NDP increase rate predicted based on the MFI-UF was assessed both with and without the correction for the effect of the surface porosity of the MFI-UF membranes (based on the outputs of the investigation addressed in the previous sections (3.3.3-3.3.6)).

3.4 RESULTS AND DISCUSSION

3.4.1 Membrane surface characterization – SEM analysis

Figure 3.9 presents the images of the surface of the 5, 10, 50 and 100 kDa membranes scanned by ultra-high resolution SEM (at a magnification of 500,000x). One important remark is that the pore openings shown in the SEM images might be narrowed or blocked just underneath the membrane surface. Therefore, the porous area scanned by SEM might be even smaller than in reality. Accordingly, the measurements of membrane surface

porosity and pore size distribution were considered as an indication and not as absolute figures.

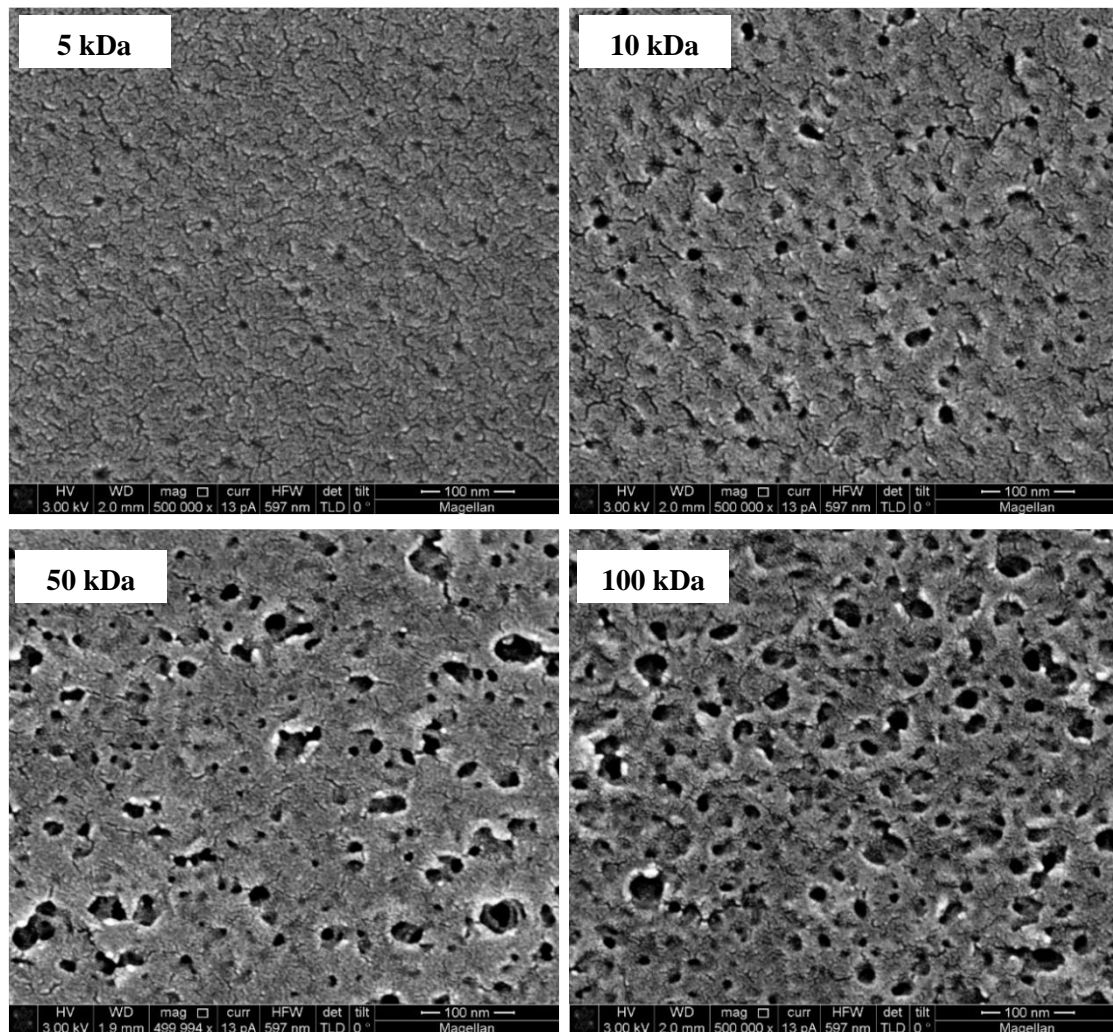


Figure 3.9: Ultra-high resolution SEM images of the surface of 5-100 kDa PES membranes (magnification of 500,000x)

Based on the SEM images, it was observed that the lower membrane MWCO, the lower the membrane surface porosity as well as the more the pores are non-uniformly distributed over membranes surface. In general, all membranes had low surface porosity; 0.6, 2.9, 6.1 and 10.5% for 5, 10, 50 and 100 kDa membrane, respectively.

The relationship between the membrane MWCO and the measured surface porosity was found to be logarithmic in the studied range, as shown in Figure 3.10. This means that the difference in surface porosity is major at lower MWCO, while it becomes less in the higher MWCO range. For instance, the difference in surface porosity between a 5 and 10 kDa membrane is a factor of 5 times, while the difference between a 95 and 100 kDa membranes is nearly negligible. This can be supported visually based in the SEM images

3. Quantifying the effect of the surface porosity of MFI-UF membrane

(Figure 3.9), where the difference in the surface porosity decreases markedly when the MWCO increases.

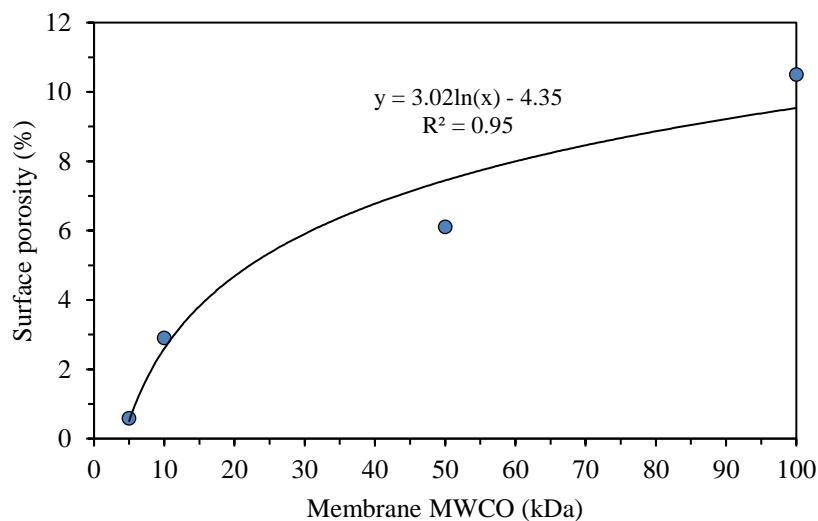


Figure 3.10: Relationship between membrane MWCO and surface porosity based on ultra-high resolution SEM analysis

Figure 3.11 shows the pore size distribution of the 5-100 kDa membranes based on a scanned area of 1 μm^2 (the pore size is the equivalent pore diameter assuming that the cross-sectional area of a pore is circular). As can be observed, the higher the membrane MWCO, the wider the pore size distribution. However, more than 60-80% of pores were within the size range of 6-12 nm. In addition, the mean pore size was similar for all membranes; 8.0, 9.2, 10.1 and 10.6 nm for 5, 10, 50 and 100 kDa membrane, respectively.

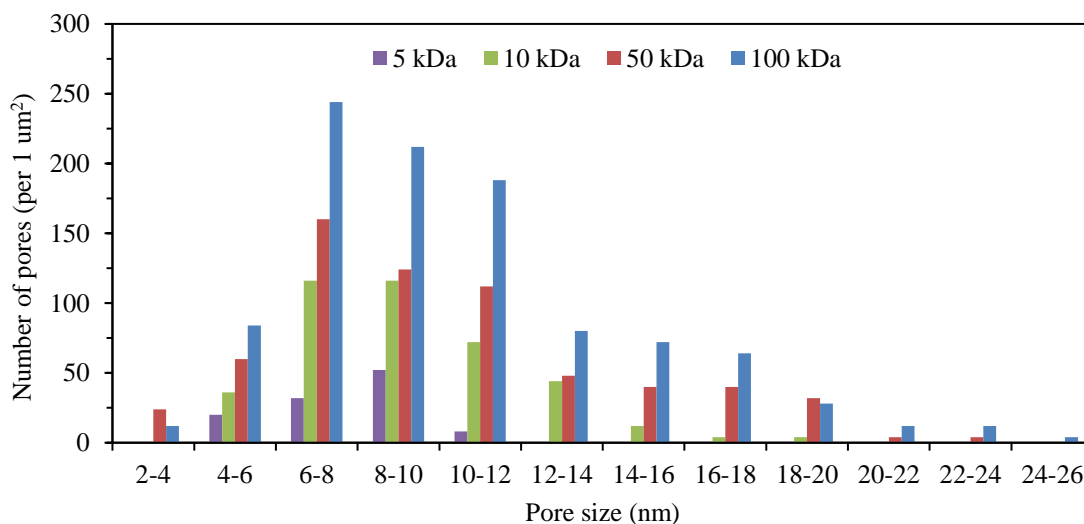


Figure 3.11: Pore size distribution of 5-100 kDa membranes based on ultra-high resolution SEM analyses

3.4.2 Theoretical effect of membrane surface porosity during the MFI-UF testing

Figure 3.12 shows the theoretical time required until the membrane surface area is completely covered by a particle-cake during an MFI-UF test, such that the effective filtration area is independent of the membrane surface porosity. The time was calculated assuming that membrane pores are uniformly distributed over the surface. This was done following to the steps explained in section 3.3.4, based on the measured membrane surface porosity and mean pore size characterized by ultra-high resolution SEM (section 3.4.1). As can be observed, the extent of the effect of membrane surface porosity was inversely correlated to the membrane MWCO (i.e. surface porosity as well). This is because the formed cake hemispheres (Figure 3.3 (b)) require more time to overlap and cover the entire membrane surface in case the interspacing between the membrane pores is larger (due to lower surface porosity).

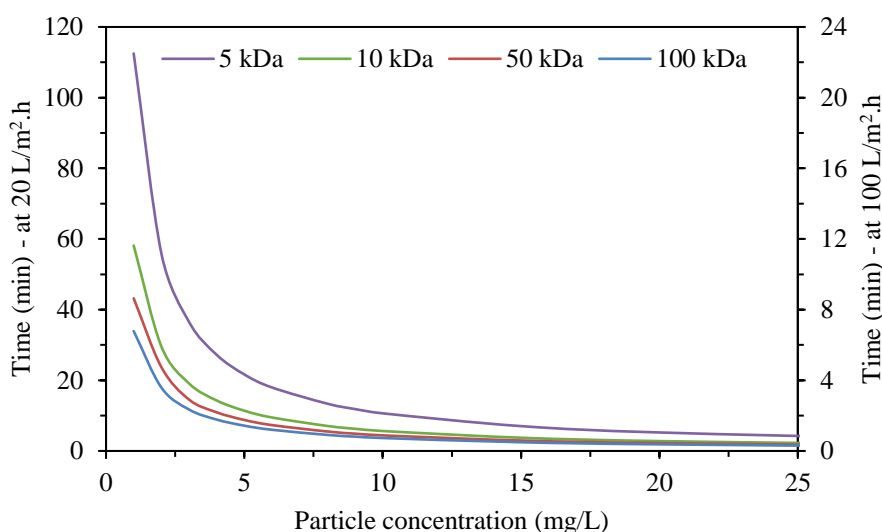


Figure 3.12: Time required until membrane surface is entirely covered by cake, assuming that the membrane pores are uniformly distributed over the surface

In addition, the theoretical calculations showed that the effect of membrane surface porosity is highly dependent on the flux rate applied in the MFI-UF test. This is because the lower the flux, the lower the load of particles depositing on the membrane surface over time, thus requiring more time for the particle-cake to cover the entire membrane surface. Accordingly, in Figure 3.12, since the difference between the flux of 20 L/m².h (left Y-axis) and 100 L/m².h (right Y-axis) is to a factor of 5, thus the calculated time required until the particle-cake covers the entire membranes surface at a flux of 20 L/m².h was 5 times longer than that at 100 L/m².h.

Moreover, based on Figure 3.12, the effect of membrane surface porosity appeared to dramatically decrease when the particle concentration increased (particularly at the

concentration range of 1-5 mg/L), where the cake formation takes relatively shorter time to cover the entire membrane surface since the load of particles depositing on membrane surface over time becomes higher. In the worst-case studied scenario; at 1 mg/L concentration, 5 kDa membrane and 20 L/m².h flux rate, the effect of membrane surface porosity would last for around 110 minutes. Whereas this duration decreases to 22 minutes when the particle concentration increases to 5 mg/L. Based on this theoretical calculation (Figure 3.12), it could be suggested that if the MFI-UF test was carried out for prolonged periods of time, then the measured MFI-UF value would be (theoretically) independent of the membrane surface porosity (i.e. the effect of membrane surface porosity would be temporary and diminishes in time as long as the MFI-UF test lasts long enough for a particle-cake to form on the entire membrane surface).

3.4.3 Quantifying the effect of membrane surface porosity on the measured MFI-UF

Figure 3.13 shows the MFI-UF of the feed suspension of washed polystyrene particles measured at a constant flux of 100 L/m².h, using a range of membranes (5, 10, 50 and 100 kDa) with different surface porosities. Complete particle retention was verified with all membranes, as shown in Figure 3.7. This means that the observed increase in the MFI-UF values could be attributed to the reduction in the surface porosity of the membrane and was independent of the membrane pore size.

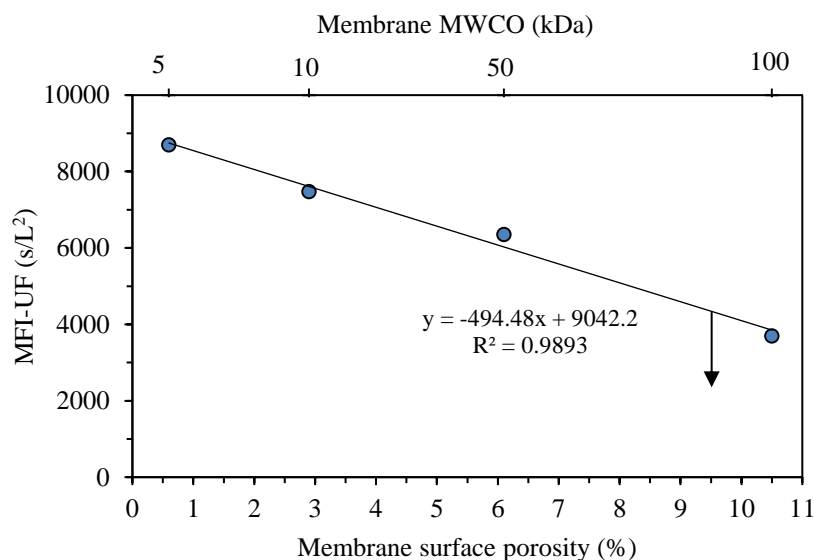


Figure 3.13: Relationship between MFI-UF of washed polystyrene particles suspension, membrane surface porosity and membrane MWCO

The measured MFI-UF value was linearly correlated to the membrane surface porosity, where the MFI-UF increased by around 500 s/L² per 1% decrease in the membrane surface porosity. However, by extrapolating the regression line, the MFI-UF value will

approach zero at higher surface porosity (18.3%), which is not possible. This means that the correlation between the MFI-UF and membrane surface porosity observed in Figure 3.13 is probably valid only in the studied range, while the correlation at higher surface porosities ($> 10.5\%$) should be further investigated.

However, the result of the MFI-UF dependency on the membrane surface porosity shown in Figure 3.13 is in conflict with the theoretical calculation illustrated in section 3.4.2. Whereas, based on Figure 3.12, the effect of membrane surface porosity should have diminished after less than 1 min of cake filtration at the same flux ($100 \text{ L/m}^2\cdot\text{h}$) and particle concentration (65 mg/L after polystyrene washing). Nevertheless, the effect of membrane surface porosity on the (experimentally) measured MFI-UF shown in Figure 3.13 was still observed although the duration of the MFI-UF tests was longer than 60 min.

The reason for this contradiction was attributed mainly to the pattern of surface porosity; i.e. the uniformity of pore distribution over the membrane surface. In the theoretical calculation, the pores were assumed to be identical in size and uniformly distributed over the membrane surface (equal inter-pores spacing). As it can be observed from Figure 3.9, the pore distribution shows non-uniformity across the membrane surface; with areas of the membrane surface being completely non-porous and other regions showing the presence of pores. This is exacerbated as the membrane MWCO decreases (mostly observed with the 5 and 10 kDa membranes). Consequently, cake formation might be permanently limited to the porous regions only, as illustrated in the schematic diagram in Figure 3.14 (left). In this case, the effective filtration area (A_{eff}) of the membrane is less than the geometric surface area (A). Subsequently, at constant pump flow (Q), the actual local flux through the formed cake (i.e. Q/A_{eff}) will be higher than that when the cake is evenly distributed over the entire membrane surface (Figure 3.14 (right)), which eventually results in higher (i.e. overestimated) MFI-UF.

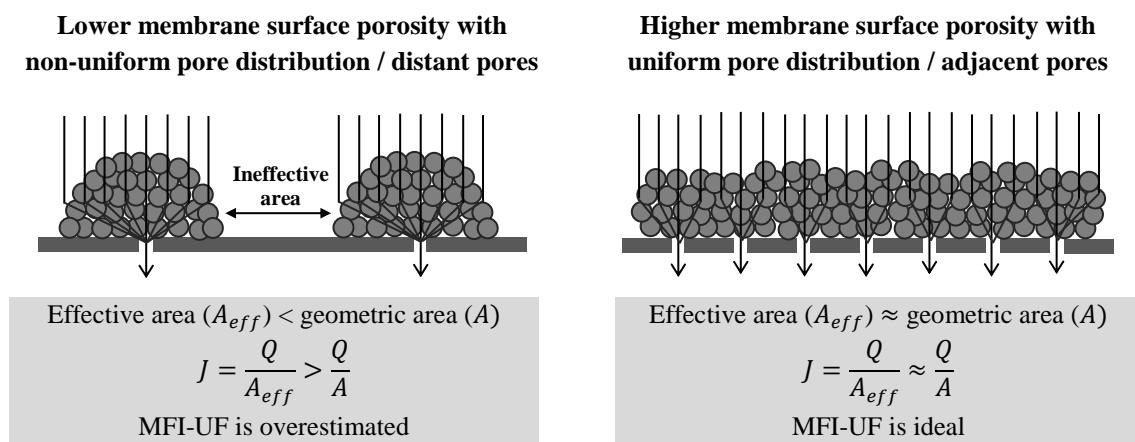


Figure 3.14: Schematic diagram illustrating the structure of the polystyrene particle cake formed on membrane with uniform and non-uniform pore distribution

According to the above explanation illustrated in Figure 3.14 and based on the results shown in Figure 3.9 and Figure 3.13, it could be concluded that the lower the membrane MWCO, the lower the membrane surface porosity, and the more non-uniformly the membrane pores are distributed and the greater the distance between the pores. Consequently, this results in smaller effective membrane filtration area, and subsequently higher local flux, which eventually leads to overestimation of the MFI-UF.

3.4.4 Correcting the effect of membrane surface porosity on the measured MFI-UF

In order to eliminate the effect of membrane surface porosity, the measured MFI-UF has to be corrected based on a reference/standard MFI-UF value where the effect of non-uniform membrane surface porosity is very low/negligible. Ideally, a theoretical reference MFI-UF value for the polystyrene particle suspension should have been calculated (using Equation (3.6)) where no effect of membrane surface porosity (i.e. cake covers the entire membrane surface) exists. However, the porosity of the cake formed on membrane surface is not known. Consequently, the reference MFI-UF has to be found experimentally. Based on the available ultra-high resolution SEM images (Figure 9), the 100 kDa membrane was identified as the membrane with the most uniformly distributed pores over membrane surface as well as with the shortest distance between membrane pores. Accordingly, it was expected that the effect of non-uniform surface porosity is low with this membrane. Therefore, the MFI-UF measured based on 100 kDa membrane was chosen as a reference to correct the effect of surface porosity of the other UF membranes with lower MWCO (and lower surface porosity). Nevertheless, the selection of a 100 kDa UF membrane as a reference should be further investigated to prove that the distribution of pores is indeed uniform across the membrane.

Since the MFI-UF increase due to the effect of membrane surface porosity was linear (Figure 3.13), the MFI-UF values could be corrected linearly in relation to the MFI-UF of a 100 kDa membrane. Accordingly, based on Figure 3.13, the identified correction factors are shown in Table 3.2. For example, the correction factor for the 5 kDa membrane = $\text{MFI-UF}_{100 \text{ kDa}}/\text{MFI-UF}_{5 \text{ kDa}} = 3700/8700 \text{ s/L}^2 = 0.4$.

Table 3.2: MFI-UF correction factors for the effect of membrane surface porosity (identified based on washed polystyrene particle suspension)

Membrane MWCO	5 kDa	10 kDa	50 kDa	100 kDa
MFI-UF correction factor	0.4	0.5	0.6	1.0

3.4.5 Effect of membrane holder support on membrane surface porosity

Figure 3.15 shows the R_m of 10 and 100 kDa membranes, measured with each side of the membrane holder support pad (Figure 3.8). As can be observed for each membrane MWCO, the average measured R_m was very similar for both sides of the support pad despite the major difference in the permeable area of the two sides (factor of 2). This could indicate that neither side of the support pad had any influence on membrane surface porosity and thus on the measured MFI-UF.

However, this result is in contrast with the findings of Nahrstedt and Camargo-Schmale (2008) and Salinas Rodriguez et al. (2019), where a strong effect was observed due to the membrane holder support pad on the surface porosity of a 0.45 μm MF membrane. The main reason can be attributed to the difference in the cross-sectional structure of the MF and UF membranes. The cross-section of the 0.45 MF membrane consists of only one layer where the pores extend from the top to the bottom of the membrane (Alhadidi et al., 2011d). Therefore, in the study of Nahrstedt and Camargo-Schmale (2008) and Salinas Rodriguez et al. (2019), the pores of the MF membrane were in direct contact with the support pad. As a result, the non-permeable part of the pad blocked the pores which were in contact with it, and consequently reduced the surface porosity of the MF membrane. On the other hand, the cross-section of the UF membranes used in this study has a composite structure consisting of two main parts; a filtration layer with interconnected pores in the top, and a supporting base layer in the bottom (Salinas-Rodríguez et al., 2015). Therefore, the top filtration layer of UF membrane (i.e. membrane pores) was not affected by the pad as there was no direct contact with it, as the bottom layer of membrane (support layer) was in between. In addition, the interconnectivity of the pores of UF membranes could also allow the water to flow through the membrane via different routes even if the pad blocked some of membrane pores.

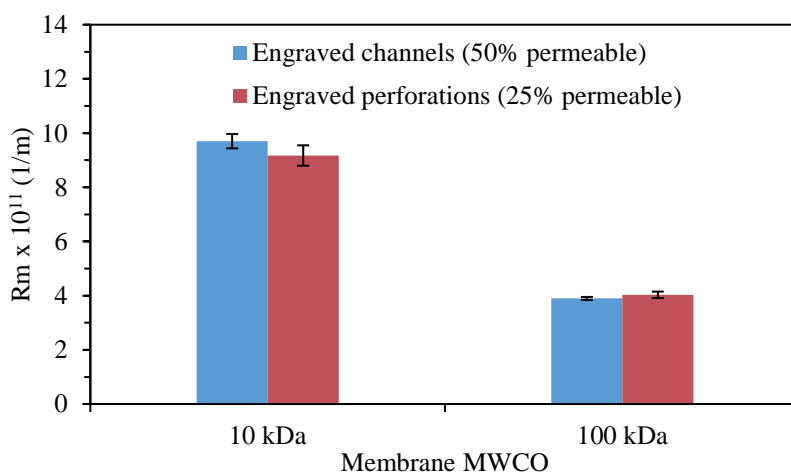


Figure 3.15: R_m of 10 and 100 kDa membranes measured based on both sides of the holder support pad

3.4.6 Effect of membrane surface porosity on the prediction of particulate fouling in a full-scale RO plant

Table 3.3 and Figure 3.16 show the inputs and the outputs of the MFI-UF fouling prediction model (Equation (3.7)), respectively. The MFI-UF values were calculated both before and after correcting for the effect of non-uniform membrane surface porosity. No further correction for the membrane holder support pad was incorporated since no impact was found on the MFI-UF due to the support pad (as illustrated in section 3.4.5).

3.4.6.1 Actual fouling observed in the RO plant

Figure 3.16 shows the actual NDP increase observed in an RO plant in the period after MFI-UF measurements. It should be noted that the observed NDP increase in the RO plant can be due to a number of fouling phenomena such as scaling, biological fouling, organic fouling and/or particulate/colloidal fouling or a combination of all of the above. Although, the various types cannot be ruled out completely, fouling in this plant was attributed mainly to particulates/colloids (i.e. formation of cake/gel by particles/colloids accumulated on the RO membrane surface) for the following reasons.

Firstly, even though the concentrate in first stage ($R = 57\%$) is supersaturated with respect to calcium carbonate (saturation index $SI = 1$) and barium sulphate ($SI = 2.4$), scaling is not expected to occur in the plant as antiscalant is dosed to the RO feed water (1.8 mg/L) to prevent precipitation of sparingly soluble salts. Moreover, the resulting saturation indices for both calcium carbonate and barium sulphate were low and in the range which can be easily controlled by the addition of antiscalant (Boerlage et al., 2002a; Mangal et al., 2022).

Secondly, the biofouling potential is also believed to be very low as the AOC concentration was below 10 ug/L in the RO feed water during the prediction period, which is often referred to as the threshold level to avoid biological fouling (van der Wielen and van der Kooij, 2010; Abushaban et al., 2019; Sousi et al., 2020a; Sousi et al., 2020b). Moreover, the TEP concentration in the RO feed water, which may help to kick-start biological fouling, was also very low, i.e. 0.26 mgXeq/L (Villacorte et al., 2015).

Thirdly, organic fouling (DOC concentration < 2.6 mg/L) due to the adsorption of organic matter directly onto the surface of the RO membrane is expected to occur prior to cake/gel formation when new/clean membranes are put into operation. However, in this case the RO membranes were already in operation for around 6 months (with membrane cleaning in place (CIP) performed only 2 times per year). Hence, the contribution of organic fouling is believed to be low and limited to the period of operation prior to cake/gel formation on the membrane.

Based on the above, the most likely type of fouling to occur in the RO plant is particulate/colloidal fouling reflected by the MFI-UF measured for the RO feed water.

The presence of particulate/colloidal matter in the RO feed (particularly after UF pre-treatment) may be due to (i) the passage of small colloids through the UF (150 kDa) which could be captured by the MFI-UF membrane (5-10 kDa), (ii) loss of integrity of the UF (i.e. broken fibres) which could allow particles/colloids to pass into the permeate stream (the UF integrity test is performed regularly in the plant, but loss in integrity might have occurred during the prediction period), (iii) re-aggregation of small particles/colloids that passed through the UF in the buffer tank located after the UF and prior to the RO, and/or (iv) re-growth of bacteria on the permeate side of the UF membrane (which are considered as particles).

3.4.6.2 Comparing actual and predicted particulate fouling rates in the RO plant

The NDP increase predicted based on the MFI-UF measured with 10 and 5 kDa membranes were substantially overestimated before correcting the effect of membrane surface porosity, i.e. the predicted rates of increase in NDP were about 3.0-4.5 times higher than the actual rate of increase in NDP observed in the RO plant. However, after correcting the effect of membrane surface porosity, the difference between the predicted and observed NDP decreased to 1.6-1.8 times, improving the prediction by around 50-60%.

Despite the improvement obtained by correcting the effect of membrane surface porosity, the NDP increase predicted based on the 10 and 5 kDa membranes was still overestimated. The reason is most likely due to the fact that the correction factors were obtained based on a feed suspension of (synthetic) monodisperse polystyrene particles, which are rigid and thus hardly compressible. On the other hand, natural water (i.e. RO feed) comprises many different types of particles which are likely to be more deformable and compressible (such as the particulate/colloidal organic material released by bacteria and algae). In addition, particles in natural water are expected to have a wider range of sizes, shapes and densities. Subsequently, small particles can fill the voids between the larger particles in the cake formed on the MFI-UF membranes. Hence, the cake formed by natural particles might be more compressed and less porous than that formed by polystyrene particles. Consequently, since the MFI-UF is highly dependent on cake porosity (Equation (3.6)), the effect of non-uniform distribution of membrane pores on the cake and thus on the MFI-UF might be greater for real RO feed/concentrate than for a polystyrene particle suspension. As a result, the correction factors estimated based on the (synthetic) polystyrene particles might have underestimated the effect of non-uniform membrane surface porosity on the MFI-UF of real RO feedwater.

Therefore, future research on understanding the effect of non-uniform membrane surface porosity should focus on searching for and testing different types of particles (and mixtures of particles) which exhibit similar properties to natural particles existing in real water (i.e. RO feed).

3. Quantifying the effect of the surface porosity of MFI-UF membrane

Table 3.3: Main inputs of the MFI-UF fouling prediction model (Equation (3.7))

Membrane MWCO	10 kDa	5 kDa
MFI-UF of RO feed (without with correction)	1580 s/L ² 790 s/L ²	2130 s/L ² 850 s/L ²
MFI-UF of RO conc. (without with correction)	2440 s/L ² 1220 s/L ²	3200 s/L ² 1280 s/L ²
Deposition factor (Ω)	0.59	0.62
Flux (J)	26 L/m ² .h	
Viscosity (normalized temp of 25 °C)	0.00089 N.s/m ²	

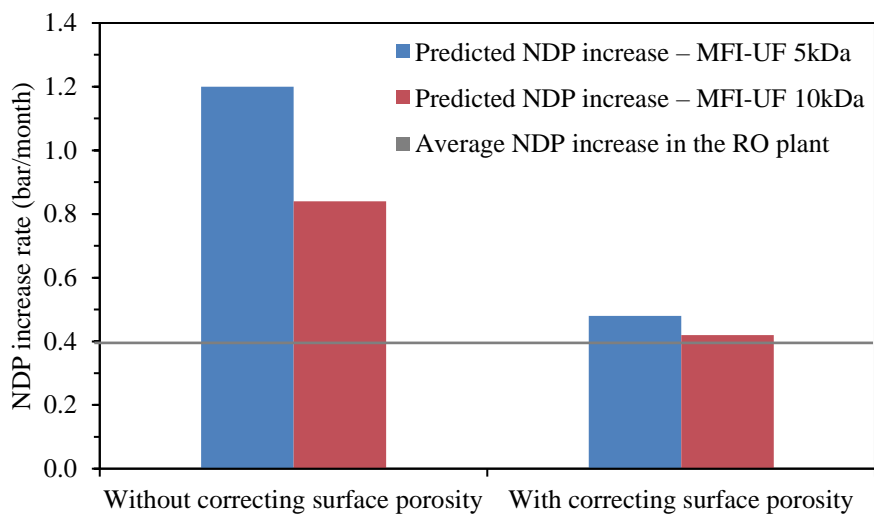


Figure 3.16: Predicted NDP increase rates with and without correcting the MFI-UF for the effect of non-uniform membrane surface porosity

3.5 CONCLUSIONS

This study investigated the effect of membrane surface porosity on the MFI-UF, measured at constant flux, with flat-sheet PES UF membranes with a MWCO of 5, 10, 50 and 100 kDa. The following were the main conclusions:

- Ultra-high resolution SEM analysis showed that the lower the membrane MWCO, the lower the membrane surface porosity, and the more non-uniformly the pores are distributed over membrane surfaces.
- A new approach, using suspensions of pre-washed polystyrene particles (75 nm), was successfully developed and applied to experimentally verify and quantify the effect of membrane surface porosity on the MFI-UF independently of membrane pore size.

- Based on the results of the newly developed approach, the MFI-UF was found to be highly dependent on membrane surface porosity; i.e. pore distribution over the membrane surface. The results indicated that in case of a non-uniform distribution of pores, cake formation might not be distributed evenly over the entire membrane surface and may be limited only to the porous regions. This results in a smaller effective filtration area, and subsequently a higher local flux, which eventually leads to overestimation of the measured MFI-UF.
- Accordingly, correction factors of 0.4, 0.5, 0.6 and 1.0 were identified to correct the MFI-UF for the effect of surface porosity of the 5, 10, 50 and 100 kDa membrane, respectively.
- Correcting the MFI-UF for the effect of membrane surface porosity significantly improved the prediction of particulate fouling in a full-scale RO plant, by around 50-60%. Nevertheless, despite the improvement, the predicted particulate fouling rate was still overestimated. The reason was attributed to the difference in the properties of polystyrene particles (used to estimate the correction factors) and natural particles which exist in real RO feed water (i.e. the cake formed by natural particles may have lower porosity and thus higher resistance compared to that formed by synthetic polystyrene particles).

In addition, the findings of this study can be used as a basis for recommended investigations for future research, including:

- Investigating and quantifying the effect of membrane surface porosity using different types of organic and inorganic particles (and mixtures of particles) which exhibit similar properties to particles that exist in real water (e.g. RO feed). Eventually, 'global' correction factors should be proposed for different types of feed water.
- Investigating the effect of membrane surface porosity for higher MWCO UF membranes (i.e. with higher surface porosity); verifying the assumption that there is low/negligible effect due to surface porosity on the MFI-UF with membranes of $\text{MWCO} \geq 100$ kDa. However, the size of tested particles should be further investigated in this case (as membrane pore size is expected to be higher with $\text{MWCO} \geq 100$ kDa) to ensure the criterion of complete particle retention (i.e. to quantify the effect of membrane surface porosity independently of membrane pore size).
- In addition to the effect of membrane surface porosity investigated in this study, further work is required to examine also the effect of pore size distribution on the measured MFI-UF and thus on the predicted particulate fouling rate. This can give a more complete picture of the overall effect of membrane surface properties on particulate fouling prediction.

3.6 ANNEXES

Annex 3.6.1: Particle technical sheet

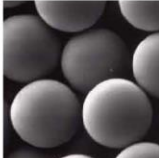
Polystyrene particles (75 nm)



Bangs Laboratories, Inc.
BEADS ABOVE THE REST

Polystyrene Microspheres

Product Data Sheet 732



DESCRIPTION

Polystyrene microspheres present a flexible platform for applications in diagnostics and bioseparations. They may be coated with ligands such as antibodies, antigens, peptides, or nucleic acid probes, and can be loaded with hydrophobic dyes and other compounds. Polystyrene microspheres also are used extensively as standards for instrument set-up and calibration.

Plain polystyrene microspheres may be protein coated via adsorption, and have been utilized in a range of diagnostic tests and assays. Reference *TechNote 204, Adsorption to Microspheres*, for a general protocol and additional information & references.

Surface-modified microspheres are available with carboxyl or primary amine groups for covalent ligand attachment. *TechNote 205, Covalent Coupling*, details a basic foundation for successful attachment of a variety of ligands through coupling protocols, buffer recipes, blockers, and references. See bangslabs.com for available coupling reagents and kits.

Our polystyrene spheres are synthesized via emulsion polymerization, and are available in diameters from ~20nm to 20µm, with typical CVs of 5-10%. For applications requiring highly stringent CVs (e.g. 2-5%), please contact our Customer Service group.

CHARACTERISTICS

Mean Diameter:	20nm - 20µm
Particle Concentration:	10% solids (100 mg/mL)
Surface Functionality:	COOH - titrated Lot-specific values provided on our website or CoFA NH ₂ - ninhydrin confirmation (non-quantitative)

STORAGE AND STABILITY

Store at 2-8°C. Freezing, drying, or aggressive centrifugation of microsphere suspension may result in irreversible aggregation and loss of binding activity. Uncoated polymer microspheres are not assigned expiration dates.

SAFETY

These particle suspensions may contain sodium azide. Sodium azide may react with lead and copper plumbing to form explosive metal azides. Upon disposal of material, flush with a large volume of water to prevent azide accumulation. Please consult the product specific SDS for more information.

These products are for research use only and are not intended for use in humans or for *in vitro* diagnostic use.

ORDERING INFORMATION - Standard units available are 0.5g, 1.0g, 1.5g, or 5.0g

PLAIN POLYSTYRENE MICROSPHERES

Catalog Number	Diameter	Diameter Range	Catalog Number	Diameter	Diameter Range
PS02001	0.025µm	0.015-0.035	PS03002	0.600µm	0.570-0.630
PS02002	0.050µm	0.040-0.060	PS03003	0.700µm	0.670-0.730
PS02003	0.075µm	0.065-0.085	PS03004	0.800µm	0.770-0.830
PS02004	0.100µm	0.090-0.110	PS03005	0.900µm	0.870-0.930
PS02005	0.125µm	0.115-0.135	PS04001	1.00µm	0.95-1.05
PS02006	0.150µm	0.140-0.160	PS05001	2.00µm	1.80-2.20
PS02007	0.175µm	0.165-1.185	PS05002	3.00µm	2.80-3.20
PS02008	0.200µm	0.190-0.210	PS05003	4.00µm	3.80-4.20
PS02009	0.300µm	0.270-0.330	PS06001	5.00µm	4.80-5.20
PS02010	0.400µm	0.370-0.430	PS06002	5.50µm	5.30-5.70
PS03001	0.500µm	0.470-0.530	PS06003	6.00µm	5.80-6.20

9025 Technology Dr. Fishers, IN 46038 • www.bangslabs.com • info@bangslabs.com • 317.570.7020 • fax 317.570.7034

PDS 732 Rev #005, Active: 17/January/2019 Page 1 of 2

PDS 732

PLAIN POLYSTYRENE MICROSPHERES CONTINUED

Catalog Number	Diameter	Diameter Range
PS06004	7.00µm	6.80-7.20
PS06005	7.50µm	7.30-7.70
PS07001	10.00µm	9.50-10.50
PS07002	15.00µm	14.50-15.50
PS07003	20.00µm	19.00-21.00
PS08001	>25.µm	>25.µm

CARBOXYL POLYSTYRENE MICROSPHERES

Catalog Number	Diameter	Diameter Range
PC02001	0.025µm	0.015-0.035
PC02002	0.050µm	0.040-0.060
PC02003	0.070µm	0.060-0.080
PC02004	0.100µm	0.090-0.110
PC02005	0.125µm	0.115-0.135
PC02006	0.150µm	0.140-0.160
PC02007	0.175µm	0.165-0.185
PC02008	0.200µm	0.190-0.210
PC02009	0.300µm	0.270-0.330
PC02010	0.350µm	0.340-0.360
PC02011	0.400µm	0.370-0.430
PC03001	0.500µm	0.470-0.530
PC03002	0.600µm	0.570-0.630
PC03003	0.800µm	0.770-0.830
PC03004	0.900µm	0.870-0.930
PC04001	1.00µm	0.95-1.05
PC05001	2.00µm	1.80-2.20
PC05002	2.50µm	2.30-2.70
PC05003	3.00µm	2.80-3.20
PC05004	4.00µm	3.80-4.20
PC05005	4.50µm	4.30-4.70
PC06001	5.00µm	4.80-5.20
PC06002	5.50µm	5.30-5.70
PC06003	6.00µm	5.80-6.20
PC06004	7.00µm	6.80-7.20
PC07001	10.00µm	9.50-10.50
PC07002	15.00µm	14.50-15.50
PC07003	20.00µm	19.00-21.00
PC08001	>25.µm	>25.µm

AMINE POLYSTYRENE MICROSPHERES

Catalog Number	Diameter	Diameter Range
PA02001	0.200µm	0.190-0.210
PA03001	0.500µm	0.470-0.530
PA03002	0.750µm	0.740-0.760
PA04001	1.00µm	0.95-1.05

ADDITIONAL RESOURCES

TN203 Washing Microspheres
 TN204 Adsorption to Microspheres
 TN205 Covalent Coupling
 TSD 0300 Buffers
 PDS 731 Fluorescent Microspheres
 Microsphere Reagent Guide

Order online anytime at www.bangslabs.com.

3. Quantifying the effect of the surface porosity of MFI-UF membrane

Silver particles (80 nm)

SIGMA-ALDRICH[®]

sigma-aldrich.com

3050 Spruce Street, Saint Louis, MO 63103, USA

Website: www.sigmaaldrich.com

Email USA: techserv@sial.com

Outside USA: eurtechserv@sial.com

Product Specification

Product Name:

Silver nanospheres - 80 nm avg. part. size, 0.02 mg/mL in water, PVP functionalized

Product Number: 795992

Storage Temperature: 2 - 8 °C

TEST	Specification
Appearance (Color)	Light Yellow to Yellow and Light Brown to Brown
Appearance (Form)	Liquid
Wavelength	
Report Result	
ICP Major Analysis	Confirmed
Confirms Silver Component	
Diameter	
Hydrodynamic (Report Result)	
Surface Area	
Report Result (TEM)	
Concentration	
Mass (Ag)(Report Result)	
Particles/ml	Confirmed
7.4E+ 09 particles/mL	
Diameter	Confirmed
80 nm	
Miscellaneous Supplier Data	
Zeta Potential (mV)(Report Result)	
pH	
Report Result	
Silver (Ag)	Confirmed
99.99%	
Miscellaneous Supplier Data	Confirmed
Particle Surface: PVP	
Recommended Retest Period	-----
1 year	

Sigma-Aldrich warrants, that at the time of the quality release or subsequent retest date this product conformed to the information contained in this publication. The current Specification sheet may be available at Sigma-Aldrich.com. For further inquiries, please contact Technical Service. Purchaser must determine the suitability of the product for its particular use. See reverse side of invoice or packing slip for additional terms and conditions of sale.

SIGMA-ALDRICH[®]*sigma-aldrich.com*

3050 Spruce Street, Saint Louis, MO 63103, USA

Website: www.sigmaaldrich.comEmail USA: techserv@sial.comOutside USA: eurtechserv@sial.com

Product Specification

Product Name:

Silver nanospheres - 80 nm avg. part. size, 0.02 mg/mL in water, PVP functionalized

Product Number: **795992**

Storage Temperature: 2 - 8 °C

TEST**Specification**

Specification: PRD.1.ZQ5.10000054639

Sigma-Aldrich warrants, that at the time of the quality release or subsequent retest date this product conformed to the information contained in this publication. The current Specification sheet may be available at Sigma-Aldrich.com. For further inquiries, please contact Technical Service. Purchaser must determine the suitability of the product for its particular use. See reverse side of invoice or packing slip for additional terms and conditions of sale.

2 of 2

Pullulan particles (800 kDa)

SIGMA-ALDRICH

3050 Spruce Street, Saint Louis, MO 63103 USA
 Email USA: techserv@sial.com Outside USA: eurtechserv@sial.com

Certificate of Analysis

Product Name: Pullulan Standard 800,000
 certified reference material, certified according to DIN, for GPC

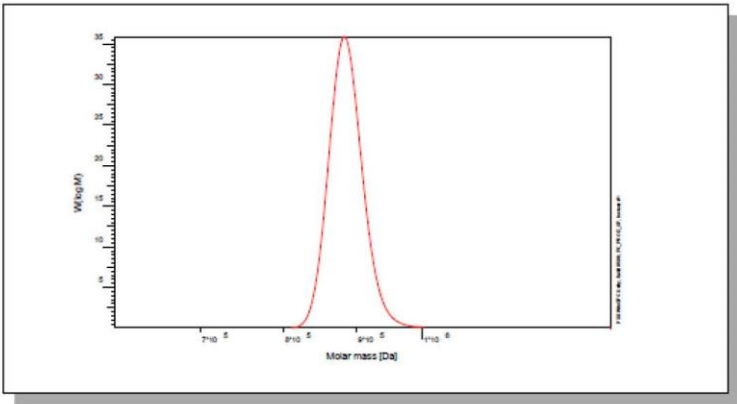
Product Number: 18789

Batch Number: BCBV1207

Brand: Sigma-Aldrich

Expire Date: EXPIRY DATE PRINTED ON LABEL

Molar Mass Distribution



GPC/SEC - Conditions

Sample concentration	0,70 g/l	Inject volume	100 µl
Solvent	Water, Sodium azide 0.02%	Flow rate	1,00 ml/min
Precolumn [8 x 50 mm]	PSS SUPREMA 10µm	Temperature	30 °C
Columns [analytical, each 8 x 300 mm]	PSS SUPREMA 10µm 100Å / 10 000Å		
Data Acquisition Software	PSS WinGPC		

GPC/SEC - Results

Detector	Mw [Da]	Mn [Da]	Mp [Da]	PDI [Mw/Mn]
Agilent RID	805000	636000	708000	1,27

Additional Methods - Results

Method	Mw [Da]
Light Scattering, on-line	855 000

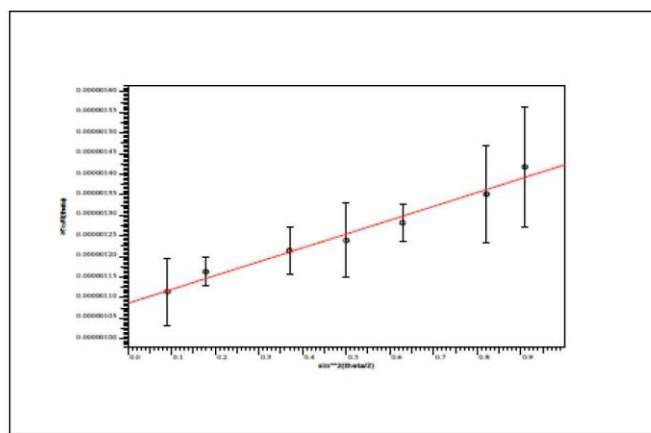
Note: All analysis run according to ISO EN 13885 and DIN 55672
 Mw = Weight average molecular weight
 Mn = Number average molecular weight
 Mp = Molar mass at the peak maximum
 PDI = Polydispersity Index

Sigma-Aldrich
Certificate of Analysis - Product 18789 Lot BCBV1207
Page 1 of 2

SIGMA-ALDRICH3050 Spruce Street, Saint Louis, MO 63103 USA
Email USA: techserv@sial.com Outside USA: eurtechserv@sial.com**Light Scattering - Conditions**

Light Scattering run on-line, based on Toluene Rayleigh Ratio $R_{\theta} = 1.404 \cdot 10^{-5} \text{ cm}^{-1}$ at 633 nm.
System and instrument validation based on DIN-Pullulan Lot No: p-100di.

Instrument	PSS SLD7000 MALLS detector, 637 nm
Data Acquisition Software	using 7 angles: 35°, 50°, 75°, 90°, 105°, 130°, 145°
Solvent	Water, Sodium azide 0.02%
Temperature	30 °C
Flow rate	1,00 ml/min
Precolumn [8 x 50 mm]	PSS SUPREMA 10µm
Columns [analytical, each 8 x 300 mm]	PSS SUPREMA 10µm 100Å / 10 000Å
Sample concentration	0,70 g/l
Inject volume	100 µl
Sample dn/dc	0.148 ml/g

Light Scattering - Zimm Plot

09 MAY 2017

Dr. Claudia Geitner
Manager Quality Control
Buchs, Switzerland

Sigma-Aldrich warrants that at the time of the quality release or subsequent retest date this product conformed to the information contained in this publication. The current specification sheet may be available at Sigma-Aldrich.com. For further inquiries, please contact Technical Service. Purchaser must determine the suitability of the product for its particular use. See reverse side of invoice or packing slip for additional terms and conditions of sale.

Annex 3.6.2: Preliminary investigations of polystyrene particle washing

Polystyrene particles were washed to remove the small components resulted by the manufacturing process (i.e. small particle fractions and surfactant). For this purpose, several washing techniques were investigated, addressed below in details.

Centrifugation

Centrifugation is one of the simplest techniques to wash the particles. In this technique, a particle suspension is placed in a tube which rotates in a defined speed. As a result, a centrifugal force is applied on the particles, and thus the particles can be separated and settled. Settling velocity depends highly on the particle size. Hence, while the large particles are settled, the existing small components may still remain in suspension. In this way, the large settled particles can be collected from the tube base and re-suspended again.

Settling velocity (V) of polystyrene particles could be calculated based on the Stokes' Law described by Equation (A - 3.1).

$$V = \frac{g \cdot d^2 \cdot (\rho_1 - \rho_2)}{18 \cdot \eta} \quad (A - 3.1)$$

Where d is the particle diameter (75 nm), ρ_1 is the particle density (1.05 g/cm³), ρ_2 is the suspending water density (1 g/cm³), η is the water viscosity (at room temperature of 22 °C), and g is the gravitational force (relative centrifugation force). The definition of g value was challenging; where high g can lead to re-suspend the settled particles, while low g may be insufficient for particles separation. Based on g value of 10,000, V will be 0.000164 cm/s. With using a centrifugal tube of 10 cm, then the required centrifugation duration will be around 17 hours. However, the centrifugation process should be repeated several times to ensure the complete removal of all existed small components, and this will subsequently require longer time. Therefore, using the centrifugation technique for washing the polystyrene particles (75 nm) seemed to be problematic, since it may need much time and effort to optimize the operation conditions (particularly g force and frequency), and this was out of the scope of this study. Consequently, washing the polystyrene particles by centrifugation was not proceeded.

Dialysis

Particles can be also washed by dialysis, where the small components associated in the particle suspension can be removed by diffusion through a dialysis membrane tube. This can be done as follows. The particles suspension is filled in a dialysis tube with pore size smaller than the particles to be washed but larger than the small components to be removed. The tube is then placed in a container containing blank water (dialysate). The particles and all other existing small components will tend to diffuse through the dialysis

membrane due to the difference in concentration between inside and outside the tube. As a result, all the components smaller than the membrane pore size will pass to the dialysate while the larger particles will be rejected and remain in the feed inside the tube. The time required for the dialysis to be accomplished depends on many factors; concentration differential, membrane pore size, ratio of the tube surface area to volume, and temperature. The dialysis process can be accelerated by placing the dialysis system on a shaker or a magnetic stirrer.

The dialysis of polystyrene particles was done using cellulose ester dialysis membrane tube with MWCO of 300 kDa and flat width of 31 mm (Repligen). A polystyrene particle suspension of 100 mg/L was prepared and placed in a dialysis tube with a length of 10 cm. The tube was closed and placed in a dialysate of ultra-pure water (Milli-Q, Millipore). Since the optimum duration of the dialysis was unknown in advance, the dialysis experiment was performed along 15 days, while the dialysate was being replaced on a daily basis.

Figure A - 3.1 shows the MFI-UF of the suspension of polystyrene particles washed by dialysis. As can be observed, washing was not effective, where the complete particle retention was not achieved as indicated by the high MFI-UF values of the permeates. Moreover, the MFI-UF of washed particle suspension was much higher than the MFI-UF of same polystyrene particle suspension before particles washing. The increase in the MFI-UF could be likely due to the bacterial growth since the dialysis process was performed for a long duration (15 days) in presence of organic matter (surfactant). Other reasons could be attributed to the micelles formation of the surfactant associated with the polystyrene particles, and/or leaching of some substances from the dialysis membrane. However, these reasons were not further investigated.

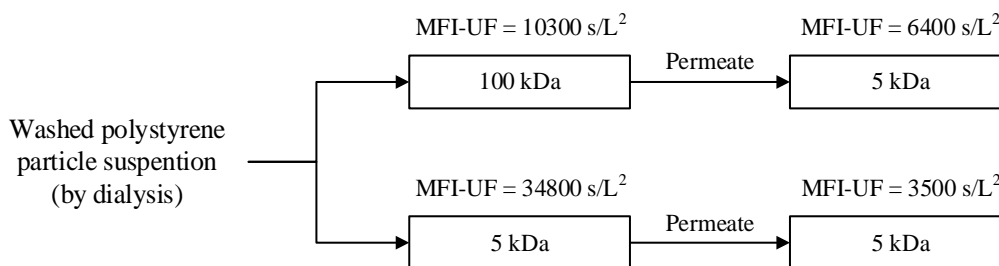


Figure A - 3.1: Verifying the effect of membrane surface porosity on the MFI-UF using a suspension of polystyrene particles washed by dialysis

Unstirred dead-end filtration

Unstirred dead-end filtration is the simplest way to wash the particles; where the particles suspension can be filtered in dead-end mode through a membrane which have a pore size smaller than the particles to be washed but larger than the other small components in the

suspension which should be removed. After that, the membrane surface is flushed well with blank water to re-suspend the retained washed particles.

The efficiency of unstirred dead-end filtration to wash the polystyrene particles was examined by filtering a polystyrene particles suspension with 100 mg/L concentration through a 100 kDa membrane. This was done at constant flux of 100 L/m².h using the MFI-UF set-up. After the filtration was done, the membrane was flushed to re-suspend the retained polystyrene particles using 100 mL of ultra-pure water (Milli-Q, Millipore).

As shown in Figure A - 3.2, the washing was insufficient, where the criterion of complete particle retention was not satisfied as it could be indicated from the MFI-UF values of the permeates which were considerably high. The reason could be because during the washing (i.e. dead-end filtration), the components smaller than the pore size of the washing membrane could be also retained due to the membrane pore blocking, particle bridging, and/or trapping between the larger particles in the formed cake (Boerlage et al., 2003a). As a result, these small components could be still associated with the washed particles.

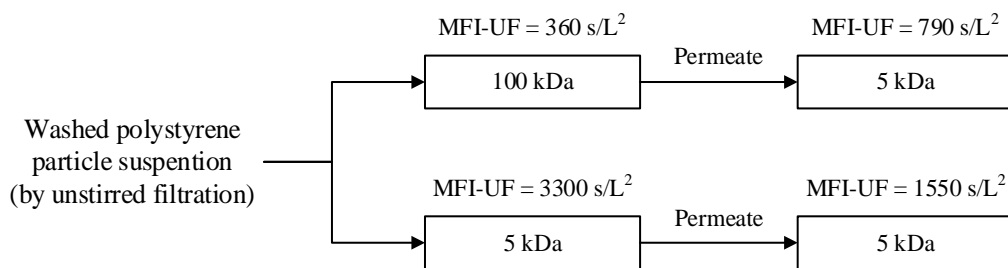


Figure A - 3.2: Verifying the effect of membrane surface porosity on the MFI-UF using a suspension of polystyrene particles washed by unstirred dead-end filtration

Stirred dead-end filtration

Stirred dead-end filtration is dead-end filtration enhanced by stirring which generates shear force across the membrane surface preventing/limiting the cake formation. As a result, small components may not be trapped in the cake (as in the case of unstirred filtration), and thus can pass through the membrane.

Washing polystyrene particles by stirred dead-end filtration was done at constant pressure using 200 mL stirred UF cell (Amicon, Millipore) including a 500 kDa PES membrane (Biomax, Millipore). The cell was connected to a pressure vessel filled with an ultra-pure water (Milli-Q, Millipore) for the washing purpose. A suspension sample of polystyrene particles was placed in the filtration cell. During the filtration (i.e. washing) process, the suspension sample was being diluted by the ultra-pure water and simultaneously filtered through the membrane. The quality of filtrate water was checked along the filtration time

in terms of TOC. The washing was considered acceptable when the TOC of filtrate became equal to that of the ultra-pure water ($\text{TOC} < 0.2 \text{ mg/L}$).

The efficiency of stirred dead-end filtration process was initially examined at a constant pressure of 250 mbar, while the filtration process lasted for around 6 hours (after reaching the stopping criterion mentioned above). As can be observed from Figure A - 3.3, the washing was insufficient, similarly as the case of washing by dialysis and unstirred dead-end filtration illustrated above.

Therefore, the washing was further enhanced with replacing the membrane twice (i.e. 3 membranes in total were used) at a lower pressure of 100 mbar (i.e. lower flux), while the overall filtration was performed for a duration of around 8 hours. Particle washing at these conditions achieved the criterion of complete particle retention where the MFI-UF of the permeate was below the LOD value ($< 200 \text{ s/L}^2$) with all membranes, which indicated that the particles in the feed suspension were completely retained on the 5-100 kDa membranes. Accordingly, this approach was adopted to wash the polystyrene particles, and consequently verify the effect of membrane surface porosity on measured MFI-UF.

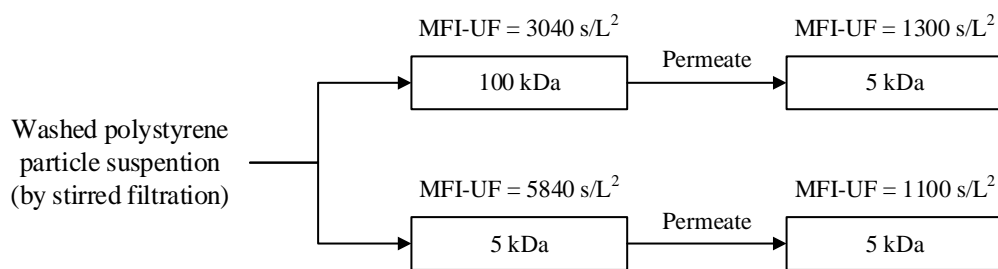


Figure A - 3.3: Verifying the effect of membrane surface porosity on the MFI-UF using a suspension of polystyrene particles washed by stirred dead-end filtration at 250 mbar using 1 membrane (500 kDa)

4

PREDICTION OF PARTICULATE FOULING IN FULL-SCALE REVERSE OSMOSIS PLANTS USING THE MFI-UF METHOD

This study aimed at applying and verifying the MFI-UF method to predict particulate fouling in RO plants. Two full-scale RO plants treating surface water, with average capacity of 800-2,000 m³/h, were studied. Firstly, the MFI-UF of RO feed and concentrate was measured using 5-100 kDa membranes at same flux applied in the RO plants (20-26 L/m².h). Subsequently, the particle disposition factor (Ω) was calculated to simulate particle deposition in RO cross-flow filtration. Finally, particulate fouling rates were predicted based on the measured MFI-UF and Ω , and compared with the actual fouling rates in the plants. For plant A, the results showed that the fouling rates predicted using MFI-UF measured with 100 kDa membrane have the best agreement with the actual fouling (with 3-11% deviation). For plant B, the fouling rates predicted based on both 10 and 100 kDa membranes agreed well with the actual fouling (with 2% and 15% deviation, respectively). However, the fouling predicted based on 5 kDa membrane was considerably overestimated for both plants, which is attributed to the effect of the low surface porosity of 5 kDa membrane. More widespread applications of MFI-UF in full-scale RO plants are required to demonstrate the most suitable MFI-UF membranes for fouling prediction.

4.1 INTRODUCTION

Reverse osmosis (RO) technology has been rapidly growing in the water treatment sector due to the continuous advancements in both design and operation (DesalData, 2020). However, RO membrane fouling still remains a key challenge. Fouling can cause a decline in the RO membrane permeability. Consequently, higher energy and more frequent membrane cleaning are required to maintain water production, which eventually results in increased O&M costs.

Particulate fouling, due to the deposition of particles and colloids on the membrane, is one of the types of fouling which is persistently experienced in RO plants. Therefore, there is a need for a reliable method which can accurately measure and predict the particulate fouling, allowing the performance of RO plants to be assessed and monitored. The existing ASTM standard assessment methods; silt density index (SDI) (ASTM, 2014) and modified fouling index (MFI-0.45) (ASTM, 2015), simulate particulate fouling using a 0.45 μm membrane. Thus, the effect of small colloids ($< 0.45 \mu\text{m}$), which are more likely to be responsible for RO membrane fouling, is not evaluated in either method (Schippers et al., 1981). Consequently, a more promising method; the modified fouling index – ultrafiltration (MFI-UF) was developed, whereby a UF membrane is used in order to capture smaller colloids (Boerlage et al., 1997; Boerlage et al., 1998; Boerlage et al., 2000; Boerlage et al., 2003a; Boerlage et al., 2003b). The MFI-UF was performed initially at constant pressure (as is the MFI-0.45 and SDI). Later, the method was developed further to be measured at constant flux in order to simulate the operation of RO plants in practice (Boerlage et al., 2004; Salinas-Rodríguez et al., 2015). Furthermore, the measured MFI-UF (at constant flux) can be used in a model to predict the rate of particulate fouling during RO system operation (Schippers et al., 1981; Salinas-Rodríguez et al., 2015).

The MFI-UF test is performed in dead-end filtration mode. Hence, all particles in the feed water move directly towards the surface of the MFI-UF membrane during the test. However, RO plants are typically operated in cross-flow filtration mode, where the particles in the RO feed water either move towards the RO membrane surface or are transported to the concentrate (Tang et al., 2011). The portion of particles depositing on RO membranes can be determined by the particle deposition factor proposed by Schippers et al. (1981), by taking in account the difference in particle concentration between the RO feed and RO concentrate. Consequently, the particle deposition factor is incorporated in the MFI-UF model to consider only that portion of particles depositing on RO membranes during cross-flow filtration (Schippers et al., 1981; Salinas-Rodríguez et al., 2015).

Sim et al. (2010) and Sim et al. (2011a) proposed another approach to simulate particle deposition in RO filtration, i.e. using a cross-flow sampler (CFS) prior to the MFI-UF set-

up. The function of the CFS is to fractionate the particles in the feed water under the same hydrodynamic conditions as in RO cross-flow filtration. For this purpose, a non-retentive membrane with large straight-through pores ($\geq 5 \mu\text{m}$) is used in the CFS, so that all particles moving near the membrane surface can permeate through. Subsequently, the permeate collected from the CFS should contain all potential particles which will likely deposit on the RO membrane. Despite the innovation of this method in simulating RO cross-flow filtration, it does not consider the potential detachment of particles deposited on the RO membrane during actual operation. In RO cross-flow filtration, particle deposition is not static and the particles already deposited on the membrane can be re-suspended and transported away from the membrane as a result of the hydrodynamic forces induced on the particles by the tangential flow as well as upon the collision with other flowing particles (Boerlage et al., 2003a; Henry et al., 2012). Accordingly, the MFI-UF method incorporating the concept of a particle deposition factor has the advantage that it can reflect both the deposition as well as the detachment of particles by considering the ratio of actual particle load in both the RO feed and RO concentrate.

Particulate fouling rates predicted based on the MFI-UF depend strongly on the testing conditions applied during the MFI-UF test, namely; flux rate and UF membrane molecular weight cut-off (MWCO), as explained below.

The measured MFI-UF can be greatly affected by the flux rate applied during the MFI-UF test. At higher flux (i.e. higher permeation rate), the particles in the cake can be re-arranged, and simultaneously the cake can be compressed. As a result, the cake resistance and thus the measured MFI-UF will increase. Hence, the MFI-UF should be typically measured at the same flux rate as is applied in the RO system (typically $\sim 10\text{-}35 \text{ L/m}^2\text{.h}$). However, for a fixed feed volume, the filtration time and thus the time required to build a cake/gel on the MFI-UF membrane is significantly longer at lower flux. Therefore, to deal with this problem, Salinas-Rodríguez et al. (2012) proposed to measure the MFI-UF at higher flux rates (e.g. $50\text{-}350 \text{ L/m}^2\text{.h}$) and extrapolate to the actual flux rate in the RO system. However, the MFI-UF values determined by both approaches (i.e. direct measurement and extrapolation) have not yet been compared, and hence, it is unknown whether both approaches yield similar MFI-UF results.

The MWCO of the MFI-UF membrane can also substantially affect the measured MFI-UF. The lower the membrane MWCO, the smaller the membrane pore size and the more the particles that can be retained by the MFI-UF membrane, which eventually leads to higher MFI-UF value (Salinas-Rodríguez et al., 2015). In addition, as demonstrated in Chapter 3 (Abunada et al., 2022), it was found that MFI-UF membranes with lower MWCO have lower surface porosity and more non-uniform pore distribution, and thus smaller effective filtration area. This results in a higher local flux during the MFI-UF test and subsequently an overestimation of the MFI-UF value. The effect of membrane surface porosity on the measured MFI-UF was quantified using a suspension of polystyrene

particles. As a result, a correction factor of 0.4-1.0 was proposed for the MFI-UF measured with 5-100 kDa, respectively. Accordingly, there is a need to further investigate the effect of MFI-UF membrane MWCO (i.e. both pore size and surface porosity) on the particulate fouling rate prediction.

This study aims to apply and verify the MFI-UF method to predict the rate of particulate fouling under various MFI-UF testing conditions. For this purpose, the MFI-UF was measured at two full-scale RO plants, using 5-100 kDa UF membranes. The objectives were as follows.

- (1) To measure the MFI-UF of RO feed and RO concentrate at the same (low) flux applied in RO plants. The MFI-UF was measured (1) directly at the same low flux applied in the RO plants, and (2) at higher flux rates (50-200 L/m².h) and then the MFI-UF was extrapolated to the same low flux as was applied in the RO plant. Finally, the MFI-UF values measured by both approaches were compared.
- (2) To predict the particulate fouling rate (based on the measured MFI-UF of RO feed and deposition factor), and compare it with the actual fouling rate observed in the RO plants.

4.2 THEORETICAL BACKGROUND

During the filtration of a feed water through a membrane, particulate fouling occurs typically in three subsequent mechanisms; (i) pore blocking, (ii) cake/gel filtration, and (iii) cake/gel compression, as shown in Figure 4.1. However, for RO membranes, cake/gel filtration is considered the dominant particulate fouling mechanism (Zhu and Elimelech, 1997). Therefore, the MFI-UF method was derived based on the cake/gel filtration to closely simulate particulate fouling in RO systems, as explained below.

At constant flux (i.e. the operation mode in the most of RO systems), cake/gel filtration can be described by the fundamental model shown in Equation (4.1) (Boerlage et al., 2004).

$$J = \frac{\Delta P}{\eta \cdot (R_m + R_c)} \quad (4.1)$$

Where J is the flux, ΔP is the transmembrane pressure, η is the water viscosity, R_m is the clean membrane resistance and R_c is the cake/gel resistance. R_c can be described as a function of time, as shown in Equation (4.2) (Boerlage et al., 2004).

$$R_c = J \cdot I \cdot t \quad (4.2)$$

The parameter I is the fouling index, which describes the fouling potential due to cake/gel formed on the membrane surface.

With combining and rearranging Equation (4.1) and (4.2), cake/gel filtration at constant flux can be then defined by Equation (4.3).

$$\Delta P = J \cdot \eta \cdot R_m + J^2 \cdot \eta \cdot I \cdot t \quad (4.3)$$

Cake/gel filtration in RO can be simulated during MFI-UF test (i.e. by filtering the feed water through UF membrane at constant flux), as shown in Figure 4.1.

Subsequently, the value of I (fouling index) is determined from the slope of the linear cake/gel filtration phase, as shown in Equation (4.4).

$$I = \frac{1}{J^2 \cdot \eta} \cdot \text{slope} \quad (4.4)$$

By definition, the MFI-UF is the I value corrected to reference testing conditions, as shown in Equation (4.5) (Schippers and Verdouw, 1980).

$$MFI-UF = \frac{\eta_{20^\circ\text{C}} \cdot I}{2 \cdot \Delta P_o \cdot A_o^2} \quad (4.5)$$

Where ΔP_o , $\eta_{20^\circ\text{C}}$ and A_o are, respectively, the reference pressure (200 kPa), water viscosity (1×10^{-6} kPa.s) and surface membrane area (13.8×10^{-4} m²) (Schippers and Verdouw, 1980).

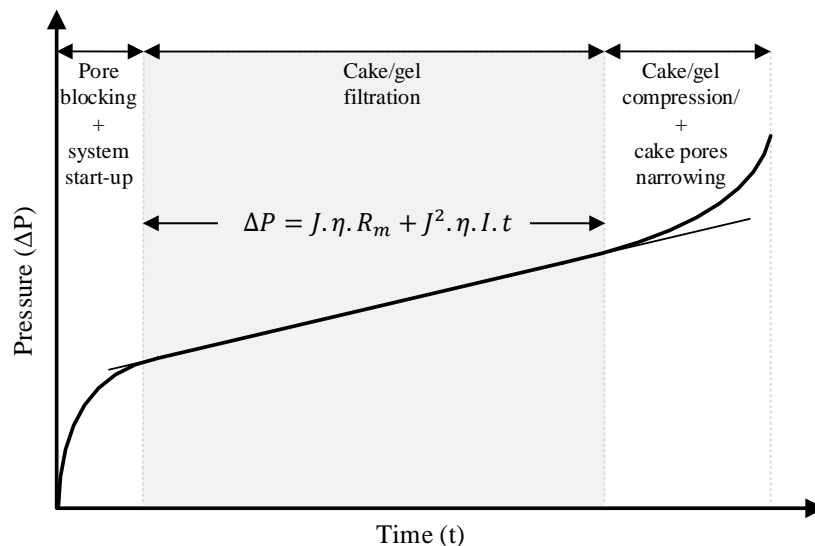


Figure 4.1: Typical particulate fouling mechanisms during MFI-UF test performed at constant flux

4.2.1 MFI-UF fouling prediction model

Particulate fouling development rate at constant flux filtration can be described by the increase of the net driving pressure (NDP) over a certain time, assuming that the NDP increase is mainly attributable to the cake/gel formed by particulate matter with a negligible contribution by scaling and biofouling. Accordingly, the NDP increase (ΔNDP) during a certain period of time (t) can be determined by integrating Equation (4.3) from $t = 0$ to $t = t$, as shown in Equation (4.6), where $\Delta P_{t=0}$ is an initial NDP pressure value at a reference time and $\Delta P_{t=t}$ is the NDP pressure value after time (t).

$$\Delta NDP = \Delta P_{t=t} - \Delta P_{t=0} = J^2 \cdot \eta \cdot I \cdot t \quad (4.6)$$

By substituting the value of I from Equation (4.5), the NDP increase rate can be then predicted based on the measured MFI-UF using the model shown in Equation (4.7) (Schippers et al., 1981).

$$\frac{\Delta NDP}{t} = \frac{2\Delta P_o \cdot A_o^2 \cdot J^2 \cdot \eta \cdot \Omega \cdot MFI-UF_{feed}}{\eta_{20^\circ C}} \quad (4.7)$$

The particle deposition factor (Ω) incorporated in the prediction model (Equation (4.7)) simulates the portion of particles depositing on the RO membrane during cross-flow filtration. The deposition factor can be determined by Equation (4.8), based on R (recovery rate; the ratio of RO permeate flow to RO feed flow), $MFI-UF_{feed}$ (MFI-UF of RO feed) and $MFI-UF_{concentrate}$ (MFI-UF of RO concentrate). Ideally, the Ω has a value between 0 and 1; where, $\Omega = 0$ indicates no particle deposition, and $\Omega = 1$ indicates that all particles presented in the feed water passing the RO membrane deposited and remained on its surface (Schippers et al., 1981; Salinas-Rodriguez, 2011; Salinas-Rodríguez et al., 2015).

$$\Omega = \frac{1}{R} + \frac{MFI-UF_{concentrate}}{MFI-UF_{feed}} \cdot \left(1 - \frac{1}{R}\right) \quad (4.8)$$

4.3 MATERIALS AND METHODS

To achieve the objectives of this study aiming at verifying the MFI-UF method to predict the particulate fouling rate in full-scale RO plants, the main steps shown in Figure 4.2 were followed, where the materials/methods applied in each step are explained in detail in the following sections (4.3.1-4.3.5).

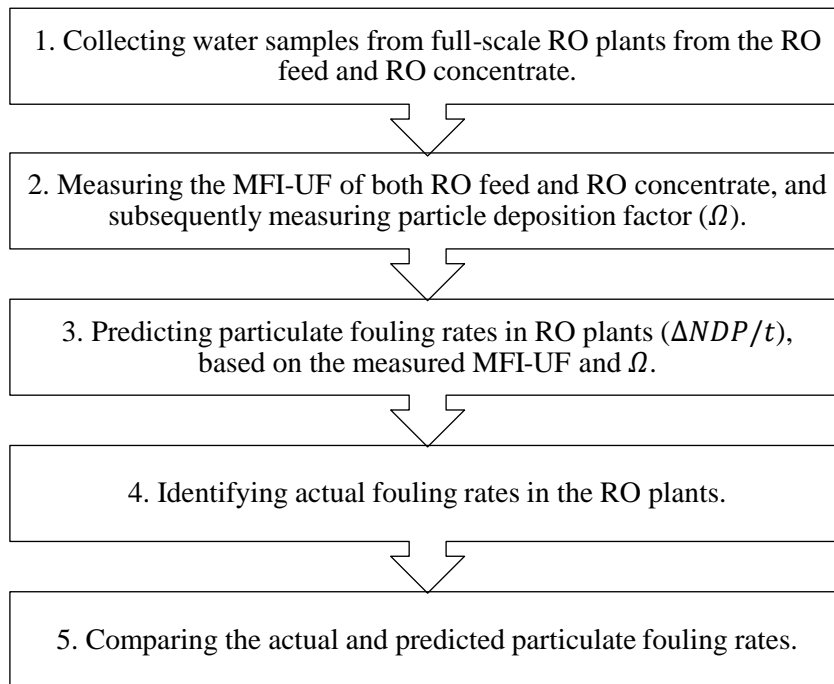


Figure 4.2: Methodology followed to verify the MFI-UF method to predict the particulate fouling rate in full-scale RO plants

4.3.1 Full-scale RO plants and sample collection

4.3.1.1 RO plant description

The MFI-UF was applied to predict the particulate fouling rate in two different full-scale RO plants treating surface water, located in the Netherlands. The scheme of the main treatment processes of each plant is shown in Figure 4.3.

Plant A (Figure 4.3 (top)) is a full-scale RO plant, producing drinking water with an average capacity of 2000 m³/h. The plant receives raw water from a lake. The raw water is treated first by serial conventional pre-treatment processes, including micro strainers, coagulation/flocculation (using 20 mg/L Fe³⁺ as coagulant), sedimentation, and rapid sand filtration (10-20 m/h). The pre-treated water is then transported via 80 km pipeline and filtered through 150 kDa UF membranes (X-flow XIGA 40, Pentair). To prevent the occurrence of scaling, a dose of 1.8 mg/L of antiscalant is injected into the feed water after the UF. Finally, the feed water is pumped into 8 parallel units of 8-in RO membranes (ESPA3 24, Hydranautics) with a total recovery of 80%. All RO units receive same RO feed and operate at same conditions. In addition, all RO units have same configuration, consisting of 2 stages (24:12 pressure vessels - 7 RO membrane elements per vessel).

Plant B (Figure 4.3 (bottom)) is a full-scale RO plant, producing industrial water with an average capacity of 800 m³/h, by treating raw water received from a river. The raw water is first conventionally pre-treated by strainers and combined coagulation (2 mg/L Fe³⁺), dissolved air flotation (DAF) and media filtration. Subsequently, the scaling compounds in the pre-treated water are removed by a softening process (ion exchange) which is followed by NaOH addition to adjust the pH (to pH = 9.3) to prevent the biofouling in the downstream RO units. The water is then prefiltered through cartridge filters (CF) with pore size of 10 µm, and finally pumped to 4 parallel units of 8-in RO membranes (FILMTEC ECO PRO-440i, Dupont) with a total recovery of 85%. All RO units receive same RO feed and operate at same conditions. In addition, all RO units have same configuration, consisting of 3 stages (24:12:6 pressure vessels - 6 RO membrane elements per vessel).

The detailed specifications of RO membranes installed in both plants are shown in Annex 4.6.1.

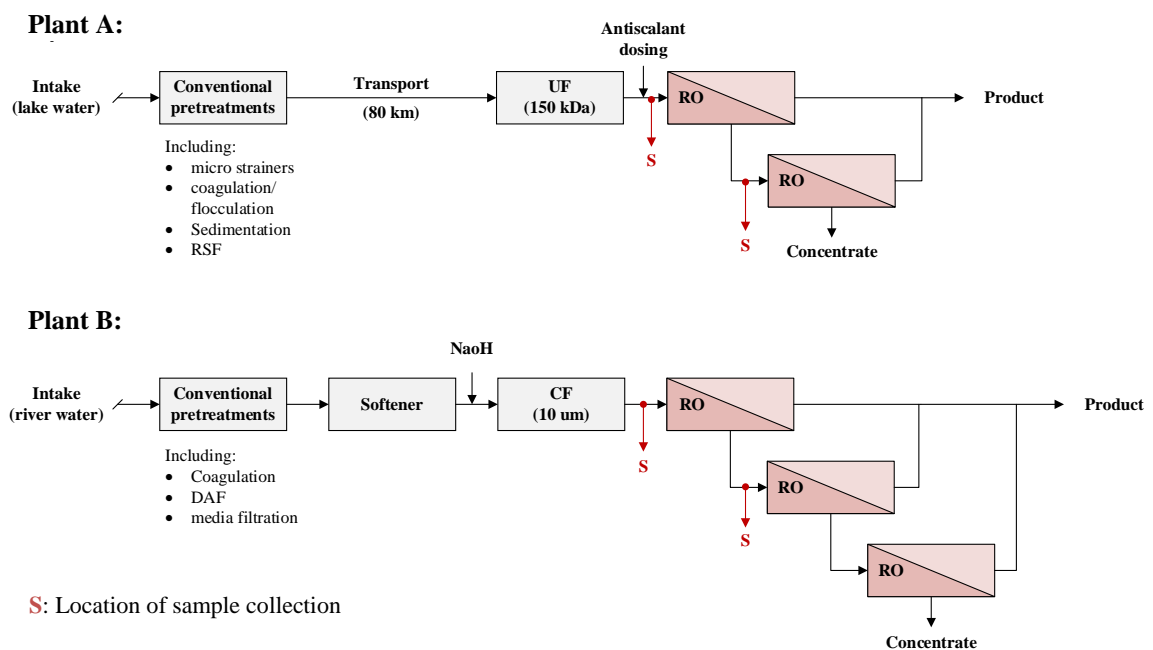


Figure 4.3: Treatment process schemes of the studied RO plants

4.3.1.2 Water samples

Four different sets of water samples were collected from the RO plants as described in Figure 4.3 and Table 4.1. One RO unit was targeted from each plant, as the operation conditions were similar in all the units of each plant (as explained in section 4.3.1.1). Water samples were collected from the RO feed and RO concentrate of the first stages only (as shown in Figure 4.3) to eliminate as much as possible the potential effect of

scaling on the NDP (since membrane scaling usually occurs in the last stage). The quality of RO feed at the collection time is summarized in Table 4.2.

Table 4.1: Summary of water samples collection and operational data

	Trial (#)	Time	RO stage	Avg. J (L/m ² .h)	R (%)
Plant A	1	January 2019	Stage 1	23	55
	2	January 2021	Stage 1	26	57
	3	March 2021	Stage 1	26	57
Plant B	1	December 2019	Stage 1	20	51
			Stage 2	20	53

Table 4.2: Characteristics of RO feed during collection time

Parameter	Plant A	Plant B
<i>Cations:</i>		
Calcium	57-65 mg/L	< 3 mg/L
Magnesium	11-17 mg/L	< 0.4 mg/L
Sodium	66-122 mg/L	-
Iron	< 0.01 mg/L	< 0.005 mg/L
Barium	0.03-0.04 mg/L	-
Strontium	0.36-0.46 mg/L	-
<i>Anions:</i>		
Carbonate	< 5 mg/L	-
Chloride	130-220 mg/L	-
Silicate	1.4-4.2 mg/L	5 mg/L
Sulphate	56-76 mg/L	54 mg/L
Bicarbonate	148-152 mg/L	160 mg/L
<i>Other parameters:</i>		
Temperature	4-5 °C	7 °C
pH	7.8-8.0	9.3
EC	690-980 uS/cm	780 uS/cm
TDS	450-640 mg/L	510 mg/L

4.3.2 MFI-UF measurement

4.3.2.1 MFI-UF set-up

MFI-UF measurements of RO feed and RO concentrate were performed using the set-up schemed in Figure 4.4. The set-up consists of three main items: (i) infusion syringe pump (PHD ULTRA, Harvard Apparatus), (ii) pressure transmitter (PXM409, Omega and PMC51, Endress+Hauser), and (iii) membrane holder (Whatman) where the UF membrane is placed. The accuracy of MFI-UF set-up was checked frequently during this study.

The MFI-UF was measured by filtering the feed water through the membrane at constant flow. Pump flow (Q) was set based on the membrane surface area (A) and the required flux rate (J), where $Q = A \times J$. The data of the transmembrane pressure (ΔP) development over time (t) observed during the MFI-UF test was recorded by the pressure transmitter (every 10 seconds). Finally, the relationship of ΔP against t was plotted, and then the MFI-UF value was calculated as described in section 4.2.

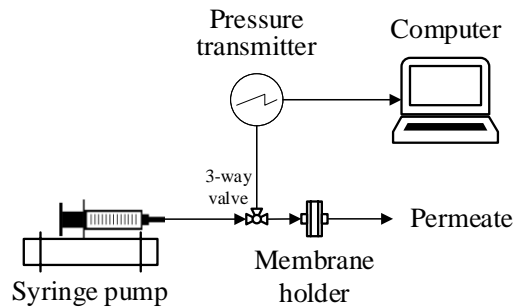


Figure 4.4: Scheme of MFI-UF set-up at constant flux filtration

4.3.2.2 MFI-UF membranes

MFI-UF measurements were performed with Polyethersulfone (PES) UF membranes (Biomax, Millipore) with MWCO of 5, 10, and 100 kDa. The membranes had a flat-sheet configuration and had a diameter of 25 mm.

All membranes were cleaned before use to remove the preservation coating. This was done by filtering at least 100 mL of ultra-pure water (Milli-Q, Millipore) through the membrane at a flux of 200-300 L/m².h. Subsequently, the clean membrane resistance (R_m) was measured using Equation (4.9) to ensure that the membrane is well-manufactured and not damaged.

$$R_m = \frac{\Delta P}{J \cdot \eta} \quad (4.9)$$

4.3.2.3 Flux rate

The MFI-UF was measured based on two flux approaches; (1) directly at the same average flux applied in RO plant (20-26 L/m².h), and (2) at higher flux rates (50-200 L/m².h) and then extrapolated to the same average RO flux as proposed by Salinas-Rodríguez et al. (2012). The outputs of both approaches were compared.

4.3.2.4 MFI-UF correction for membrane surface porosity effect

In Chapter 3 (Abunada et al., 2022), the effect of surface porosity of MFI-UF membranes was quantified, using a suspension of washed polystyrene particles. It was found that the lower the membrane surface porosity, the more non-uniformly the membrane pores are distributed, and the smaller the effective membrane filtration area, which subsequently results in a higher local flux rate during the MFI-UF test and eventually leads to an overestimated MFI-UF value. This effect is exacerbated as the MWCO of the MFI-UF membrane reduces from 100 down to 5 kDa. Accordingly, a correction factor of 0.4 and 0.5 were proposed to correct the MFI-UF measured with 5 and 10 kDa membranes, respectively, while the MFI-UF measured with 100 kDa membrane was not corrected as the effect of membrane surface porosity was expected to be minimal as the pores appeared to be evenly distributed over the membrane surface of the 100 kDa MFI-UF membrane.

Therefore, all MFI-UF values measured with 5 and 10 kDa membranes in this study were corrected to eliminate the effect of membrane surface porosity based on the aforementioned correction factors.

4.3.3 Prediction of particulate fouling rates in RO plants

Particulate fouling rate in the RO plants was predicted using Equation (4.7) based on the measured MFI-UF of RO feed and the particle deposition factor (Equation (4.8)). The prediction was determined based on the average flux applied in the RO plant (Table 4.1), at reference temperature condition (25 °C).

4.3.4 Identification of actual fouling observed in RO plants

The actual fouling rate in the RO plants was described by the rate of NDP increase observed over time. However, to verify that the NDP increase is dominated by particulate fouling, the role of the other types of fouling; i.e. scaling, biofouling and organic fouling was also investigated, as follows.

For scaling, the saturation index (SI) of the scaling compounds were determined for the RO concentrate to assess the occurrence of scaling in the RO plants.

Biofouling potential was measured using both bacterial growth potential (BGP) and assimilable organic carbon (AOC) methods. These two methods indicate the potential of

bacteria to grow by utilizing biodegradable organic matter present in the sample. BGP was measured as described by Abushaban et al. (2017), where water samples were pasteurized to inactivate microorganisms present in the samples and thereafter distributed in triplicate into 30 mL carbon-free vials and each vial was inoculated with an indigenous microbial consortium from the intake of the RO plant (10,000 intact cells/mL measured by flow cytometry). Bacterial growth was monitored using microbial adenosine triphosphate (ATP) measurement (Abushaban, 2019). The maximum growth was converted to carbon concentration using a calibration line (between glucose and maximum bacterial growth). Whereas AOC was measured following the protocol proposed by Kooij (1992) which has similar concept of BGP. However, in the AOC test, the samples were incubated by *Pseudomonas fluorescens* P17 and *Spirillum* sp. NOX bacteria and the bacterial growth was monitored by heterotrophic plate counting (HPC). To convert bacterial growth to carbon, acetate is used for AOC test while glucose is used for BGP measurements.

Finally, the organic carbon content of the RO feed was measured as dissolved organic carbon (DOC).

4.3.4.1 NDP calculation and normalization

The actual fouling in the RO plants was determined by calculating the NDP overtime, using Equation (4.10).

$$NDP_{act} = P_f - \frac{dP}{2} - \Delta P_{osm} - P_p \quad (4.10)$$

Where P_f is the feed pressure, P_p is the permeate pressure, dP is the average pressure drop across the RO membrane (feed pressure - concentrate pressure), and ΔP_{osm} is the differential osmotic pressure.

However, the actual NDP development observed in RO plant could be attributable not only to membrane fouling but also the variations in operational parameters, namely; (i) permeate flux, and (ii) water temperature (based on Equation (4.3)). For this reason, the NDP had to be normalized based on a reference flux and temperature to ensure that the NDP increase in the plant is only due to membrane fouling and not to changes in flux rate and/or water temperature. Accordingly, the NDP was normalized based on Equation (4.11)-(4.13).

$$NDP_{nor} = NDP_{act} \cdot \frac{FCF}{TCF} \quad (4.11)$$

$$FCF = \frac{J_r}{J_a} \quad (4.12)$$

$$TCF = e^{3020\left(\frac{1}{T_a+273}-\frac{1}{T_r+273}\right)} \quad (4.13)$$

FCF is the flux correction factor. It corrects the NDP for the flux linearly (since the NDP is linearly correlated to the flux based on Equation (4.1)). J_r is the reference flux. It was substituted by the average flux in the RO plant during the fouling prediction period (Table 4.1). J_a is the actual flux. *TCF* is the temperature correction factor. T_r is the reference water temperature at standard condition (25 °C). T_a is the actual water temperature.

4.3.5 Comparison between predicted and observed fouling rates in RO plants

Finally, the fouling rates (i.e. NDP increase rates) predicted based on MFI-UF prediction model (Equation (4.7)) were plotted together with the normalized NDP increase observed in the RO plants, to verify the accuracy of MFI-UF method. The comparison between the predicted and observed fouling rates was based on the assumption that no variation in the quality of RO feed occurs after sample collection. Nevertheless, as this might not be the case in reality, the comparison between the predicted and observed fouling rates was limited to 30 days after sample collection, assuming minor variation in the quality of RO feed water may occur during this period. However, for plant B, the fouling rates were predicted only over 7 days, since the RO membranes in the plant were cleaned on weakly basis (due to the high pressure drop observed in the plant) during the time of this work.

4.4 RESULTS AND DISCUSSION

4.4.1 MFI-UF of RO feed and RO concentrate

Figure 4.5 shows the MFI-UF of RO feed and RO concentrate of stage 1 in plant A (Trial #1) using 5, 10 and 100 kDa membranes. The MFI-UF was measured based on two flux approaches; (1) directly at the same average RO flux applied in the plant which was 23 L/m².h (open points), and (2) at higher flux rates; 50, 100 and 200 L/m².h (solid points) and then extrapolated linearly at the average RO flux in the plant (disconnected lines). As can be observed in all cases, the MFI-UF values measured directly at 23 L/m².h and those extrapolated were very similar, with a difference of around ±5%. Hence, the results indeed confirmed that even at low flux rates the MFI-UF can be measured directly or extrapolated from the MFI-UF values measured at higher flux rates, as both approaches eventually yield similar output.

Accordingly, the MFI-UF was measured in the two RO plants selected for this study based on both approaches (the results are presented in Annex 4.6.1). The MFI-UF measurement

based on the second approach (i.e. extrapolation from higher flux rates) was also investigated based on other flux ranges; where the MFI-UF was extrapolated based on only 2 flux rate experiments (100 and 200 L/m².h) as well as with 3 flux rate experiments with equal increment (100, 150 and 200 L/m².h). The results showed that the MFI-UF extrapolated based on the 3 flux rate experiments appeared more accurate. This is because in the case of 2 flux rate experiments, the regression line is defined by only 2 data points, and therefore, any uncertainty in the MFI-UF measured at the higher flux rates (i.e. 100 and 200 L/m².h) will impact the MFI-UF value extrapolated at the low RO flux. In addition, the results showed that measuring the MFI-UF at higher flux rates with equal-increments (i.e. 100, 150 and 200 L/m².h) could eliminate the potential influence of high leverage on the resulted regression line and thus on the extrapolated MFI-UF value.

The linear correlation between the MFI-UF and flux rate found in this study agree with the observation of Salinas-Rodríguez et al. (2012) who also found a linear correlation for various types of feed water. However, the relationship of the MFI-UF and flux rate may not be ultimately linear for all types of feed water. This is because the rate of cake compressibility due to the increasing flux may not be constant (as the case in this study) and it may vary depending on the characteristics of particles existing in the feed water.

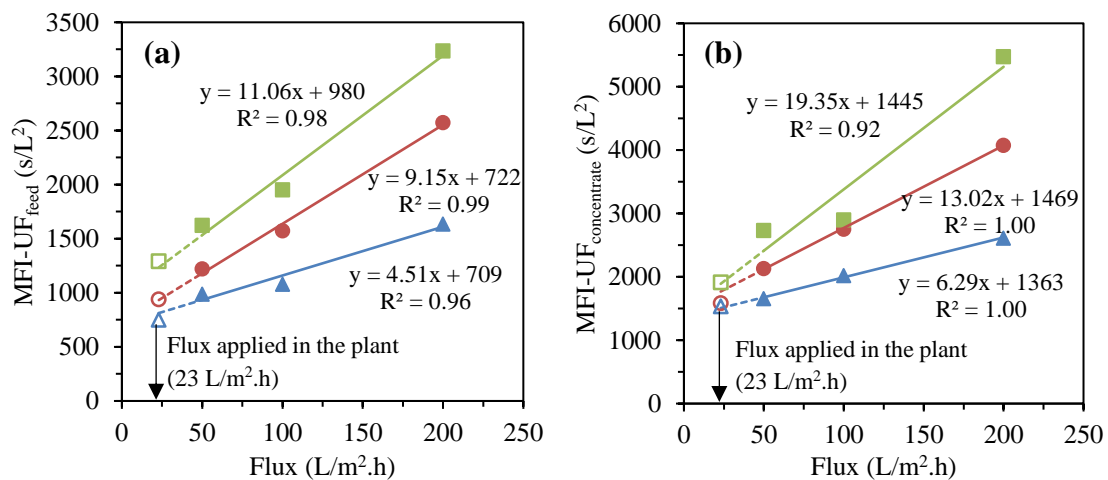


Figure 4.5: MFI-UF measured in plant A – stage 1 (Trial #1): (a) RO feed, and (b) RO concentrate; (i) MFI-UF measured directly at same RO flux applied in the plant (Δ 100 kDa, \circ 10 kDa, \square 5 kDa), and (ii) MFI-UF measured at higher flux rates (\blacktriangle 100 kDa, \bullet 10 kDa, \blacksquare 5 kDa) and extrapolated (disconnected lines) at the applied RO flux

4.4.1.1 Dependency of MFI-UF test duration on the applied flux

Table 4.3 shows the duration range of the MFI-UF measurements discussed above in relation to the flux rate applied during the MFI-UF test. As it can be clearly observed, the duration of the MFI-UF measurement performed based on flux approach (1) was substantially longer than that performed based on approach (2). The reason is because the

lower the flux, the lower the load of particles depositing on the membrane. Consequently, the depositing particles take longer time to interconnect and build-up a complete cake in even layers on the membrane surface, as demonstrated in Chapter 3 (Abunada et al., 2022).

In addition, in this study, the overall time of the MFI-UF measurements performed based on approach (2) was much faster than in the case of approach (1). However, approach (2) had one disadvantage in that it requires more effort and cost since multiple MFI-UF measurements should be performed to determine the MFI-UF at the actual RO flux, while only one MFI-UF measurement is required in case approach (1) is applied. Accordingly, the best approach can be selected by trading off the time against the cost and effort.

It is important to mention that the duration of MFI-UF tests listed in Table 4.3 depended mainly on the characteristics of water measured in this study. Therefore, different duration might be required for other types of water.

Table 4.3: Approximate duration of MFI-UF test in relevance to the applied flux

	Flux	MFI-UF test duration
Approach (1): MFI-UF measured directly at the same flux applied in the RO plant	20-26 L/m ² .h	500-800 min
Approach (2): MFI-UF measured at higher flux rates and then extrapolated at the same flux applied in the RO plant	50 L/m ² .h	90-120 min
	100 L/m ² .h	60-90 min
	150 L/m ² .h	60-70 min
	200 L/m ² .h	30-60 min

4.4.1.2 Particle deposition factor

Table 4.4 shows the particle deposition factors (Ω) in the full-scale RO plants. In general, higher particle deposition factor (Ω) was found when the MFI-UF was measured using lower MWCO UF membrane (for plant A - Trial #2, the difference in the Ω was minor). Exceptionally, in plant A (Trail #3), the particle deposition factor (Ω) measured based on the 5 kDa membrane was negative. The negative Ω value indicates that the load of particles detached from the RO membrane was higher than that of particles depositing on the membrane (Boerlage et al., 2003a). However, since the Ω values measured based on both 10 and 100 kDa membranes were positive, this could indicate that particle detachment occurred only for particles smaller than 10 kDa. This could be explained by the effect of cross-flow hydrodynamic conditions on the cake stratification, which could result in smaller particles concentrating on the top of the cake and larger particles in the bottom (Yoon, 2015). As a result, the smaller particles might detach from the top of the cake by the hydrodynamic forces induced on the particles by the tangential flow as well

as due to the collision with other flowing particles (Henry et al., 2012). The reason that particle detachment occurred only in this Trial (i.e. not in Trial #1 nor 2) might be because the thickness of the cake accumulated on the RO membranes was higher during the time of this Trial, and thus the chance of particle detachment due to the acting tangential forces was higher (Boerlage et al., 2003a).

Interestingly, for plant B, particle deposition factor (Ω) in stage 1 were higher than the corresponding values for stage 2, although both stages operated at similar flux and cross-flow velocity. This could be because the concentration (i.e. load) of particles in the feed of stage 2 was higher, as indicated from the MFI-UF values. Hence, there was a higher chance of collision between the particles moving by the tangential flow across the RO membranes and the particles which already deposited. Consequently, this collision might have reduced the particle deposition on RO membrane, which eventually resulted in lower Ω values. However, this hypothesis/explanation needs further investigation.

Table 4.4: Particle deposition factor (Ω) measured at same flux applied in RO plants

	Trial (#)	RO stage	Ω value		
			100 kDa	10 kDa	5 kDa
Plant A	1	Stage 1	0.12	0.44	0.61
	2	Stage 1	0.57	0.59	0.62
	3	Stage 1	0.70	0.81	-0.72
Plant B	1	Stage 1	0.67	0.89	0.90
		Stage 2	0.38	0.42	0.60

4.4.2 Actual fouling observed in the RO plants

Figure 4.6 and Figure 4.7 show the actual fouling observed in plant A and B, respectively, expressed in NDP increase overtime. In principle, the NDP increase can be due to scaling, biological fouling, organic fouling and/or particulate fouling. However, the NDP increase in the RO plants was assumed to be mainly due to particulate fouling (i.e. formation of cake/gel by particles/colloids accumulated on the RO membrane surface), as indicated by the measured fouling indices/parameters shown in Table 4.5 and explained below.

4.4.2.1 Plant A

For plant A, scaling is controlled by dosing antiscalant to the RO feed (1.8 mg/L). In the RO concentrate, calcium carbonate and barium sulphate were slightly supersaturated (SI = 0.7-1.0 and 1.9-2.8, respectively) and their saturation level was in the range which can be controlled by the antiscalant (Boerlage et al., 2002a; Mangal et al., 2022).

Biofouling is not expected to be the reason for the NDP increase, since the measured AOC concentration in the RO feed is very low (3-6 ug/L). Weinrich et al. (2009) reported that bacterial growth in the absence of a chlorine residual can be observed at AOC concentration of 10 ug/L or higher. Moreover, Vrouwenfelder and van der Kooij (2001) observed RO biofouling when AOC concentration in the feed water exceeded 80 ug/L.

Organic fouling due to the adsorption of dissolved organic matter onto the surface of RO membranes was not expected to be a problem in plant A, as organic fouling is assumed to occur prior to cake/gel formation when new/clean membranes are put into operation. However, the RO membranes of plant A was already in operation for around 6 months and any adsorption onto the RO membrane would have already taken place. The negligible effect of organic fouling (and also biofouling) can be supported by the observed pressure drop (dP), which was stable (i.e. not increasing) during the fouling prediction period (see Annex 4.6.1). It is important to mention that the stable pressure drop does not rule out the particulate fouling in the plant, since the particles/colloids existed in the RO feed might have passed through the feed spacers in the RO membranes (i.e. did not cause any increase in the pressure drop) but deposited and accumulated on the surface of the membranes, resulting in NDP increase.

According to the above explanation, it could be concluded that particulate fouling is most likely the main reason for the NDP increase in plant A. The existence of particles/colloids in the RO feed after the extensive pre-treatment enhanced by UF, could be a result of several reasons; (i) the passage of small colloids through the UF, (ii) loss of integrity of the UF which could allow to the particles/colloids to pass into the permeate side (i.e. RO feed), (iii) re-aggregation of small particles/colloids that passed through the UF, and/or (iv) re-growth of bacteria on the permeate side of the UF membranes (which are considered as particles).

4.4.2.2 Plant B

In plant B, the concentrations of sparingly soluble compounds were reduced substantially prior to the RO units by the softening process (as shown in Table 4.2). Therefore, the scaling compounds were undersaturated in the RO concentrate, and hence scaling was not expected to occur in the plant.

Biofouling is also not expected to be the reason behind the NDP increase in plant B since the pH of the RO feed is adjusted to 9.3 (by adding NaOH) after softening process, in which most bacteria cannot grow or even survive. Moreover, when the pH is corrected to around 8, low BGP concentrations were measured (< 78 ug/L). Abushaban et al. (2019) reported a BGP concentration of 70 ug/L in SWRO feed water, where the CIP (cleaning in place) is performed every 3 years.

However, the RO membranes in plant B were cleaned almost every week due to the high pressure drop observed in the plant (around 2.8 bar per stage, normalized based on the worst-case conditions; maximum flow and minimum temperature). The increase in the pressure drop could be due to organic and/or particulate fouling (whereas biofouling effect is considered minor as explained above). Nevertheless, the concentration of DOC in the RO feed was low (1.2-1.5 mg/L), which might indicate less effect due to organic fouling.

Therefore, it could be concluded that particulate fouling is most likely the dominant type of fouling in plant B, while the effect of organic fouling could not be excluded completely.

Table 4.5: Scaling, biological and organic fouling potential indices/parameters for plant A and B

Index/parameter	Plant A	Plant B
Scaling:		
SI – CaCO ₃	0.7-1.0	-
SI – BaSO ₄	1.9-2.8	-
Biofouling potential:		
AOC	3-6 ug/L	-
BGB	-	55-78 ug/L
Organic fouling:		
DOC	2.6-3.6 mg/L	1.2-1.5 mg/L

4.4.3 Comparison between predicted and observed fouling rates in RO plants

The comparison between the observed and predicted NDP development (i.e. fouling rate) is presented in Figure 4.6 and Figure 4.7 for plant A and plant B, respectively. As mentioned in section 4.3.5, for plant A, the prediction of NDP increase was limited to 30 days, assuming that minor variation in the quality of RO feed water may occur during this period. For plant B, the fouling rates were predicted over only 7 days, since the RO membranes in the plant were cleaned almost every week (due to the high pressure drop observed in the plant).

For plant A – Trial #1 (Figure 4.6 (a)), the observed NDP was apparently affected by the flux variation in the plant, particularly in the earlier phase (i.e. 0-13 days), although the observed NDP was already normalized for the flux (section 4.3.4.1). This is because the flux normalization could correct only the hydrodynamic effect of the flux on the NDP, but it does not take into account the effect of flux on cake compression (i.e. cake

resistance). Consequently, the observed NDP rapidly increased on day 1 and 6 due to the cake compression resulting from the flux increase (from 23 to 26 L/m².h), while it suddenly declined on day 4 and 13 as the cake relaxed when the flux decreased again (from 26 to 23 L/m².h). Accordingly, once the flux applied in the plant became constant at 23 L/m².h (day 13-30), the observed NDP development was stable. During this phase, the NDP predicted based on the MFI-UF measured using the 100 kDa membrane showed the best agreement with the observed NDP trend, where the deviation between the predicted and actual fouling rate was around 11% (Table 4.6).

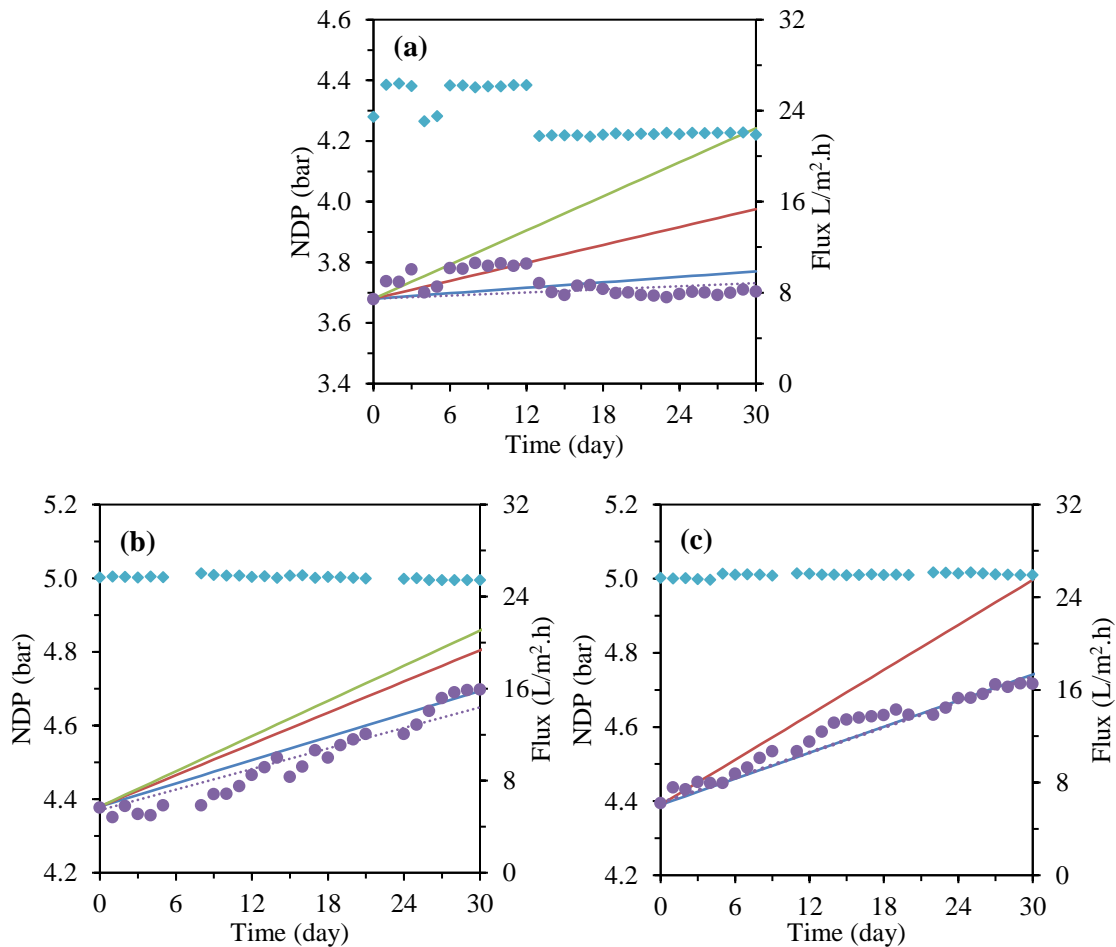


Figure 4.6: Predicted and observed NDP increase along with the flux applied in plant A – stage 1 (where day 0 is the day of sample collection); (a) Trial #1, (b) Trial #2, and (c) Trial #3

Predicted NDP - MFI-UF_{100 kDa} (—), predicted NDP - MFI-UF_{10 kDa} (—), predicted NDP - MFI-UF_{5 kDa} (—), observed NDP (●), observed NDP trend (···), and flux (◆)

In the other trials with plant A (Figure 4.6 (b) and (c)), the observed NDP trend was similar. The sudden NDP decline observed during the prediction period was due to turning the RO unit off as some maintenance work were carried out. However, no

membrane flushing nor CIP took place during the shut-down period (based on the information obtained from the plant operator). Hence, the NDP dropped probably as a result of cake relaxation due to switching the RO unit off. Nevertheless, the NDP drop was minor (< 0.05 bar). In both trails (Figure 4.6 (b) and (c)), the rate of in NDP increase predicted based on the MFI-UF measured with the 100 kDa membrane showed good agreement with the NDP observed in the plant with a deviation of 8% and 3% for Trial #2 and #3, respectively (Table 4.6).

For plant B – stage 1 (Figure 4.7 (a)), the observed NDP was significantly affected by the unsteady daily operation of the plant, where it was even difficult to determine the NDP development over time. This was attributed, as mentioned above, to the variation in cake compression resulting from the variable flux applied in the plant. Accordingly, it was not possible to verify the prediction of NDP increase for stage 1. For stage 2 (Figure 4.7 (b)), the effect of the variation in the applied flux on the observed NDP was lower in comparison with stage 1. The reason might be due to the lower load of particles deposited on the RO membranes in stage 2 (as indicated from the Ω values in Table 4.4), which resulted in a thinner cake layer on RO membranes. Hence, the variation in the applied flux might have less effect on cake compression. In this case, the NDP increase rate predicted based on the MFI-UF measured with 10 kDa membrane agreed closely with the NDP trend observed in the plant with 2% deviation (Table 4.6). The rate of increase in NDP predicted based on the 100 kDa membrane showed also good agreement with the observed NDP with a deviation of 15% (Table 4.6).

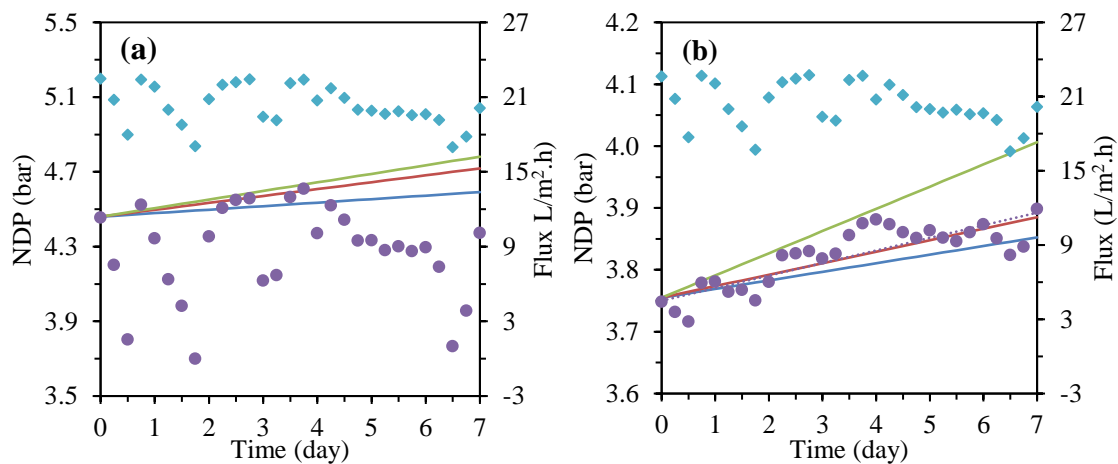


Figure 4.7: Predicted and observed NDP increase along with the flux applied in plant B (where day 0 is the day of sample collection); (a) stage 1, and (b) stage 2
 Predicted NDP - MFI-UF_{100 kDa} (—), predicted NDP - MFI-UF_{10 kDa} (—), predicted NDP - MFI-UF_{5 kDa} (—), observed NDP (●), observed NDP trend (⋯), and flux (◆)

Table 4.6: Summary of the NDP increase rates predicted based on MFI-UF and the NDP increase rates observed in the RO plants

	Predicted NDP increase rate (bar/month)		
	[Deviation between predicted and observed NDP increase]		
	100 kDa	10 kDa	5 kDa
Plant A: Figure 4.6 (a)	0.06 [11%]	0.30 [100%]	0.56 [>100%]
Plant A: Figure 4.6 (b)	0.31 [8%]	0.42 [29%]	0.48 [37%]
Plant A: Figure 4.6 (c)	0.35 [3%]	0.60 [36%]	* *
Plant B: Figure 4.7 (a)	0.56 **	1.06 **	1.46 **
Plant B: Figure 4.7 (b)	0.45 [15%]	0.56 [2%]	1.08 [43%]

* The NDP was not predicted since the Ω had a negative value.

** The observed NDP increase could not be identified as the NDP trend was highly unstable.

However, it was expected that the fouling prediction would more closely match the actual values when the MWCO of the MFI-UF membrane was lower, since more smaller particles can be captured and evaluated. Nevertheless, this was not the case in the results discussed above; where the fouling rates predicted based on the MFI-UF measured with the 10 and 5 kDa membranes in plant A and the 5 kDa membrane in plant B overestimated the increase in NDP observed over time (by around 30-100% variation). This could be attributed to the effect of the non-uniform surface porosity of the MFI-UF membrane, as explained in Chapter 3 (Abunada et al., 2022). Although the MFI-UF values were already corrected for the effect of surface porosity (as explained in section 4.3.2.4), the correction factors might be still overestimated as these factors were identified based on polystyrene particles which are hardly compressible and are well-defined in size and shape. On the other hand, the real particles present in RO feed water are most likely more compressible and flexible, and they comprise a wide particle size range so that small particles could fill the voids in the formed cake (Boerlage et al., 1998; Boerlage et al., 2003b). Consequently, the cake formed by particles present in real water (i.e. RO feed) may be more compressed and less porous than a cake formed by polystyrene particles. Therefore, the effect of membrane surface porosity on the cake and thus on the measured MFI-UF may be greater

for RO feed water in comparison with a polystyrene particle suspension. As a result, as discussed above, the fouling rates predicted based on the 5-10 kDa membranes were mostly overestimated. In addition, the results also indicated that the correction of MFI-UF for membrane surface porosity effect was dependent on the type of RO feed, where the fouling rate predicted based on 10 kDa membrane was overestimated for plant A but not for plant B, which requires more investigations in the future research.

On the other hand, interestingly, the fouling rates predicted based on the 100 kDa membrane (i.e. the highest MWCO membrane) showed in all cases fairly good agreement with the actual fouling development observed in the RO plant. This could be because the difference in the particle retention by 5, 10 and 100 kDa membranes is small as indicated by the particle deposition factors (Table 4.4), however, the higher fouling rates predicted based on the MFI-UF measured with the 5 and 10 kDa membranes was dominated mainly by the effect of surface porosity as explained above. This could be supported by the scanning electron microscope (SEM) analysis presented in Chapter 3 (Abunada et al., 2022) which showed that 60-80% of the pores of the 5-100 kDa membranes had similar size range (6-12 nm), and thus similar particles retention might be expected with the 5-100 kDa membranes. Furthermore, Boerlage et al. (2002b) claimed that similar retention of particles could be obtained with different MWCO membranes since the cake built-up on the membrane surface could eventually act as a new membrane layer and dominate the filtration, while the role of membrane pore size becomes less dominant over time.

4.5 CONCLUSIONS

The MFI-UF method was applied in two full-scale RO plants to predict particulate fouling rate (described by the NDP increase rate). MFI-UF was measured at same flux rates applied in the plants (20-26 L/m².h) using 5-100 kDa membranes. The following are the main findings:

- For plant A, the particulate fouling rates predicted based on the MFI-UF measured with the 100 kDa membranes had the best agreement with the fouling rates observed in the plant with a deviation of 3-11%.
- For plant B, the particulate fouling rate predicted based on the 10 kDa membrane agreed the best with the fouling observed in the plant with only 2% deviation. Nevertheless, the fouling rate predicted based on the 100 kDa membrane showed also a good agreement with the observed fouling rate with 15% deviation.
- Particulate fouling rates predicted based on 5 kDa membrane were considerably overestimated in both RO plants. The reason could be attributed to the effect of surface porosity of 5 kDa membrane, although the MFI-UF values were corrected for

this effect. This is because the factors used to correct the MFI-UF for the effect of membrane surface porosity were identified using a suspension of synthetic polystyrene particles (as explained previously in Chapter 3 (Abunada et al., 2022)) which have properties different than those of natural particles in the RO feed.

Accordingly, the findings of this study indicated that the 10-100 kDa is the suitable range of MFI-UF membranes to predict particulate fouling in RO plants. Nevertheless, it is recommended to apply the MFI-UF method in more RO plants operating with different feed water and different conditions, and eventually demonstrate the most suitable range of UF membranes to be used in the MFI-UF measurement for accurate particulate fouling prediction.

In addition, since the accuracy of particulate fouling prediction could be affected by the variation in flux rate and/or feed water quality in RO plants over time, it is recommended to perform the MFI-UF measurement online (i.e. in real-time) over shorter periods (e.g. on monthly basis such as in plant A, or shorter in case the variation is high such as in plant B). Therefore, further research is required to develop a new online and automated MFI-UF measurement system.

4.6 ANNEXES

Annex 4.6.1: Supplementary data

Table A - 4.1: Specifications of RO membranes installed in the RO plants

Parameter	Plant A	Plant B
Manufacture	Hydranautics	Dupont
Module	ESPA3 24	FILMTEC ECO PRO-440i
Diameter	8 in	8 in
Length	1 m	1 m
Permeate flow	55 m ³ /d	48 m ³ /d
Min salts rejection	98.5%	99.7%
Total surface area	37 m ²	41 m ²
Max operating pressure	4.16 MPa	4.10 MPa
Max pressure drop per element	70 kPa	100 kPa
Max operating temperature	45 °C	45 °C
Chlorine tolerance	< 0.1 mg/L	< 0.1 mg/L
pH of feed water	3-10	2-11

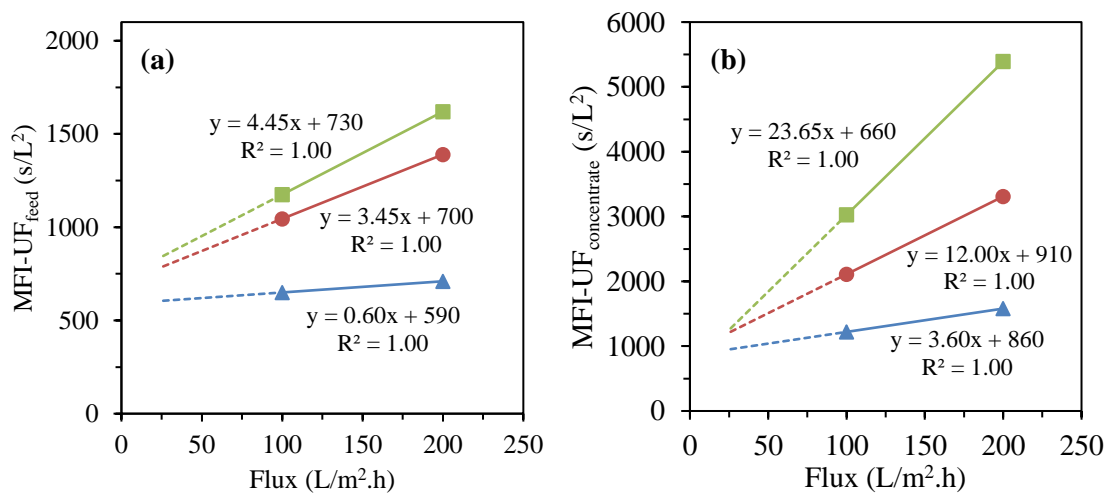


Figure A - 4.1: MFI-UF in plant A – stage 1 (Trial #2): (a) RO feed, and (b) RO concentrate; measured at higher flux rates (100 and 200 L/m².h) and extrapolated at the same average flux applied in the RO plant (26 L/m².h)
(▲ 100 kDa, ● 10 kDa, ■ 5 kDa)

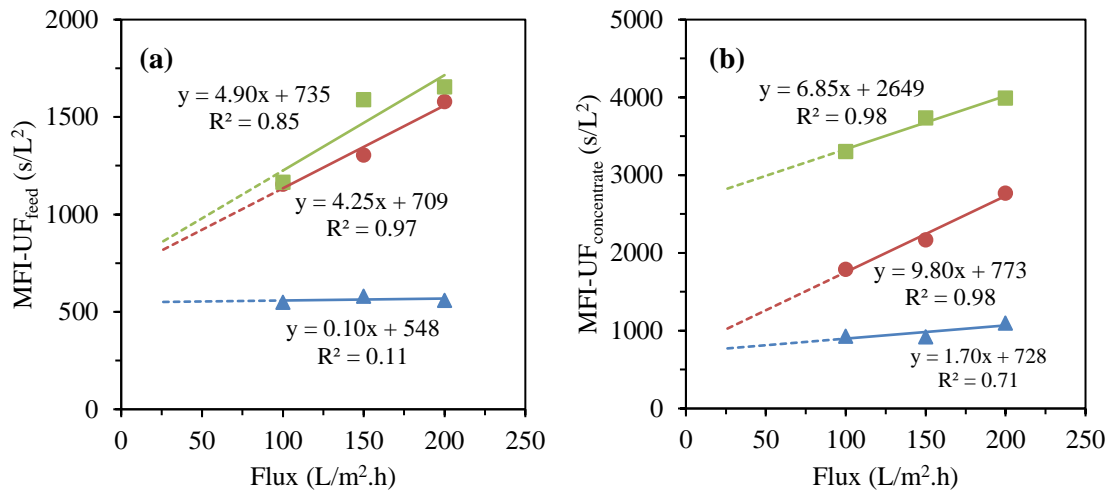


Figure A - 4.2: MFI-UF in plant A – stage 1 (Trial #3): (a) RO feed, and (b) RO concentrate; measured at higher flux rates (100, 150 and 200 L/m².h) and extrapolated at the same average flux applied in the RO plant (26 L/m².h)
(▲ 100 kDa, ● 10 kDa, ■ 5 kDa)

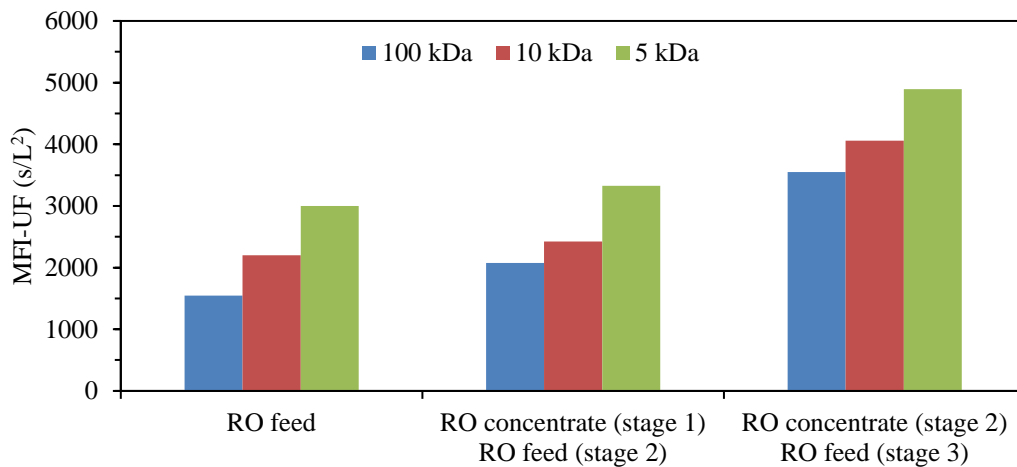


Figure A - 4.3: MFI-UF in plant B – stage 1 and 2; measured at same average applied RO flux (20 L/m².h)

4. Prediction of Particulate Fouling in Full-Scale Reverse Osmosis Plants Using the MFI-UF Method

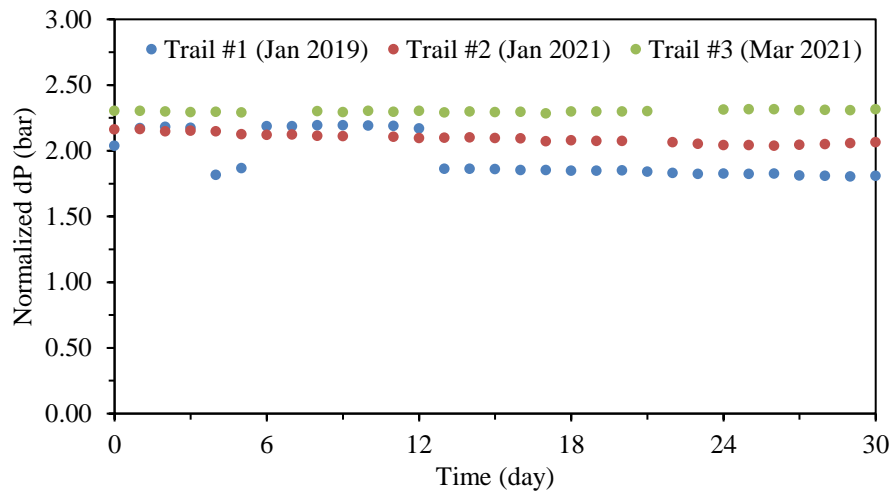


Figure A - 4.4: Normalized pressure drop (dp) in plant A – stage 1

5

PROTOCOL FOR THE MFI-UF AT CONSTANT FLUX TO MEASURE PARTICULATE FOULING IN REVERSE OSMOSIS

The existing ASTM methods, i.e. Silt Density Index (SDI) and Modified Fouling Index (MFI) cannot be used to predict particulate fouling in reverse osmosis (RO) systems as these tests are performed at constant pressure while RO systems operate mostly at constant flux. In addition, both methods use 0.45 μm membrane to simulate RO membrane fouling. Consequently, the MFI-UF method was developed to operate at a constant flux using ultrafiltration (UF) membrane to capture small colloids which are more likely to be responsible for RO fouling. However, unlike the SDI and MFI, there is no standard protocol for the MFI-UF method. Therefore, this research aims to describe the various procedures required to perform the MFI-UF measurement accurately and consistently. It addresses all details related to the MFI-UF set-up, membranes, operating conditions and calculation. The protocol focuses on MFI-UF measurement at constant flux in the range of 20-200 $\text{L}/\text{m}^2\cdot\text{h}$ using flat-sheet polyethersulfone (PES) UF membranes with MWCO of 5-100 kDa. The developed protocol is considered a first step to standardize the MFI-UF method. More work is recommended to integrate the protocol with a fully automated MFI-UF system which can be connected online in RO plants to measure and report particulate fouling potential in real time.

5.1 INTRODUCTION

Particulate fouling due to the deposition of particles/colloids on membrane surface is one of the problems experienced in many reverse osmosis (RO) systems. Fouling can reduce the permeability of RO membranes, which consequently requires higher energy consumption and more frequent membrane cleaning and replacement to maintain constant water supply. Therefore, a method to measure and predict particulate fouling is very important to optimize the performance of RO systems.

The ASTM-D4189 Silt Density Index (SDI) is the most method used worldwide to assess the particulate fouling in RO (ASTM, 2014). However, several doubts related to the SDI accuracy have been growing, as (i) it is not based on any fouling mechanism, (ii) it has nonlinear correlation with particle concentration, and (iii) it is not corrected for the reference testing conditions (Alhadidi et al., 2011a). Consequently, the ASTM-D8002 Modified Fouling Index (MFI) was introduced by ASTM as alternative method to the SDI to overcome the aforementioned inaccuracies (ASTM, 2015). The MFI was originally developed by Schippers and Verdouw (1980), based on cake/gel filtration which is assumed to be the dominant fouling mechanism in RO (Zhu and Elimelech, 1997).

MFI method simulates the fouling of RO membrane through filtering the feed water at a constant pressure (2 bar) through a 0.45 μm microfiltration (MF) membrane. Hence, the particles smaller than 0.45 μm , which are likely to be responsible for RO membrane fouling, are not considered by the method (Schippers et al., 1985). For this reason, the MFI-UF method was developed, where an ultrafiltration (UF) membrane is used in the place of 0.45 μm membrane to capture smaller particles (Boerlage et al., 1997; Boerlage et al., 1998; Boerlage et al., 2000; Boerlage et al., 2003a; Boerlage et al., 2003b). However, it was found that the (initial) flux observed during the MFI-UF test performed at constant pressure is around 10-1000 times higher than the flux applied in RO systems in practice. As a result, since high filtration fluxes can result in cake compression, it was observed that the cake formed on MFI-UF membranes under constant pressure filtration may be more compressed in comparison with the cake formed on RO membranes, and thus predicted particulate fouling may be overestimated (Boerlage et al., 2004). Therefore, to more accurately assess particulate fouling in RO, the MFI-UF was developed further to operate at constant flux (Boerlage et al., 2004; Salinas-Rodríguez et al., 2015). The MFI-UF at constant flux was initially measured using hollow fibre UF membranes (Boerlage et al., 2004), and it was afterwards developed using flat-sheet membranes (Salinas-Rodríguez et al., 2015).

The measured MFI-UF value is used as an input in a mathematical model to predict the particulate fouling rate in RO systems over time (Schippers et al., 1981). The accurate prediction of particulate fouling is very important in order to identify the cleaning frequency of RO membranes, optimizing the operation conditions of the RO system,

improving/upgrading the pre-treatment of RO feed (Goh et al., 2018). This results in minimizing the use of energy and chemicals as well as reducing the frequency of RO membrane replacement, which eventually leads to improved overall efficiency of the RO system and thus reduced total operation cost.

However, unlike the MFI, there is no standard protocol for the MFI-UF method, which can affect the accuracy, reproducibility as well as applicability of the method to predict particulate fouling in RO systems. Therefore, the aim of this work is to develop a detailed protocol for the MFI-UF method at constant flux to ensure the accuracy and consistency of MFI-UF measurement and thus particulate fouling prediction. The protocol was developed in six sections, including:

- (1) Introduction: defines the scope and significance of the MFI-UF method.
- (2) MFI-UF setup: describes the MFI-UF set-up, including the specifications of each set-up component and the procedure to be applied to verify the accuracy and reproducibility of the set-up.
- (3) MFI-UF membrane: describes specifications of UF membranes that should be used in the MFI-UF test and the procedure to be applied to clean and inspect the membranes.
- (4) MFI-UF testing conditions: illustrates the operation conditions of the MFI-UF test, namely: feed water temperature, flux rate and test duration.
- (5) MFI-UF calculation: explains the calculation steps of the MFI-UF value, and introduces a new automated numerical algorithm to calculate the MFI-UF value.
- (6) MFI-UF testing protocol manual: describes step-by-step the procedure required to measure the MFI-UF.

5.1.1 MFI-UF theoretical background

The MFI-UF method was developed based on cake/gel filtration (Boerlage et al., 2004), which is assumed to be the dominant fouling mechanism in RO (Zhu and Elimelech, 1997). At constant flux, cake/gel filtration is described by Equation (5.1) (Boerlage et al., 2004).

$$\Delta P = J \cdot \eta \cdot R_m + J^2 \cdot \eta \cdot I \cdot t \quad (5.1)$$

Where ΔP is the transmembrane pressure, t is the filtration time, J is the constant flux, η is the feed water viscosity, R_m is the clean membrane resistance, and I is the fouling index which describes the fouling potential of a feed water.

The value of I can be determined through an MFI-UF test, whereby the water sample is filtered through a UF membrane at a constant flux in dead-end mode. During the test,

membrane fouling takes place in three phases; (i) pore blocking, (ii) cake/gel filtration, and (iii) cake/gel compression and/or cake/gel pores narrowing, as shown in Figure 5.1. Subsequently, I is determined from the slope of the linear phase of cake/gel filtration, as shown by Equation (5.2).

$$I = \frac{1}{J^2 \cdot \eta} \cdot \text{slope} \quad (5.2)$$

The MFI-UF, by definition, is the value of I corrected to the reference conditions, as shown in Equation (5.3) (Schippers and Verdouw, 1980).

$$MFI-UF = \frac{\eta_{20^\circ\text{C}} \cdot I}{2 \cdot \Delta P_o \cdot A_o^2} \quad (5.3)$$

Where ΔP_o , $\eta_{20^\circ\text{C}}$ and A_o are the reference pressure (2 bar), water viscosity (0.001 N.s/m²) and surface membrane area (0.00138 m²), respectively (Schippers and Verdouw, 1980).

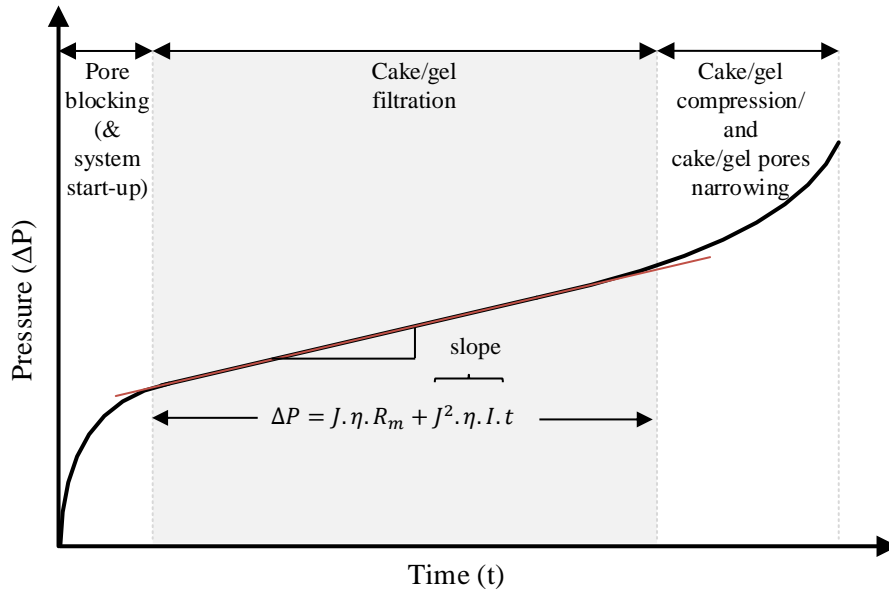


Figure 5.1: Typical filtration phases during MFI-UF test performed at constant flux

The MFI-UF value can be used as an input in the mathematical model shown in Equation (5.4) to predict the particulate fouling rate in RO systems. The particulate fouling rate is described by the increase in the net driving pressure (ΔNDP) over time due to the cake/gel formation on RO membrane, assuming no contribution by scaling and biofouling (Schippers et al., 1981).

$$\frac{\Delta NDP}{t} = \frac{2\Delta P_o \cdot A_o^2 \cdot J^2 \cdot \eta \cdot \Omega \cdot MFI-UF_{feed}}{\eta_{20^\circ\text{C}}} \quad (5.4)$$

The particle deposition factor (Ω) is incorporated in the prediction model (Equation (5.4)) to simulate the portion of particles depositing on RO membrane during cross-flow filtration. The deposition factor can be measured using Equation (5.5), based on the MFI-UF of RO feed, MFI-UF of RO concentrate and recovery rate (R). Ideally, the Ω value may vary between 0 and 1; where $\Omega = 0$ indicates no particle deposition, and $\Omega = 1$ indicates that all particles existed in the water passing the RO membrane deposited and remained on its surface (Salinas-Rodríguez et al., 2015).

$$\frac{\Delta NDP}{t} = \frac{2\Delta P_o \cdot A_o^2 \cdot J^2 \cdot \eta \cdot \Omega \cdot MFI-UF_{feed}}{\eta_{20^\circ C}} \quad (5.5)$$

5.2 MFI-UF SET-UP

The following sections (5.2.1 and 5.2.2) describe the MFI-UF set-up used in this work, including (1) the assembly of the MFI-UF set-up, and (2) the procedure applied to control the set-up quality.

5.2.1 Set-up assembly

The scheme of the MFI-UF set-up is shown in Figure 5.2. The set-up consists of three main components: (i) infusion pump, (ii) pressure transmitter, and (iii) membrane holder which comprises the MFI-UF membrane. The set-up works simply as follows. The pump pushes the feed water through a UF membrane at a constant flow rate. The pressure transmitter records the transmembrane pressure (ΔP) development over the filtration time (t) and transfers the data to the connected computer. The transferred data (ΔP vs t) is then used to calculate the MFI-UF value (refer to section 5.5).

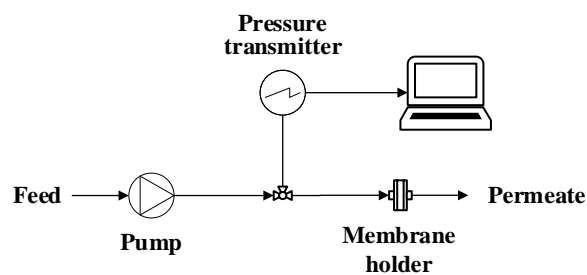


Figure 5.2: Scheme of MFI-UF set-up at constant flux filtration

5.2.1.1 Pump

The pump to be used in the MFI-UF set-up must not cause any pulsations or vibrations which can affect the properties of cake/gel formed on the MFI-UF membrane. Therefore, in this work, infusion syringe pumps were used (from Harvard Apparatus). The technical specifications of the pumps are summarized in Table 5.1.

5. Protocol for the MFI-UF at Constant Flux to Measure Particulate Fouling in Reverse Osmosis

Syringe pumps operate by pushing the feed water by an axial force at a constant displacement rate. The syringes used were made of plastic, with 60/140 mL volume, with a Luer-Lok tip (from BD). A new syringe was used for each MFI-UF measurement, as the plastic syringe wall may deviate with the frequent use.

Table 5.1: Technical specifications of used pumps (from Harvard Apparatus)

	PHD ULTRA standard	PHD ULTRA 4400	PHD ULTRA HPSI
Operating flow range	1.5 pL/min to 216 mL/min	3 pL/min to 216 mL/min	60 nL/min to 144 mL/min
Maximum operating pressure (based on 60 mL syringe)	6 bar	16 bar	35 bar
No. of syringes installed in parallel	2	1	4

5.2.1.2 Pressure transmitter

Two different pressure transmitters were used; Cerabar PMC51 (from Endress+Hauser) and PXM409 (from Omega). Both transmitters had a pressure measuring range from 0 to 10 bar. The transmitters were connected to a computer to transfer the data (ΔP and t) using a software provided by the manufacturer.

5.2.1.3 Membrane holder

MFI-UF membrane was placed in a 25 mm diameter dead-end plastic holder, with a pressure withstanding capacity of 10 bar (from Whatman). The holder consists of two caps assembled together with a rubber O-ring to prevent water leakage from the holder during filtration, as shown in Figure 5.3. The holder contains a support pad on which the MFI-UF membrane is placed, with an effective diameter of 21 mm.



Figure 5.3: Membrane holder with 25 mm nominal diameter (from Whatman)

5.2.1.4 Tubes

The set-up components (i.e. pump, pressure transmitter and membrane holder) were connected together using flexible plastic tubes of 6 mm diameter (from Festo). The tubes are resistant to chemicals, aging and abrasion, and could withstand pressure up to 10 bar.

All tubes used were transparent in order to monitor the presence of air bubbles which may affect the MFI-UF measurement (refer to section 5.2.2.2).

5.2.2 Set-up quality control

The accuracy of the MFI-UF measurement depends strongly on the quality of the set-up. The quality of the MFI-UF set-up is controlled by (1) periodic monitoring of the accuracy and reproducibility of the instruments used in the set-up, i.e., the pump and pressure transmitter, (2) the detection of trapped air, and (3) the detection of water leakage from the set-up. The procedure applied in this work to control the quality of MFI-UF set-up is explained in detail in the sections below (5.2.2.1-5.2.2.3).

5.2.2.1 Accuracy and reproducibility of pump and pressure transmitter

The accuracy and reproducibility of the pump and pressure transmitter installed in the MFI-UF set-up was checked quarterly/half-yearly (depending on the number of measurements), by following the procedure explained below (section 5.2.2.1.1 and 5.2.2.1.2). The pumps and pressure transmitters were directly maintained and calibrated (by the manufacturer) once a significant deviation in the accuracy and reproducibility was observed during the check ($\leq 5\%$ error was considered acceptable).

5.2.2.1.1 Pump check

Any error in the pump flow will be directly reflected in the applied flux rate during the MFI-UF test (since the flux equals the pump flow divided by the surface area of the MFI-UF membrane). Based on the fouling index I equation (Equation (5.2)), the difference in I value (and thus in the MFI-UF value as well) due to an error in the flux is raised to a power of 2. For example, if the required flux (ideal flux) is $100 \text{ L/m}^2\cdot\text{h}$ and there is an error in the pump of -10% (i.e. the actual flux is $90 \text{ L/m}^2\cdot\text{h}$), then the measured I value (and thus the MFI-UF) will be overestimated by around 23% , assuming no change in the slope of cake/gel filtration phase (i.e. assuming negligible effect by the flux variation on the cake compression), as shown below:

$$I_{with\ error} = \frac{J_{ideal}^2}{J_{with\ error}^2} \cdot I_{ideal} = \frac{100^2}{90^2} \cdot I_{ideal} = 1.23 I_{ideal} \quad (5.6)$$

In this work, pump accuracy was checked at different flow rates in the range of $6.93\text{-}69.30 \text{ mL/h}$. This flow range is equivalent to a flux rate of $20\text{-}200 \text{ L/m}^2\cdot\text{h}$, which is the flux range applied during this work (refer to section 5.4.2). At each flow rate, the pumped water was collected and weighed using an electronic balance. Accordingly, the water volume and thus water flow rate was measured over time.

Figure 5.4 demonstrates an example of the pump flow rate check, where the set flow value was 34.6 mg/L (i.e. equivalent to flux of $100 \text{ L/m}^2\cdot\text{h}$). As shown, the variation in the flow

rates (measured every 2 minutes) was low and random, whereas the standard deviation was 0.32 mL/h. The actual average pump flow (33.7 mL/h) was less than the set pump flow (34.6 mL/h) by less than 3%. According to the manufacturing technical sheet, this systematic error (3%) is likely due to the inevitable deviation in the wall of the plastic syringes used in the test, and it is not related to the pump instrument itself. Using steel syringes could solve the issue of syringe wall deviation, but it was not adopted in this work as the air bubbles inside the syringe cannot be observed.

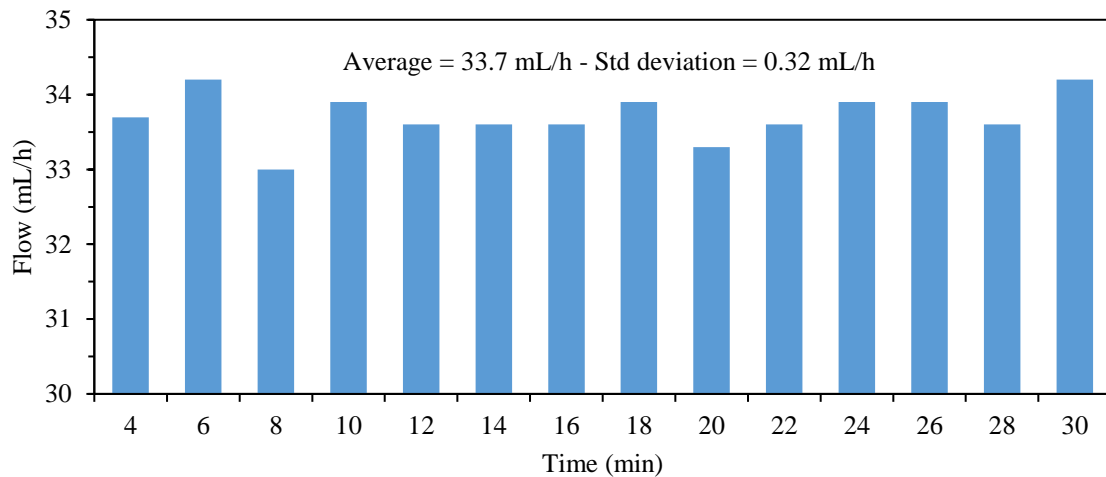


Figure 5.4: Pump (PHD ULTRA standard) flow at 34.6 mL/h (100 L/m².h)

For all pumps used in this work (Table 5.1), the maximum difference between the actual and set pump flow over the entire testing range (20-200 L/m².h) was always $\leq 5\%$, which is considered acceptable. In addition, the average flow rate was very reproducible with all pumps, where the variation did not exceed $\pm 1\%$ (Figure 5.5).

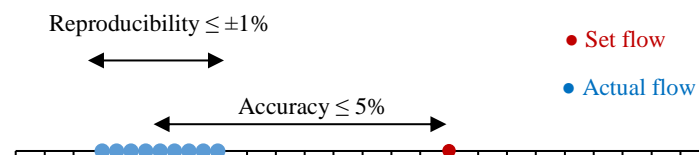


Figure 5.5: Accuracy and reproducibility of used pumps (expressed in max error%)

5.2.2.1.2 Pressure transmitter check

The MFI-UF is calculated based on the slope of the cake/gel filtration phase observed during the test (Figure 5.1). Therefore, any (systematic) error in the pressure measurement will result in inaccurate transmembrane pressure readings and thus a misleading slope of cake/gel filtration phase. Consequently, the measured MFI-UF may be incorrect. For example, assuming that there is an increment of 10 mbar in the transmembrane pressure over 30 min of filtration due to a systematic error in the pressure transmitter, then there will be an additional slope of 0.33 mbar/min due to this error. The equivalent increase in

the MFI-UF value due to this error is around 950 s/L^2 at a flux $100 \text{ L/m}^2\cdot\text{h}$ and a temperature of $20 \text{ }^\circ\text{C}$ (based on Equation (5.2) and (5.3)).

The accuracy of pressure transmitters was checked within a pressure range of 20-5000 mbar, which is the transmembrane pressure range mostly observed during the MFI-UF tests performed in this work (using 5-100 kDa membranes at a flux of $20\text{-}200 \text{ L/m}^2\cdot\text{h}$ (refer to section 5.3.1 and 5.4.2)). For this purpose, the pressure transmitter was connected to a pressure vessel, where the pressure was set using a pressure regulator, and then the transmitter readings were compared with the outputs of a calibrated manometer.

Figure 5.6 shows an example of the pressure transmitter check in the range of 1000 mbar. As shown, the pressure readings were random and very close to each other, where the standard deviation was only 0.2 mbar. Moreover, the actual average pressure (1091.9 mbar) was very similar to that measured by the calibrated manometer, where the difference was only 0.3%.

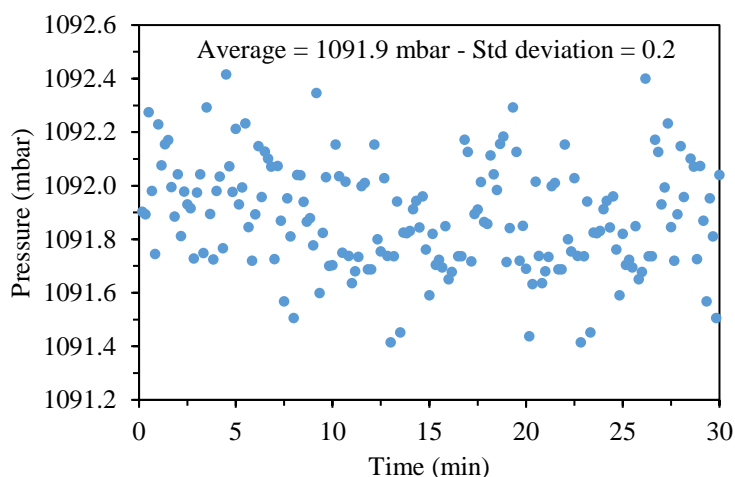


Figure 5.6: Pressure transmitter (Omega) readings at constant pressure in the range of 1000 mbar

For all pressure transmitters used in this work, the difference between the readings of the pressure transmitter and the outputs of the calibrated manometer was less than $\pm 1\%$ over the entire testing range (20-5000 mbar). In addition, the average pressure readings of the pressure transmitter were reproducible, where the variation was $< \pm 1\%$ (Figure 5.7).

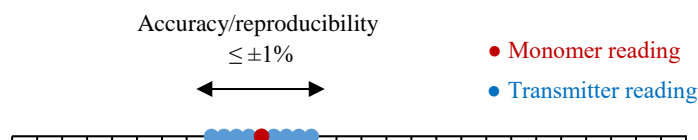


Figure 5.7: Accuracy and reproducibility of used pumps (expressed in max error%)

5.2.2.2 Trapped air detection

The presence of trapped air bubbles in the MFI-UF set-up (specifically inside the syringe, connecting tubes and membrane holder) may lead to artificially-high transmembrane pressure, due to the air compression and/or because of the bubble point of the MFI-UF membrane (in case the air bubbles are trapped over the MFI-UF membrane). As a result, an overestimated MFI-UF can be obtained. Therefore, trapped air should be removed before starting the MFI-UF test. This can be done by disconnecting the part including the air bubbles from the set-up and re-filling it gently with the feed water and then connecting it again to the set-up.

5.2.2.3 Water leakage detection

Water leakages from the MFI-UF set-up components can reduce the water flow (i.e. flux) through the UF membrane. Thus, the real flux rate can be lower than the flux required. Consequently, the measured MFI-UF can be underestimated. Therefore, to avoid the erratic MFI-UF measurement, water leakages should be detected and fixed before starting the MFI-UF test. In case water leakages were observed during the test performance, then the output of MFI-UF measurement might be incorrect.

5.3 MEMBRANE

The measured MFI-UF value is also highly dependent on the properties of the UF membrane used in the test. The following sections (5.3.1-5.3.5) describes (1) the selection of MFI-UF membranes, (2) membrane cleaning, (3) membrane resistance and inspection, (4) effect of membrane surface porosity, and (5) membrane surface plane direction.

5.3.1 Membrane selection

The UF membrane used in the MFI-UF test can have, in principle, any configuration as long as the membrane can be connected to the MFI-UF set-up. Boerlage et al. (2004) measured the MFI-UF using a custom hollow fibre UF modules which could be backwashed (from Pall Corporation). Afterward, Salinas-Rodríguez et al. (2015) performed the MFI-UF test with single-use flat-sheet UF membranes which are commercially available (From Millipore).

The pore size of the MFI-UF membrane (expressed by molecular weight cut-off (MWCO)) should be as small as possible in order to capture the particles that can deposit on an RO membrane. However, the pore size should not be too small so that the salt molecules or dissolved organic matter in feed water can be retained by the membrane during the MFI-UF test. This is because the MFI-UF method is derived based on cake/gel filtration mechanism, and does not account for the resistance caused by the osmotic pressure and concentration polarization resulting from the retention of salt and small organic molecules

on the MFI-UF membrane. However, due to the effect of cross-flow hydrodynamic conditions in RO filtration, only particles with a selective size range may deposit on an RO membrane and cause fouling (Lu and Ju, 1989). Therefore, to investigate the particles causing membrane fouling, the MFI-UF test can be applied using different MWCO membranes.

In this work, flat-sheet polyethersulfone (PES) UF membranes were used, with a wide range of MWCO; 5, 10, 50, and 100 kDa (from Millipore).

5.3.2 Membrane cleaning

UF membranes are usually coated with glycerine ($C_3H_8O_3$) to prevent the membranes drying and to maintain pore structure (Millipore, 2018). The quantity of glycerine depends mainly on the membrane properties; surface area, pore size and thickness (Wright et al., 2005).

Therefore, membranes should be cleaned before use in the MFI-UF test to remove the preservation glycerine coating which can hinder the water transport through the membrane. The importance of membrane cleaning is demonstrated in Figure 5.8. Figure 5.8 (a) shows the case where an ultra-pure water (i.e. no presence of particles) was filtered through uncleaned 100 kDa membrane at a flux of $100 \text{ L/m}^2\cdot\text{h}$. As it can be observed, the transmembrane pressure was decreasing along the filtration as the glycerine coating was being flushed out from the membrane over time. This decrease in the pressure (around 10 mbar per 30 min) is equivalent to negative MFI-UF of about -950 s/L^2 (based on Equation (5.2) and (5.3)). On the other hand, Figure 5.8 (b) shows how the transmembrane pressure became stable (~ 0 slope) after the membrane was cleaned.

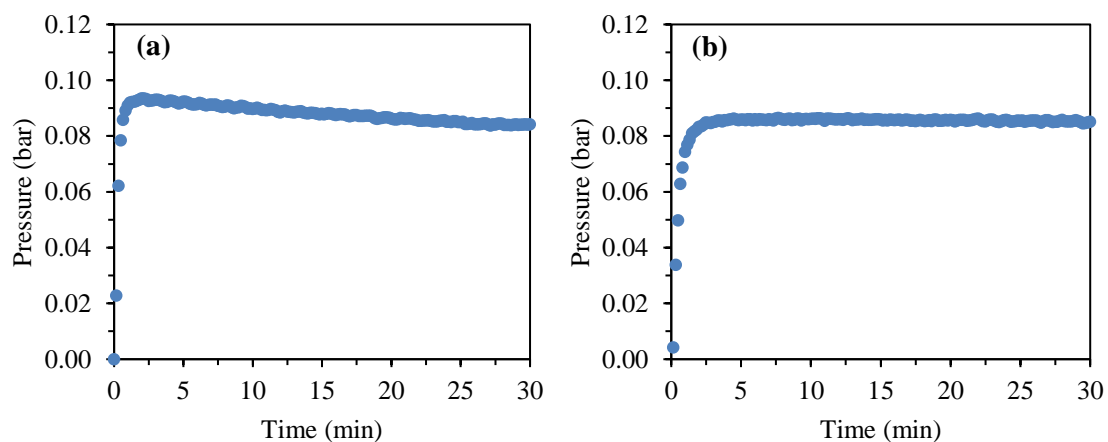


Figure 5.8: Transmembrane pressure over time during the filtration of ultra-pure water through 100 kDa membrane at $100 \text{ L/m}^2\cdot\text{h}$; (a) before and (b) after membrane cleaning by filtering 100 ml of ultra-pure water

Therefore, during the MFI-UF test, the slope of cake/gel filtration phase may be affected if the membrane was not pre-cleaned, as the slope would be a resultant of both (i) transmembrane pressure decline due to the release of preservation glycerine coating over time (as in Figure 5.8 (a)), and (ii) transmembrane pressure increase due to cake/gel formation. As a result, the measured MFI-UF may be inaccurate.

5.3.2.1 Cleaning approach

According to the technical sheet of membrane manufacturer (Millipore), membranes can be cleaned by soaking the membrane in ultra-pure water for one hour with changing the water at least three times. Alternatively, membranes can be cleaned by filtering ultra-pure water for at least five minutes at a pressure of 0.7 and 3.8 bar for the membranes with MWCO ≥ 100 kDa and < 100 kDa, respectively (Millipore, 2018). Nevertheless, these procedures were found (after several trials) to be insufficient to remove the glycerine coating completely, where the transmembrane pressure decline was still observed as shown in Figure 5.8 (a).

Consequently, a new cleaning approach was investigated by filtering 100 mL of ultra-pure water (Milli-Q, Millipore) at a flux rate of 100-1000 L/m².h (\equiv pump flow of 34.6-346 mL/h). As a worst-case scenario, membrane cleaning was investigated using 100 kDa membrane as it has the highest MWCO (i.e. largest pore size) and thus it is expected that it has the largest quantity of coating in comparison with the other used membranes having lower MWCO (Wright et al., 2005). At each applied flux, 5 membranes were cleaned in parallel, where all the membranes were obtained from the same manufacturing batch. During filtration, the permeate was collected in sequential discrete batches of 20 mL volume, and the TOC was measured accordingly (using TOC-L model from Shimadzu).

Figure 5.9 shows the removal of glycerine coating expressed by the TOC of permeate (it is important to mention that the TOC may also include organic matters released by the membrane material itself). As observed, 90-95% of coating removal was achieved in the first 20 mL of filtered volume. However, the removal was more efficient when the applied flux was lower. This is because the lower the flux, the longer the filtration duration, and thus the longer the contact time between the water and membrane. Consequently, the diffusion of glycerine from the membrane was higher (Wright et al., 2005; Arenillas et al., 2017). At 100 L/m².h (the lowest applied flux), the cleaning was sufficient after filtering 80 mL, where the TOC of the permeate reached the limit of detection (LOD) of the used TOC equipment (0.2 mg/L). On the other hand, at 1000 L/m².h (the highest applied flux), the cleaning was not sufficient even after filtering 100 mL, where the TOC of the permeate was still higher than 3 mg/L.

Nevertheless, cleaning the membrane at a flux of 100 L/m².h (34.6 mL/h) was time consuming, where the filtration of 100 mL lasted for around 3 hours. On the other hand, membrane cleaning at 1000 L/m².h (346 mL/h) was much faster, as the filtration of 100

mL lasted only for 0.3 hour, however, the cleaning was insufficient as mentioned above. Therefore, in this work, membrane cleaning by filtering 100 mL of ultra-pure water at 300 L/m².h was mostly adopted, where the filtration (i.e. cleaning) time was 1 hour and the cleaning was sufficient.

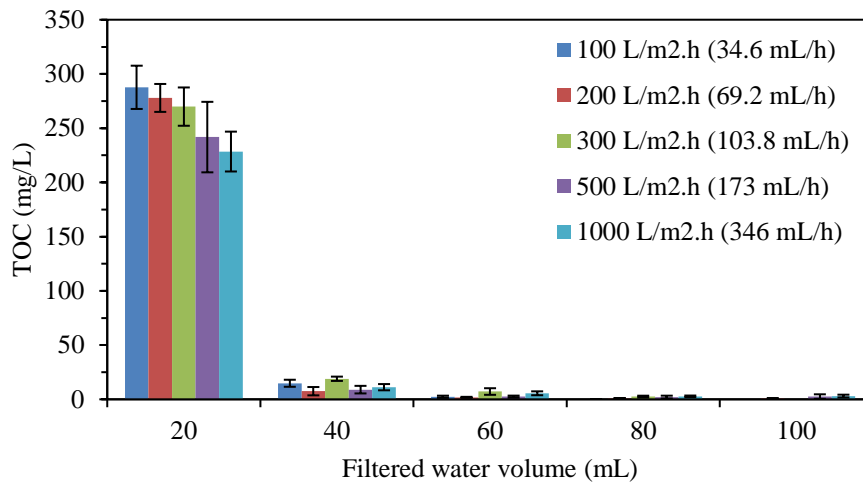


Figure 5.9: TOC of permeate collected in sequent discrete batches of 20 mL during the filtration of ultra-pure water through 100 kDa membranes at a flux rate of 100-1000 L/m².h

In case the MFI-UF is measured for a feed water with high fouling potential (e.g. raw water), membrane cleaning with less water volume (e.g. 50 mL) can be also sufficient. This is because the effect of uncomplete coating removal will be insignificant in comparison with the effect of membrane fouling.

In addition, it is expected that membrane cleaning can be further improved by heating the ultra-pure water. This is because the higher the water temperature, the higher the diffusion rate of glycerine from the membrane (Wright et al., 2005). However, the temperature of ultra-pure water should be lower than the operational temperature limit of the membranes (50 °C for the PES UF membranes used in this work). However, the effect of water temperature on enhancing coating removal still needs further investigation.

5.3.3 Membrane resistance

Membrane should be inspected prior to the MFI-UF test to verify that the membrane is not damaged. This can be done by measuring the membrane resistance. Accordingly, membranes with a resistance value outside of the expected range can be excluded.

Membrane resistance (R_m) is the reciprocal of membrane permeability. It can be defined according to Hagan-Poiseuille formula as a function of membrane thickness (Δx), tortuosity (τ), surface porosity (ε_s) and pore radius (r_p), as described by Equation (5.7).

$$R_m = \frac{8 \cdot \Delta x \cdot \tau}{\varepsilon_m \cdot r_p^2} \quad (5.7)$$

The aforementioned membrane properties are usually not provided by the membrane manufacturer, and also very difficult to measure separately for each membrane. Therefore, R_m can be determined experimentally after membrane cleaning (refer to section 5.3.2) by filtering ultra-pure water using same MFI-UF set-up (Figure 5.2). The R_m value is then calculated using Equation (5.8).

$$R_m = \frac{\Delta P}{J \cdot \eta} \quad (5.8)$$

R_m can be measured at any flux as long as the applied flux is not too high to compact the membrane. The effect of the flux on the membrane compaction was tested for 100 kDa membrane, by measuring the transmembrane pressure during the filtration of ultra-pure water (i.e. no presence of particles) at different flux rates (100-1000 L/m².h). As shown in Figure 5.10, the transmembrane pressure was linearly correlated to the flux. This means that increasing the flux did not compact the membrane, and thus did not affect the R_m .

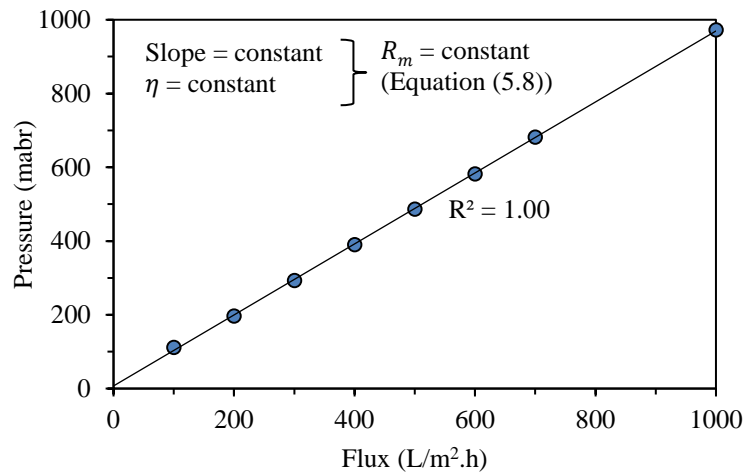


Figure 5.10: Transmembrane pressure against flux during the filtration of ultra-pure water through 100 kDa membrane

Table 5.2 lists the R_m range of UF membranes used in this work, where the outliers were removed based on Tukey's method (Hoaglin et al., 1986). The observed variation in R_m value could be due to one or multiple membrane properties (Equation (5.7)), which can differ from one membrane to another (Mulder, 2012). However, assuming that the membrane surface properties (i.e. the pore size and surface porosity) play a major role in the R_m variation, then the characteristics of the cake/gel formed on the membrane and thus the measured MFI-UF value might be different for the same feed water if the used membranes had different R_m values. Therefore, for each batch of MFI-UF tests, it is

recommended to use membranes with similar R_m value, to eliminate as much as possible the effect of membrane properties variation on the measured MFI-UF. This is more essential for the 5 kDa membranes since the variation in R_m is higher (Table 5.2). Nevertheless, further work is still required to investigate the membrane properties dominating the R_m variation.

Table 5.2: R_m range of used PES membranes with MWCO of 5-100 kDa

Membrane MWCO	5 kDa	10 kDa	50 kDa	100 kDa
No. of membranes	154	262	6	287
Average (1/m)	6.90×10^{12}	9.44×10^{11}	5.75×10^{11}	3.68×10^{11}
Minimum (1/m)	4.50×10^{12}	8.00×10^{11}	5.56×10^{11}	3.02×10^{11}
Maximum (1/m)	10.7×10^{12}	11.2×10^{11}	5.99×10^{11}	4.43×10^{11}
Standard deviation (1/m)	1.50×10^{12}	0.68×10^{11}	0.18×10^{11}	0.32×10^{11}
Coefficient of variation (%)	21.7	7.2	3.2	8.7

5.3.4 Effect of membrane surface porosity

In Chapter 3 (Abunada et al., 2022), it was found that the lower the MWCO of the MFI-UF membrane, the lower the surface porosity and thus the smaller the effective filtration area. This results in a higher local flux during the MFI-UF test and subsequently an overestimated MFI-UF value. The effect of membrane surface porosity on the measured MFI-UF was quantified using a suspension of pre-washed polystyrene particles. As a result, a correction factors of 0.4-1.0 were proposed for the MFI-UF measured with 5-100 kDa membranes, respectively. The study also recommended to quantify the effect of membrane surface porosity using (a mixture of) different types of organic and inorganic particles which exhibit similar properties to particles that exist in real water such as RO feed water.

5.3.5 Membrane plane direction

The direction of the membrane surface plane can be either vertical or horizontal. This means that the membrane holder can be installed in the set-up either vertically or horizontally. However, as a special case, when the feed sample is prepared from synthetic inert particles (e.g. polystyrene particles), the direction of the membrane surface plane should be horizontal. This is because inert particles may not adhere to the membrane surface and to each other, and thus the formed cake can fall/creep due to gravity if the membrane surface plane is vertical. This can be more significant at low flux rates, where the permeation force becomes insufficient to hold the particles/cake on the membrane

surface. The aforementioned creep phenomenon is demonstrated and explained in detail in Annex 5.8.1.

5.4 MFI-UF TESTING CONDITIONS

The operating conditions during the MFI-UF test can have a significant effect on the occurrence and extent of cake/gel formation (Figure 5.1) and thus on the measured MFI-UF. Based on Equation (5.1), which describes the fundamental equation of cake/gel formation at constant flux filtration, the increase in the transmembrane pressure (ΔP) is a function of fouling resistance (I) as well as the following conditions: (i) feed temperature (i.e. viscosity), (ii) applied flux rate, and (iii) filtration duration (i.e. test duration). The effect of these operating conditions is discussed in detail in the sections below (5.4.1-5.4.3).

5.4.1 Feed water temperature

The temperature of the feed water sample may be different than the temperature where the MFI-UF test is performed. However, it is important to allow the sample to reach ambient temperature so that it remains constant during the MFI-UF test. This is because any variation in feed water temperature can affect the permeability of water through the MFI-UF membrane and thus the transmembrane pressure development during the test. As a result, the observed slope of the cake/gel filtration phase can be attributed not only to the effect of fouling but also to the variation in feed water temperature (as shown in Equation (5.1)). Consequently, erratic MFI-UF results may be obtained.

The effect of water temperature variation on the transmembrane pressure (ΔP) can be described by Equation (5.9), where ΔP_i is the initial transmembrane pressure at the start of cake/gel filtration phase, and ΔP_f is the final transmembrane pressure at the end of cake/gel filtration phase, and η_i and η_f are the initial and final feed water viscosity (i.e. at the start and end of cake/gel filtration phase), respectively.

$$\Delta P_f = \Delta P_i \left(\frac{\eta_f}{\eta_i} \right) \quad (5.9)$$

For instance, for a feed water with initial temperature of 20 °C ($\eta_i = 0.001 \text{ N.s/m}^2$), the ΔP would change by around $\pm 2.5\%$ if the temperature varied by $\pm 1 \text{ }^\circ\text{C}$ ($\pm 0.000025 \text{ N.s/m}^2$) during the cake/gel filtration phase. Based on Equation (5.9), the effect of water temperature variation on the ΔP can be greater if the ΔP_i is higher (which can likely occur when the applied flux rate is higher and/or the membrane MWCO is lower). For example, with using 5 kDa membrane at a flux of 100 L/m².h in an MFI-UF test, the ΔP_i can be around 2 bar at 20 °C. Assuming that the feed water temperature varied by $\pm 1 \text{ }^\circ\text{C}$ during

30 minutes of cake/gel filtration, then ΔP will change by ± 0.05 bar ($2.5\% \times 2$ bar) in 30 min due to this temperature variation in the feed water. This is equivalent to MFI-UF of around ± 5000 s/L² (based on Equation (5.2) and (5.3)), which is considered substantial. The effect of feed water temperature variation can be more significant if the feed water has low fouling potential. In this case, the cake/gel filtration phase and thus the measured MFI-UF will be dominated by the variation of the water temperature rather than the effect of membrane fouling.

In case the variation in feed water temperature could not be prevented during the MFI-UF test, then the slope of cake/gel filtration phase should be corrected before calculating the MFI-UF. This can be done using Equation (5.10), where $slope_{cor}$ and $slope_{act}$ are the corrected and actual slope of the cake/gel filtration phase, respectively, and t_c is the duration of the cake/gel filtration phase (the derivation of the equation is explained in detail the Annex 5.8.2).

$$Slope_{cor} = \left((\Delta P_i + slope_{act} \times t_c) \cdot \left(\frac{\eta_i}{\eta_f} \right) - \Delta P_i \right) \cdot \frac{1}{t_c} \quad (5.10)$$

The equation above (Equation (5.10)) was derived based on the assumption that (i) the variation rate of water temperature is constant during cake/gel filtration, and (ii) both membrane resistance and specific cake resistance are not affected by the water temperature variation (as found by Boerlage et al. (2003b)). However, it was observed that the variation rate of feed water temperature (if any) is usually not constant as assumed above, whereby the variation in water temperature may be higher at the beginning of filtration. Therefore, Equation (5.10) is considered an approximate (i.e. not absolute) correction for the effect of feed temperature variation.

5.4.2 Flux rate

The measured MFI-UF is highly dependent on the flux rate applied during the test. At higher flux rate, the particles deposited on the MFI-UF membrane can be re-arranged and the formed cake can be compressed, which can result in a less porous cake and consequently higher MFI-UF value (Boerlage et al., 2004; Salinas-Rodríguez et al., 2012; Salinas-Rodríguez et al., 2015). Therefore, the MFI-UF should be measured at the same flux as is applied in the RO system to be assessed (typically ~ 10 - 35 L/m².h (DOW, 2011)). Alternatively, since an MFI-UF test at such a low flux may take a long time (refer to section 5.4.3), the MFI-UF can be measured at higher flux rates and then extrapolated linearly to the actual RO flux. For example, Figure 5.11 shows the MFI-UF of RO feed water (collected from RO plant treating surface water) measured by both aforementioned approaches; (i) directly at RO flux of 23 L/m².h (open points), and (ii) at higher flux rates (solid points) and then extrapolated to 23 L/m².h (disconnected lines). As it can be

observed, the MFI-UF obtained by both approaches was very similar in all cases, where the difference was around $\pm 5\%$.

For the latter approach (i.e. extrapolation), MFI-UF measurement at flux rates higher than $200 \text{ L/m}^2\cdot\text{h}$ is not recommended, since cake compression can occur very quickly and thus it would be difficult to identify the cake filtration phase (especially for feed water with a high fouling potential). In addition, to eliminate the potential influence of high leverage on the resulted regression line and thus on the extrapolated MFI-UF value, the test should be performed at higher flux rates with equal-increment (e.g. 50, 100, 150 and $200 \text{ L/m}^2\cdot\text{h}$).

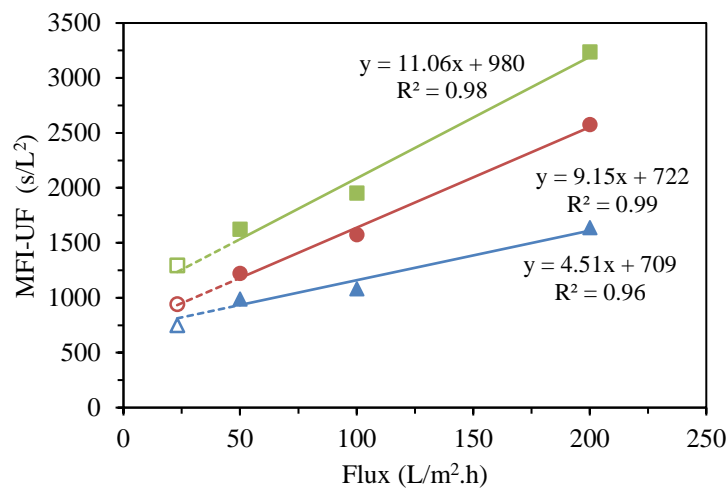


Figure 5.11: MFI-UF measured (i) directly at same RO flux (Δ 100 kDa, \circ 10 kDa, \square 5 kDa), and (ii) at higher flux rates (\blacktriangle 100 kDa, \bullet 10 kDa, \blacksquare 5 kDa) and then extrapolated to the RO flux (disconnected lines)

5.4.3 Test duration

The duration of the MFI-UF test should be sufficient to observe a stable cake/gel filtration phase. To know how long the MFI-UF test should last, it is important to understand the mechanism of cake/gel formation on the MFI-UF membrane during the test, as explained below.

Once the MFI-UF test starts, particles in the filtered feed water flow with the water stream toward the membrane pores, which eventually results in pore blocking. Subsequently, particles start to accumulate over the pores forming separated clumps/mounds of particles (Figure 5.12 (right)). The clumps/mounds will grow until the cake starts to be built up in a uniform structure of even layers (Figure 5.12 (left)). Afterwards, the built-up of cake layers will remain stable and take over the filtration until the particles in the cake start to re-arrange simultaneously with cake compaction, whereby cake compression becomes the dominant filtration mechanism.

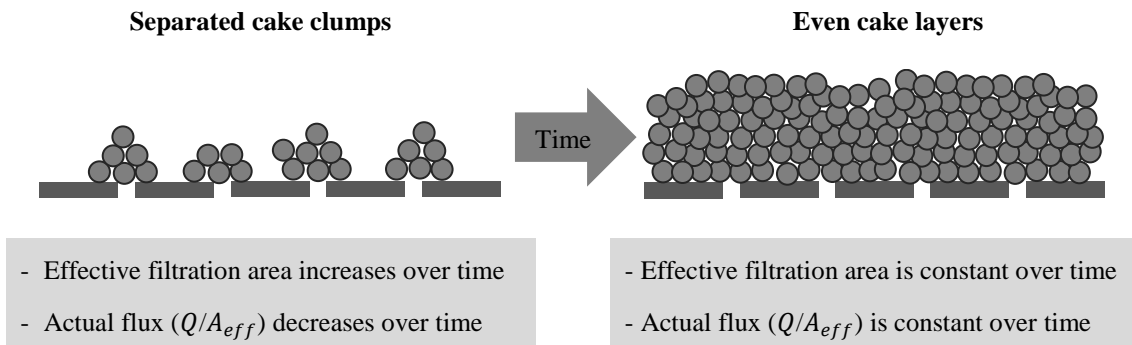


Figure 5.12: Schematic diagram illustrating cake development on a membrane surface during an MFI-UF test

The explanation above is further demonstrated in Figure 5.13 which shows the transmembrane pressure development during an MFI-UF test with canal water using a 10 kDa membrane at a flux of $20 \text{ L/m}^2\cdot\text{h}$ (i.e. at 6.9 mL/h). As it can be observed during the cake/gel filtration phase, the increase rate of transmembrane pressure was initially not constant and continuously decreasing over time during the period where cake clumps/mounds are formed on the membrane surface (0.5-2.5 h), while afterwards, it became stable when the cake build-up occurred in even layers (2.5-10 h). This is because the effective filtration area (A_{eff}) was increasing gradually as the cake clumps/mounds were growing. As a result, since the pump flow was constant (6.9 mL/h), then the actual flux (Q / A_{eff}) was decreasing with cake clumps/mounds growth over time. Simultaneously, based on Equation (5.1), the increase rate of transmembrane pressure was decreasing. However, once the cake growth over the membrane became stable (such as in Figure 5.12 (right)), the A_{eff} remained constant, and consequently the actual flux and thus the increase rate of transmembrane pressure was stable over time.

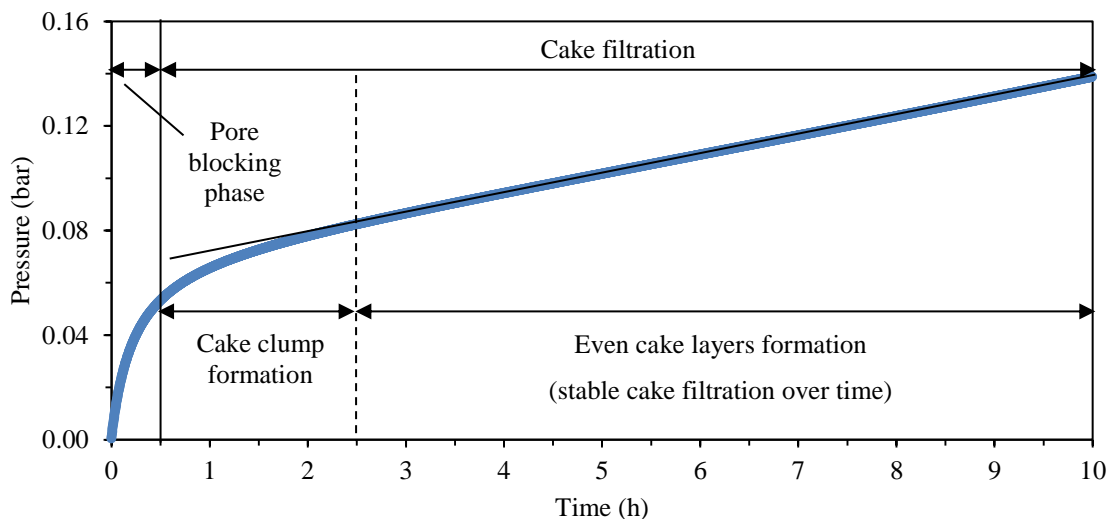


Figure 5.13: Transmembrane pressure development over time during filtration of canal water through 10 kDa membrane at $20 \text{ L/m}^2\cdot\text{h}$

Accordingly, as observed in Figure 5.13, if the MFI-UF test was stopped during the phase of cake clump/mound formation (i.e. before 2.5 h), then the calculated MFI-UF would be overestimated as the slope of cake filtration phase is higher than the slope during the phase of even cake layers formation (i.e. after 2.5 h). In this case, the MFI-UF calculated based on the period of 0.5-2.5 h (13,500 s/L²) was around 47% higher than that obtained based on the period of 2.5-10 h (9,200 s/L²).

5.4.3.1 Factors affecting test duration

As mentioned above, the MFI-UF test duration depends on observing stable cake/gel filtration during the test. The start of the stable cake/gel filtration phase can be strongly influenced by three factors, namely; (i) concentration of particles in the feed water, (ii) applied flux rate, and (iii) surface porosity of the MFI-UF membrane. At lower particle concentrations and/or lower flux rates, the load of particles depositing over time on the MFI-UF membrane is lower. As a result, the growth of cake clumps/mounds (Figure 5.12 (left)) will be slower, and thus more time is required until the cake starts to build up evenly on the membrane surface. In addition, the formation of even cake layers on the MFI-UF membrane can take more time when the membrane has a lower surface porosity (i.e. lower MWCO). This is because the lower the surface porosity, the larger the distance between the membrane pores. Consequently, cake clumps/mounds will take more time to form continuous/even cake layers. In summary, the MFI-UF test duration should be longer with lower flux rate, particle concentration and/or membrane surface porosity.

Ideally, the MFI-UF test is complete when cake/gel compression phase (Figure 5.1) is observed during the test. However, if the cake compression phase is not observed, then it is recommended to stop the MFI-UF test once stable cake filtration has been observed for more than 75% of the elapsed test time. This rule of thumb was concluded based on a large number of MFI-UF measurements.

As an indication, Table 5.3 shows the approximate duration of the MFI-UF tests for canal water diluted to different concentrations; from 100% (raw canal water) to 1% (i.e. 1% of raw canal water mixed with 99% of a dilute solution of filtered tap water). The quality of raw canal water was as follows: turbidity ranged from 1.5 to 3.0 NTU, TOC from 11 to 18 mg/L, and EC from 600 to 800 uS/cm. The MFI-UF tests were performed at fluxes of 20, 100 and 200 L/m².h using 5, 10, 100 kDa membranes. The measured MFI-UF values were presented in Chapter 2 (Abunada et al., 2023a) and were in the range of 100-70000 s/L².

The shortest and longest test duration shown in Table 5.3 refer to the canal water with 100% and 1% concentration, respectively (e.g. for the MFI-UF measured at 20 L/m².h using 5 kDa membrane, 8 h refers to the 100% canal water sample and the 20 h refers to the 1% canal water sample). As observed, the effect of particle concentration and flux rate have the greatest impact on MFI-UF test duration in comparison with the membrane MWCO (i.e. membrane surface porosity). Accordingly, considering the longest MFI-UF

test duration as a ‘safe’ scenario, then the MFI-UF test can be stopped generally once the test duration exceeds 20, 3 and 1 h at a flux of 20, 100 and 200 L/m².h, respectively. The test duration at other flux rates can be approximated relatively. For example, at a flux of 150 L/m².h, the MFI-UF test duration can be estimated as 2 hours.

Table 5.3: Approximate range of MFI-UF test duration (for canal water samples with a concentration of 1-100%, where raw canal water has turbidity ranged from 1.5 to 3.0 NTU, TOC from 11 to 18 mg/L, and EC from 600 to 800 uS/cm)

Membrane	Flux		
	20 L/m ² .h	100 L/m ² .h	200 L/m ² .h
5 kDa	8 – 20 h	1 – 3 h	0.50 – 1 h
10 kDa	6 – 18 h	1 – 2 h	0.25 – 1 h
100 kDa	5 – 15 h	0.5 – 2 h	0.25 – 1 h

5.5 MFI-UF CALCULATION

By the completion of the MFI-UF test, the data of transmembrane pressure (ΔP) and time (t) recorded during the test is plotted. The plot typically consists of three subsequent fouling phases (as shown in Figure 5.1); pore blocking, cake/gel filtration and cake/gel compression. Subsequently, the MFI-UF value is calculated based on the slope of the stable (linear) cake/gel filtration phase using Equation (5.2) and (5.3).

The boundaries (i.e. the start and end) of the stable cake/gel filtration phase can be identified manually (i.e. visually). To identify the boundaries more precisely, the x- and y-axis can be zoomed-in and re-scaled. This can be further supported by drawing a parallel line (such as the red line in Figure 5.1). The drawn line helps to prevent selecting a part of the pore blocking, cake/gel compression as well as the phase of cake clump/mound formation (shown in Figure 5.13). An example of manual calculation steps of MFI-UF is illustrated in Annex 5.8.3.

However, since it can be difficult (particularly for non-professional) to identify visually the exact boundaries of cake/gel filtration phase, and as the visual identification of cake/gel filtration boundaries can be subjective and different from one person to another, this may eventually result in inaccurate and/or unreproducible MFI-UF calculation. Therefore, a new numerical algorithm was developed to calculate the MFI-UF automatically (i.e. not manually/visually). The new calculation algorithm was developed based on regression modelling, where the actual data obtained during the MFI-UF test (ΔP against t) can be modelled/fitted and then the slope of cake/gel filtration phase could be determined by finding the 1st derivative of the fitting curve. Four regression models

were selected and tested. The results showed that the model so-called Rational 3/2 (Equation (5.11), where α and β are the model parameters (NIST, 2012)) is the most robust model, where it could greatly fit the ΔP vs t data for different levels of fouling potential (i.e. different levels of MFI-UF), and the minimum slope of cake/gel filtration phase was found where it was expected, as shown in Figure 5.14.

$$P = \frac{\alpha_0 + \alpha_1 t + \alpha_2 t^2 + \alpha_3 t^3}{\beta_0 + \beta_1 t + \beta_2 t^2} \quad (5.11)$$

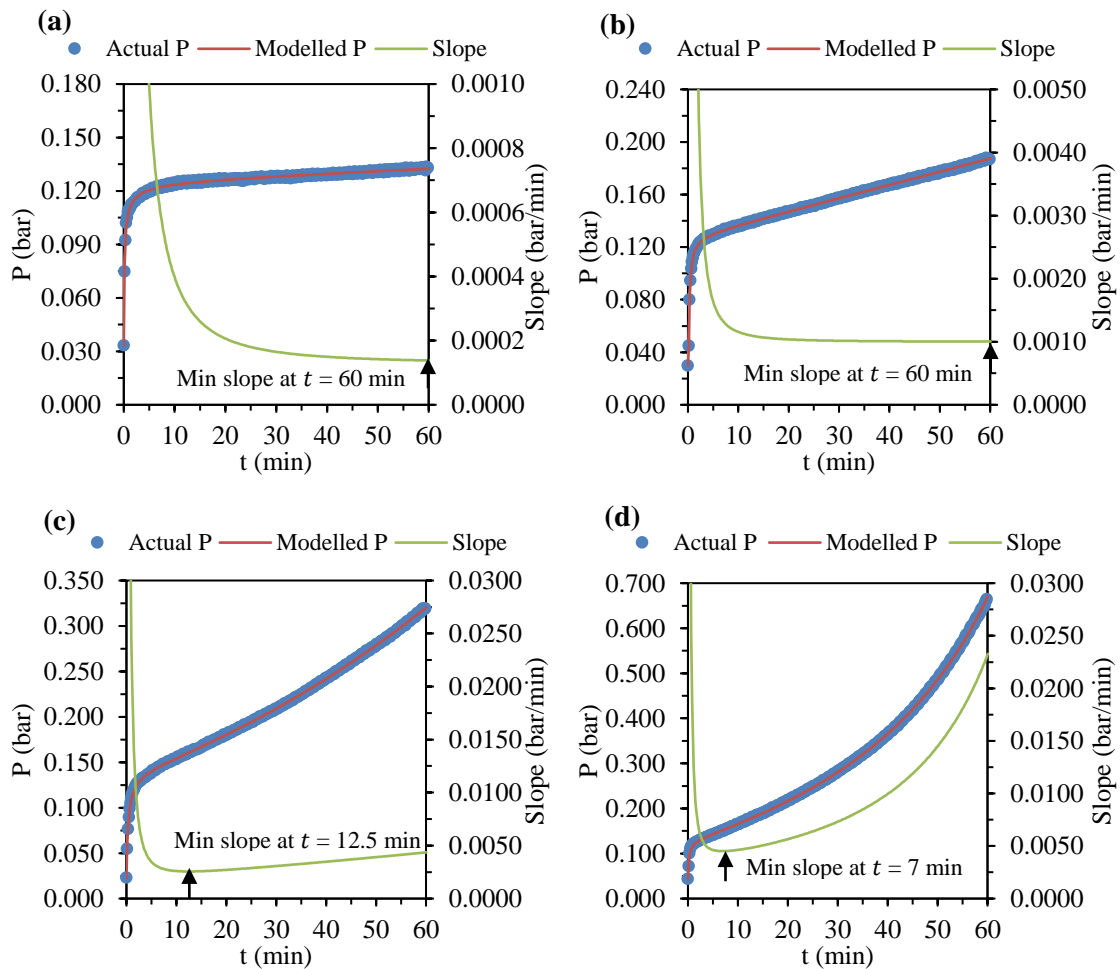


Figure 5.14: MFI-UF calculation based on Rational 3/2 model for different MFI-UF levels (P vs t data is for canal water samples with (a) 5%, (b) 25%, (c) 50% and (d) 100% concentration, measured at $100 \text{ L/m}^2 \cdot \text{h}$ using 100 kDa membrane)

The comparison between both MFI-UF calculation approaches (i.e. manual and automatic) is shown Table 5.4. The maximum difference (8%) was found for the lowest concentration water sample. Nevertheless, this difference is equivalent to MFI-UF of 50

s/L^2 which is considered very low and below the limit of detection calculated in Chapter 3 (Abunada et al., 2022).

The developed MFI-UF calculation algorithm was further validated using additional MFI-UF data (ΔP vs t) of various water samples at different testing conditions (at 20-200 $L/m^2.h$ flux using 5-100 kDa membranes). The results confirmed the precision and reproducibility of calculated MFI-UF values. The development of the automated calculation algorithm is addressed in more details in Annex 5.8.4.

Table 5.4: MFI-UF calculated based on manual and automatic approach for canal water samples measured at 100 $L/m^2.h$ using 100 kDa membrane

Canal water concentration	5%	25%	50%	1000%
Manual MFI-UF calculation	450 s/L^2	3000 s/L^2	7600 s/L^2	13400 s/L^2
Automatic MFI-UF calculation (based on Rational 3/2 model)	400 s/L^2	3000 s/L^2	8000 s/L^2	14200 s/L^2
Coefficient of variation	8%	0%	4%	4%

5.6 STEP-BY-STEP MFI-UF TESTING PROCEDURE

The following is the step-by-step procedure to measure the MFI-UF, based on the details addressed in the previous sections (section 5.1-5.5).

1. Introduction

- 1.1. This protocol covers the determination of the MFI-UF at constant flux to measure particulate fouling in RO systems.
- 1.2. The MFI-UF method is a water quality method, developed based on the MFI method, to evaluate the effect of the small particles/colloids which are more likely to be responsible for RO membrane fouling.

Note - The MFI-UF method can be also used to determine and profile the efficiency of water pre-treatment processes in removing particulate matter.

2. MFI-UF set-up

- 2.1. The MFI-UF set-up is assembled as shown in Figure 5.2. The set-up consists mainly of a pump, pressure transmitter, dead-end membrane holder containing UF membrane, and connecting tubes/fittings (the specifications of each set-up component are explained in detail in section 5.2.1).

- 2.2. The set-up works as follows. The pump pushes the feed water through a UF membrane at a constant flow rate. The pressure transmitter records the transmembrane pressure over time and transfers the data to a connected computer. The transferred data is then used to calculate the MFI-UF value (refer to point 5. MFI-UF calculation).
- 2.3. Pump:
- 2.3.1. This protocol is based on using a syringe infusion pump.
- 2.3.2. The pump should not generate vibration that may affect the properties of cake/gel formed on the MFI-UF membrane.
- 2.3.3. The accuracy and reproducibility of the pump should be checked periodically (this depends on the measurement load recommended by the manufacturer). The procedure of checking the accuracy and reproducibility of the pump is explained in detail in section 5.2.2.1.1.
- 2.3.4. Pump flow is set based on the required flux rate, using Equation (5.12), where Q is the pump flow, J is the flux, and A is the active membrane surface area.

$$Q = J \cdot A \tag{5.12}$$

Table 5.5 shows the pump flow at given flux rates based on active membrane surface diameter of 21 mm (refer to point 3. MFI-UF membrane).

Table 5.5: Pump flow at given flux rates

Flux (L/m ² .h)	Pump flow (mL/h)
20	6.9
100	34.6
150	51.9
200	69.2

- 2.4. Pressure transmitter:
- 2.4.1. Pressure transmitter should be connected to a computer screen displaying the pressure readings in real-time during the test.
- 2.4.2. The zero level of the pressure transmitter should be set at the same elevation of the membrane holder. This can be verified by checking the pressure transmitter reading while the pump is off which should be around zero.

- 2.4.3. The accuracy and reproducibility of the pressure transmitter should be checked periodically (this depends on the measurement load recommended by the manufacturer). The procedure of checking the accuracy and reproducibility of the pressure transmitter is explained in detail in section 5.2.2.1.2.
- 2.5. Membrane holder:
 - 2.5.1. The holder should hold a flat-sheet membrane in dead-end mode. This protocol is based on using a membrane holder of 25 mm nominal diameter and 21 mm active diameter (refer to point 3. MFI-UF membrane).
 - 2.5.2. The holder should be sealed with a rubber O-ring to prevent the water leakage from the holder during the test.
 - 2.5.3. The holder should be transparent to detect any trapped air bubbles.
 - 2.5.4. Holder material should be resistant to the chemicals, aging and abrasion.
- 2.6. Connecting tubes and fittings:
 - 2.6.1. Tubes and fittings should be transparent to detect any trapped air bubbles.
 - 2.6.2. Material should be resistant to the chemicals, aging and abrasion.
- 2.7. All set-up components should be compatible with the operating pressure range observed during the MFI-UF test. The operating pressure depends mainly on the applied flux rate, MWCO of the MFI-UF membrane, and quality of feed water. For the scope of this protocol, the operating pressure is expected to be in the range of around 0-5 bar.
- 2.8. Trapped air and water leakages in the MFI-UF setup should be detected and eliminated before starting the test (refer to section 5.2.2.2-5.2.2.3).

3. MFI-UF membrane

- 3.1. This protocol is based on using flat-sheet polyethersulfone (PES) membranes with MWCO of 5-100 kDa and nominal surface diameter of 25 mm (the active diameter of membrane surface is 21 mm inside the membrane holder). Selection of membrane MWCO is explained in section 5.3.1.
- 3.2. Membrane should be cleaned before use to remove the preservation coating. Membrane is cleaned using same MFI-UF set-up (Figure 5.2) with filtering ultra-pure water. This can be done as follows:
 - 3.2.1. Place the MFI-UF membrane into the membrane holder:

3.2.1.1. Disassemble/open the membrane holder and remove the rubber O-ring.

3.2.1.2. Wet the membrane with the ultra-pure water and place it on the holder support pad. The glossy surface (i.e. active filtration side) should face the direction of water flow.

Note - Membrane should be placed in the holder using a clean tweezer. The tweezer should hold the membrane from the edge to avoid membrane puncturing. Membrane should not be held with hands to avoid any membrane contamination.

3.2.1.3. Re-install the rubber O-ring over the membrane, and then re-assemble/close the membrane holder. Tighten the holder gently to avoid membrane twisting.

3.2.1.4. Fill the membrane holder with ultra-pure water from the holder inlet using a needle.

3.2.2. Fill ultra-pure water in a plastic transparent syringe. 60/140 mL syringe can be typically used.

Note - Steel syringes should not be used since they are not transparent, and thus the trapped air bubbles cannot be detected.

3.2.3. Connect the membrane holder with the syringe and pressure transmitter through a 3-way valve, as shown in Figure 5.2.

3.2.4. Ensure that there are no trapped air bubbles in the syringe, membrane holder and tubes/fittings.

3.2.5. Set the pump flow (refer to point 2.3.4), and start both the pump and pressure transmitter logging simultaneously.

3.2.6. Ensure that there is no water leakage from the set-up during the test. In case any leakage is detected, the test should stop.

Note - The cleaning can be optimally done by filtering 100 mL of ultra-pure water at a flux of 300 L/m².h. This lasts for around 1 hour (other cleaning approaches are explained in detail in section 5.3.2).

- Sufficient cleaning can be verified by observing constant transmembrane pressure over time.

3.3. Membrane resistance (R_m) should be measured after membrane cleaning to verify that the membrane is not damaged.

3.3.1. R_m can be measured using Equation (5.8), where ΔP is the constant/stable transmembrane pressure observed at the end of the membrane cleaning, J is the flux rate applied during filtering ultra-pure water, and η is the viscosity of ultra-pure water.

3.3.2. R_m is expected to be in the range listed in Table 5.2. R_m which is out of the expected range should be discarded.

Note - R_m range shown in Table 5.2 is based on PES membranes of one manufacturer. The range can vary if the membrane material and/or manufacturer are different.

4. MFI-UF testing procedure

4.1. Feed water sample should be first allowed to stabilize with the ambient temperature where the MFI-UF set-up is placed (refer to section 5.4.1).

4.2. Disconnect the set-up components after membrane cleaning is completed.

4.3. Replace the ultra-pure water in the membrane holder (used during membrane cleaning) with water from the feed sample.

Note - Membrane holder should not be opened and the membrane should remain inside the holder to avoid any damage or contamination to the membrane. The ultra-pure water used in the cleaning can be removed from the holder by shaking the holder where the water can then move out from the inlet. Feed water sample can be then filled in the holder using a needle.

4.4. Fill the stabilized feed water sample in a plastic transparent syringe.

Note - Steel syringes should not be used since they are not transparent, and thus the trapped air bubbles cannot be detected.

4.5. Connect the membrane holder with the syringe and pressure transmitter through a 3-way valve, as shown in Figure 5.2.

Note - For research purpose, if the feed water sample consists of synthetic inert particle (e.g. polystyrene particles), membrane holder should be connected so that the membrane surface plane is horizontal. This is because the inert particles accumulated on the MFI-UF membrane during the test may creep (i.e. fall down) if the membrane surface plane is vertical as in Figure 5.2 (refer to section 5.3.5).

4.6. Ensure that there are no trapped air bubbles in the syringe, membrane holder and tubes/fittings.

5. Protocol for the MFI-UF at Constant Flux to Measure Particulate Fouling in Reverse Osmosis

- 4.7. Set the pump flow (refer to point 2.3.4), and start both the pump and pressure transmitter logging simultaneously.
- 4.8. Ensure that there is no water leakage from the set-up during the filtration. In case any leakage is detected, the test should stop.
- 4.9. The test can be stopped when one of the following rules of thumb is reached (refer to section 5.4.3).
 - 4.9.1. The cake/gel compression phase is observed during the test (as shown in Figure 5.1).
 - 4.9.2. Stable (linear) cake/gel filtration phase lasts for more than 75% of the total elapsed time.
 - 4.9.3. Test duration exceeds 20, 3 and 1 hour at a flux of 20, 100 and 200 L/m².h, respectively. The test duration at in-between flux rates can be approximated relatively (e.g., at a flux of 150 L/m².h, the MFI-UF test duration can be estimated at 2 hours).

- Note - A new syringe should be used in each MFI-UF test. It is not recommended to clean and re-use same syringe since the wall of plastic syringes may deviate with the frequent use.
- The MFI-UF should be measured at the actual RO flux (typically in the range 10-35 L/m².h). Since the MFI-UF measurement at such low flux may take long time, the MFI-UF can be measured at higher flux rates and then extrapolated linearly at the actual RO flux (refer to section 5.4.2). In the latter, the MFI-UF test procedures should be repeated at each applied flux rate, including all the steps in point 3 and 4.
 - For particulate fouling prediction, the MFI-UF should be measured for both the RO feed and concentrate to calculate the particle deposition factor (refer to point 5.2). This means that the MFI-UF test procedures should be repeated for both samples, including all the steps in point 3 and 4.

5. MFI-UF calculation

- 5.1. By conducting the MFI-UF test, the MFI-UF value can be calculated following the steps below. The steps below are further illustrated in one example in section 5.5.
 - 5.1.1. Plot the data of the pressure (ΔP) and time (t) transferred by the pressure transmitter. The plot ideally consists of three subsequent fouling phases; (i) pore blocking (plus pump start-up), (ii) cake/gel filtration, and (iii) cake/gel compression and/or cake/gel pores narrowing, as shown in Figure 5.1.

Note - An overlap between the fouling phases may occur while the plot still shows the same trend in Figure 5.1 where each phase represents the dominant form of fouling.

5.1.2. Identify the stable cake/gel filtration phase by identifying the linear stable region in the plot, as shown in Figure 5.1 and Figure 5.13.

5.1.3. Determine the *slope* of stable cake/gel filtration.

5.1.4. Calculate the fouling index (*I*) using Equation (5.2).

5.1.5. Calculate the MFI-UF value using Equation (5.3). The calculated MFI-UF is expressed in s/L^2 unit.

Note - MFI-UF can be alternatively calculated using a developed numerical algorithm which can calculate the MFI-UF value automatically (i.e. not manually). The automated calculation algorithm is described in section 5.5.

5.2. To predict particulate fouling, particle deposition factor should be first calculated using Equation (5.5). Subsequently, the increase in the net driving pressure (ΔNDP) is calculated using Equation (5.4).

Note - The fouling rate described by Equation (5.4) is based on the assumption that the increase in net driving pressure is due to the cake/gel formation on RO membrane, with no contribution by scaling and biofouling.

- The MFI-UF can be affected by the low surface porosity of the MFI-UF membrane. Therefore, for accurate fouling prediction, the calculated MFI-UF value should be corrected for the effect of membrane surface porosity (refer to section 5.3.4).

5.7 CONCLUSIONS

This study aimed to develop and introduce a complete protocol to measure the MFI-UF at constant flux, ensuring the accuracy and reproductivity of MFI-UF measurements. The protocol focuses on MFI-UF measurement at a flux of 20-200 $L/m^2.h$ using flat-sheet PES membranes of 5-100 kDa. The protocol addresses all details related to the MFI-UF set-up, membranes, operating conditions and calculation. The study also investigated the factors which may affect the MFI-UF measurements. The following are the key conclusions of these investigations:

- The complete removal of membrane preservation coating is essential, particularly for low fouling potential water, such as the fouling potential of RO feed. The removal of

coating was found more efficient when the membrane is flushed by filtering ultra-pure water at lower flux rate. Nevertheless, more than 90% of coating removal was achieved in the first 20 mL of filtered ultra-pure water independently of the applied flux rate (100-1000 L/m².h).

- The use of 5 kDa membrane in the MFI-UF test might be challenging, for the following reasons:
 - The variation in membrane properties, described by the membrane resistance (R_m), is considerable in the case of 5 kDa membrane ($\pm 22\%$) compared to the 10-100 kDa membranes ($\pm 7.2\%$, 3.2% and 8.7% for 10, 50 and 100 kDa membranes, respectively). This could indicate that the MFI-UF measured with 5 kDa membranes might be less reproducible.
 - 5 kDa membranes require much higher transmembrane pressure in comparison with the higher MWCO membranes. As a result, since the error of pressure transmitter is proportional (as a percentage) to the measured pressure range, the error in transmembrane pressure readings would be higher with the 5 kDa membrane, which eventually may affect the accuracy of MFI-UF measurements.
- The change in feed water temperature during the MFI-UF test will result in a variation in the transmembrane pressure, and eventually lead to inaccurate MFI-UF value. Therefore, the temperature of the feed water should be ideally allowed to reach ambient temperature before starting the MFI-UF test. Nonetheless, in case the variation in feed water temperature could not be prevented during the test, then the MFI-UF value can be corrected using a correction formula developed in this study.
- MFI-UF test duration depends mainly on the occurrence and stability of cake/gel filtration phase, which is strongly affected by three main factors, namely (i) flux rate, (ii) MFI-UF membrane MWCO (i.e. membrane surface porosity), and (iii) particle concentration in feed water. The lower the aforementioned factors, the longer the duration of an MFI-UF test.
- A new numerical algorithm to calculate the MFI-UF method automatically was successfully developed based on least-squares regression modelling. The new algorithm was tested for different levels of fouling potential (i.e. different levels of MFI-UF). The outputs of MFI-UF values calculated by the algorithm were compared with the MFI-UF values calculated based on the traditional (i.e. manual) approach. The results confirmed the accuracy and reproducibility of the developed algorithm to calculate the MFI-UF.

The developed protocol is considered a first step to standardize the MFI-UF method. More work is recommended to integrate the protocol with a fully automated MFI-UF system which can be connected online in RO plants to measure and report particulate fouling potential in real time.

5.8 ANNEXES

Annex 5.8.1: Cake creep during the filtration of feed water consisting of inert particles

The direction of membrane surface plane may affect the cake formation during the MFI-UF test. However, this could be only observed with feed water consisting of inert (i.e. non-adherent/non-sticky) particles, such as polystyrene particles. Figure A - 5.1 shows the transmembrane pressure progress over time during the filtration of a suspension of 25 nm polystyrene particles (from Bangs Laboratories) of 50 mg/L concentration through 10 kDa membrane at 50 and 100 L/m².h, where same feed was filtered when the membrane surface plane was (i) vertical and (ii) horizontal. As it can be observed, when the membrane surface plane was horizontal, the pressure increase rate was stable during the cake filtration phase at both flux rates. However, when the membrane surface plane was vertical, the pressure increase rate was stable along the filtration duration at 100 L/m².h (Figure A - 5.1 (a)), while it started to decline after 60 minutes of filtration at 50 L/m².h (Figure A - 5.1 (b)). The reason of the behaviour in Figure A - 5.1 (b) was attributed to the creep (falling down) of the cake formed on the MFI-UF membrane when the membrane plane was vertical. The reason of the cake creep at 50 L/m².h only could be because the permeation force was insufficient to push and hold the cake on the membrane surface, in contrast with the case at a higher flux rate (i.e. 100 L/m².h).

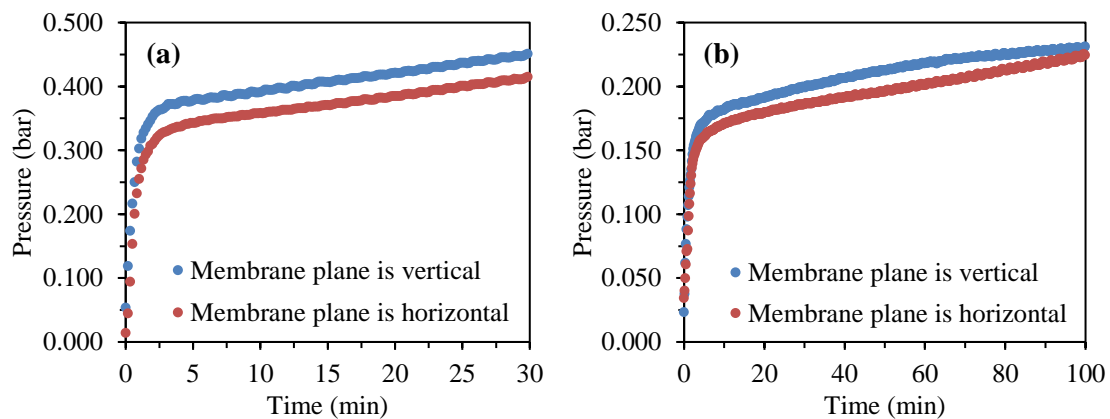


Figure A - 5.1: Transmembrane pressure development during the filtration of polystyrene particles suspension (50 mg/L) using 10 kDa membrane at: (a) 100 L/m².h, and (b) 50 L/m².h

To prove the creep hypothesis mentioned above, the MFI-UF test above was re-performed at 50 L/m².h; where the filtration continued for 1 hour then stopped for 1 hour and then resumed again for another 1 hour, as shown in Figure A - 5.2. As it can be observed, when the membrane surface plane was horizontal (Figure A - 5.2 (a)), the initial transmembrane pressure of cake filtration phase in filtration 2 started almost from the end pressure of

filtration 1. This is because the cake creep did not occur (i.e. cake did not fall down) after stopping filtration 1 since the membrane surface plane was horizontal. Hence, the cake continued to build up during the filtration 2 on the existing cake layers formed in filtration 1. On the other hand, in the case when the membrane surface plane was vertical (Figure A - 5.2 (b)), the initial pressure of cake filtration phase in filtration 2 was markedly lower than the end pressure in the filtration 1. This could indicate that the cake formed in filtration 1 mostly crept after stopping the filtration, and a new cake layers started to build up on membrane surface in filtration 2.

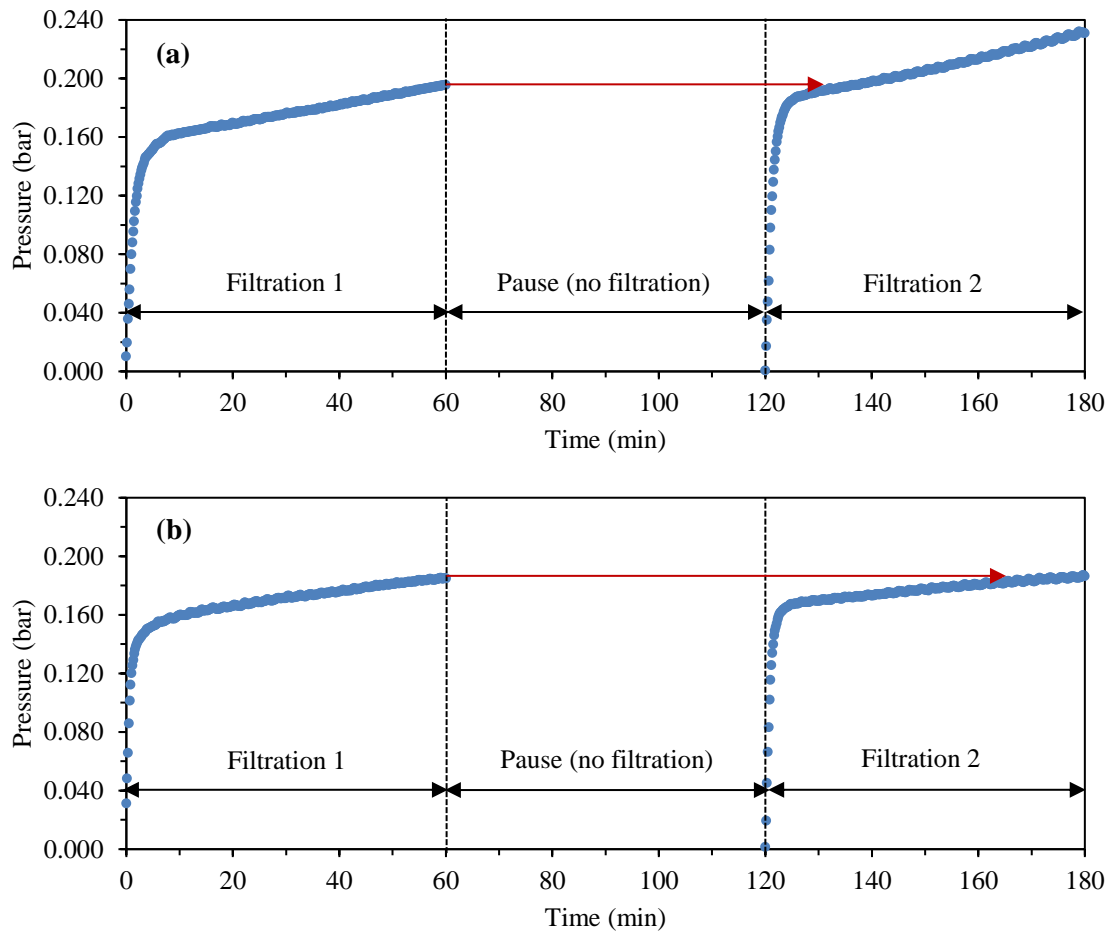


Figure A - 5.2: Transmembrane pressure development during filtration of polystyrene suspension using 10 kDa membrane at $50 \text{ L/m}^2\cdot\text{h}$, where the membrane surface plane is (a) horizontal, and (b) vertical

Furthermore, to confirm that the creep phenomenon was related to the inert nature of polystyrene particles and it was not due to another reason, the experiment presented in Figure A - 5.2 (b), was repeated using canal water (i.e. consisting of natural adherent particles). As shown in Figure A - 5.3, no cake creep was observed at $50 \text{ L/m}^2\cdot\text{h}$ despite the membrane surface plane was vertical, where the initial pressure of cake filtration phase in filtration 2 started from the end pressure of filtration 1. This is because the canal

water consists of real particles which mostly have adherence nature. As a result, the particles could adhere to the membrane surface and to each other, and thus could remain on the membrane surface and did not creep even at low flux rate.

In summary, the direction of membrane surface plane should be horizontal if the MFI-UF test was applied at low flux rate using a feed water consisting of inert particles. Otherwise, the MFI-UF measurement can be independent of the direction of membrane surface plane.

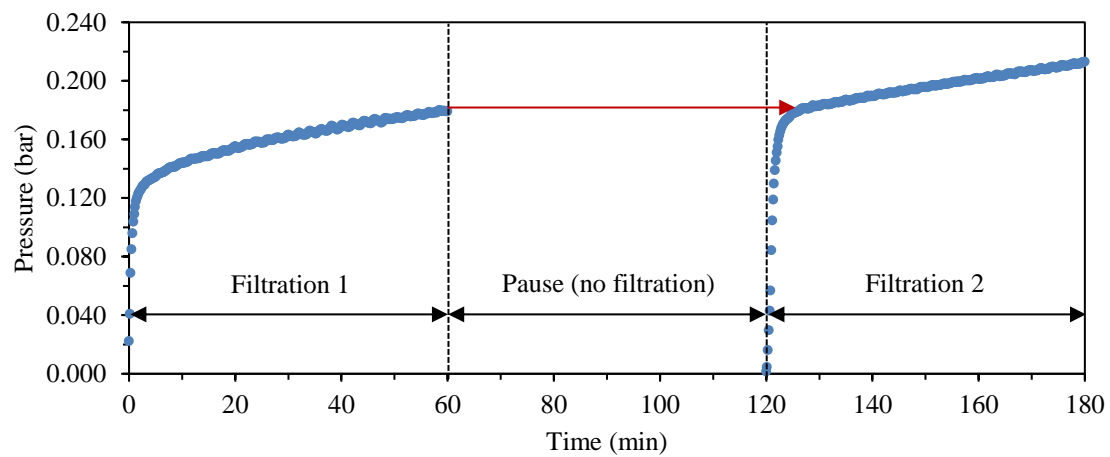


Figure A - 5.3: Transmembrane pressure development during filtration of canal water using 10 kDa membrane at 50 L/m².h, where the membrane surface plane is vertical

Annex 5.8.2: Correction of water temperature variation during MFI-UF test

The temperature of feed water may vary during the MFI-UF test if it is not balanced with the ambient temperature. Consequently, the transmembrane pressure and thus the slope of cake/gel filtration phase can be affected, which results in an erratic MFI-UF value. Therefore, the effect of feed water temperature variation should be corrected. This can be done as illustrated below.

The cake/gel filtration equation can be rearranged as shown in Equation (A - 5.1).

$$\Delta P = \eta \cdot (J \cdot R_m + J^2 \cdot I \cdot t) \quad (A - 5.1)$$

Assuming that both membrane resistance and specific cake resistance are not affected by the water temperature variation, then the parameters between the brackets can be considered constant. Therefore, for simplification, the equation above can be re-written with substituting the parameters between the brackets by the parameter X, as shown in Equation (A - 5.2).

$$\Delta P = \eta \cdot (X) \quad (A - 5.2)$$

Based on Figure A - 5.4, the black curve represents the actual cake/gel filtration phase where the water temperature varied during the MFI-UF test. On the other hand, the blue line represents the cake/gel filtration phase after the correcting the variation in feed water temperature during the test. Accordingly, after some trigonometry calculations, the slope of cake/gel filtration can be corrected using Equation (A - 5.3).

$$slope_{cor} = \left((\Delta P_i + slope_{act} \times t_c) \cdot \left(\frac{\eta_i}{\eta_f} \right) - \Delta P_i \right) \cdot \frac{1}{t_c} \quad (A - 5.3)$$

Where $slope_{cor}$ and $slope_{act}$ are the corrected and actual slope of the cake/gel filtration phase, respectively, and t_c is the duration of the cake/gel filtration phase.

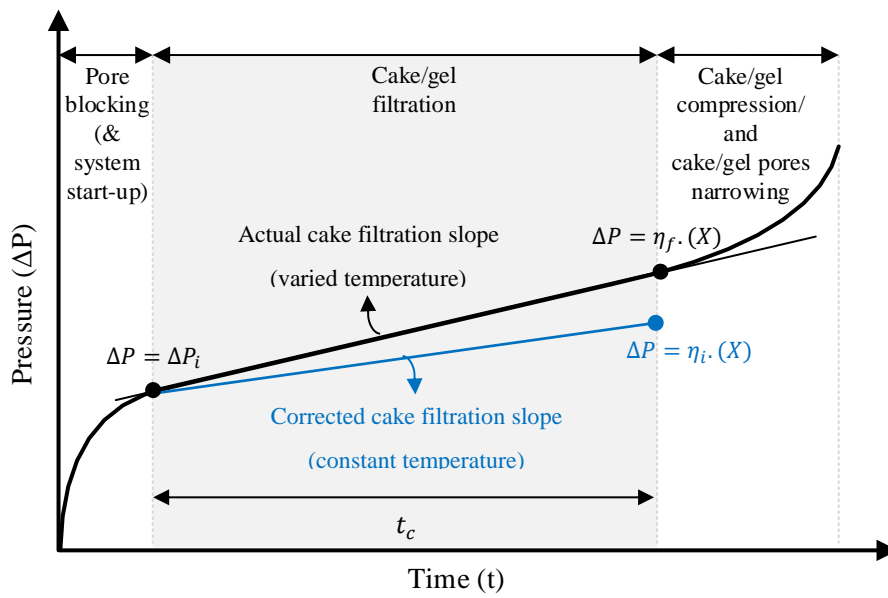


Figure A - 5.4: Filtration curve during the MFI-UF test at constant flux if the feed water temperature changed over the test

Annex 5.8.3: Example of manual MFI-UF calculation

Figure A - 5.5 shows a typical example of the output of an MFI-UF test; i.e. transmembrane pressure (ΔP) against filtration time (t). The figure shows the results of an MFI-UF measurement for a water sample using a 100 kDa membrane at a flux of 100 L/m².h. The temperature of water sample was 21 °C (room temperature).

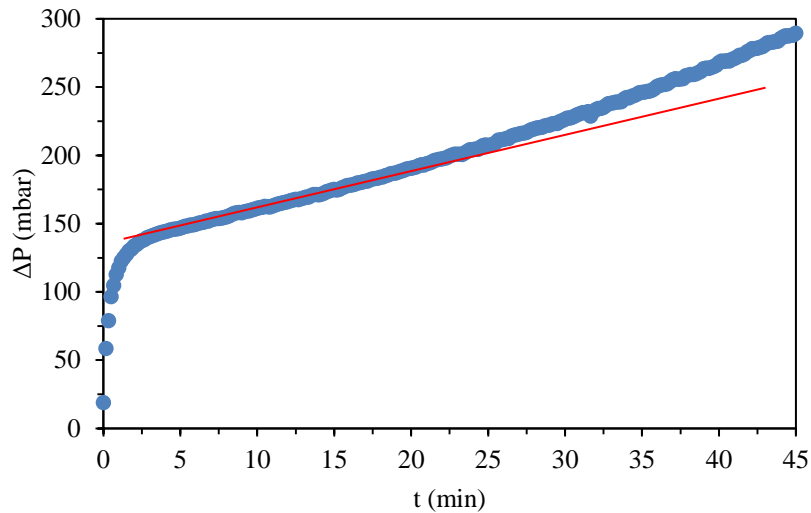


Figure A - 5.5: A typical output of an MFI-UF test (MWCO = 100 kDa, flux = 100 L/m².h, temperature = 21 °C)

To calculate the MFI-UF value, the following steps were followed. The value of main parameters used in the MFI-UF calculation are summarized in Table A - 5.1.

1. Identify the cake filtration phase: the boundaries of cake/gel filtration phase were identified visually with drawing a parallel line (red line), where the line fitted only the linear region of the curve (i.e. the line should not fit neither the pore blocking phase nor the cake compression phase). Accordingly, the cake filtration phase was identified in the period of 5-15 min.
2. Calculate the slope of cake/gel filtration phase: the slope can be calculated manually as shown below, or by using the SLOPE function in Excel.

$$\text{slope} = \frac{\Delta P}{t} = \frac{175 - 147 \text{ (mbar)}}{15 - 5 \text{ (min)}} = 2.8 \text{ mbar/min} = 0.00467 \text{ kPa/s}$$

3. Calculate the fouling index (I):

$$I = \frac{1}{J^2 \cdot \eta} \cdot \text{slope} = \frac{0.00467 \text{ (kPa/s)}}{0.000028^2 \text{ (m}^3\text{/m}^2 \cdot \text{s)}^2 \times 9.8 \times 10^{-7} \text{ (kPa} \cdot \text{s)}} = 6.2 \times 10^{12} \text{ 1/m}^2$$

4. Calculate the MFI-UF value:

$$\begin{aligned}
 MFI-UF &= \frac{\eta_{20^{\circ}\text{C}} \cdot I}{2 \cdot \Delta P_o \cdot A_o^2} = \frac{1.002 \times 10^{-6} \text{ (kPa}\cdot\text{s)} \times 6.2 \times 10^{12} \text{ (1/m}^2\text{)}}{2 \times 200 \text{ (kPa)} \times 0.00138^2 \text{ (m}^2\text{)}^2} \\
 &= 8.1 \times 10^9 \text{ s/(m}^3\text{)}^2 = 8100 \text{ s/L}^2
 \end{aligned}$$

Table A - 5.1: Summary of the main parameters used to calculate the MFI-UF

Parameter	Value
J	100 L/m ² .h (0.000028 m ³ /m ² .s)
$Temp.$	21 °C
η	0.00098 N.s/m ² (9.8×10 ⁻⁷ kPa.s)
ΔP_o	2 bar (200 kPa)
$\eta_{20^{\circ}\text{C}}$	0.001002 N.s/m ² (1.002×10 ⁻⁶ kPa.s)
A_o	0.00138 m ²

Annex 5.8.4: MFI-UF calculation algorithm

1. Introduction

MFI-UF value is calculated based on the slope of cake/gel filtration phase observed during the test. Yet, the cake/gel filtration phase is determined manually; i.e. visually. However, based on prior preliminary work entailing the calculation of MFI-UF for various water samples, it was found that the manual approach of determining the cake/gel filtration phase is problematic. First, it can be difficult (particularly for beginners), to identify visually the exact boundaries of cake/gel filtration phase, and hence this can lead to an inaccurate MFI-UF calculation. Second, and as a result of the first mentioned point, the manual/visual determination of cake/gel filtration boundaries can be subjective and different from one person to another, which may eventually result in an unreproducible MFI-UF calculation. Based on the preliminary work results, the difference in MFI-UF values obtained by different researchers reached to 30%, which is considered very high. Third, consequently, this can limit the application of MFI-UF method, since only the professional users with the required scientific background can calculate the MFI-UF value precisely. Finally, the manually-based calculation of MFI-UF value can also restrict the development of an automated MFI-UF set-up which can be equipped as an online monitor for particulate fouling in RO systems.

The main objective of this study is to develop and validate a new automated approach to calculate the MFI-UF value at constant flux filtration, to ensure the accuracy, reproducibly and applicability of the MFI-UF method. The new calculation method was developed based on the least-squares regression modelling. For this purpose, four regression models were proposed. The accuracy of each model was investigated based on several criteria using various MFI-UF data simulating different levels of particulate fouling potential. Finally, the most accurate model was selected and validated with further data obtained at wide range of testing conditions. The new MFI-UF calculation method was developed using Excel VBA with a simple user interface (UI), named as “MFI-UF Calculator”.

2. Regression modelling

Regression is a set of statistical processes to model the relationship among interrelated variables (Golberg and Cho, 2010). In general, regression model can be described by the basic form shown in Equation (A - 5.4) (NIST, 2012).

$$y = f(x, \beta) + \varepsilon \quad (A - 5.4)$$

The model includes three main parts, namely (i) y : the dependent variable, (ii) $f(x, \beta)$: the model function which includes the independent variable (x) and unknown parameter (β), and (iii) ε : the estimated error.

Accordingly, in order to define the model, it is necessary to find the value of the unknown parameter (β). There are several methods to estimate β . The least squares method is the most basic and widely used one (NIST, 2012). In the least-squares method, β is estimated by minimizing the sum of squared residuals (SSR), as shown in Equation (A - 5.5). The residual is the difference between the actual value of a dependent variable ($y_{(act)i}$) and the corresponding value estimated by the model ($y_{(mod)i}$). The smaller SSR value, the better the fit of the model to the actual data.

$$SSR = \sum_{i=1}^k (y_{(act)i} - y_{(mod)i})^2 \quad (A - 5.5)$$

2.1. Linear regression model

The regression model is identified as linear when the dependent variable (y) is linear with the unknown parameter (β), but doesn't need to be linear with the independent variable (x) (NIST, 2012). Generally, the linear regression model can be described as in Equation (A - 5.6).

$$y = \beta_0 + \beta_1 x_1 + \beta_2 x_2 + \dots + \beta_n x_n \quad (A - 5.6)$$

Based on the above description, the linear regression model is not necessarily to be only a straight line. For instance, the polynomial model is also a linear regression model although the independent variables are raised to a power of 1- n , as shown by Equation (A - 5.7).

$$y = \beta_0 + \beta_1 x + \beta_2 x^2 + \dots + \beta_n x^n \quad (A - 5.7)$$

In the linear regression modelling, the SSR is minimized in an analytical approach (usually based on matrix algebra) which leads to find a closed-form solution for the unknown parameters (β_{0-n}). This can be done, as explained by Equation (A - 5.8); based on the matrix of the independent variables (X), the transpose matrix of the independent variables (X^T), and the matrix of actual dependent variables (Y).

$$\beta = (X^T X)^{-1} X^T Y \quad (A - 5.8)$$

2.2. Nonlinear regression model

Nonlinear regression model can be in any form in which the dependent variable (y) is not linear with the model unknown parameter (β) (NIST, 2012). Accordingly, the nonlinear regression models have a broad range of forms. Examples of nonlinear model include exponential, logarithmic and power functions. The ratio of polynomial functions, defined

as rational model, is also a nonlinear regression model. The typical form of rational model can be described by Equation (A - 5.9), where m and n are the degree of the numerator and denominator, respectively, and α_{0-m} and β_{0-n} are the unknown parameters (NIST, 2012).

$$y = \frac{\alpha_0 + \alpha_1x + \alpha_2x^2 + \dots + \alpha_mx^m}{\beta_0 + \beta_1x + \beta_2x^2 + \dots + \beta_nx^n} \quad (A - 5.9)$$

Unlike the linear model, SSR cannot be minimized analytically. However, this can be done by an iterative numerical process using optimization algorithm. Most of the algorithms involve selecting initial values for the unknown parameters. Then, the initial values are refined iteratively in a successive approximation ended when the convergence criteria are satisfied. For this reason, the nonlinear regression model generally has no closed-form solution for the unknown parameters (NIST, 2012).

2.3. Goodness of fit

Goodness of fit (GOF) of a regression model describes the degree of how well the model fits the actual data. The most commonly used GOF measure is the coefficient of determination (R^2), which is applied in many statistical software. R^2 measures the proportion of the dependent variables variation explained by the regression model. In other words, it measures the scatter of the data points around the regression model curve. For a data set of k points, R^2 value can be calculated by Equation (A - 5.10) (NIST, 2012).

$$R^2 = 1 - \frac{\sum_{i=1}^k (y_{(act)i} - y_{(mod)i})^2}{\sum_{i=1}^k (y_{(act)i} - \bar{y}_{(act)})^2} \quad (A - 5.10)$$

Where $y_{(act)}$ and $y_{(mod)}$ are the actual and modelled (estimated) value of a dependent variable, respectively, and $\bar{y}_{(act)}$ is the mean of the actual values of the dependent variable.

R^2 has a value between 0 and 1. When $R^2 = 0$, this indicates that the regression model explains none of the variation of the dependent variables, and it failed completely to fit the actual data. In this case, the dependent variable values estimated by the model ($y_{(mod)}$) will always equal the mean ($\bar{y}_{(act)}$), which means that the regression model is a horizontal line. On the other hand, $R^2 = 1$ indicates that the model explains the entire variation of the dependent variables, which means that the model fits the actual data completely and all residuals are equal to zero. This interpretation is absolutely correct in case of linear regression models. However, for nonlinear regression models, several arguments arise, since R^2 could have a negative value when the model fits the actual data very poorly (worse than a horizontal line). Nevertheless, if the nonlinear model is compatible with the

actual data (which yields $R^2 \geq 0$), then R^2 can truly provide a useful descriptive measure for the GOF (Kva^oLseth, 1983; Greene, 2003).

3. MFI-UF calculation algorithm development

A new algorithm was developed to calculate the MFI-UF values, based on the least-squares regression. The algorithm involves four main processes/steps, illustrated in Figure A - 5.6 and Figure A - 5.7. Step 1 is to model the filtration curve of the transmembrane pressure (P) against time (t) obtained from the MFI-UF test. This entails the definition of the model function $P(t)$ which can describe the relationship between P and t . Step 2 is to define the first derivative of the model function $P'(t)$ to find the slope of the tangent line over time. Step 3 is to determine the slope of cake/gel filtration phase where the $P'(t)$ is minimum. Step 4 includes the calculation of MFI-UF value based on the determined minimum slope.

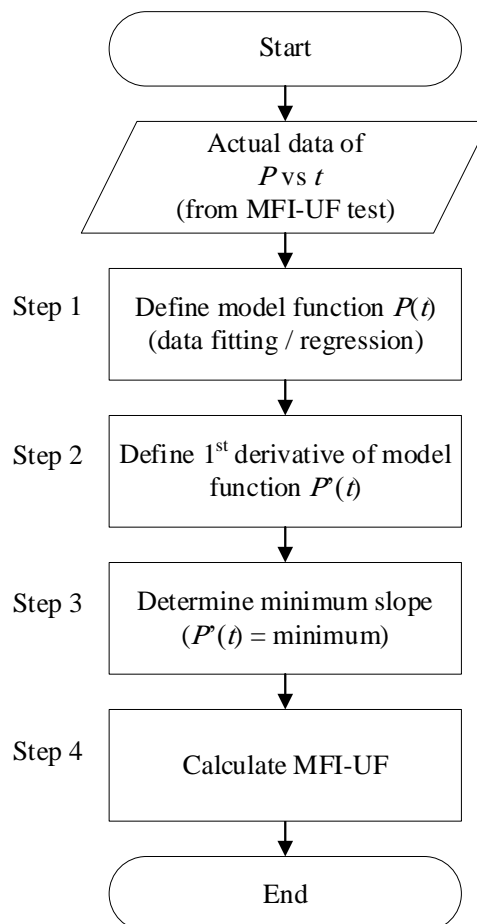


Figure A - 5.6: The MFI-UF calculation algorithm

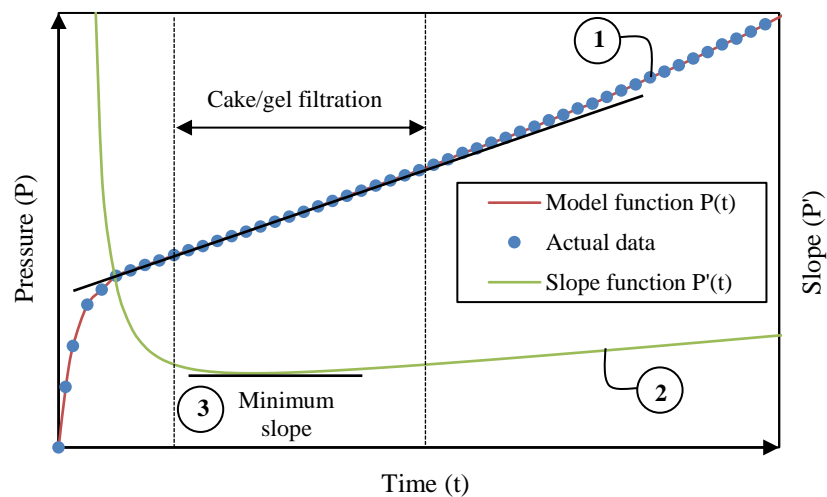


Figure A - 5.7: Detailed illustration of the MFI-UF calculation algorithm processes/steps: (1) define model function / data fitting, (2) define first derivative function (cake/gel filtration slope), and (3) determine the minimum slope

3.1. Proposed regression models

The first step/process in the MFI-UF calculation algorithm is to fit/model the actual data of P vs t obtained from the MFI-UF test (Figure A - 5.6 and Figure A - 5.7). For this purpose, four models were proposed, listed in Table A - 5.2.

The first is Polynomial model with 10th order, which is the only proposed linear model. The advantage of polynomial model is its flexibility to fit various curve shapes. The high order (10th degree) was adopted to ensure the best model fit to the actual data.

The second proposed model is Rational 3/2, which is a ratio of 3rd to 2nd order polynomial function. Rational model has an advantage over the normal polynomial model as it is less oscillated and more flexible to fit complex curve shapes. The degrees of numerator (m) and denominator (n) were selected based on the guidelines recommended by NIST (2012), where m should be $> n + 1$ if $P(\infty)$ and $P'(\infty)$ approach to infinity (∞), which is the case of the typical filtration curve (Figure A - 5.7). Rational models with higher degree could be more robust, however, this would make the regression analysis more complicated due to the higher number of unknown parameters.

The third is Creep model. It is derived from the model which describes the deformation tendency of metals under the influence of mechanical stress (Harrison et al., 2014). Although the use of this model is very far from the MFI-UF application, however, the curve shape of the Creep model function is very similar to the trend of P vs t curve obtained during MFI-UF tests (Figure A - 5.7).

The last model is Exponential Plus Linear (EPL). The advantage of this model is the existence of the power term beside the linear term, which makes the model more flexible to fit all phases in the P vs t plot obtained from the MFI-UF test.

Table A - 5.2: Models used to fit/model the relationship of P vs t

Model name	Model type	Model function*	Equation
Polynomial 10 th order	Linear	$P(t) = a_0 + a_1t + a_2t^2 + \dots + a_{10}t^{10}$	(A - 5.11)
Rational 3/2	Nonlinear	$P(t) = \frac{a_0 + a_1t + a_2t^2 + a_3t^3}{1 + b_1t + b_2t^2}$	(A - 5.12)
Creep	Nonlinear	$P(t) = a(1 - e^{-ct}) + b(e^{dt} - 1)$	(A - 5.13)
Exponential plus linear (EPL)	Nonlinear	$P(t) = a + bc^t + dt$	(A - 5.14)

* Model function represents the pressure (P) as a function of the time (t), while the other components (i.e.: a , b , c and d) are the unknown model parameters which should be estimated based on the least-squares regression.

Regression process (i.e. the estimation of unknown parameters and the definition of model function) was done using Excel 2016. For the polynomial 10th model (linear model), this was done directly using the LINEST() function.

For the other models; Rational 3/2, Creep and EPL (nonlinear models), the regression analysis was done as illustrated in Figure A - 5.8. The first step is to set initial values for the unknown model parameters (matrix β). The initial values of β are set randomly in the range between 0 and 1, using RAND() function in Excel. This range is recommended by many modelling software (e.g. MATLAB) if the best initial values are unknown. Subsequently, the GRG optimization solver (Lasdon et al., 1978) integrated in Excel is used to minimize the sum of squared residuals (SSR) to estimate the final values of β . However, since the accuracy of final β values depends strongly on the initial values which are set, diverged β values could be estimated by the solver if the set initial values were improper. To avoid this issue, the previous two steps are repeated 5 times. At each iteration, the goodness of fit (GOF) is measured by R^2 using Equation (A - 5.10). Finally, the estimated values of β corresponding the best fit (with highest R^2) are selected to define the model function $P(t)$.

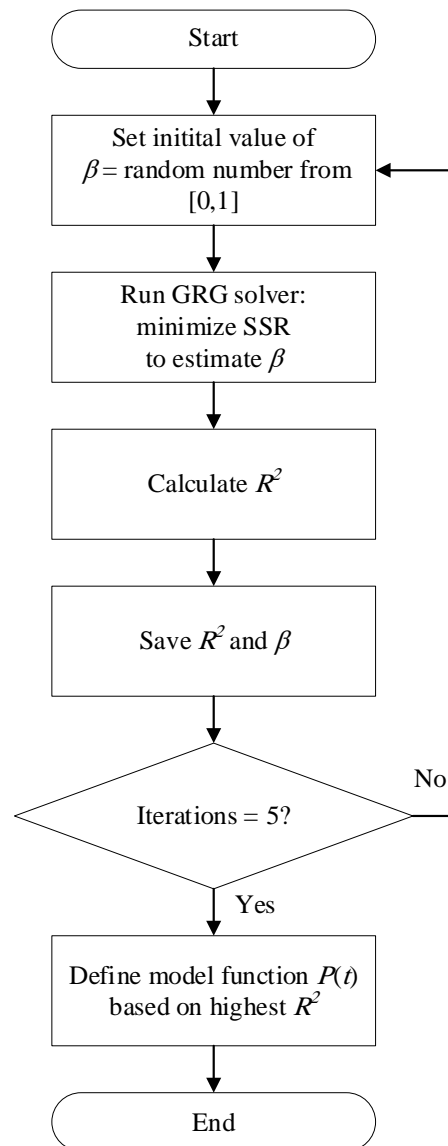


Figure A - 5.8: Steps of nonlinear least squares regression (this figure represents step 1 in Figure A - 5.6)

3.2. Model evaluation

The proposed regression models (Table A - 5.2) were evaluated using MFI-UF data (P vs t plots) of different levels of particulate fouling. Four representative examples of MFI-UF data were selected and presented to illustrate the model fitting. The data is for canal water (CW) diluted to different concentrations (5, 25, 50 and 100%), obtained based on a flux of 100 L/m².h using 100 kDa membrane. The selected data can simulate the particulate fouling potential levels along full-scale RO plants. For instance, the particulate fouling potential of DC-5% and DC-100% samples are within the range of particulate fouling potential of RO feed and raw water, respectively.

The evaluation of each model was done based on several criteria. Firstly, the goodness of fit (GOF) of the model to actual data (P vs t) was assessed. Since the R^2 value of the fitting was very high in most of the cases for all models, the GOF was assessed visually to ensure whether the model could fit perfectly the entire set of actual data. Secondly, the trend of the derived slope function was checked in correspondence to the fouling mechanisms (as in Figure A - 5.7), where the slope should decrease as the pore blocking phase is being over, then gradually be stable/horizontal during the cake/gel filtration phase, and finally start to increase once the cake compression occurs. Subsequently, it was checked if the minimum slope determined based on the model was within the cake/gel filtration phase. Thirdly, the MFI-UF value calculated based on the model was compared with the value estimated by the manual calculation approach. The purpose of this criterion is to demonstrate how much the model-based calculated MFI-UF is close or far from the expected MFI-UF value. Fourthly, the overall robustness of the model was examined by verifying the linear correlation between the model-based calculated MFI-UF and particle concentration.

Finally, the model satisfying the above criteria was selected, and then further validated using additional MFI-UF data of various water samples at a wide range of MFI-UF testing conditions; at flux of 20-200 L/m².h and membrane of 5, 10 and 100 kDa.

4. Best model selection

The MFI-UF was initially calculated based on the manual approach, where the boundaries of cake filtration phase were determined manually/visually, as shown in Figure A - 5.9. The boundaries were different depending on the sample concentration (i.e. particles concentration). This is because at lower concentration, the cake filtration phase starts later, since the particles take more time to build up even cake layers on membrane surface. On the other hand, at higher concentration, the load of particles per filtered volume is higher, and thus the development of cake layers occurs in a shorter time, and could be followed faster by cake compression. The relationship between the calculated MFI-UF values and the particle concentrations was strongly linear ($R^2 = 0.99$), which indicated the precise identification of cake filtration boundaries.

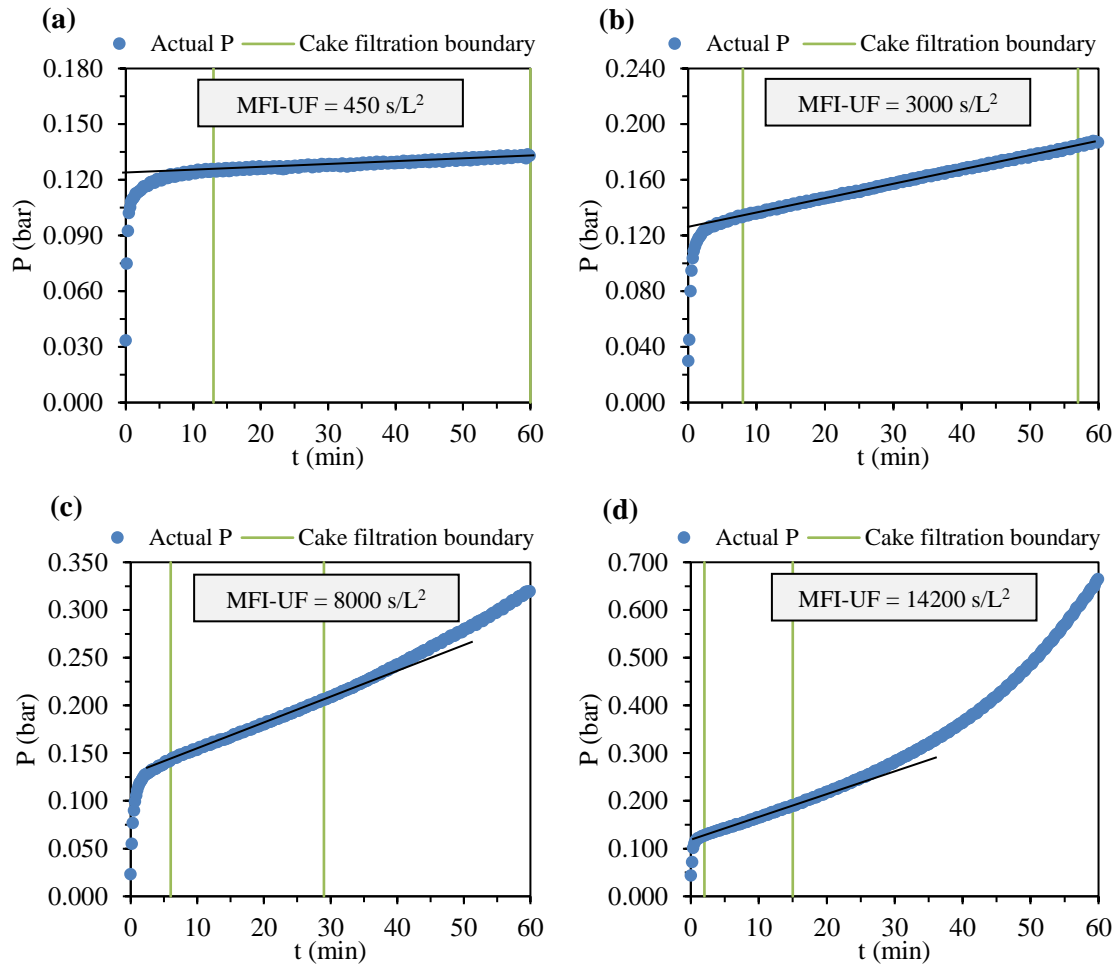


Figure A - 5.9: Actual P vs t , cake filtration boundaries and MFI-UF determined manually for (a) CW-5%, (b) CW-25%, (c) CW-50%, and (d) CW-100%

4.1. MFI-UF calculation based on Polynomial 10th model

The actual data of P vs t fitted by the Polynomial 10th model is shown Figure A - 5.10. As shown for all samples, the model highly over-fitted the actual data. This could be more pronounced by the oscillation of the slope function, which was apparently misleading. For CW-5%, CW-25% and CW-50% samples, the minimum slope had a negative value, and thus the corresponding calculated MFI-UF values were negative as well. On the other hand, for DC-100% sample, the value of minimum slope was positive and found at $t = 5.5$ min which was within the estimated cake filtration boundaries (Figure A - 5.9 (d)). However, the corresponding MFI-UF value was far from the value obtained based on the manual calculation approach.

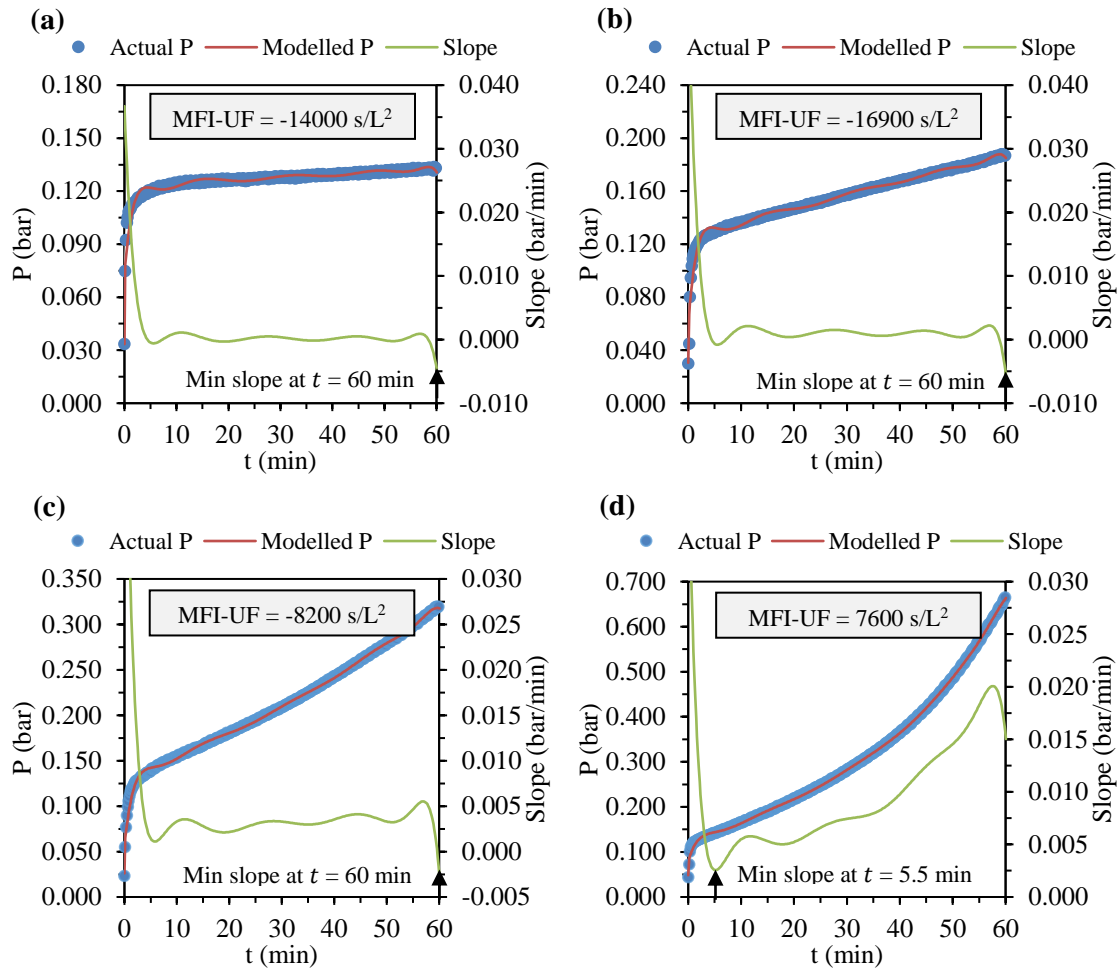


Figure A - 5.10: Actual P vs t and modelled P , the slope and MFI-UF determined based on Polynomial 10^{th} model for (a) CW-5%, (b) CW-25%, (c) CW-50%, and (d) CW-100%

4.2. MFI-UF calculation based on Rational 3/2 model

Rational 3/2 model showed perfect fit to the actual data of P vs t , as shown in Figure A - 5.11. For all samples, the minimum slope was found within the range of the estimated cake filtration boundaries (Figure A - 5.9); at $t = 60, 60, 12.5$ and 7 min for CW-5%, CW-25%, CW-50% and CW-100%, respectively. In addition, the MFI-UF values calculated based on the model were very close to those determined by the manual calculation approach. Furthermore, the relationship between the model-based calculated MFI-UF and particle concentration was strongly linear, with $R^2 = 0.99$, which could verify the accuracy of calculated MFI-UF values.

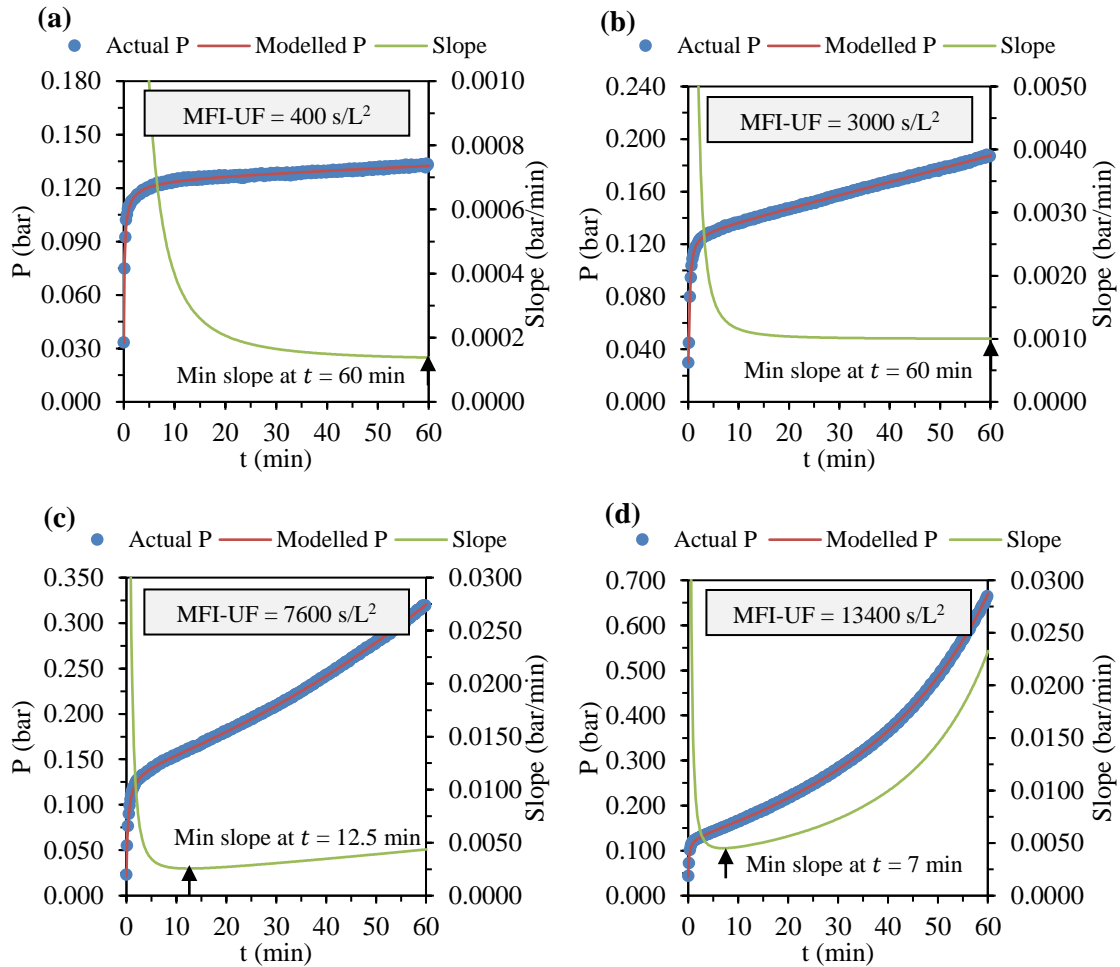


Figure A - 5.11: Actual P vs t and modelled P , the slope and MFI-UF determined based on Rational $3/2$ model for (a) CW-5%, (b) CW-25%, (c) CW-50%, and (d) CW-100%

4.3. MFI-UF calculation based in Creep model

Figure A - 5.12 shows the actual data of P vs t fitted by the Creep model. In general, the model showed good fitting. However, the model was not flexible to fit properly the transition phase between the pore blocking and cake filtration phases. This consequently affected the fitting of the actual P data during the cake filtration phase, especially in the beginning (i.e. just after pore blocking). The minimum slope was found within the estimated boundaries of cake filtration phase (Figure A - 5.9) for all samples excluding the CW-50% sample. Though, the MFI-UF values calculated based on the model were relatively far from the corresponding values estimated by the manual calculation approach, except for CW-25% sample. The inaccuracy of MFI-UF values calculated based on the model could be confirmed by the lower R^2 of the linear relationship between the MFI-UF and particle concentration which was 0.77.

Moreover, from the technical point of view, a lot of errors were shown up during the run of the Creep model. This was due to the exponential term in the model function (Equation

(A - 5.13)) which could generate enormous numbers exceeding the numeric range in Excel during estimating the model unknown parameters.

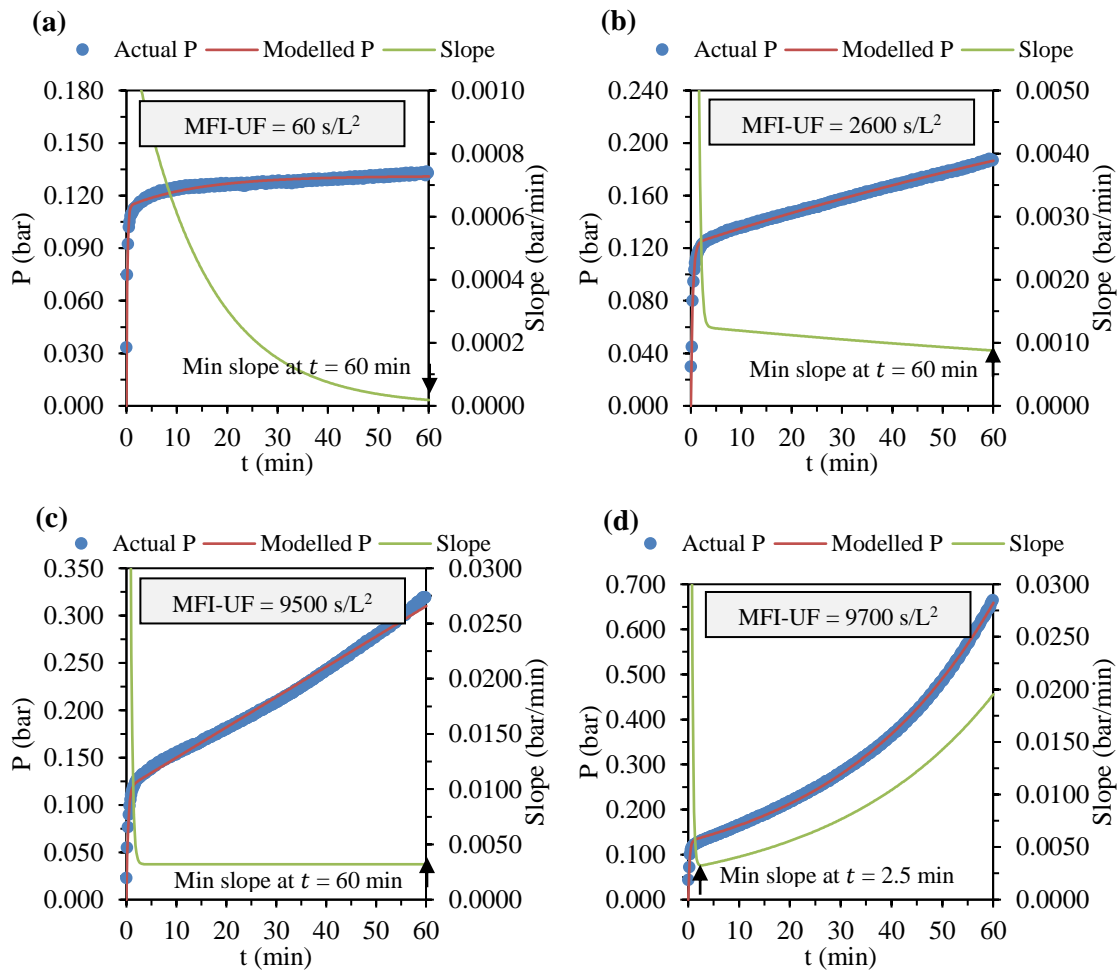


Figure A - 5.12: Actual P vs t and modelled P , the slope and MFI-UF determined based on Creep model for (a) CW-5%, (b) CW-25%, (c) CW-50%, and (d) CW-100%

4.4. MFI-UF calculation based on EPL model

The output of the EPL model is shown in Figure A - 5.13. For CW-5%, CW-25% and CW-50% samples, the model fitted the actual data similarly, where the fitting curve was entirely straight line directly after the pore blocking phase until the end of the filtration time. This could be more noticeable by the horizontal part of the slope data ($t = 5-60$ min). Accordingly, well curve fitting was observed in the case of CW-5% and CW-25% samples as the cake filtration was the dominant mechanism in both cases, and thus the minimum slope was found within the estimated range of cake filtration boundaries (Figure A - 5.9). As a result, the model-based calculated MFI-UF value was more accurate for CW-5% and CW-25% samples in comparison with the MFI-UF values estimated by the manual calculation approach. On the other hand, for CW-100% sample, the model

could fit only the cake compression phase which was the dominant fouling mechanism, and hence, the MFI-UF calculated based on the model was totally inaccurate in this case. The linear relationship between the model-based calculated MFI-UF and particle concentration was very poor, where $R^2 = 0.01$. However, this was mainly because of the incorrect MFI-UF value of CW-100% sample. With excluding this value, the fitting could be significantly improved with $R^2 = 0.97$.

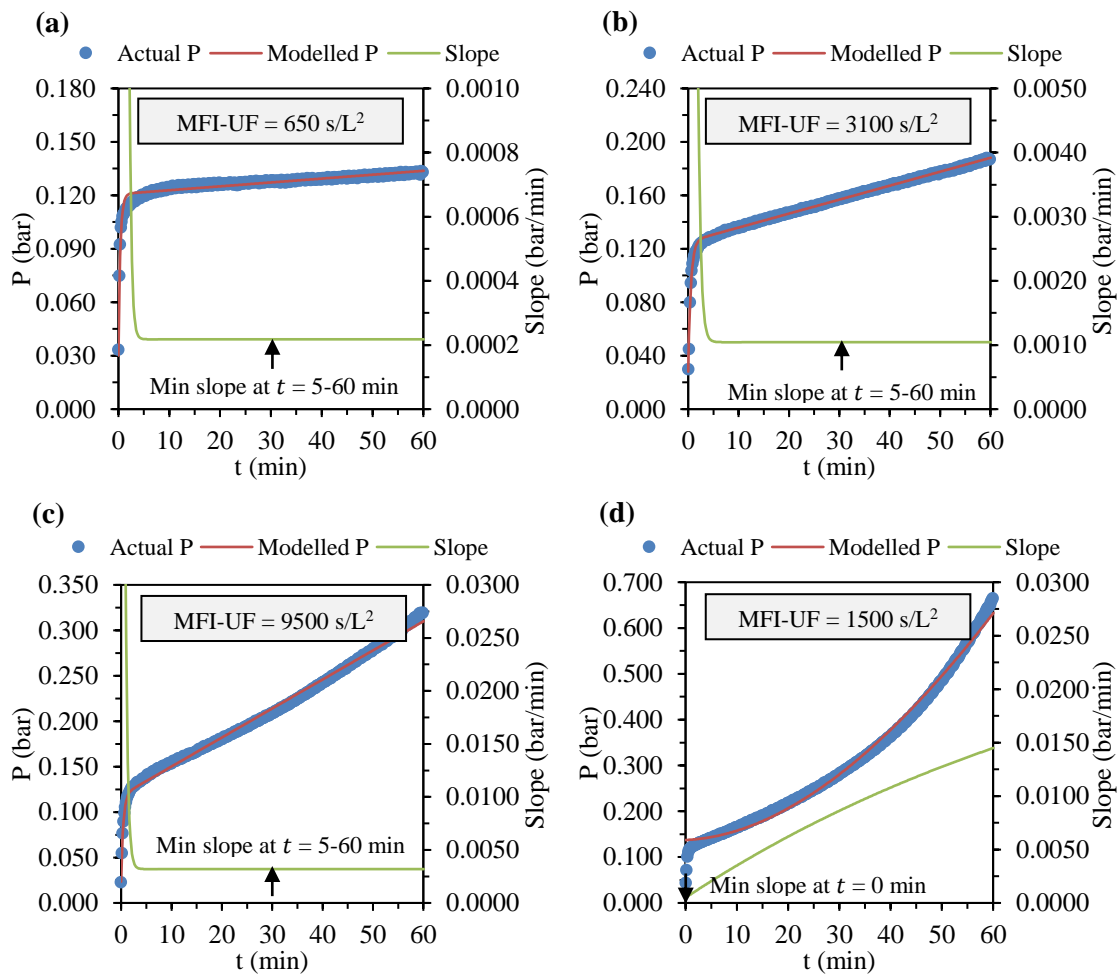


Figure A - 5.13: Actual P vs t and modelled P , the slope and MFI-UF determined based on EPL model for (a) CW-5%, (b) CW-25%, (c) CW-50%, and (d) CW-100%

4.5. Best model selection and validation

It can be concluded according to the results above that the Rational 3/2 is the best model, where it could fit perfectly the actual data of P vs t and, thus the calculated MFI-UF value was accurate for all samples. On the other hand, the Creep and EPL models were more or less successful to calculate the MFI-UF of low-mediate fouling samples (e.g. CW-25% samples), but inefficient to be used to calculate the MFI-UF of low and high fouling

samples (e.g. CW-5% and CW-100% samples, respectively). Finally, the Polynomial 10th model was invalid to be used to calculate the MFI-UF of all samples.

The best model, Rational 3/2, was further validated using additional MFI-UF data (P vs t) of various water samples at different testing conditions (at 20-200 L/m².h flux using 5-100 kDa membranes). The results confirmed the precision and reproducibility of MFI-UF value calculated based on the model.

However, the validation results showed that the fitting of cake filtration phase might be deviated when (i) the pore blocking (or start-up pressure increase) phase is unstable (i.e. pressure doesn't increase smoothly) or it relatively takes long time (e.g. when 5 kDa membrane is used) and/or (ii) when the cake compression is extreme (i.e. pressure increases sharply). As a result, the accuracy of the MFI-UF calculated based on the model could be affected in these cases. Moreover, the fitting of the model was affected in the cases when the MFI-UF data (P vs t) has outliers.

Consequently, the MFI-UF calculation algorithm has to be modified further to eliminate the effect of the aforementioned issues to ensure the accuracy of the calculated MFI-UF. This is illustrated in detail in the following section.

5. Selected model modification

The MFI-UF calculation algorithm illustrated in Figure A - 5.6 was modified by incorporating two main supplementary processes to refine the Rational 3/2 model fitting, as presented in Figure A - 5.14. The first process is to exclude the data of pore blocking and cake compression phase and fit only the cake filtration phase, and the second process is to remove the outliers.

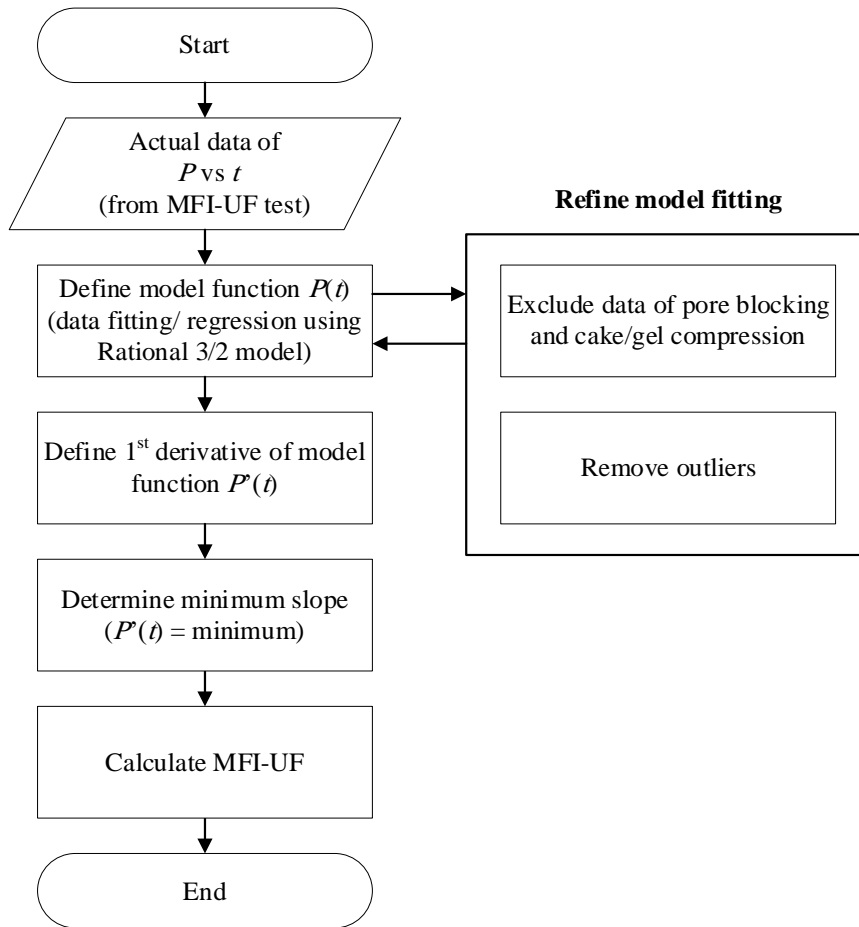


Figure A - 5.14: The modified version of the new MFI-UF calculation method

5.1. Fitting only cake filtration phase

The MFI-UF calculation algorithm was modified by limiting the fitting of Rational 3/2 model to fit only the cake/gel filtration phase. This could be done as shown in Figure A - 5.15, as follows. After the model fits all fouling mechanism phases (i.e. pore blocking, cake/gel filtration and cake/gel compression), the slope function could be defined and then the minimum slope of cake filtration phase can be determined (typically as the case before the algorithm modification). Afterward, as shown in Figure A - 5.15 (left), based on the minimum slope (ms) and the time (t_{ms}) and pressure ($P(t_{ms})$) where the minimum slope was found, a linear curve with the same slope of cake/gel filtration phase can be plotted over time (the disconnected black line). Subsequently, the cake/gel filtration phase can be detected by excluding the P data points above and below the linear curve (the hashed areas). It was found that it is sufficient to exclude the P data points which have a difference of more than 10% with the corresponding values on the linear curve. Finally, the model is re-run again to fit only the data of cake filtration phase, as shown in Figure A - 5.15 (right).

It is worthy to mention that this modification could not be adopted with the other models examined in this study (i.e. Polynomial, Creep and EPL). This is because the minimum slope could not be determined in all cases within the estimated boundaries of the cake/gel filtration phase (as illustrated in the previous section).

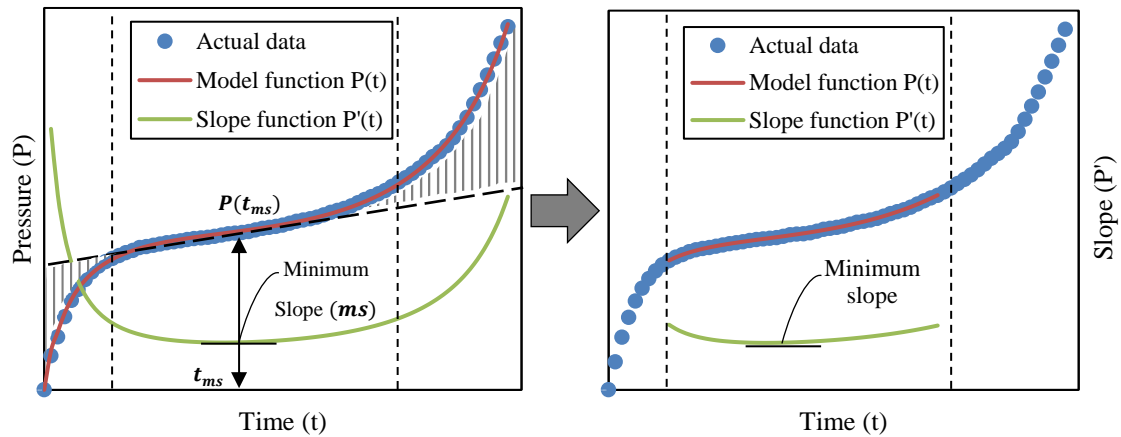


Figure A - 5.15: Limiting the model fitting to the cake/gel filtration phase only; (left) fitting all fouling phases, and (right) re-fitting based on cake/gel filtration phase only

Figure A - 5.16 shows an example where the MFI-UF was calculated based on the fitting of the Rational 3/2 model to (a) all fouling phases and (b) only cake filtration phase. In Figure A - 5.16 (a), the model was mainly governed to fit the sharp pressure increase in the pore blocking and the dominant cake compression phase, which could affect the fitting of the short cake filtration phase (this could be more visible by zooming in the graph). On the other hand, in Figure A - 5.16 (b), when the pore blocking and cake compression phases were excluded, the model could fit the cake filtration phase perfectly. As a result, the MFI-UF value was considerably improved (by more than 50%).

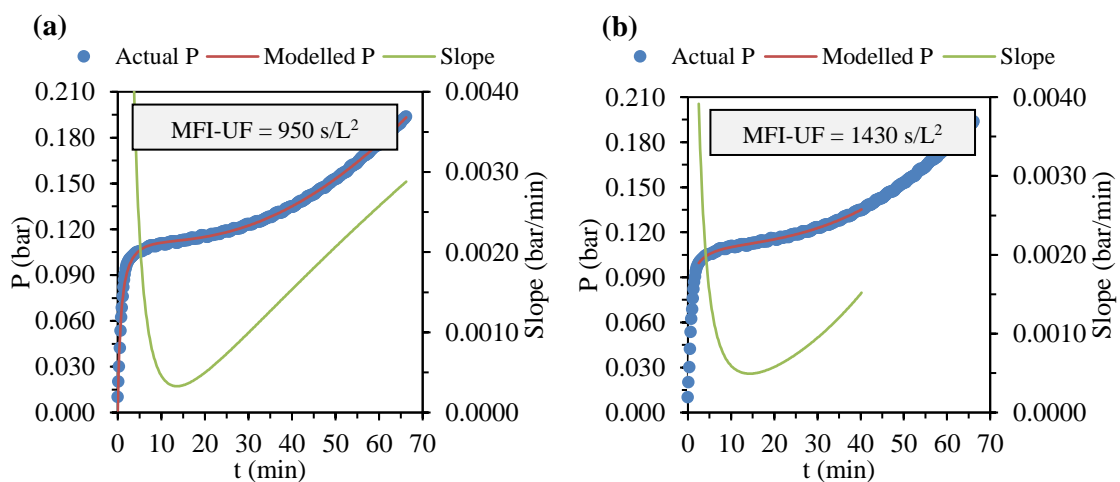


Figure A - 5.16: Actual P vs t and modelled P , slope, and MFI-UF determined based on Rational 3/2 model: (a) fitting all phases, and (b) fitting only cake filtration phase

5.2. Detecting and removing outliers

The MFI-UF calculation algorithm was modified further by refining the Rational 3/2 model fitting after the removal of the affecting outliers. The outliers could be detected based on the standardized residual, as described by Equation (A - 5.15) (NIST, 2012).

$$|\textit{standardized residual}| > d \quad (\textit{A} - 5.15)$$

The standardized residual is the ratio of the residual of a data point (difference between the actual and modelled P) and the standard deviation of all residuals. The value of d is usually set to 2 as a rule of thumb to identify the outlier. However, it was found that the value of d depends mainly on the number and the deviation of the outliers. For instance, if there are very few data points which deviate from the actual filtration curve, then the standard deviation of all residuals will be low. In this case, the value of d should be greater than 2. Otherwise, keeping the value d as 2 will result in detecting many data points which slightly deviate from the filtration curve as outliers, while these points have no effect on the model fitting. On the other hand, if there are many data points deviating significantly from the actual filtration curve, then the value of d should not be greater than 2. Otherwise, some outliers can be not detected.

Several trials have been done to detect the outliers with changing the value of d from 2 to 4. As an optimum solution, it was found that setting the value of d as 3 can be sufficient in all cases (both with low and high number of outliers) to detect the outliers which can significantly affect the model fitting and hence the calculated MFI-UF value.

Figure A - 5.17 presents an actual set of P vs t data with several outliers, where the Rational 3/2 model was applied before and after the detection and removal of outliers (based on $d = 3$). It can be observed that the fitting of cake filtration phase was deviated due to the outliers (Figure A - 5.17 (a)), while it became markedly perfect when the outliers were removed (Figure A - 5.17 (b)). The difference in the fitting can be also pronounced through the trend of the slope curve in both cases. As a result, the improvement in MFI-UF value was considerable, where the MFI-UF decreased to the half when the outliers were removed.

5.3. Exceptional cases

Despite the improvement of the Rational 3/2 model fitting, illustrated above, there are some cases where the data has poor quality due to (for example) data oscillation/instability and recording P values before the start and after the stop of the MFI-UF test, as shown in Figure A - 5.18. In these cases, the model fails to fit the actual data accurately. This poor-quality data should be eliminated in advance by utilizing a reliable MFI-UF set-up components.

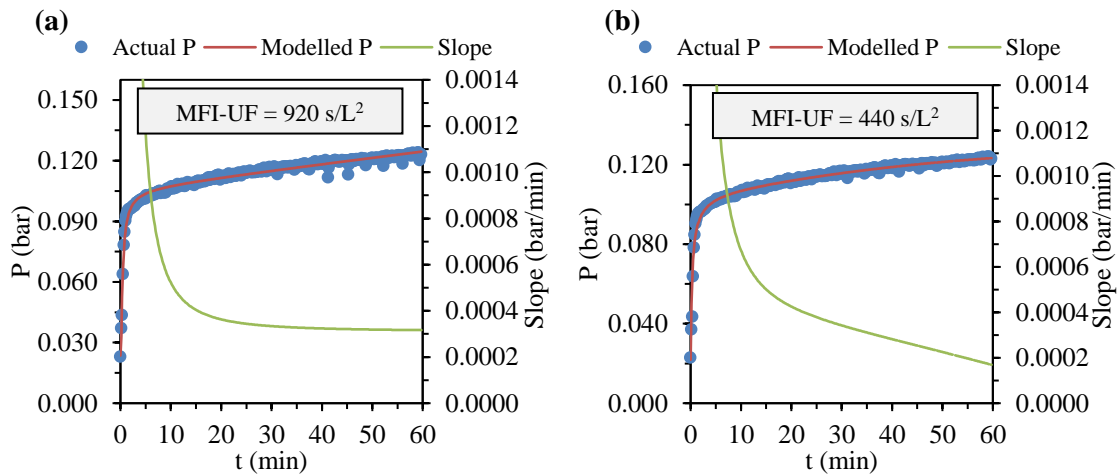


Figure A - 5.17: Actual P vs t and modelled P , slope and $MFI-UF$ determined based on Rational 3/2 model: (a) before outlier removal, and (b) after outlier removal

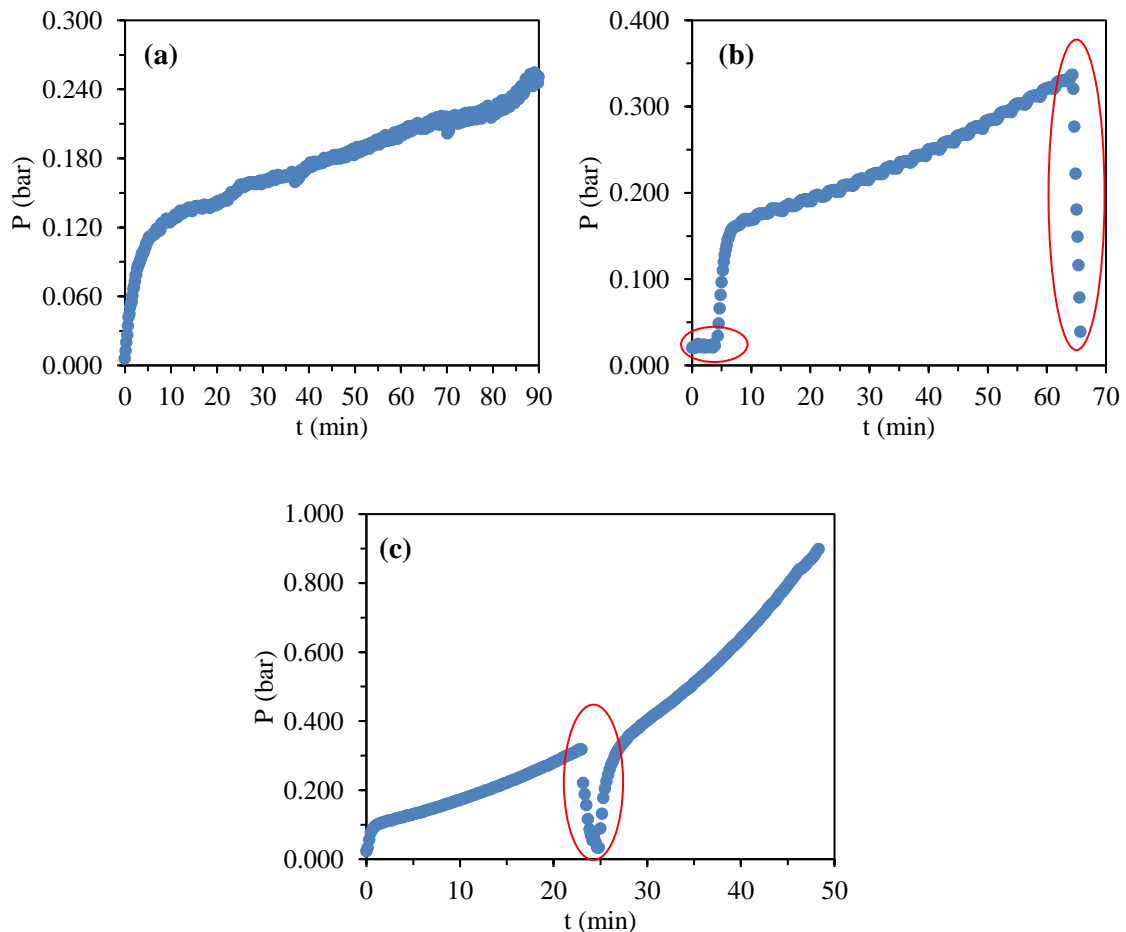


Figure A - 5.18: Examples of poor-quality P vs t data with deviated data points: (a) highly oscillated/unstable curve, (b) pressure was recorded before and after the $MFI-UF$ test (i.e. pump operation), and (c) sudden pump operation interruption

6. MFI-UF Calculator

The MFI-UF calculation algorithm was developed on Excel using VBA programming language, and named as “MFI-UF Calculator”. It has simple user interface (UI), presented in Figure A - 5.19. The UI consists of two parts; the first (left) includes the required inputs which should be entered by the user, and the second (right) presents the calculation outputs.

The inputs part is divided into four main sections. The first section requires to enter the MFI-UF testing conditions, namely: flux rate, water temperature and used membrane area. The second includes optional inputs, where the user can limit the range of data to be used in the MFI-UF calculation. This option can be useful, for example, to discard some data points which might have been recorded before or after the MFI-UF test. It can be used also for research purposes, to investigate the variation in the fitting (and thus the MFI-UF value) at different ranges of data. In case this option is not required, then the user can enter 0 and 10000 (or any high number) for the Start time and End time, respectively. The third section is related to the quality of the raw data (P vs t), and it includes two inputs; the value of the ABS(standardized residual) above which the data point is identified as an outlier (illustrated in section 5.2 of this annex), and the allowed duration in which the filtration curve trends as a U-shape (valley). In case any outliers or U-shape region are detected, a warning messages will be displayed in the outputs message box (on the right-down corner). The default values of these two inputs are set as 3 and 15, respectively. The last section in the inputs part is to calculate the MFI-UF. Here, the modification processes incorporated in the calculation algorithm (section 5 of this annex), i.e. to fit only cake/gel filtration phase and to remove outliers, are set as options. This was done for research purposes, where the user can investigate the difference in MFI-UF value with and without activating (checking) these options.

In this work, since the developed MFI-UF Calculator was not integrated yet with the MFI-UF set-up (i.e. the calculation doesn't start automatically after the end of the MFI-UF test), the user still should copy the raw MFI-UF data (P vs t) to a linked excel sheet, and then press on “Calculate MFI-UF” button after entering all required inputs.

The inputs part is accompanied with several error pop-up messages which are displayed if the user enters any improper inputs. For example, an error message will be displayed on the screen if the user enters any input with negative value, or if one of the testing conditions inputs is zero. If any error is detected, then the MFI-UF calculation will be directly terminated.

The outputs part (on the right) displays three sections. The first section (in the top) displays one chart presenting the actual P vs t data entered by the user, the curve fitted by the Rational $3/2$ model and the derived slope curve. The second section, which is the most important, shows the calculated MFI-UF value. The last section is the outputs message box which displays whether the calculation was successfully completed or there

are some errors due to any incorrect input. The box displays also a warning message in case of detection of outliers or U-shape regions. If the cake/gel filtration phase was too short (< 5 min), a warning message will be displayed as well. Another outputs section which is not displayed within the UI includes the detailed calculation outputs, where it is more convenient to present them separately.

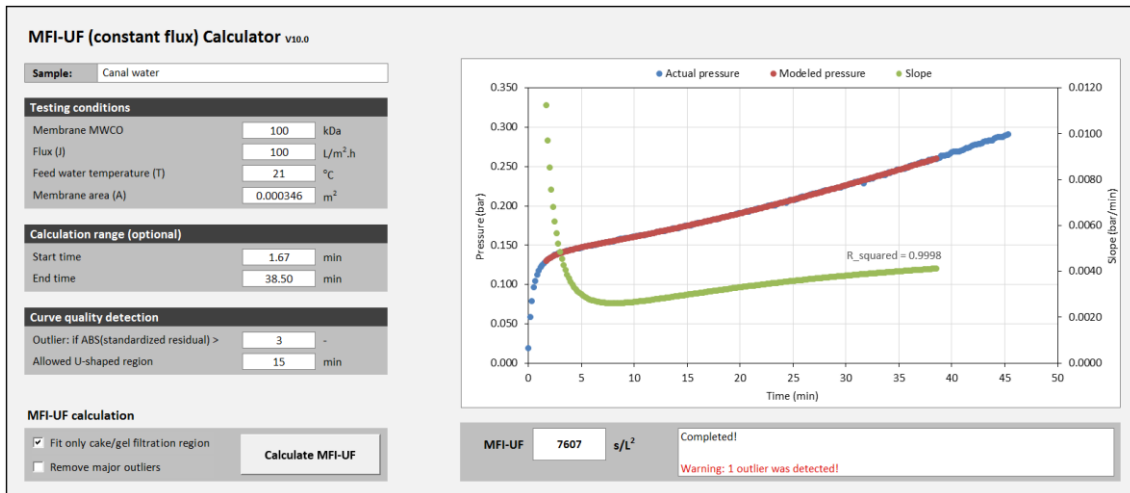


Figure A - 5.19: MFI-UF Calculator UI

The run time taken by the computer to calculate the MFI-UF depends mainly on: the specifications of used computer, size of raw data (P vs t), and the calculation options involved. The computer used in this work was a 4-years aged computer operating on Windows 7 with Core i5-6200U @ 2.3GHz processor and 8 GB RAM. Based on these specifications, the time required to calculate the MFI-UF was ± 3 seconds per 100 data points. However, with activating the calculation options of (i) fitting only cake/gel filtration phase and (ii) removing outliers, the run time reached ± 6 seconds per 100 data points. For example, the data presented in Figure A - 5.19 consisted of 270 data points and it took 12 seconds to calculate the MFI-UF (without outlier removal).

6

CONCLUSIONS AND FUTURE PERSPECTIVES

6.1. CONCLUSIONS

This research aimed to further develop and apply the MFI-UF method - constant flux, verifying its accuracy, reproducibility and applicability to predict particulate fouling in RO systems. The study concludes with the introduction of a complete testing protocol for the MFI-UF method to measure particulate fouling potential over a wide range of testing conditions; at fluxes of 20-200 L/m².h using 5, 10, 50 and 100 kDa PES flat-sheet membranes. The following is a summary of the main conclusions of the thesis.

6.1.1 Calibration and validation of the MFI-UF method

Until the date of conducting this study, neither a standard solution nor a standard procedure was available to calibrate MFI-UF measurements. Therefore, in this research, the calibration as well as the validation of the MFI-UF method were investigated in order to ensure the accuracy of particulate fouling measurements in RO.

Firstly, MFI-UF calibration was examined using two solutions of standard particles (dextran 150 kDa and polystyrene 25 nm). Two main criteria were investigated; (i) verification of MFI-UF linearity at both the lower and higher range of MFI-UF (i.e. MFI-UF of water of lower particle concentration such as RO feed and higher particle concentration such as RO concentrate and raw water), and (ii) reproducibility of MFI-UF linearity under the same testing conditions. Dextran solutions showed a strong linear relationship between the MFI-UF and particle concentration over the entire range of MFI-UF. However, the calibration was not reproducible, and different batches of dextran prepared under the same conditions produced very variable results. This was attributed to the structure of the dextran polymers which could be sensitive to slight variations in the chemical and/or physical conditions during the preparation of dextran solution, resulting in different size ranges of dextran particles (and thus different MFI-UF values) for each of the prepared dextran samples. For polystyrene solutions, a linear relationship between the MFI-UF and polystyrene particle concentration was verified at the higher range of MFI-UF (i.e. > 10,000 s/L²), while the MFI-UF values at the lower range (i.e. < 5000 s/L²) appeared to be underestimated. In addition, the slopes of the calibration lines obtained for polystyrene solutions were similar for a wide range of flux rates (50-200 L/m².h). This was attributed to the fact that the polystyrene particles could be hardly rearranged or compressed even when the flux increases since they are monodisperse and rigid in nature. As a result, the porosities of cake formed from polystyrene particles (and thus the measured MFI-UF values) were similar at different flux rates, which resulted in similar calibration lines. This result suggests that the polystyrene particle solutions may not be suitable to detect errors in the pump since the MFI-UF of a polystyrene sample would be similar even if the flux was different due to a pump error.

Secondly, natural (surface) water was used to validate the MFI-UF method under a wide range of MFI-UF testing conditions (flux rates of 20, 100 and 200 L/m².h using 5, 10 and

100 kDa UF membranes). The relationship between the MFI-UF and the particle concentration was strongly linear ($R^2 > 0.97$) in the entire range of measured MFI-UF values (up to 70,000 s/L²). Therefore, the MFI-UF method was validated and thus can be used to measure different levels of particulate fouling in RO systems. In addition, the strong correlation between the MFI-UF and particle concentration also confirmed the robustness of the MFI-UF method to detect the variation in particulate fouling potential due to a change in RO feed water quality.

6.1.2 Effect of surface porosity of the MFI-UF membrane

A new approach, using suspensions of pre-washed polystyrene particles (75 nm), was developed and applied experimentally to verify and quantify the effect of surface porosity of MFI-UF membrane of 5, 10, 50 and 100 kDa. Polystyrene particles were washed by stirred filtration (using an Amicon cell) to remove any surfactant material and particle fractions smaller than the pores of 5-100 kDa membranes. This was essential to ensure that the polystyrene particles retained on 5-100 kDa membranes are equivalent (i.e. same specific cake resistance on all membranes). Consequently, the MFI-UF of washed polystyrene particle suspensions measured by the 5-100 kDa membranes was independent of the membrane pore size and depended only on the membrane surface porosity. The MFI-UF measurements of washed polystyrene suspensions were combined with high-resolution SEM analyses to characterize the surface porosity of the 5-100 kDa membranes.

The results showed that the membrane surface porosity decreased with MWCO from 10.5% (100 kDa) to 0.6% (5 kDa), and consequently the MFI-UF increased from 3700 to 8700 s/L², respectively. This increase in MFI-UF was attributed to the non-uniform distribution of membrane pores, which is exacerbated as the surface porosity decreases. This could result in limiting the cake formation only over the porous regions of membrane surface, and consequently lead to smaller effective membrane filtration area, and thus higher local flux. Eventually, an overestimated MFI-UF was obtained with the lower membrane surface porosity. Accordingly, using the 100 kDa membrane as a reference (with the lowest/negligible surface porosity effect), correction factors of 0.4-1.0 were identified to correct the MFI-UF for the effect of surface porosity of the 5-100 kDa membranes, respectively.

6.1.3 Application of the MFI-UF method to predict particulate fouling in RO systems

In this research, the MFI-UF method using 5, 10 and 100 kDa membranes was applied to predict particulate fouling rates in two full-scale RO plants. In order to consider the effect of RO cross-flow hydrodynamic conditions on the particle deposition and detachment, the particle deposition factor (Ω) was measured (from the ratio of the MFI-UF of the RO feed and RO concentrate) and incorporated in the fouling prediction. The other types of

fouling potential (i.e. scaling, organic fouling and biofouling) were also measured and evaluated, and the results indicated minor effect due to these types of fouling, and thus the particulate fouling was considered the dominant fouling in the studied RO plants.

The results indicated that particulate fouling rates predicted based on the MFI-UF measured using UF membrane in the range of 10-100 kDa agreed well with the actual fouling observed in the two RO plants. On the other hand, the fouling rates predicted based on the MFI-UF measured with 5 kDa membrane were apparently overestimated. The reason was attributed to the correction factor used to correct the effect of surface porosity of the 5 kDa membranes, which is most likely still overestimated. This is because the correction factors (addressed in section 6.1.2) were identified using suspensions of polystyrene particles which are rigid and incompressible compared to natural particles existing in real RO feed water which are usually deformable and compressible. This means that the cake formed by natural particles might be more compact and thus less porous compared to the cake formed by polystyrene particles. As a result, the effect of membrane surface porosity on overestimating the MFI-UF is probably greater for real RO feed water compared to polystyrene particle suspensions.

6.1.4 MFI-UF testing protocol

This research proposed a complete testing protocol for the MFI-UF method – constant flux to ensure the accuracy and reproducibility of MFI-UF measurements and thus the prediction of particulate fouling in RO. The protocol describes the procedures required to perform the MFI-UF test accurately, addressing all details related to the MFI-UF set-up, membranes, operating conditions and calculation. For MFI-UF calculation, a new numerical algorithm was successfully developed based on regression modelling which calculates the MFI-UF value automatically upon the completion of the MFI-UF test. The protocol investigated also the factors/problems which may affect the MFI-UF measurements. The following, among others, are the key findings of these investigations:

- **MFI-UF membrane cleaning:** UF membranes used in the MFI-UF test are purchased with a preservation coating, which should be removed before the test by filtering ultra-pure water. With filtering same water volume, the removal of this coating was found more efficient when the applied flux was lower, since the contact time between the membrane and filtered water was longer. Nevertheless, 90-95% of coating removal was achieved in the first 20 mL of filtered water independently of the applied flux rate (100-1000 L/m².h). As an optimum cleaning approach, membrane coating can be sufficiently removed by filtering 100 mL of ultra-pure water at 300 L/m².h (cleaning time is 1 hour).
- **Feed water temperature:** the transmembrane pressure observed during the MFI-UF depends highly on the temperature (i.e. viscosity) of the tested feed water. Any change in feed water temperature during the MFI-UF test will result in a variation in the

transmembrane pressure, which will subsequently affect the slope of the cake/gel filtration phase, and eventually lead to inaccurate MFI-UF values. To avoid this, the temperature of the feed water should be allowed to reach the ambient temperature before starting the MFI-UF test. In case the variation in feed water temperature could not be prevented during the MFI-UF test, then the slope of cake/gel filtration phase can be corrected using a correction formula developed in this research.

- MFI-UF test duration: the MFI-UF test can be stopped when an even cake continuously builds up over the membrane surface. The formation of even cake layers can take longer time when the flux rate, particle concentration or membrane surface porosity (i.e. MWCO) is lower. It was found that the duration of MFI-UF is sufficient once; (1) the cake compression phase is observed during the test, (2) a stable linear cake filtration phase lasts for more than 75% of the total elapsed time, or (3) test duration exceeds 20, 3 and 1 hour at a flux of 20, 100 and 200 L/m².h, respectively (these durations are considered as a ‘safe’ rule of thumb, where the durations were estimated based on MFI-UF measurements of very low fouling water sample; i.e. tap water filtered by 10 kDa membrane).
- It was found that the use of 5 kDa membrane in the MFI-UF test might be challenging, for the following reasons:
 - The variation in membrane properties, described by the membrane resistance (R_m), was considerable in the case of 5 kDa membrane ($\pm 22\%$) compared to the 10-100 kDa membranes ($< \pm 9\%$). This could indicate that the MFI-UF measured with 5 kDa membranes might be less reproducible.
 - 5 kDa membranes require much higher transmembrane pressure in comparison with the higher MWCO membranes (transmembrane pressure of the 5 kDa membrane is around 10 times higher than the pressure of the 10 kDa membrane at same flux rate). As a result, since the error of pressure transmitter is proportional (expressed as a percentage) to the measured pressure range, the error in transmembrane pressure readings would be higher with the 5 kDa membrane which eventually might affect the accuracy of measured MFI-UF. In addition, the effect of insufficient membrane cleaning and/or feed water temperature variation during the test (mentioned above) will be higher, since the effect of both factors is proportional to the transmembrane pressure (i.e. the higher the transmembrane pressure, the higher the effect).
 - As mentioned in section 6.1.2, the effect of the very low surface porosity of 5 kDa membranes was significant even after the use of a correction factor for MFI-UF.

6.2 FUTURE PERSPECTIVES

The findings of this research can be used as a basis for future research, as summarised below:

- In this research, the MFI-UF calibration was examined using synthetic solutions of standard dextran particles and monodisperse polystyrene spheres. The solution of polystyrene particles is considered more promising as it is stable and reproducible compared to dextran solutions. However, as mentioned in section 6.1.1, the calibration lines obtained for polystyrene solutions were similar over a wide range of flux rates (50-200 L/m².h), which was attributed to the fact that the polystyrene particles could be hardly rearranged or compressed even when the flux was increased since they were monodisperse and rigid in nature. Therefore, further investigation is needed to select, prepare and test a suitable heterogenous mixture of polystyrene particles (with different particle sizes and shapes) as well as particles which mimic the particles in natural water and thus overcome the limitations of calibration obtained with the monodisperse rigid polystyrene particles.
- Correcting the effect of the low surface porosity of the MFI-UF membrane is important for accurate prediction of particulate fouling. However, as mentioned in section 6.1.2, the proposed correction factors were determined using the 100 kDa membrane as a reference, assuming that the membranes with MWCO of ≥ 100 kDa have a negligible effect due to surface porosity. Therefore, a further research is required to verify this assumption, with investigating the effect of surface porosity of the membranes with MWCO of ≥ 100 kDa. In addition, as mentioned in section 6.1.3, the correction factors appeared to be still overestimated, particularly the correction factor for the 5 kDa membrane. Therefore, further research is still required to quantify the effect of membrane surface porosity using different types of particles which exhibit similar properties to particles that exist in real water. Eventually, 'global' correction factors should be proposed for different types of feed water.
- In this research, the MFI-UF was applied in two RO plants treating surface water. Therefore, it is recommended to apply and verify the MFI-UF method to predict particulate fouling rates in other RO plants operating with different feed water and different conditions.
- A fully automated MFI-UF equipment (i.e. measuring and calculating the MFI-UF automatically) should be developed. The automatic MFI-UF equipment can be connected online on the RO feed and concentrate of each train in the RO plant, providing real-time MFI-UF measurements and particulate fouling rates prediction. This can further improve the accuracy and reproducibility and enhance the applicability of MFI-UF measurements to predict particulate fouling in RO plants.

- The MFI-UF method has been used in several researches. However, it is difficult to compare the outputs of these researches as the MFI-UF measurements have been carried out based on different set-ups and testing procedures. This study introduced a complete testing protocol for the MFI-UF method. A next step is required to standardize the method.

REFERENCES

- Abbas, A., & Al-Bastaki, N. (2005). Modeling of an RO water desalination unit using neural networks. *Chemical Engineering Journal*, 114(1), 139-143.
- Abunada, M., Dhakal, N., Andyar, W. Z., Ajok, P., Smit, H., Ghaffour, N., Schippers, J. C., & Kennedy, M. D. (2022). Improving MFI-UF constant flux to more accurately predict particulate fouling in RO systems: Quantifying the effect of membrane surface porosity. *Journal of Membrane Science*, 660, 120854.
- Abunada, M., Dhakal, N., Andyar, W. Z., Li, Y., Ajok, P., Ghaffour, N., Schippers, J. C., & Kennedy, M. D. (2023a). Calibrating and Validating the MFI-UF Method to Measure Particulate Fouling in Reverse Osmosis. *Membranes*, 13(5), 535.
- Abunada, M., Dhakal, N., Gulrez, R., Ajok, P., Li, Y., Abushaban, A., Smit, H., Moed, D., Ghaffour, N., Schippers, J. C., & Kennedy, M. D. (2023b). Prediction of particulate fouling in full-scale reverse osmosis plants using the modified fouling index – ultrafiltration (MFI-UF) method. *Desalination*, 553, 116478.
- Abushaban, A., Salinas-Rodriguez, S. G., Dhakal, N., Schippers, J. C., & Kennedy, M. D. (2019). Assessing pretreatment and seawater reverse osmosis performance using an ATP-based bacterial growth potential method. *Desalination*, 467, 210-218.
- Abushaban, M. (2019). *Assessing Bacterial Growth Potential in Seawater Reverse Osmosis Pretreatment: Method Development and Applications*.
- Abushaban, M., Mangal, M. N., Salinas-Rodriguez, S. G., Nnebuo, C., Mondal, S., Goueli, S., Schippers, J., & Kennedy, M. (2017). Direct measurement of ATP in seawater and application of ATP to monitor bacterial growth potential in SWRO pre-treatment systems. *Desalination and Water Treatment*, 99.
- Ahmed, F. E., Hashaikeh, R., & Hilal, N. (2020). Hybrid technologies: The future of energy efficient desalination – A review. *Desalination*, 495, 114659.
- Aish, A. M., Zaqoot, H. A., & Abdeljawad, S. M. (2015). Artificial neural network approach for predicting reverse osmosis desalination plants performance in the Gaza Strip. *Desalination*, 367, 240-247.
- Al-Shayji, K. A., & Liu, Y. A. (2002). Predictive Modeling of Large-Scale Commercial Water Desalination Plants: Data-Based Neural Network and Model-Based Process Simulation. *Industrial & Engineering Chemistry Research*, 41(25), 6460-6474.
- Alhadidi, A., Blankert, B., Kemperman, A. J. B., Schippers, J. C., Wessling, M., & van der Meer, W. G. J. (2011a). Effect of testing conditions and filtration mechanisms on SDI. *Journal of Membrane Science*, 381(1–2), 142-151.
- Alhadidi, A., Kemperman, A. J. B., Blankert, B., Schippers, J. C., Wessling, M., & van der Meer, W. G. J. (2011b). Silt Density Index and Modified Fouling Index relation, and effect of pressure, temperature and membrane resistance. *Desalination*, 273(1), 48-56.

- Alhadidi, A., Kemperman, A. J. B., Schippers, J. C., Blankert, B., Wessling, M., & van der Meer, W. G. J. (2011c). SDI normalization and alternatives. *Desalination*, 279(1–3), 390-403.
- Alhadidi, A., Kemperman, A. J. B., Schippers, J. C., Wessling, M., & van der Meer, W. G. J. (2011d). The influence of membrane properties on the Silt Density Index. *Journal of Membrane Science*, 384(1–2), 205-218.
- Alhadidi, A., Kemperman, A. J. B., Schurer, R., Schippers, J. C., Wessling, M., & van der Meer, W. G. J. (2012). Using SDI, SDI+ and MFI to evaluate fouling in a UF/RO desalination pilot plant. *Desalination*, 285, 153-162.
- Alpatova, A., Qamar, A., Al-Ghamdi, M., Lee, J., & Ghaffour, N. (2020). Effective membrane backwash with carbon dioxide under severe fouling and operation conditions. *Journal of Membrane Science*, 611, 118290.
- Arenillas, S., Drouin, M., Monnin, E., & Moulin, P. (2017). Glycerin Removal from Ultrafiltration Flat Sheet Membranes by Filtration and Soaking. *Journal of Membrane Science and Research*, 3(2), 102-108.
- ASTM. (2014). ASTM D4189-07, standard test method for silt density index (SDI) of water. In. West Conshohocken, PA, USA.
- ASTM. (2015). ASTM D8002-15, standard test method for modified fouling index (MFI-0.45) of water. In. West Conshohocken, PA, USA.
- Au, K.-K., Alpert, S. M., & Pernitsky, D. J. (2011). Chapter 1 - Particle and Natural Organic Matter Removal in Drinking Water Treatment. In *Operational Control of Coagulation and Filtration Processes - Manual of Water Supply Practices, M37* (3rd ed., pp. 1-16). USA: American Water Works Association (AWWA).
- Barello, M., Manca, D., Patel, R., & Mujtaba, I. M. (2014). Neural network based correlation for estimating water permeability constant in RO desalination process under fouling. *Desalination*, 345, 101-111.
- Barger, M., & Carnahan, R. P. (1991). Fouling prediction in reverse osmosis processes. *Desalination*, 83(1), 3-33.
- Belfort, G., Davis, R. H., & Zydney, A. L. (1994). The behavior of suspensions and macromolecular solutions in crossflow microfiltration. *Journal of Membrane Science*, 96(1), 1-58.
- Boerlage, S. F. E., Kennedy, M., Aniye, M. P., & Schippers, J. C. (2003a). Applications of the MFI-UF to measure and predict particulate fouling in RO systems. *Journal of Membrane Science*, 220(1–2), 97-116.
- Boerlage, S. F. E., Kennedy, M., Tarawneh, Z., De Faber, R., & Schippers, J. C. (2004). Development of the MFI-UF in constant flux filtration. *Desalination*, 161(2), 103-113.
- Boerlage, S. F. E., Kennedy, M. D., Aniye, M. P., Abogrean, E., Tarawneh, Z. S., & Schippers, J. C. (2003b). The MFI-UF as a water quality test and monitor. *Journal of Membrane Science*, 211(2), 271-289.

- Boerlage, S. F. E., Kennedy, M. D., Aniye, M. p., Abogrean, E. M., El-Hodali, D. E. Y., Tarawneh, Z. S., & Schippers, J. C. (2000). Modified fouling index ultrafiltration to compare pretreatment processes of reverse osmosis feedwater. *Desalination*, 131(1), 201-214.
- Boerlage, S. F. E., Kennedy, M. D., Aniye, M. P., Abogrean, E. M., Galjaard, G., & Schippers, J. C. (1998). Monitoring particulate fouling in membrane systems. *Desalination*, 118(1), 131-142.
- Boerlage, S. F. E., Kennedy, M. D., Bonne, P. A. C., Galjaard, G., & Schippers, J. C. (1997). Prediction of flux decline in membrane systems due to particulate fouling. *Desalination*, 113(2), 231-233.
- Boerlage, S. F. E., Kennedy, M. D., Bremere, I., Witkamp, G. J., Van der Hoek, J. P., & Schippers, J. C. (2002a). The scaling potential of barium sulphate in reverse osmosis systems. *Journal of Membrane Science*, 197(1), 251-268.
- Boerlage, S. F. E., Kennedy, M. D., Dickson, M. R., El-Hodali, D. E. Y., & Schippers, J. C. (2002b). The modified fouling index using ultrafiltration membranes (MFI-UF): characterisation, filtration mechanisms and proposed reference membrane. *Journal of Membrane Science*, 197(1-2), 1-21.
- Brant, J. A., & Childress, A. E. (2002). Assessing short-range membrane–colloid interactions using surface energetics. *Journal of Membrane Science*, 203(1-2), 257-273.
- Carman, P. C. (1938). Fundamental principles of industrial filtration (A critical review of present knowledge). *Trans. Instn Chem. Engrs*, 16, 168-188.
- Chandler, M., & Zydney, A. (2006). Effects of membrane pore geometry on fouling behavior during yeast cell microfiltration. *Journal of Membrane Science*, 285(1), 334-342.
- Choi, J.-S., Hwang, T.-M., Lee, S., & Hong, S. (2009). A systematic approach to determine the fouling index for a RO/NF membrane process. *Desalination*, 238(1), 117-127.
- DesalData. (2020). *IDA Desalination Plants Inventory*. Retrieved from: www.desaldata.com
- DOW. (2011). FILMTEC™ Reverse Osmosis Membranes - Technical Manual. In.
- Ethier, C. R., & Kamm, R. D. (1989). The hydrodynamic resistance of filter cakes. *Journal of Membrane Science*, 43(1), 19-30.
- Fane, A. G., Fell, C. J. D., Hodgson, P. H., Leslie, G., & Marshall, K. C. (1991). Microfiltration of biomass and biofluids: Effects of membrane morphology and operating conditions. *Filtration & Separation*, 28(5), 332-331.
- Giddings, J., Yang, F., & Myers, M. (1976). Flow-field-flow fractionation: a versatile new separation method. *Science*, 193(4259), 1244-1245.
- Goh, P. S., Lau, W. J., Othman, M. H. D., & Ismail, A. F. (2018). Membrane fouling in desalination and its mitigation strategies. *Desalination*, 425, 130-155.

- Golberg, M., & Cho, H. (2010). *Introduction to Regression Analysis*.
- Greene, W. H. (2003). *Econometric Analysis*: Prentice Hall.
- Gregory, J. (2005). *Particles in water: properties and processes*. London: IWA Publishing.
- Gregory, J. (2006). *Particles in Water: Properties And Processes*: CRC/Taylor & Francis.
- Güell, C., & Davis, R. H. (1996). Membrane fouling during microfiltration of protein mixtures. *Journal of Membrane Science*, *119*(2), 269-284.
- Harrison, W., Abdallah, Z., & Whittaker, M. (2014). A Model for Creep and Creep Damage in the γ -Titanium Aluminide Ti-45Al-2Mn-2Nb. *Materials*, *7*(3), 2194-2209.
- Hartmann, R. L., & Williams, S. K. R. (2002). Flow field-flow fractionation as an analytical technique to rapidly quantitate membrane fouling. *Journal of Membrane Science*, *209*(1), 93-106.
- Henry, C., Minier, J.-P., & Lefèvre, G. (2012). Towards a description of particulate fouling: from single particle deposition to clogging. *Advances in Colloid and Interface Science*, *185–186*, 34-76.
- Hoaglin, D. C., Iglewicz, B., & Tukey, J. W. (1986). Performance of Some Resistant Rules for Outlier Labeling. *Journal of the American Statistical Association*, *81*, 991-999.
- Hoek, E. M. V., & Elimelech, M. (2003). Cake-Enhanced Concentration Polarization: A New Fouling Mechanism for Salt-Rejecting Membranes. *Environmental Science & Technology*, *37*(24), 5581-5588.
- Hong, K., Lee, S., Choi, S., Yu, Y., Hong, S., Moon, J., Sohn, J., & Yang, J. (2009). Assessment of various membrane fouling indexes under seawater conditions. *Desalination*, *247*(1), 247-259.
- Hund, D., Antonyuk, S., & Ripperger, S. (2017). Simulation of Bridging at the Static Surface Filtration by CFD-DEM Coupling. *EPJ Web of Conferences*, *140*, 09033.
- Hydranautics. (2016). Technical Service Bulletin - Procedure for Measuring Silt Density Index (SDI). In.
- Jafar, M. M., & Zilouchian, A. (2002). Prediction of Critical Desalination Parameters Using Radial Basis Functions Networks. *Journal of Intelligent and Robotic Systems*, *34*(2), 219-230.
- Ju, Y., Hong, I., & Hong, S. (2015). Multiple MFI measurements for the evaluation of organic fouling in SWRO desalination. *Desalination*, *365*, 136-143.
- Ju, Y., & Hong, S. (2014). Nano-colloidal fouling mechanisms in seawater reverse osmosis process evaluated by cake resistance simulator-modified fouling index nanofiltration. *Desalination*, *343*, 88-96.
- Khayet, M., Cojocar, C., & Essalhi, M. (2011). Artificial neural network modeling and response surface methodology of desalination by reverse osmosis. *Journal of Membrane Science*, *368*(1), 202-214.

- Khirani, S., Ben Aim, R., & Manero, M.-H. (2006). Improving the measurement of the Modified Fouling Index using nanofiltration membranes (NF–MFI). *Desalination*, *191*(1), 1-7.
- Khoo, Y. S., Lau, W. J., Hasan, S. W., Salleh, W. N. W., & Ismail, A. F. (2021). New approach of recycling end-of-life reverse osmosis membranes via sonication for microfiltration process. *Journal of Environmental Chemical Engineering*, *9*(6), 106731.
- Kim, S., Lee, S., Kim, C.-H., & Cho, J. (2009). A new membrane performance index using flow-field flow fractionation (fl-FFF). *Desalination*, *247*(1), 169-179.
- Kooij, D. v. d. (1992). Assimilable Organic Carbon as an Indicator of Bacterial Regrowth. *Journal AWWA*, *84*(2), 57-65.
- Kutscher, H. L., Chao, P., Deshmukh, M., Singh, Y., Hu, P., Joseph, L. B., Reimer, D. C., Stein, S., Laskin, D. L., & Sinko, P. J. (2010). Threshold size for optimal passive pulmonary targeting and retention of rigid microparticles in rats. *Journal of Controlled Release*, *143*(1), 31-37.
- Kva^oLseth, T. O. (1983). Note on the R2 measure of goodness of fit for nonlinear models. *Bulletin of the Psychonomic Society*, *21*(1), 79-80.
- Lasdon, L. S., Waren, A. D., Jain, A., & Ratner, M. (1978). Design and Testing of a Generalized Reduced Gradient Code for Nonlinear Programming. *ACM Trans. Math. Softw.*, *4*(1), 34–50.
- Lee, Y. G., Lee, Y. S., Jeon, J. J., Lee, S., Yang, D. R., Kim, I. S., & Kim, J. H. (2009). Artificial neural network model for optimizing operation of a seawater reverse osmosis desalination plant. *Desalination*, *247*(1), 180-189.
- Li, Q., & Elimelech, M. (2004). Organic Fouling and Chemical Cleaning of Nanofiltration Membranes: Measurements and Mechanisms. *Environmental Science & Technology*, *38*(17), 4683-4693.
- Li, Y., Gao, F., Wei, W., Qu, J.-B., Ma, G.-H., & Zhou, W.-Q. (2010). Pore size of macroporous polystyrene microspheres affects lipase immobilization. *Journal of Molecular Catalysis B: Enzymatic*, *66*(1), 182-189.
- Libotean, D., Giralt, J., Giralt, F., Rallo, R., Wolfe, T., & Cohen, Y. (2009). Neural network approach for modeling the performance of reverse osmosis membrane desalting. *Journal of Membrane Science*, *326*(2), 408-419.
- Lipp, P., Müller, U., Hetzer, B., & Wagner, T. (2009). Characterization of nanoparticulate fouling and breakthrough during low-pressure membrane filtration. *Desalination and Water Treatment*, *9*(1-3), 234-240.
- Lohaus, J., Perez, Y. M., & Wessling, M. (2018). What are the microscopic events of colloidal membrane fouling? *Journal of Membrane Science*, *553*, 90-98.
- Long, G. L., & Winefordner, J. D. (1983). Limit of Detection A Closer Look at the IUPAC Definition. *Analytical Chemistry*, *55*(07), 712A-724A.
- Lu, W.-M., & Ju, S.-C. (1989). Selective particle deposition in crossflow filtration. *Separation Science and Technology*, *24*(7-8), 517-540.

- Mangal, M. N., Yangali-Quintanilla, V. A., Salinas-Rodriguez, S. G., Dusseldorp, J., Blankert, B., Kemperman, A. J. B., Schippers, J. C., Kennedy, M. D., & van der Meer, W. G. J. (2022). Application of a smart dosing pump algorithm in identifying real-time optimum dose of antiscalant in reverse osmosis systems. *Journal of Membrane Science*, 658, 120717.
- March, H. (2015). The politics, geography, and economics of desalination: a critical review. *Wiley Interdisciplinary Reviews: Water*, 2(3), 231-243.
- Millipore. (2018). User guide: Ultrafiltration Membranes - Operating Instructions. In.
- Moon, J., & Cho, J. (2005). Investigation of nano-colloid transport in UF membranes using flow field-flow fractionation (flow FFF) and an irreversible thermodynamic transport model. *Desalination*, 179(1), 151-159.
- Moradi, A., Mojarradi, V., & Sarcheshmehpour, M. (2013). Prediction of RO membrane performances by use of artificial neural network and using the parameters of a complex mathematical model. *Research on Chemical Intermediates*, 39(7), 3235-3249.
- Mulder, M. (2012). *Basic Principles of Membrane Technology*: Springer Netherlands.
- Nahrstedt, A., & Camargo-Schmale, J. (2008). New insights into silt density index and modified fouling index measurements. *Water Science and Technology: Water Supply*, 8(4), 401-411.
- Niemi, H., Bulsari, A., & Palosaari, S. (1995). Simulation of membrane separation by neural networks. *Journal of Membrane Science*, 102, 185-191.
- NIST. (2012). *e-Handbook of Statistical Methods*. USA.
- Niu, C., Li, X., Dai, R., & Wang, Z. (2022). Artificial intelligence-incorporated membrane fouling prediction for membrane-based processes in the past 20 years: A critical review. *Water Research*, 216, 118299.
- Park, J. Y., Cho, J., & Park, K. (2009a). Evaluation of quantitative performance of the membrane filtration-differential mobility analyzer (MF-DMA) counting technique to determine suspended particles and dissolved solids in water. *Desalination*, 247(1), 316-325.
- Park, J. Y., Lim, S., & Park, K. (2013). A new approach for determination of fouling potential by colloidal nanoparticles during reverse osmosis (RO) membrane filtration of seawater. *Journal of Nanoparticle Research*, 15(4), 1548.
- Park, K., Park, J. Y., Lee, S., & Cho, J. (2009b). Measurement of size and number of suspended and dissolved nanoparticles in water for evaluation of colloidal fouling in RO membranes. *Desalination*, 238(1), 78-89.
- Pellegrino, J., Wright, S., Ranvill, J., & Amy, G. (2005). Predicting membrane flux decline from complex mixtures using flow-field flow fractionation measurements and semi-empirical theory. *Water Science and Technology*, 51(6-7), 85-92.
- Rachman, R. M., Ghaffour, N., Wali, F., & Amy, G. L. (2013). Assessment of silt density index (SDI) as fouling propensity parameter in reverse osmosis (RO) desalination systems. *Desalination and Water Treatment*, 51(4-6), 1091-1103.

- Salgado-Reyna, A., Soto-Regalado, E., Gómez-González, R., Cerino-Córdova, F. J., García-Reyes, R. B., Garza-González, M. T., & Alcalá-Rodríguez, M. M. (2015). Artificial neural networks for modeling the reverse osmosis unit in a wastewater pilot treatment plant. *Desalination and Water Treatment*, 53(5), 1177-1187.
- Salinas-Rodríguez, S. G. (2011). *Particulate and organic matter fouling of seawater reverse osmosis systems: characterization, modelling and applications* (1st Edition ed.). London, UK: CRC Press/Balkema.
- Salinas-Rodríguez, S. G., Amy, G. L., Schippers, J. C., & Kennedy, M. D. (2015). The modified fouling index ultrafiltration constant flux for assessing particulate/colloidal fouling of RO systems. *Desalination*, 365, 79-91.
- Salinas-Rodríguez, S. G., Boerlage, S. F. E., Schippers, J. C., Kennedy, M. D., Salinas-Rodríguez, S. G., Schippers, J. C., Amy, G. L., Kim, I. S., & Kennedy, M. D. (2021). Particulate fouling. In *Seawater Reverse Osmosis Desalination: Assessment and Pre-treatment of Fouling and Scaling* (pp. 0): IWA Publishing.
- Salinas-Rodríguez, S. G., Kennedy, M. D., Amy, G. L., & Schippers, J. C. (2012). Flux dependency of particulate/colloidal fouling in seawater reverse osmosis systems. *Desalination and Water Treatment*, 42(1-3), 155-162.
- Salinas Rodríguez, S. G., Sithole, N., Dhakal, N., Olive, M., Schippers, J. C., & Kennedy, M. D. (2019). Monitoring particulate fouling of North Sea water with SDI and new ASTM MFI0.45 test. *Desalination*, 454, 10-19.
- Sawe, B. E. (2017, 25 April). Countries Who Rely on Desalination. WorldAtlas. Retrieved from <https://www.worldatlas.com/articles/countries-who-rely-on-desalination.html>
- Schäfer, A. I., Fane, A. G., & Waite, T. D. (1998). Nanofiltration of natural organic matter: Removal, fouling and the influence of multivalent ions. *Desalination*, 118(1), 109-122.
- Schippers, J. C., Folmer, H. C., Verdouw, J., & Scheerman, H. J. (1985). Reverse osmosis for treatment of surface water. *Desalination*, 56, 109-119.
- Schippers, J. C., Hanemaayer, J. H., Smolders, C. A., & Kostense, A. (1981). Predicting flux decline of reverse osmosis membranes. *Desalination*, 38, 339-348.
- Schippers, J. C., & Verdouw, J. (1980). The modified fouling index, a method of determining the fouling characteristics of water. *Desalination*, 32, 137-148.
- Sim, L. N., Ye, Y., Chen, V., & Fane, A. G. (2010). Crossflow Sampler Modified Fouling Index Ultrafiltration (CFS-MFIUF)—An alternative Fouling Index. *Journal of Membrane Science*, 360(1-2), 174-184.
- Sim, L. N., Ye, Y., Chen, V., & Fane, A. G. (2011a). Comparison of MFI-UF constant pressure, MFI-UF constant flux and Crossflow Sampler-Modified Fouling Index Ultrafiltration (CFS-MFIUF). *Water Research*, 45(4), 1639-1650.
- Sim, L. N., Ye, Y., Chen, V., & Fane, A. G. (2011b). Investigations of the coupled effect of cake-enhanced osmotic pressure and colloidal fouling in RO using crossflow sampler-modified fouling index ultrafiltration. *Desalination*, 273(1), 184-196.

- Singh, R. S., Saini, G. K., & Kennedy, J. F. (2008). Pullulan: Microbial sources, production and applications. *Carbohydr Polym*, 73(4), 515-531.
- Sousi, M., Liu, G., Salinas-Rodriguez, S. G., Chen, L., Dusseldorp, J., Wessels, P., Schippers, J. C., Kennedy, M. D., & van der Meer, W. (2020a). Multi-parametric assessment of biological stability of drinking water produced from groundwater: Reverse osmosis vs. conventional treatment. *Water Research*, 186, 116317.
- Sousi, M., Salinas-Rodriguez, S. G., Liu, G., Schippers, J. C., Kennedy, M. D., & van der Meer, W. (2020b). Measuring Bacterial Growth Potential of Ultra-Low Nutrient Drinking Water Produced by Reverse Osmosis: Effect of Sample Pre-treatment and Bacterial Inoculum. *Frontiers in Microbiology*, 11.
- Spettmann, D., Eppmann, S., Flemming, H.-C., & Wingender, J. (2007). Simultaneous visualisation of biofouling, organic and inorganic particle fouling on separation membranes. *Water Science and Technology*, 55(8-9), 207-210.
- Taheri, A. H., Sim, S. T. V., Sim, L. N., Chong, T. H., Krantz, W. B., & Fane, A. G. (2013). Development of a new technique to predict reverse osmosis fouling. *Journal of Membrane Science*, 448, 12-22.
- Tang, C. Y., Chong, T. H., & Fane, A. G. (2011). Colloidal interactions and fouling of NF and RO membranes: a review. *Advances in Colloid and Interface Science*, 164(1-2), 126-143.
- Trinh, T. A., Li, W., & Chew, J. W. (2020). Internal fouling during microfiltration with foulants of different surface charges. *Journal of Membrane Science*, 602, 117983.
- UNESCO. (2020). *United Nations World Water Development Report 2020: Water and Climate Change* (UNESCO Ed.). Paris.
- United Nations. (2017). *Factsheet: People and Oceans*. Paper presented at the The Ocean Conference, New York, USA.
- van der Wielen, P. W. J. J., & van der Kooij, D. (2010). Effect of water composition, distance and season on the adenosine triphosphate concentration in unchlorinated drinking water in the Netherlands. *Water Research*, 44(17), 4860-4867.
- Villacorte, L. O., Ekowati, Y., Calix-Ponce, H. N., Schippers, J. C., Amy, G. L., & Kennedy, M. D. (2015). Improved method for measuring transparent exopolymer particles (TEP) and their precursors in fresh and saline water. *Water Research*, 70, 300-312.
- Vrouwenvelder, J. S., & van der Kooij, D. (2001). Diagnosis, prediction and prevention of biofouling of NF and RO membranes. *Desalination*, 139(1), 65-71.
- Weinrich, L. A., Giraldo, E., & LeChevallier, M. W. (2009). Development and Application of a Bioluminescence-Based Test for Assimilable Organic Carbon in Reclaimed Waters. *Applied and Environmental Microbiology*, 75(23), 7385-7390.
- World Bank. (2019). *The Role of Desalination in an Increasingly Water-Scarce World*. Retrieved from Washington, DC:
- Wright, S., Pellegrino, J., & Amy, G. (2005). Humectant release from membrane materials. *Journal of Membrane Science*, 246(2), 227-234.

-
- Wright, S., Ranville, J., & Amy, G. (2001). Relating complex solute mixture characteristics to membrane fouling. *Water Supply*, 1(5-6), 31-38.
- Yang, H., Yu, X., Liu, J., Tang, Z., Huang, T., Wang, Z., Zhong, Q., Long, Z., & Wang, L. (2022). A Concise Review of Theoretical Models and Numerical Simulations of Membrane Fouling. *Water*, 14(21), 3537.
- Yiantsios, S. G., & Karabelas, A. J. (1998). The effect of colloid stability on membrane fouling. *Desalination*, 118(1), 143-152.
- Yiantsios, S. G., Sioutopoulos, D., & Karabelas, A. J. (2005). Colloidal fouling of RO membranes: an overview of key issues and efforts to develop improved prediction techniques. *Desalination*, 183(1), 257-272.
- Yoon, S. H. (2015). *Membrane Bioreactor Processes: Principles and Applications*: CRC Press.
- Yu, Y., Lee, S., Hong, K., & Hong, S. (2010). Evaluation of membrane fouling potential by multiple membrane array system (MMAS): Measurements and applications. *Journal of Membrane Science*, 362(1-2), 279-288.
- Zhu, X., & Elimelech, M. (1997). Colloidal Fouling of Reverse Osmosis Membranes: Measurements and Fouling Mechanisms. *Environmental Science & Technology*, 31(12), 3654-3662.

LIST OF ACRONYMS

AI	Artificial intelligence
ANN	Artificial neural networks
AOC	Assimilable organic carbon
ASTM	American society for testing and materials
ATP	Adenosine triphosphate
BGP	Bacterial growth potential
CEOP	Cake enhance osmotic pressure
CFI	Combined fouling index
CFS	Cross-flow sampler
CIP	Cleaning in place
CW	Canal water
DMA	Differential mobility analyser
DOC	Dissolved organic carbon
ED	Electrodialysis
EPL	Exponential plus linear (model)
EPS	Extracellular polymer substances
FFM	Feed fouling monitor
FI-FFF	Flow field-flow fractionation
GOF	Goodness of fit
HPC	Heterotrophic plate counting
LOD	Limit of detection
MED	Multi-effect distillation
MF	Microfiltration
MFI	Modified fouling index
MFI-NF	Modified fouling index – nanofiltration
MFI-UF	Modified fouling index – ultrafiltration
MSF	Multi-stage flash

MWCO	Molecular weight cut off
NDP	Net driving pressure
NF	Nanofiltration
NOM	Natural organic matter
PAN	Polyacrylonitrile
PES	Polyethersulfone
RO	Reverse Osmosis
SDI	Silt density index
SEM	Scanning electron microscope
SI	Saturation index
TEP	Transparent exopolymer particles
TOC	Total organic carbon
UF	Ultrafiltration
UTDR	Ultrasonic time domain reflectometry
VBA	Visual basic for applications
VC	Vapour compression
ZP	Zeta potential

LIST OF TABLES

Table 1.1: Range of SDI values.....	8
Table 2.1: Testing conditions applied to examine the MFI-UF calibration using dextran and polystyrene solutions	30
Table 2.2: Testing conditions applied to assess the MFI-UF linearity using CW.....	31
Table 3.1: LOD of MFI-UF at 100 L/m ² .h.....	51
Table 3.2: MFI-UF correction factors for the effect of membrane surface porosity (identified based on washed polystyrene particle suspension).....	62
Table 3.3: Main inputs of the MFI-UF fouling prediction model (Equation (3.7))	66
Table 4.1: Summary of water samples collection and operational data	87
Table 4.2: Characteristics of RO feed during collection time	87
Table 4.3: Approximate duration of MFI-UF test in relevance to the applied flux	93
Table 4.4: Particle deposition factor (Ω) measured at same flux applied in RO plants .	94
Table 4.5: Scaling, biological and organic fouling potential indices/parameters for plant A and B.....	96
Table 4.6: Summary of the NDP increase rates predicted based on MFI-UF and the NDP increase rates observed in the RO plants	99
Table 5.1: Technical specifications of used pumps (from Harvard Apparatus).....	110
Table 5.2: <i>Rm</i> range of used PES membranes with MWCO of 5-100 kDa.....	119
Table 5.3: Approximate range of MFI-UF test duration (for canal water samples with a concentration of 1-100%, where raw canal water has turbidity ranged from 1.5 to 3.0 NTU, TOC from 11 to 18 mg/L, and EC from 600 to 800 uS/cm).....	125
Table 5.4: MFI-UF calculated based on manual and automatic approach for canal water samples measured at 100 L/m ² .h using 100 kDa membrane.....	127
Table 5.5: Pump flow at given flux rates.....	128

LIST OF FIGURES

Figure 1.1: Global desalination capacity increase between 1970 and 2020 (DesalData, 2020).....	3
Figure 1.2: Global market share of the different desalination technologies (DesalData, 2020).....	3
Figure 1.3: Global RO capacity with regards to the water source (DesalData, 2020)	3
Figure 1.4: Mechanisms of particulate fouling: (a) complete blocking, (b) standard blocking, (c) intermediate blocking, and (d) cake/gel formation (Yang et al., 2022)	6
Figure 1.5: Scheme of SDI set-up (adapted from ASTM (2014)).....	7
Figure 1.6: Typical filtration curve at constant pressure (t/V vs V) and at constant flux (ΔP vs t) (Boerlage et al., 1998; Boerlage et al., 2004)	10
Figure 1.7: Scheme of MFI-UF set-up at constant flux filtration.....	13
Figure 2.1: Typical filtration phases during the MFI-UF test performed at constant flux	28
Figure 2.2: Scheme of MFI-UF set-up at constant flux filtration.....	29
Figure 2.3: Relationship between MFI-UF and dextran concentration	32
Figure 2.4: MFI-UF of dextran samples (50 mg/L) prepared with two diluting buffer solutions (where MFI-UF was measured in triplicate).....	33
Figure 2.5: Relationship between MFI-UF and polystyrene concentration	35
Figure 2.6: Hypothesized illustration of the cake formed by polystyrene particles in case of (a) lower particle concentration (b) higher particle concentration	35
Figure 2.7: Relationship between MFI-UF and particle concentration in surface canal water at various testing conditions; at 20, 100 and 200 L/m ² .h using 5, 10 and 100 kDa membranes (the raw canal water used to prepare the dilutions was different at each testing condition; turbidity = 1.5-3.0 NTU, TOC = 11-18 mg/L and EC = 600-800 uS/cm)	37
Figure 3.1: Typical filtration curve during an MFI-UF test at constant flux.....	46
Figure 3.2: Scheme of MFI-UF set-up at constant flux filtration.....	47
Figure 3.3: Schematic diagram illustrating the hypothesized cake development on the membrane surface during MFI-UF test; (a) separated mounds, (b) overlapping hemispheres, and (c) continuous/even layers	48
Figure 3.4: The newly developed approach to verify the effect of membrane surface porosity on the MFI-UF measured at constant flux.....	50

Figure 3.5: Preliminary investigation to verify the effect of membrane surface porosity on measured MFI-UF using feed suspensions/solutions of (a) unwashed polystyrene particles (75 nm), (b) silver particles (80 nm), and (c) pullulan particles (800 kDa).....	52
Figure 3.6: Polystyrene particle washing approach using stirred UF filtration at constant pressure.....	54
Figure 3.7: Verified the effect of membrane surface porosity on the MFI-UF using a suspension of polystyrene particles washed by stirred dead-end filtration (Amicon cell)	55
Figure 3.8: Membrane holder support pad; (a) channelled side, and (b) perforated side	56
Figure 3.9: Ultra-high resolution SEM images of the surface of 5-100 kDa PES membranes (magnification of 500,000x)	57
Figure 3.10: Relationship between membrane MWCO and surface porosity based on ultra-high resolution SEM analysis	58
Figure 3.11: Pore size distribution of 5-100 kDa membranes based on ultra-high resolution SEM analyses	58
Figure 3.12: Time required until membrane surface is entirely covered by cake, assuming that the membrane pores are uniformly distributed over the surface	59
Figure 3.13: Relationship between MFI-UF of washed polystyrene particles suspension, membrane surface porosity and membrane MWCO	60
Figure 3.14: Schematic diagram illustrating the structure of the polystyrene particle cake formed on membrane with uniform and non-uniform pore distribution	61
Figure 3.15: <i>R_m</i> of 10 and 100 kDa membranes measured based on both sides of the holder support pad	63
Figure 3.16: Predicted NDP increase rates with and without correcting the MFI-UF for the effect of non-uniform membrane surface porosity	66
Figure 4.1: Typical particulate fouling mechanisms during MFI-UF test performed at constant flux	83
Figure 4.2: Methodology followed to verify the MFI-UF method to predict the particulate fouling rate in full-scale RO plants	85
Figure 4.3: <i>Treatment process schemes of the studied RO plants</i>	86
Figure 4.4: Scheme of MFI-UF set-up at constant flux filtration.....	88
Figure 4.5: MFI-UF measured in plant A – stage 1 (Trial #1): (a) RO feed, and (b) RO concentrate; (i) MFI-UF measured directly at same RO flux applied in the plant (Δ 100	

kDa, \circ 10 kDa, \square 5 kDa), and (ii) MFI-UF measured at higher flux rates (\blacktriangle 100 kDa, \bullet 10 kDa, \blacksquare 5 kDa) and extrapolated (disconnected lines) at the applied RO flux 92

Figure 4.6: Predicted and observed NDP increase along with the flux applied in plant A – stage 1 (where day 0 is the day of sample collection); (a) Trial #1, (b) Trial #2, and (c) Trial #3 97

Figure 4.7: Predicted and observed NDP increase along with the flux applied in plant B (where day 0 is the day of sample collection); (a) stage 1, and (b) stage 2..... 98

Figure 5.1: Typical filtration phases during MFI-UF test performed at constant flux. 108

Figure 5.2: Scheme of MFI-UF set-up at constant flux filtration..... 109

Figure 5.3: Membrane holder with 25 mm nominal diameter (from Whatman)..... 110

Figure 5.4: Pump (PHD ULTRA standard) flow at 34.6 mL/h (100 L/m².h) 112

Figure 5.5: Accuracy and reproducibility of used pumps (expressed in max error%). 112

Figure 5.6: Pressure transmitter (Omega) readings at constant pressure in the range of 1000 mbar 113

Figure 5.7: Accuracy and reproducibility of used pumps (expressed in max error%). 113

Figure 5.8: Transmembrane pressure over time during the filtration of ultra-pure water through 100 kDa membrane at 100 L/m².h; (a) before and (b) after membrane cleaning by filtering 100 ml of ultra-pure water 115

Figure 5.9: TOC of permeate collected in sequent discrete batches of 20 mL during the filtration of ultra-pure water through 100 kDa membranes at a flux rate of 100-1000 L/m².h 117

Figure 5.10: Transmembrane pressure against flux during the filtration of ultra-pure water through 100 kDa membrane 118

Figure 5.11: MFI-UF measured (i) directly at same RO flux (\triangle 100 kDa, \circ 10 kDa, \square 5 kDa), and (ii) at higher flux rates (\blacktriangle 100 kDa, \bullet 10 kDa, \blacksquare 5 kDa) and then extrapolated to the RO flux (disconnected lines) 122

Figure 5.12: Schematic diagram illustrating cake development on a membrane surface during an MFI-UF test..... 123

Figure 5.13: Transmembrane pressure development over time during filtration of canal water through 10 kDa membrane at 20 L/m².h 123

Figure 5.14: MFI-UF calculation based on Rational 3/2 model for different MFI-UF levels (P vs t data is for canal water samples with (a) 5%, (b) 25%, (c) 50% and (d) 100% concentration, measured at 100 L/m².h using 100 kDa membrane)..... 126

ABOUT THE AUTHOR

- Oct. 2021 – Present **Investment Manager**
Invest International, the Hague, Netherlands
- Oct. 2016 – Oct. 2023 **PhD Researcher**
Delft University of Technology and IHE-Delft Institute for
Water Education, Delft, Netherlands
- Jul. 2014 – Oct. 2016 **Deputy Area Manager**
GVC Onlus, Gaza, Palestine
- Nov. 2013 – Jul. 2014 **Procurement Engineer**
Saqqa and Khoudary General Contracting Co. Ltd., Gaza,
Palestine
- Aug. 2011 – Apr. 2013 **MSc in Urban Water Engineering and Management**
IHE-Delft Institute for Water Education, Delft, Netherlands
- Mar. 2011 – Aug. 2011 **Cost Control Engineer**
Saqqa and Khoudary General Contracting Co. Ltd., Gaza,
Palestine
- Jul. 2010 – Mar. 2011 **Project Coordinator**
University College of Applied Sciences, Gaza, Palestine
- Oct. 2009 – Apr. 2010 **Project Engineer**
Saqqa and Khoudary General Contracting Co. Ltd., Gaza,
Palestine
- Sep. 2008 – Sep. 2009 **Program Coordinator**
University College of Applied Sciences, Gaza, Palestine
- Aug. 2003 – Jul. 2008 **BSc in Civil Engineering**
Islamic University of Gaza, Gaza, Palestine

Journals publications

Abunada, M., Dhakal, N., Gulrez, R., Ajok, P., Li, Y., Abushaban, A., Smit, H., Moed, D., Ghaffour, N., Schippers, J. C., & Kennedy, M. D. (2023). Prediction of particulate fouling in full-scale reverse osmosis plants using the modified fouling index – ultrafiltration (MFI-UF) method. *Desalination*, 553, 116478. doi:<https://doi.org/10.1016/j.desal.2023.116478>

Abunada, M., Dhakal, N., Andyar, W. Z., Li, Y., Ajok, P., Ghaffour, N., Schippers, J. C., & Kennedy, M. D. (2023). Calibrating and Validating the MFI-UF Method to Measure Particulate Fouling in Reverse Osmosis. *Membranes*, 13(5), 535. Retrieved from <https://www.mdpi.com/2077-0375/13/5/535>

Abunada, M., Dhakal, N., Andyar, W. Z., Ajok, P., Smit, H., Ghaffour, N., Schippers, J. C., & Kennedy, M. D. (2022). Improving MFI-UF constant flux to more accurately predict particulate fouling in RO systems: Quantifying the effect of membrane surface porosity. *Journal of Membrane Science*, 660, 120854. doi:<https://doi.org/10.1016/j.memsci.2022.120854>

Trifunović, N., **Abunada, M.**, Babel, M., & Kennedy, M. (2015). The role of balancing tanks in optimal design of water distribution networks. *Journal of Water Supply: Research and Technology - Aqua*, 64(5), 610-628. doi:10.2166/aqua.2014.04

Conference proceedings

Abunada, M., Li, Y., Dhakal, N., Schippers, J. C., & Kennedy, M. D. (2019). The modified fouling index ultrafiltration to predict the particulate fouling in reverse osmosis and ultrafiltration. The International Desalination Association World Congress, Dubai, UAE, 20-24 October 2019

Abunada, M., Trifunović, N., Kennedy, M., & Babel, M. (2014). Optimization and reliability assessment of water distribution networks incorporating demand balancing tanks. *Procedia Engineering*, 70, 4-13. doi:<https://doi.org/10.1016/j.proeng.2014.02.002>

Book chapters

Dhakal, N., Abushaban, A., Mangal, M.N., **Abunada, M.**, Schippers, J.C., Kennedy, M.D., (2020). Chapter 12: Membrane fouling and scaling in Reverse Osmosis. In, *Membrane Desalination: from nanoscale to real world applications*, CRC press. ISBN:9780367030797



*Netherlands Research School for the
Socio-Economic and Natural Sciences of the Environment*

D I P L O M A

for specialised PhD training

The Netherlands research school for the
Socio-Economic and Natural Sciences of the Environment
(SENSE) declares that

Mohanad Abunada

born on 15th April 1985 in Benghazi, Libya

has successfully fulfilled all requirements of the
educational PhD programme of SENSE.

Delft, \ 202

Chair of the SENSE board

Prof. dr. Martin Wassen

The SENSE Director

Prof. Philipp Pattberg

The SENSE Research School has been accredited by the Royal Netherlands Academy of Arts and Sciences (KNAW)



K O N I N K L I J K E N E D E R L A N D S E
A K A D E M I E V A N W E T E N S C H A P P E N



The SENSE Research School declares that **Mohanad Abunada** has successfully fulfilled all requirements of the educational PhD programme of SENSE with a work load of 40.1 EC, including the following activities:

SENSE PhD Courses

- Linear models, PE&RC and SENSE (2017)
- Basic statistics, PE&RC and SENSE (2017)
- Environmental research in context (2017)
- Research in context activity: 'Organization of a PhD social event: SENSE beach walk & IHE PhD barbecue' (2019)

Other PhD and Advanced MSc Courses

- Surface water treatment I, IHE-Delft (2017)
- Advanced water treatment and re-use, IHE-Delft (2017)
- Presenting scientific research, TU Delft (2017)
- Academic writing, IHE-Delft (2018)
- Scientific writing workshop, IHE-Delft (2019)
- Career development, TU Delft (2019)
- The basics of transport phenomena, TU Delft (2020)

Management and Didactic Skills Training

- Membership of PhD Association Board of IHE-Delft (2018-2020)
- Organizing online seminar: Human Rights and International Humanitarian Law: the Case of Palestine (2021)
- Supervising four MSc student with thesis (2018-2021)
Practical assistance in the MSc course 'Advanced water treatment and re-use' (2019-2021)

Oral Presentations

- *Development of a Standard Protocol for MFI-UF to Assess Particulate Fouling in RO Systems.* European Desalination Society Conference, Desalination for the Environment: Clean Water and Energy, 3-6 September 2018, Athens, Greece
- *The Modified Fouling Index Ultrafiltration to Predict the Particulate Fouling Rate in Reverse Osmosis.* IHE-Delft PhD Symposium: Innovation for Sustainability: Tackling Water and Climate Change Related Challenges, 10-11 October 2019, Delft, Netherlands
- *The MFI-UF to Predict Particulate Fouling in Reverse Osmosis and Ultrafiltration.* International Desalination Association (IDA) World Congress: Crossroads to Sustainability, 20-24 October 2019, Dubai, United Arab Emirates

SENSE coordinator PhD education

Dr. ir. Peter Vermeulen

Particulate fouling, due to the deposition of particles and colloids onto RO membranes, is one of the persistent problems, resulting in higher energy consumption and more frequent membrane cleaning and replacement. Hence, a reliable method to accurately predict particulate fouling is very important to optimize the performance of RO systems. Therefore, this PhD research aimed to further develop and apply the MFI-UF method to more accurately predict particulate fouling in RO systems.

Firstly, MFI-UF calibration was studied examining standard polystyrene and dextran particles. The study concluded that a heterogenous mixture of polystyrene particles is considered promising for MFI-UF calibration. Moreover, real surface water was also used to validate MFI-UF measurements. Results demonstrated that the MFI-UF method can be used to measure different levels of particulate fouling under a wide range of testing conditions (at fluxes of 20-200 L/m².h using 5, 10, 50 and 100 kDa UF membranes).

Furthermore, the effect of surface porosity of MFI-UF membranes was investigated, quantified and corrected using a new approach. Firstly, the surface porosity of MFI-UF membranes (5-100 kDa) was determined using ultra-high resolution SEM. Thereafter, the MFI-UF was measured using suspensions of standard polystyrene particles that were

pre-washed to remove particle fractions smaller than the pores of MFI-UF membranes, thus ensuring that variations in measured MFI-UF values were due to the membrane surface porosity and not membrane pore size. The results showed that the lower the MWCO of MFI-UF membrane, the lower the surface porosity, and the more non-uniform the distribution of pores is on the membrane surface. This results in lower effective membrane area and higher local fluxes, which eventually lead to overestimation of the measured MFI-UF. Consequently, correction factors of 0.4-1.0 were proposed for the MFI-UF measured with 5-100 kDa membranes, respectively. Correcting the surface porosity improved fouling prediction in a full-scale RO plant by 50-60%.

Subsequently, the improved MFI-UF method was applied in two full-scale RO plants. The study showed that particulate fouling predicted based on the 10-100 kDa membrane had the best agreement with the actual fouling observed in the studied RO plants. Finally, the research concludes with the introduction of a complete testing protocol for the MFI-UF method, providing a reliable tool to accurately measure and predict the rate of particulate fouling in RO systems, which can support engineers, operators and researchers to design, operate and monitor RO systems more effectively and sustainably.